LEABHARLANN CHOLÁISTE NA TRÍONÓIDE, BAILE ÁTHA CLIATH | TRINITY COLLEGE LIBRARY DUBLIN
Ollscoil Átha Cliath | The University of Dublin

Terms and Conditions of Use of Digitised Theses from Trinity College Library Dublin

Copyright statement

All material supplied by Trinity College Library is protected by copyright (under the Copyright and Related Rights Act, 2000 as amended) and other relevant Intellectual Property Rights. By accessing and using a Digitised Thesis from Trinity College Library you acknowledge that all Intellectual Property Rights in any Works supplied are the sole and exclusive property of the copyright and/or other IPR holder. Specific copyright holders may not be explicitly identified. Use of materials from other sources within a thesis should not be construed as a claim over them.

A non-exclusive, non-transferable licence is hereby granted to those using or reproducing, in whole or in part, the material for valid purposes, providing the copyright owners are acknowledged using the normal conventions. Where specific permission to use material is required, this is identified and such permission must be sought from the copyright holder or agency cited.

Liability statement

By using a Digitised Thesis, I accept that Trinity College Dublin bears no legal responsibility for the accuracy, legality or comprehensiveness of materials contained within the thesis, and that Trinity College Dublin accepts no liability for indirect, consequential, or incidental, damages or losses arising from use of the thesis for whatever reason. Information located in a thesis may be subject to specific use constraints, details of which may not be explicitly described. It is the responsibility of potential and actual users to be aware of such constraints and to abide by them. By making use of material from a digitised thesis, you accept these copyright and disclaimer provisions. Where it is brought to the attention of Trinity College Library that there may be a breach of copyright or other restraint, it is the policy to withdraw or take down access to a thesis while the issue is being resolved.

Access Agreement

By using a Digitised Thesis from Trinity College Library you are bound by the following Terms & Conditions. Please read them carefully.

I have read and I understand the following statement: All material supplied via a Digitised Thesis from Trinity College Library is protected by copyright and other intellectual property rights, and duplication or sale of all or part of any of a thesis is not permitted, except that material may be duplicated by you for your research use or for educational purposes in electronic or print form providing the copyright owners are acknowledged using the normal conventions. You must obtain permission for any other use. Electronic or print copies may not be offered, whether for sale or otherwise to anyone. This copy has been supplied on the understanding that it is copyright material and that no quotation from the thesis may be published without proper acknowledgement.

MODULATION OF ACTIVATED PROTEIN C (APC) ANTICOAGULANT AND CYTOPROTECTIVE FUNCTION

A Thesis Submitted to the University of Dublin, Trinity College, for the Degree of Doctor of Philosophy in the Faculty of Medicine

Submitted August 2011

Revised October 2011

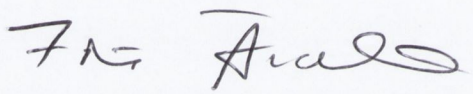
Fionnuala Bríd Ní Áinle M.B., B.Ch., B.A.O., M.R.C.P.I., F.R.C.Path.

Haemostasis Research Group
Room 2.101
Institute of Molecular Medicine
Trinity College
Dublin 8

DECLARATION

I, Fionnuala Ní Áinle, declare that this work has not been submitted as an exercise for a degree at this or any other university. It is entirely my own work. I agree that the College Library may lend or copy this thesis upon request.

Signed:



Fionnuala Ní Áinle, M.B., B.Ch., B.A.O., M.R.C.P.I., F.R.C.Path.

Date:

14 / 11 / 11

TRINITY COLLEGE
22 OCT 2012
LIBRARY DUBLIN
Thesis 9694

SUMMARY

Activated protein C (APC) is an anticoagulant glycoprotein that attenuates thrombin generation. Moreover, it has recently been demonstrated that APC possesses anti-inflammatory, anti-apoptotic and endothelial cell barrier stabilizing properties.

The first goal of this thesis was to study the role of N-linked carbohydrates (glycans) in modulating APC anticoagulant function and endothelial cytoprotective signalling via the endothelial cell protein C receptor (EPCR) and protease activated receptor 1 (PAR1). It was determined that removal of APC N-linked glycans using the enzyme PNGase resulted in a ~6-fold reduction in the APC concentration required to achieve half-maximal inhibition of thrombin-induced endothelial cell barrier permeability. Furthermore, deglycosylation enhanced APC anti-apoptotic function on endothelial cells compared to untreated APC. Recombinant APC variants were generated in which each Asn-linked glycan attachment site was eliminated by amino acid substitution. The variant APC-*N329Q* displayed up to 5-fold enhanced protection of the endothelial barrier compared to wild type APC. Moreover, an APC variant (APC-*L38D/N329Q*) was generated which possessed minimal anticoagulant activity but 5-fold improved endothelial barrier protective function compared to wild type APC.

These results have identified that APC N-linked glycosylation modulates EPCR-dependent, PAR1-mediated cytoprotective signaling. These data also suggest that β-protein C, a naturally occurring glycoform characterized by lack of N-linked glycosylation at Asn-329, may play a role in APC cytoprotective function *in vivo*.

Protamine sulphate is used to reverse heparin-induced anticoagulation. Paradoxically, it is associated with unwanted anticoagulant properties which can be associated with bleeding complications *in vivo.* The molecular mechanisms underlying these anticoagulant properties have been poorly understood. The second goal of this project was to elucidate these mechanisms. Protamine sulphate was found to prolong plasma clotting times and to attenuate thrombin generation *in vitro,* reducing endogenous thrombin potential (ETP) by 41±7%. Protamine sulphate profoundly enhanced the anticoagulant properties of APC in thrombin generation and activated partial thromboplastin time (APTT) assays. In an assay of procoagulant factor V (FV) activation, protamine was found to greatly reduce the rate of FV activation both by thrombin and by factor Xa (FXa). Moreover, administration of pharmacological doses of protamine sulphate to BALB/c mice prolonged tail bleeding time *in vivo.* These novel findings represent the molecular mechanism underlying the anticoagulant properties of protamine sulphate in plasma.

ACKNOWLEGEMENTS

I wish to express my sincere gratitude to my supervisors, Dr Roger Preston and Professor James O'Donnell, for their dedicated and expert supervision of my PhD project.

I also acknowledge the critical contributions of Professor Pádraig Fallon and Dr Hendrik Nel (Inflammation and Immunity Research Group, Insitute of Molecular Medicine, Trinity College) to work characterizing the *in vivo* anticoagulant function of protamine sulphate.

Finally, this thesis is dedicated to my husband and greatest friend, Ross Emerson and to my children, Muireann and Dónall. Tiomnaím an tráchtas seo freisin do mo thuismitheoirí, Íde agus Cathal Ó Háinle, a thug gach deis dom agus mé ag teacht in inmhe, agus arbh iad i gcónaí na múinteoirí ba thábhachtaí a bhí agam. Le mórghrá agus ardmheas.

PUBLICATIONS ARISING FROM THIS THESIS

1. **Ní Áinle F,** O'Donnell JS, Johnson JA, Brown L, Gleeson EM, Smith OP, Preston RJS. Activated protein C N-linked glycans modulate cytoprotective signaling function on endothelial cells. **J Biol Chem**. 2011; 286(2): 1323-30*.

2. **Ní Áinle F**, Preston RJ, Jenkins PV, Nel HJ, Johnson JA, Smith OP, White B, Fallon PG, O'Donnell JS. Protamine sulfate down-regulates thrombin generation by inhibiting factor V activation. **Blood** 2009; 114(8): 1658-65*.

3. Preston RJ, Tran S, Johnson JA, **Ní Áinle F**, Harmon S, White B, Smith OP, Jenkins PV, Dahlbäck B, O'Donnell JS. Platelet factor 4 impairs the anticoagulant activity of activated protein C. **J Biol Chem.** 2009; 284(9):5869-75.

4. Harmon S, Preston RJ, **Ní Áinle F**, Johnson JA, Cunningham MS, Smith OP, White B, O'Donnell JS. Dissociation of activated protein C functions by elimination of protein S cofactor enhancement. **J Biol Chem**. 2008; 283(45):30531-9.

* Directly related to the work described in this thesis.

TABLE OF CONTENTS

SUMMARY..... 3

ACKNOWLEGEMENTS 5

PUBLICATIONS ARISING FROM THIS THESIS 6

TABLE OF CONTENTS 7

LIST OF FIGURES 16

LIST OF TABLES 19

ABBREVIATIONS 20

CHAPTER 1: INTRODUCTION 25

1.1: BLOOD COAGULATION 25

1.1.1 Overview 25

1.1.2 Primary haemostasis 26

1.1.3 Coagulation cascade 29

1.1.4 Vitamin K-dependent proteins 35

1.1.5 Coagulation regulation 37

1.2: THE PROTEIN C ANTICOAGULANT AND CYTOPROTECTIVE PATHWAY 38

1.2.1 Protein C gene and structure. 38

1.2.2 EPCR 43

1.2.3 Protein C activation 46

1.2.4 APC anticoagulant function 47

1.2.5 APC inhibition 48

1.2.6 Protein C glycosylation 49

1.2.7 Protective signalling properties of APC 54

1.2.8 *In vivo* cytoprotective effects mediated by APC. 65

1.2.9 Conclusion 75

1.3: AIMS OF THESIS 76

CHAPTER 2: MATERIALS AND METHODS 77

2.1: Glycosidase treatment of APC or protein C 77

2.2: SDS-PAGE and Western blot analysis 79

2.3: Total carbohydrate detection 80

2.4: Sialic acid detection 82

2.5: Activation of protein C variants using Protac 83

2.6: Determination of amidolytic activity of recombinant APC preparations. 83

2.7: Protein C activation on the surface of an endothelial cell line 84

2.8: Assessment of APC anticoagulant activity in protein C-deficient plasma 85

2.9: Preparation of normal platelet poor plasma 86

2.10: Assessment of heparin-stimulated APC inhibition in plasma 86

2.11: Phospholipid preparation 87

2.12: Protein S-independent FVa inactivation by APC variants. 88

2.13: Protein S-dependent FVa inactivation by APC variants 89

2.14: Measurement of APC-mediated endothelial barrier protection. 90

2.15: Assessment of APC-mediated protection against endothelial cell apoptosis by TUNEL staining and flow cytometry 91

2.16: Assessment of APC-mediated protection against apoptosis by measurement of *bax* and *bcl-2* mRNA expression. 93

2.17: Measurement of APC-mediated protection against apoptosis: Apopercentage® assay 98

2.18: Generation of protein C mutants 99

2.18.1: Human protein C mammalian expression vector 99

2.18.2: Site-directed mutagenesis of pRc/CMV/PC plasmid 101

2.18.3: Agarose gel electrophoresis 103

2.18.4: Luria-Bertani (LB) agar plate preparation 103

2.18.5: DNA transformation into NovaBlue Singles® competent *E.coli* cells. 104

2.18.6: Preparation of plasmid minipreps 105

2.19: Recombinant protein C expression 108

2.19.1: Cell culture 108

2.19.2: Stable transfection of mammalian cell line 109

2.19.3: Protein C ELISA 110

2.19.4: Partial purification of recombinant protein C variants 111

2.20: Assessment of protein C binding to soluble EPCR 114

2.21: Measurement of thrombin generation and tail bleeding time in mice.....116

2.22: Activated partial thromboplastin time (APTT) and prothrombin time (PT) measurement.....117

2.23: Characterization of APC-mediated FVIIIa proteolysis in the presence of protamine sulphate.....117

2.24: Determination of rate of FV activation.....118

CHAPTER 3: FUNCTIONAL EFFECT OF MODIFYING ACTIVATED PROTEIN C GLYCOSYLATION BY TREATMENT WITH SPECIFIC GLYCOSIDASES..... 119

3.1: Digestion of APC with PNGase F results in removal of N-linked glycan residues.....119

3.2: PNGase F treatment of APC does not affect active site amidolytic activity..122

3.3: PNGase F treatment of protein C does not influence EPCR-dependent protein C activation on the surface of EA.hy926 cells.....125

3.4: PNGase treatment of APC results in enhanced anticoagulant function. 127

3.5: PNGase treatment of APC does not influence its rate of inactivation in normal pooled plasma.....130

3.6: Enhancement of APC anticoagulant function by PNGase treatment is not mediated by increased rate of substrate proteolysis.....132

3.7: PNGase treatment of APC results in enhanced EPCR/PAR1-dependent endothelial barrier protection.....135

3.8: Assessment of endothelial cell apoptosis by TUNEL staining and flow cytometry.....139

3.9: PNGase treatment of APC results in improved protective signalling against staurosporine-induced apoptosis.....141

3.10: α2-3,6,8,9 neuraminidase treatment of APC has no effect upon amidolytic or anticoagulant activity.....144

3.11: Removal of sialic acid moieties from APC does not affect EPCR and PAR-dependent barrier protective properties.....148

CHAPTER 4: MODIFICATION OF ACTIVATED PROTEIN C GLYCOSYLATION BY SITE-DIRECTED MUTAGENESIS.....150

4.1: Generation of recombinant protein C cDNA glycosylation site variants.....150

4.2: Stable expression of recombinant protein C *N*-linked glycosylation site variants.....152

4.3: Anticoagulant function of protein C variants generated by site-directed mutagenesis of protein C heavy chain *N*-linked glycan attachment sites.....156

4.4 Site-directed mutagenesis at Asn-329 results in enhanced endothelial cell barrier-protection.....158

4.5 Characterizing modulation of staurosporine-induced endothelial cell apoptosis by recombinant APC *N*-linked glycan variants using an assay of apoptosis-specific dye uptake.....161

4.6 Characterizing modulation of staurosporine-induced endothelial cell apoptosis by recombinant APC N-linked glycan variants using an assay of pro- and anti-apoptotic gene expression. 164

4.7 EPCR affinity of protein C-*N329Q* 166

4.8: Enzymatic removal of *N*-linked glycans from a non-anticoagulant recombinant APC variant results in enhancement of EPCR-dependent, PAR-1 mediated cytoprotective signalling. 168

4.9: A recombinant non-anticoagulant APC variant lacking a glycan attachment site at Asn *329* due to glutamine substitution (APC-*L38D/N329Q).* 170

4.10: APC-*L38D/N329Q* exhibits enhanced endothelial barrier protective function 172

4.11: APC-*L38D/N329Q* exhibits enhanced anti-apoptotic function 174

CHAPTER 5: DISCUSSION OF RESULTS DESCRIBED IN CHAPTERS 3 AND 4 177

5.1 ROLE OF GLYCOSYLATION IN PROTEIN FUNCTION 177

5.2 ROLE OF APC GLYCOSYLATION IN ANTICOAGULANT FUNCTION AND IN SIGNALLING FUNCTION EFFICIENCY ON ENDOTHELIAL CELLS 178

5.2.1 Role of N-linked glycans in modulating APC amidolytic function 179

5.2.2 Role of N-linked glycans in modulating protein C activation 180

5.2.3 Role of N-linked glycans in modulating APC anticoagulant function 181

5.2.4 Role of N-linked glycans in modulating APC cytoprotective function ... 183

5.3 β-APC LACKS GLYCOSYLATION AT ASN-329 AND MAY REPRESENT A PHYSIOLOGICAL MEANS OF MODULATING APC CYTOPROTECTIVE FUNCTION 187

5.4 RATIONALE FOR GENERATING RECOMBINANT APC VARIANTS WITH ENHANCED CYTOPROTECTIVE PROPERTIES AND REDUCED ANTICOAGULANT FUNCTION 189

5.6 CONCLUSION 191

CHAPTER 6: PROTAMINE SULPHATE ENHANCES APC ANTICOAGULANT PROPERTIES AND DOWNREGULATES THROMBIN GENERATION BY INHIBITING FACTOR V ACTIVATION 192

6.1 INTRODUCTION 192

6.1.1 Work leading up to this chapter 192

6.1.2 Protamine structure and function 193

6.1.3 Clinical use of protamine sulphate in reversal of systemic heparinization 194

6.1.4 *In vitro* anticoagulant properties of protamine sulphate 195

6.1.5 *In vivo* anticoagulant properties of protamine sulphate 197

6.1.6 Molecular mechanisms underlying anticoagulant effects of protamine sulphate 199

6.2 RESULTS 200

6.2.1 Protamine sulphate prolongs normal pooled plasma clotting times 200

6.2.2 Protamine sulphate attenuates TF-initiated thrombin generation in normal platelet-poor plasma.....202

6.2.3 Protamine sulphate alters specific parameters of a TF-initiated thrombin generation curve in normal platelet-poor plasma. 204

6.2.4 Anticoagulant effects of protamine sulphate following reversal of heparin-induced anticoagulation. 206

6.2.5 Anticoagulant effects of protamine sulphate following reversal of low molecular weight heparin (LMWH) 208

6.2.6 Protamine sulphate enhances APC-mediated APTT prolongation in normal pooled plasma.....210

6.2.7 Protamine sulphate enhances APC-mediated APTT prolongation in normal pooled plasma.....212

6.2.8 Protamine sulphate enhances APC-mediated attenuation of thrombin generation in heparinized normal pooled plasma. 213

6.2.9 Protamine sulphate does not enhance the anticoagulant effect of APC by influencing rate of FVa proteolysis.....215

6.2.10 Protamine sulphate does not enhance the anticoagulant effect of APC by influencing rate of FVIIIa proteolysis.....217

6.2.11 Protamine sulphate inhibits thrombin -mediated activation of coagulation factor V. 219

6.2.12 Protamine sulphate inhibits FXa- mediated activation of coagulation factor V. 222

6.2.13 Preactivation of FV greatly reduces the anticoagulant effect of protamine in plasma.....223

6.2.14: Characterization of *in vivo* anticoagulant properties of protamine sulphate.....226

6.3 DISCUSSION 229

REFERENCES 235

APPENDICES 246

APPENDIX I: COMPOSITION OF BUFFERS.....246

APPENDIX II: OLIGONUCLEOTIDE PRIMER SEQUENCES 251

ACCEPTED FOR PUBLICATION..... 253

LIST OF FIGURES

Figure 1.1: Mechanism by which exposure of subendothelial collagen and tissue factor trigger primary haemostasis. 28

Figure 1.2: The coagulation cascade 31

Figure 1.3: Amino acid sequence of the nascent protein C polypeptide 39

Figure 1.4: Functionally important surface loops in the protein C serine protease domain. 42

Figure 1.5: Interaction of the protein C "ω" loop with EPCR 45

Figure 1.6: Initiation of N-linked glycan biosynthesis 50

Figure 1.7: Proposed mechanism of APC-mediated endothelial barrier protection 63

Figure 2.1: Sites of cleavage of glycosidase enzymes 78

Figure 2.1: The pRc/CMV/Protein C cDNA vector 100

Figure 3.1: Removal of N-linked glycans from APC by enzymatic digestion with PNGase F. 121

Figure 3.2: Chromogenic substrate hydrolysis by APC-*DesGly*. 124

Figure 3.3: Activation of protein C-*DesGly* on the surface of endothelial cells. 126

Figure 3.4: Anticoagulant function of APC-*DesGly*. 129

Figure 3.5: Inhibition of APC-*DesGly* in normal plasma. 131

Figure 3.6: FVa proteolysis by APC-*DesGly*. 134

Figure 3.7: EPCR/PAR-1 dependent endothelial barrier protective function of APC-*DesGly*. 138

Figure 3.8: Assessment of endothelial cell apoptosis by flow cytometry 140

Figure 3.9: Inhibition of staurosporine-induced apoptosis on EA.hy926 cells by APC-*DesGly*. 143

Figure 3.10: Sialic acid removal from APC by enzymatic digestion with α2-3,6,8,9 neuraminidase. 147

Figure 3.11: EPCR/PAR-1 dependent endothelial barrier protective function of *Asialo*-APC. . 149

Figure 4.1: Generation of recombinant N-linked glycan variants of a protein C cDNA plasmid. 151

Figure 4.2: Characterization of recombinant protein C *N*-linked glycan variants by SDS-PAGE/Western blotting. 155

Figure 4.3: APC anticoagulant function following removal of protein C *N*-linked glycan attachment sites at Asn-248, Asn-313 or Asn-329 by glutamine substitution. 157

Figure 4.4: Site-directed mutagenesis at Asn-329 results in enhanced endothelial cell barrier-protection. 160

Figure 4.5: Inhibition of endothelial cell apoptosis by recombinant APC *N*-linked glycan variants in an assay measuring uptake of an apoptosis-specific dye. 163

Figure 4.6: Modulation of endothelial cell apoptosis by recombinant APC *N*-linked glycan variants using an assay of pro- and anti-apoptotic gene expression. 165

Figure 4.7: Affinity of protein C-*N329Q* for sEPCR. 167

Figure 4.8: Enzymatic deglycosylation of non-anticoagulant APC variant APC-*L38D* with PNGase F enhances APC-L38D-mediated endothelial cell barrier protection. 169

Figure 4.9: Assessment of anticoagulant function of APC-*L38D/N329Q* 171

Figure 4.10: APC-*L38D/N329Q* possesses enhanced endothelial barrier protective function. 173

Figure 4.11: APC-*L38D/N329Q* exhibits enhanced endothelial anti-apoptotic function. 176

Figure 5.1: The N-linked glycan at Asn-329 is conserved and proximal to a PAR1 binding exosite on APC 186

Figure 6.1: Protamine prolongs clotting time of normal pooled plasma *in vitro.* 201

Figure 6.2: Protamine inhibits TF-initiated thrombin generation in normal plasma. 203

Figure 6.3: Protamine inhibits specific thrombin generation curve parameters in normal plasma 205

Figure 6.4: Protamine inhibits thrombin generation in heparinised normal pooled plasma when it is present at a higher concentration than is required for full reversal of heparin. 207

Figure 6.5: Excess protamine inhibits thrombin generation in normal pooled plasma containing LWMH. 209

Figure 6.6: Plasma APTT prolongation by APC is enhanced by protamine sulphate. 211

Figure 6.7: APC-mediated attenuation of thrombin generation is enhanced by protamine. .. 212

Figure 6.8: Excess protamine enhances the anticoagulant effect of APC in heparinised plasma. 214

Figure 6.9: Enhancement by protamine of the anticoagulant effect of APC is not mediated by enhanced FVa hydrolysis. 216

Figure 6.10: Enhancement by protamine of the anticoagulant effect of APC is not mediated by enhanced FVIIIa hydrolysis. 218

Figure 6.11: Protamine inhibits activation of coagulation factor V by thrombin. 221

Figure 6.12: Protamine inhibits activation of coagulation factor V by Xa. 222

Figure 6.13: The anticoagulant effect of protamine is greatly reduced by preactivation of FV to FVa. 225

Figure 6.13: Protamine prolongs bleeding time *in vivo* 228

LIST OF TABLES

Table 1.1: Phase 3 randomized clinical trials of recombinant human APC (DAA) administration in sepsis..... 71

Table 2.1: Components of 2X Reverse Transcription Master Mix using the High Capacity cDNA reverse transcription kit (Applied Biosystems)..... 94

Table 2.2: Thermal cycling parameters for reverse transcription by PCR. 95

Table 2.3: PCR thermal cycling parameters for protein C mutagenesis 102

ABBREVIATIONS

ACT	activated clotting time
ADP	adenosine diphosphate
AIF	apoptosis-inducing factor
Ala; A	Alanine
ALS	amyotrophic lateral sclerosis
APACHE	acute physiology and chronic health evaluation
APC	activated protein C
ApoER2	apolipoprotein E receptor 2
APTT	activated partial thromboplastin time
Arg; R	Arginine
Asn; N	Asparagine
Asp; D	Aspartate
AT	antithrombin
BSA	bovine serum albumin
cDNA	complementary deoxyribonucleic acid
CD	cluster of differentiation
CPB	cardiopulmonary bypass
C-terminal	carboxy terminal
Cys; C	Cysteine
DIC	disseminated intravascular coagulation
DNA	deoxyribonucleic acid
dNTP	doxynucleoside triphosphate

DOPC	dioleoyl-phosphatidylcholine
DOPE	dioleoyl-phosphatidylethanolamine
DOPS	dioleoyl-phosphatidylserine
dUTP	deoxyuridine triphosphate
E.coli	*Escherischia coli*
EDTA	ethylenediaminetetraacetic acid
EGF	epidermal growth factor
ELISA	enzyme linked immunosorbent assay
EPCR	endothelial protein C receptor
ER	endoplasmic reticulum
ERK	extracellular signal-regulated kinase
ETP	endogenous thrombin potential
FII	prothrombin
FIIa	thrombin
FV(a)	(activated) factor V
FVII(a)	(activated) factor VII
FVIII(a)	(activated) factor VIII
FIX(a)	(activated) factor IX
FX(a)	(activated) factor X
FXI(a)	(activated) factor XI
FXII(a)	(activated) factor XII
FXIII(a)	(activated) factor XIII
FCS	Foetal Calf Serum
FPLC	fast protein liquid chromatography

Fuc	fucose
G418	geneticin sulphate
Gal	galactose
Gla	γ-carboxyglutamic acid
Glc	glucose
GlcNAc	N-Acetyl-D-glucosamine
Gln; Q	Glutamine
Glu; E	Glutamic acid
Gly; G	Glycine
Gp	glycoprotein
HBSS	Hank's buffered salt solution
HEK293	hamster embryonic kidney-293 cell line
His; H	Histidine
HRP	horse radish peroxidise
HUVEC	human umbilical vein endothelial cell
ICAM-1	intercellular adhesion molecule-1
IL	interleukin
kDa	kilodaltons
LB	Luria-Bertani
Leu; L	Leucine
LPS	lipopolysaccharide
Lys; K	Lysine
mAb	monoclonal antibody
Man	mannose

MEM	Minimal Essential Medium Eagle
MHC	major histocompatibility complex
mRNA	messenger RNA
NFκB	nuclear factor kappa B
NMDA	N-Methyl-D-aspartate
N-terminal	amino terminal
OD	optical density
OST	oligosaccharyltransferase
PAI-1	plasminogen activator inhibitor-1
PAR1	protease activated receptor 1
PBS	phosphate buffered saline
PCI	protein C inhibitor
PDI	protein disulfide isomerase
PI	propidium iodide
PI3K	phosphoinositide 3-kinase
PPP reagent	platelet-poor plasma reagent
Pro; P	Proline
PSGL	P-selectin glycoprotein ligand
PT	prothrombin time
RT-PCR	reverse transcription polymerase chain reaction
S1P	sphingosine-1 phosphate
S1P1	S1P receptor 1
SEM	standard error of the mean
SDS-PAGE	sodium dodecyl sulphate polyacrylamide gel electrophoresis

Ser; S	Serine
SHBG	sex hormone-binding globulin
SphK1	sphingosine kinase-1
TBE	Tris/Borate/EDTA
TdT	terminal deoxynucleotidyl transferase
TF	tissue factor
TFPI	Tissue Factor Pathway Inhibitor
T_h-2 cell	T helper-2 cell
Thr; T	Threonine
TM	thrombomodulin
TNF-α	tumour necrosis factor-α
tPA	tissue plasminogen activator
TRAIL	TNF-related apoptosis-inducing ligand
TRMP-2	testosterone repressed prostatic message-2
TUNEL	terminal deoxynucleotide transferase nick end labelling
Tyr; Y	Tyrosine
UFH	unfractionated heparin
uPA	urokinase plasminogen activator
VCAM-1	vascular cell adhesion molecule-1
VKOR	vitamin K epoxide reductase multiprotein complex
v/v	volume per unit volume
VWF	von Willebrand factor
w/v	weight per unit volume

CHAPTER 1: INTRODUCTION

1.1: BLOOD COAGULATION

1.1.1 Overview

When vascular injury occurs, a series of events is initiated which results in sealing of the wound and prevention of bleeding. These events include vasoconstriction, recruitment of von Willebrand factor (VWF) and platelets to the site of injury to generate a platelet plug (a process known as "primary haemostasis"), activation of the coagulation cascade and formation of a stable cross-linked fibrin clot. Initiation of coagulation involves generation of picomolar amounts of the serine protease thrombin, followed by assembly of activated coagulation proteases and cofactors on the activated platelet surface, to generate a stable fibrin blood clot.

1.1.2 Primary haemostasis

Primary haemostasis is the process by which platelets adhere to the site of tissue damage, become activated and spread on the exposed subendothelial surface to form large platelet aggregates [1]. This process is critically dependent upon VWF, a large multimeric glycoprotein stored in endothelial cells and platelets [2]. VWF interacts with cell surface and platelet receptors to facilitate platelet binding to exposed collagen [3, 4].

The subendothelial matrix is composed of collagens, tissue factor, fibronectin, laminin and other glycoproteins [5]. Vascular damage exposes the subendothelial matrix to blood, which under normal circumstances, is prevented by the endothelium. Following vascular damage, VWF binds to collagen [2]. VWF-collagen interaction "tethers" VWF. In the presence of shear stress, VWF unwinds, exposing multiple platelet binding sites. VWF captures platelets by binding to platelet glycoprotein (Gp) 1b/V/IX [6]. Collagen also binds directly to the platelet receptor Gp VI [7]. These binding interactions begin the process of platelet adhesion to the site of vascular injury [8].

During platelet adhesion, platelet tethering and rolling occurs first, via VWF-Gp 1b/V/IX and Gp VI interactions. For stable adhesion of platelets to the subendothelium, activation of platelet integrins must occur [9]. Signalling induced by collagen-GpVI results in a conformational change in platelet integrins $\alpha_{iib}\beta_3$ and $\alpha_2\beta_1$ [10-12]. This conformational change converts these integrins from a low to high ligand-affinity state and enables formation of strong bonds with VWF/fibrinogen and collagen respectively [9]. Therefore, initial platelet rolling on collagen and VWF is

converted to stable platelet adhesion [9]. In turn, this mediates enhanced collagen-GpVI signalling [13]. Once anchored at the site of injury, platelet activation results in the release of adenosine diphosphate (ADP), serotonin and thromboxane A_2, which activates more platelets [1]. The events which occur during primary haemostasis are summarized in **Figure 1.1**.

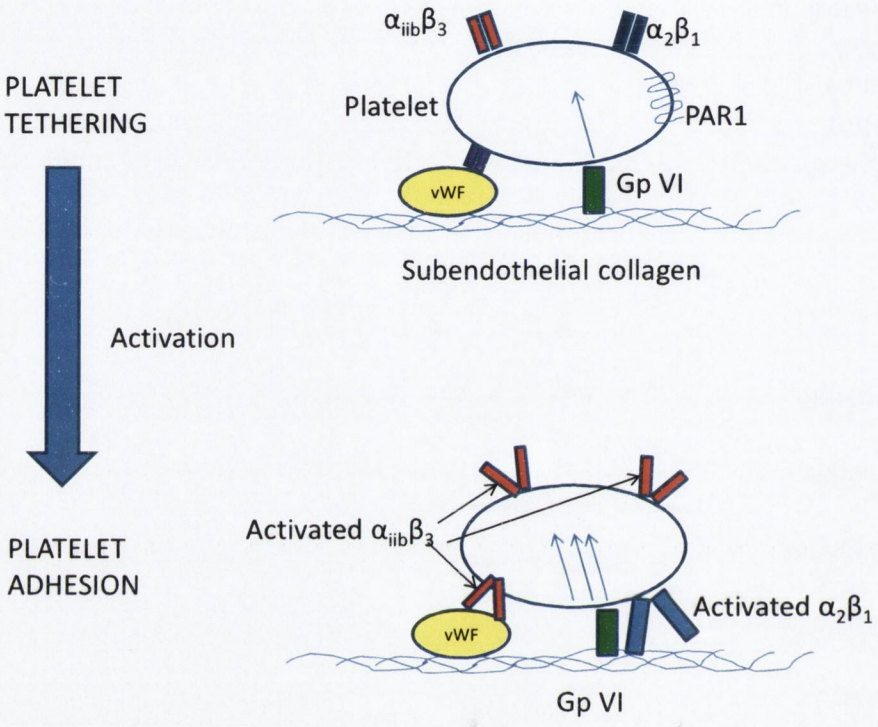


Figure 1.1: Mechanism by which exposure of subendothelial collagen and tissue factor trigger primary haemostasis.

Tethering of platelets to collagen in the extracellular matrix is mediated by interactions between Gp1b/V/IX and GpVI with VWF and collagen respectively. GpVI binding to collagen triggers signalling pathways which lead to a conformational change in platelet integrins $\alpha_{iib}\beta_3$ and $\alpha_2\beta_1$ favouring high-affinity binding, and release of platelet agonists. Firm adhesion of platelets to collagen is mediated by activated $\alpha_{iib}\beta_3$ and $\alpha_2\beta_1$, which further enhances GpVI-mediated signalling.

1.1.3 Coagulation cascade

Upon vascular injury, the tissue factor (TF)-dependent, or *extrinsic* pathway of blood coagulation is initiated when TF on the surface of extravascular cells in the subendothelial matrix is exposed. Blood coagulation is initiated by the complex of activated serine protease factor VII (FVIIa) and TF, which catalyzes the activation of vitamin K-dependent zymogens **(1.1.4)** factor X (FX) and FIX to FXa and FIXa respectively **(Figure 1.2)**.

TF is a 47-kDa transmembrane glycoprotein expressed in subendothelial tissue, which, upon exposure to blood, acts as the physiological trigger of coagulation [14]. TF is constitutively expressed in pericytes, adventitial fibroblasts and in the parenchyma of vascularised organs (for example lung, brain and placenta) [15-17]. Under normal circumstances, therefore, TF is separated from blood. Cellular TF expression is induced upon cellular stress and inflammation. TF plays a key role in sepsis-induced disseminated intravascular coagulation (DIC) in baboons [18] and its expression can be induced in peripheral blood monocytes in response to bacterial lipopolysaccharide (LPS) exposure [19]. Endothelial cells have also been shown to express TF following exposure to LPS [20] and viral nucleic acid [21], however it remains uncertain whether endothelial cells can express TF *in vivo* [14].

TF binds coagulation zymogen FVII or the activated enzyme FVIIa [22]. FVIIa is constitutively present in plasma at approximately 1-2% of total FVII [23]. TF assembles with FVIIa on the cell surface to form an active enzyme/cofactor complex, whose

optimal activity requires FVIIa insertion into a phosphatidylserine-rich phospholipid bilayer [24].

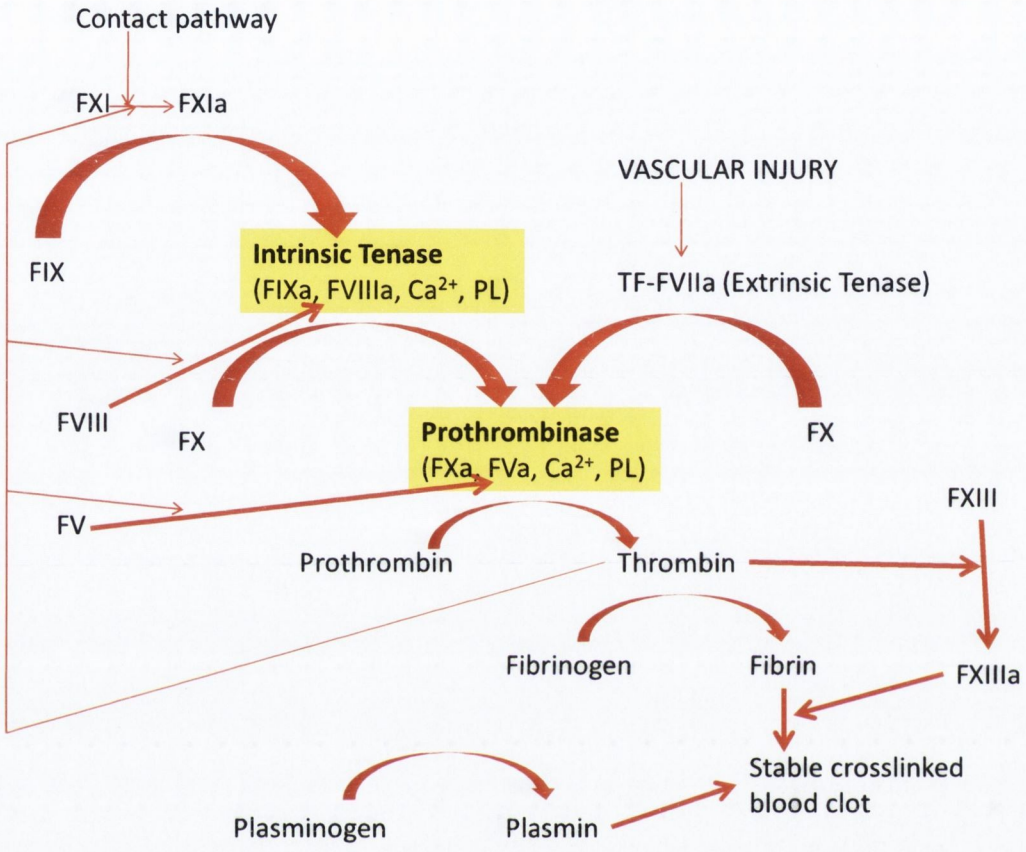


Figure 1.2: The coagulation cascade.

During blood coagulation, protease-cofactor complexes assemble on a negatively charged membrane surface. The extrinsic tenase complex (TF/FVIIa), the intrinsic tenase complex (FVIIIa/FIXa) and the prothrombinase complex (FVa/FXa) are the three major enzyme complexes which assemble during coagulation. All of these complexes require the presence of Ca^{2+} and phospholipid in order to function. The end result of blood coagulation is the formation of a fibrin clot.

TF binding to FVIIa induces a conformational change in the FVIIa serine protease domain which results in its activation [25]. The FVII(a) Gla domain **(1.1.4)** binds negatively charged phospholipids and enhances the association of FVII(a) with TF [26]. TF/FVIIa forms a ternary complex with zymogens FX or FIX and converts them to FXa and FIXa respectively [27].

The TF-mediated initiation phase of blood coagulation is regulated by TFPI [28]. TFPI is a 276 amino acid Kunitz-type serine protease inhibitor (43 kDa) consisting of three Kunitz domains, an acidic N-terminal region and a highly basic C-terminal region [29]. The active sites of TF-bound FVIIa and FXa are bound and inhibited by the first and second TFPI Kunitz domains respectively [30]. The third Kunitz domain is thought to be involved in cell-surface binding [31]. A model proposed for inhibition of TF-dependent coagulation by TFPI postulates that TFPI binds reversibly to FXa, followed by binding of TFPI/FXa to the TF/FVIIa complex [30] to form an inactive quaternary complex. An alternative model suggests that TFPI binds to FXa bound to the TF/FVIIa complex [32]. Recent studies indicate that protein S **(1.2.5)** enhances inhibition of the TF pathway by enhancing the interaction between TFPI and FXa [33].

While vascular injury leads to TF-initiated blood coagulation, an alternative process exists known as the "contact pathway". In this pathway, components entirely contained within the vasculature initiate blood coagulation, resulting in activation of FXI. High molecular weight kininogen, pre-kallikrein and FXII are responsible for FXI activation however their congenital deficiency is not associated with a bleeding phenotype. In contrast, FXI deficiency is associated with a variable bleeding tendency,

however the severity of bleeding correlates poorly with the baseline FXI level [34]. The result of this pathway is FXIa-mediated FIX activation, which activates FX.

Upon FX activation, FXa can activate prothrombin to generate the procoagulant enzyme thrombin, albeit inefficiently. Limited thrombin generation enhances coagulation by activating procoagulant cofactors FV and FVIII in a process of feedback amplification, generating FVa and FVIIIa respectively [35, 36]. This results in rapid amplification in thrombin generation due to generation of active cofactors for the prothrombinase and intrinsic tenase complexes respectively.

The prothrombinase complex consists of vitamin K-dependent serine protease FXa, active cofactor FVa, Ca^{2+} and phospholipid [37]. This complex proteolytically converts prothrombin to thrombin [38], and cleaves prothrombin 300,000 times more efficiently than FXa alone [39].

Activation of FVIII enables the formation of the intrinsic tenase complex, which consists of vitamin K-dependent serine protease FIXa and active cofactor FVIIIa, Ca^{2+} and phospholipid [40]. Binding of FIXa to its cofactor, FVIIIa, increases its ability to cleave FX 200,000-fold [41]. FVIII circulates in a complex with VWF, which stabilizes it in circulation [42]. During the amplification phase of coagulation the intrinsic tenase complex replaces the extrinsic tenase complex as principal activator of FX [43].

Thrombin cleaves fibrinopeptides from fibrinogen to generate fibrin, the main protein constituent of the final blood clot [44]. This causes fibrin to polymerize, forming an insoluble fibrous mesh which incorporates platelets and VWF [1]. This fibrin "clot" is

stabilized by FXIII. FXIII is a transglutaminase which is activated by thrombin, with fibrin polymer acting as a cofactor [44]. FXIIIa covalently cross-links fibrin at Gln and Lys residues [45]. This increases fibrin clot resistance to proteolytic degradation [44].

Once formed, the stable blood clot is broken down by a tightly regulated process known as fibrinolysis. Plasminogen, the principal zymogen in the fibrinolytic pathway (92 kD), is activated by proteolytic cleavage at Arg 560 to generate active serine protease plasmin [46, 47] which in turn degrades fibrin. The two major plasminogen activators are tissue plasminogen activator (tPA) and urokinase plasminogen activator (uPA) [47]. Serine protease inhibitors (serpins) plasminogen activator inhibitor-1 (PAI-1), PAI-2 and α_2-antiplasmin inhibit fibrinolysis. PAI-1 regulates both tPA and uPA and is the principal inhibitor of plasminogen activation [47]. Release of PAI-1 from platelets at the site of injury protects the developing thrombus from fibrinolysis [48]. In contrast, tPA, plasminogen and plasmin are bound to fibrin later during clot development [47].

1.1.4 Vitamin K-dependent proteins

Vitamin K-dependent proteins are characterized by a negatively charged domain (γ-carboxyglutamic acid or "Gla" domain) which mediates binding to phospholipid membranes, two epidermal growth factor (EGF)-like domains and a C-terminal serine protease domain [49]. This domain structure is shared by prothrombin (FII; which possesses two Kringle domains in place of two EGF-like domains), coagulation zymogens FVII, IX and X and anticoagulant protein C **(1.2)** [50]. Protein S **(1.2.4)** shares a similar structure, with the substitution of a serine protease domain for a sex hormone-binding globulin (SHBG) domain [51]. In addition, protein S possesses two further EGF-like domains and a thrombin-sensitive region. Protein Z is also structurally similar to zymogens FVII, IX X and to protein C, but contains a C-terminal pseudocatalytic domain rather than a serine protease domain [52, 53]. The pseudocatalytic domain contains lysine and aspartic acid residues in place of histidine and serine of the usual active site catalytic triad [54] and lacks proteolytic function. Protein Z is a cofactor to protein Z-dependent protease inhibitor, which plays a role in factor Xa inhibition [55]. Vitamin K-dependent proteins require γ-carboxylation of specific glutamic acid residues located in their Gla domain for optimal function. During γ-carboxylation, these glutamic acid residues are converted to γ-carboxyglutamic acid by the action of vitamin K [56, 57]. This process is dependent upon on the vitamin K epoxide reductase multiprotein complex (VKOR). This modification is critical in order for the Gla domain to be correctly folded (a process which is dependent upon interaction of negatively charged Gla residues with Ca^{2+}) and therefore for functional activity.

1.1.5 Coagulation regulation

Blood coagulation is tightly regulated by TFPI **(1.1.3)**, serine protease inhibitor (serpin) antithrombin (AT) and the protein C pathway **(1.2).** AT exerts its anticoagulant function by inhibition of thrombin, FIXa, FXa and FXIa [48]. AT inhibits its target proteases in two steps. In the first step, an encounter complex is formed, in which the target protease recognizes the sequence of the AT reactive site loop. Ser-195 of the protease attacks the peptide bond between the P1 and P1' residues, resulting in formation of a covalent bond between P1 and active site Ser 195. This is followed by protease conformational change and loss of enzymatic activity [48, 58].

Heparan sulphate and heparin molecules interact with AT and enhance its anticoagulant function [59]. Heparan sulphate is a negatively charged linear polysaccharide found on the surface of most cells. It is closely related to heparin, a synthetic glycosaminoglycan molecule used clinically as a parenteral anticoagulant. When heparan sulphate or heparin binds to specific AT lysine residues, AT undergoes a conformational change. This change alters the AT reactive centre, such that AT becomes a rapid serine protease inhibitor rather than a slow progressive one [60]. Covalent binding of this AT reactive centre to the active site of thrombin and other coagulation proteases irreversibly eliminates their procoagulant function. AT interacts with heparin via a specific unique heparin pentasaccharide sequence [61].

1.2: THE PROTEIN C ANTICOAGULANT AND CYTOPROTECTIVE PATHWAY

Protein C exists in a zymogen form which is activated to activated protein C (APC) by the complex of thrombin bound to thrombomodulin (TM). APC attenuates coagulation by proteolysis of the cofactors FVa and FVIIIa, which is dependent upon the presence of the anticoagulant cofactor protein S in plasma **(1.2.4)**. In addition, APC has recently been shown to possess signalling properties **(1.2.7)**, which mediate anti-inflammatory, anti-apoptotic and endothelial barrier protective effects.

1.2.1 Protein C gene and structure.

The human protein C (*PROC*) gene spans 11 kilobases of DNA [62] and consists of 8 exons and 7 introns. The protein C coding sequence consists of a light chain characterized by a 33 amino acid (AA) "signal peptide" and a nine amino acid "linking" propeptide (AA -42 to -1), a γ-carboxylation (Gla) domain (AA 1-45) and two epidermal growth factor (EGF)-like domains (AA 46-91 and 92-137). The heavy chain consists of an activation peptide region (AA 144-169) and a serine protease domain (AA 170-419), which contains the active site required for substrate proteolysis [63] **(Figure 1.3)**.

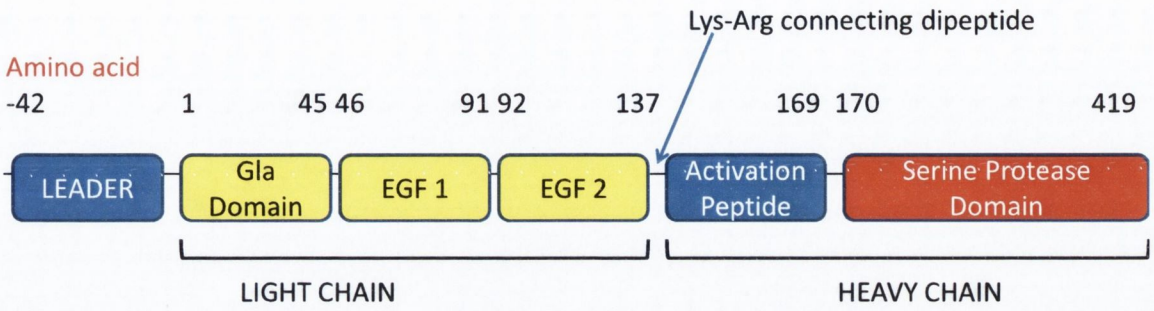


Figure 1.3: Amino acid sequence of the nascent protein C polypeptide

The nascent protein C polypeptide is composed of a leader sequence, a light chain (composed of a γ-carboxylation (Gla) domain and two EGF domains) and a heavy chain (composed of an activation peptide and the serine protease domain).

Protein C is synthesized as a single chain linked by a Lys-Arg dipeptide. The dipeptide is removed by proteolysis during protein C processing, which converts the single chain polypeptide to a light and heavy chain connected by a disulfide bond. Single-chain protein C and protein C heavy and light chains have molecular weights of 62 kD, 41 kDa and 21 kDa respectively [64].

Like prothrombin, FIX, FX and protein S, protein C biosynthesis involves the post-translational modification γ-carboxylation **(1.1.4)**. Protein C activation **(1.2.3)** is modulated by binding of the protein C Gla domain to the endothelial protein C receptor (EPCR) [65]. Protein C contains 9 γ-carboxyglutamic acid residues in its Gla domain.

It is thought that the two protein C EGF domains are involved in mediating protein-protein interactions, however their precise role remains unclear. EGF-1 possesses a Ca^{2+} binding site [66], suggesting that the region is of functional importance. The first protein C EGF-like domain contains a β-hydroxy aspartic acid at residue 71 [67]. The biological significance of this modification is not known.

The protein C serine protease domain contains two six stranded antiparallel β barrel domains [67]. At the junction of the barrels is a trypsin-like active site. Overall, the APC surface is "polarised", with a positively and negatively charged N- and C-terminal half respectively. A Ca^{2+} binding loop consisting of 10 residues (c70-80 of the chymotrypsin numbering system [68]) is similar to the trypsin Ca^{2+} binding loop and includes five acidic residues. A cluster of positively charged amino acids is present in a surface region similar to the positively charged anion binding exosite 1 of thrombin. Another

patch of eight basic residues is located in the lower right quadrant of the serine protease domain **(Figure 1.4)**. The APC serine protease domain possesses an active site consists of three amino acid residues: serine (c195), histidine (c57) and aspartate (c102). Moreover, the APC serine protease domain has several prominent surface loops, including the basic "60 loop" (c60-67) and "37 loop" (c37-39; **Figure 1.4**).

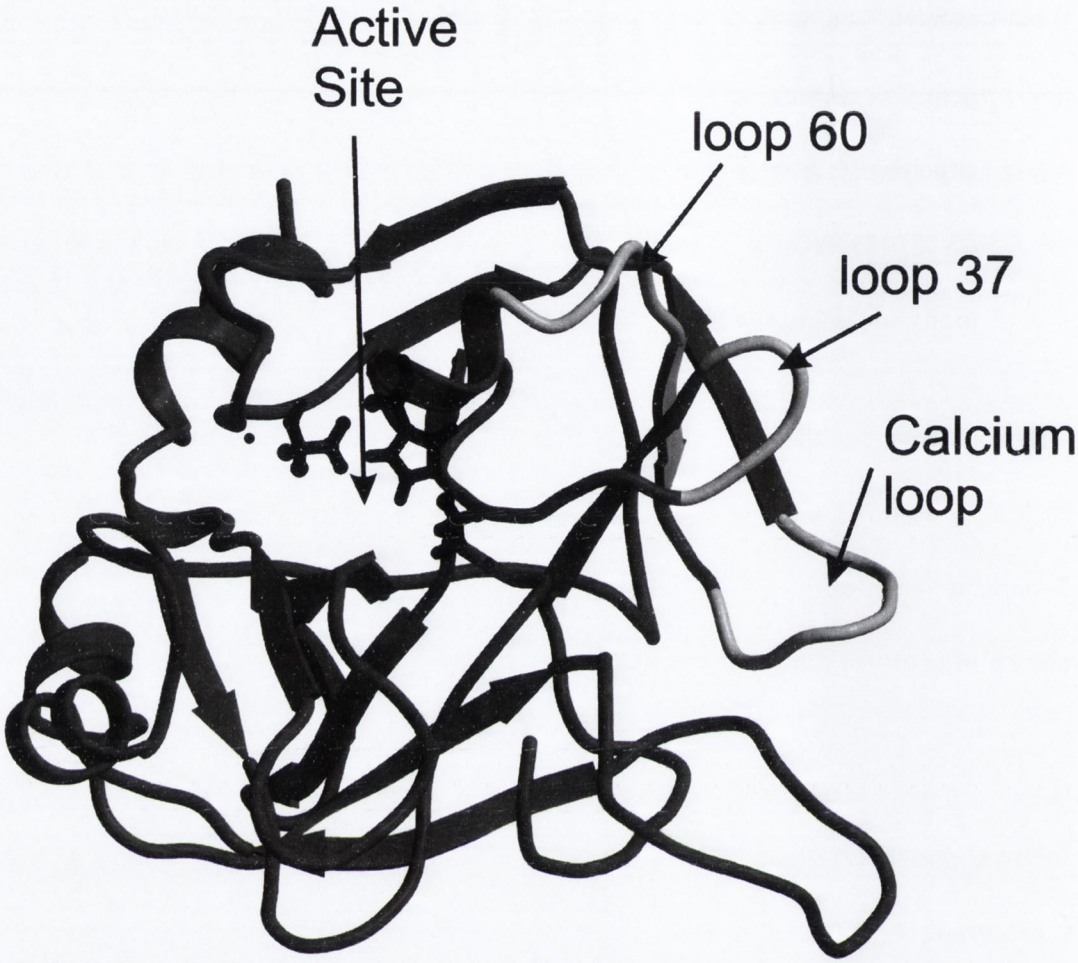


Figure 1.4: Functionally important surface loops in the protein C serine protease domain. Reproduced from Gale AJ *et al* [69]

The APC serine protease domain is shown. On it, the locations of the active site triad (black) and three functionally important structural and ligand-binding loops (grey) are indicated. These include the calcium-binding loop (c70-80; "calcium loop"), loop 37 (c37-39) and loop 60 (c60-67).

1.2.2 EPCR

EPCR is a type 1 transmembrane glycoprotein which binds protein C and enhances its activation **(1.2.3)**. In addition, EPCR-bound APC signals on the surface of endothelial and other cells via protease activated receptor 1 (PAR1; **1.2.7**) EPCR shares significant sequence homology with the major histocompatibility complex class 1 (MHC class 1) and CD1 families [70, 71]. The EPCR coding sequence consists of 1302 base pairs and encodes a mature protein of 223 amino acids [70]. EPCR is expressed on the surface of endothelium [72]. Its expression is mostly confined to the endothelium of large blood vessels, with very little expressed in the microvasculature [72]. EPCR consists of two extracellular domains, α1 and α2, a transmembrane domain and a short cytoplasmic tail [70, 73]. The extracellular domain has four sites of potential N-linked glycosylation [70]. The α1 and α2 domains of EPCR are structurally homologous with the same domains of the CD1 family [73, 74]. EPCR contains a groove which is filled with a phospholipid molecule [73]. Binding of the protein C Gla domain to EPCR requires Ca^{2+}, which exposes and stabilizes a hydrophobic "ω" loop formed by the N-terminal portion of the Gla domain [73]. Protein C "ω" loop residues Phe-4 and Leu-8 bind EPCR and are predicted to contribute the majority of the binding energy for this interaction **(Figure 1.5)** [73]. In addition, Gla residues 7,25 and 29 bind EPCR [73]. Leu-8 of the protein C "ω" loop makes close hydrophobic contacts with EPCR residue Leu-82. Phe-4 similarly interacts with EPCR residues Tyr-154 and Tyr 157 [73]. In addition, EPCR Gln-150, Tyr-154 and Leu-82 form hydrogen bonds with protein C Gla-7, while EPCR Arg-87 forms a hydrogen bond with Gla-25 [73]. EPCR Glu-86 co-ordinates one of the Ca^{2+} ions bound to the protein C Gla domain. This represents the only contact made

between Gla-bound Ca^{2+} ions and EPCR [73]. Glu-86 is also within hydrogen binding distance of protein C Gla-7, Gla-25 and Gla-29 [73]. Similarly to CD1 family proteins, EPCR may be able to translocate from the plasma membrane to the nucleus [75, 76].

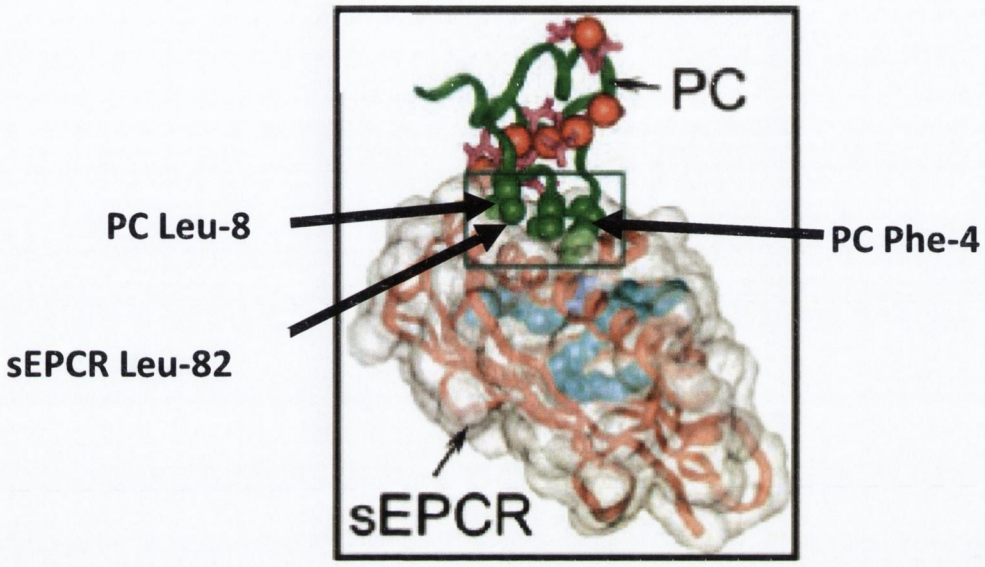


Figure 1.5: Interaction of the protein C "ω" loop with EPCR

Residues Phe-4 and Leu-8 of the protein C "ω" loop and protein C Gla residues 7, 25 and 29 make contact with residues in soluble EPCR (sEPCR). Leu-8 of the protein C "ω" loop makes close hydrophobic contacts with EPCR residue Leu-82. Reproduced from Preston *et al*, JBC 2006; 281:28850-57 [77].

1.2.3 Protein C activation

Inactive zymogen protein C is activated by proteolytic cleavage to generate activated protein C (APC). Activation is mediated by thrombin bound to the cell surface glycoprotein thrombomodulin (TM) [78]. During activation, thrombin cleaves the Arg-Leu bond (situated at residue 169 in the N-terminal region of the heavy chain), resulting in generation of a new heavy chain N-terminus and release of an activation dodecapeptide [64].

TM is expressed in the vascular endothelium, and consists of a C-type lectin-like domain, six EGF-like domains, a serine/threonine-rich region, a transmembrane section and a short cytoplasmic tail. Thrombin binds to EGF 5 and 6, while protein C binds to EGF 4 during activation [79]. Binding interactions between loops 37, 60 and 70 of the protein C serine protease domain with thrombin-TM facilitate optimal activation [80, 81]. TM binding effectively switches the function of thrombin from procoagulant to anticoagulant. TM binding causes thrombin to lose its procoagulant properties, because exosite I (which is required for substrate binding) becomes occupied by TM domains [82].

Protein C activation by the thrombin-TM complex is modulated by EPCR binding [65]. EPCR monoclonal antibodies directed at the Protein C binding site inhibit its activation ~5-fold by reduction of the K_m for protein C activation. EPCR also plays a major role in protein C activation *in vivo* [83]. Baboons infused with thrombin exhibit an 88% reduction in APC generation in the presence of an antibody which blocks protein C-EPCR interaction.

1.2.4 APC anticoagulant function

APC mediates its anticoagulant function by cleaving and inactivating cofactors FVa [84] and FVIIIa [85]. Both FV and FVIII share a similar domain structure. There are three APC cleavage sites in FVa, at positions Arg 306, Arg 506 and Arg 679 [82]. Arg 506 cleavage is favoured kinetically to Arg 306 cleavage and results in partial loss of FVa cofactor activity [86].

APC inactivation of FVa in plasma is dependent upon protein S [82]. Protein S is a vitamin K-dependent glycoprotein comprised of an N-terminal Gla domain, a thrombin-sensitive region, four EGF-like domains and two laminin G-type domains [82]. It binds negatively charged phospholipids with high affinity and forms a membrane-bound complex with APC. By binding to APC, protein S is postulated to position APC for optimal FVa and FVIIIa proteolysis. Protein S strongly stimulates APC-mediated cleavage of FVa at Arg-306, and to a lesser extent, at Arg-506. Protein S-stimulated inactivation of FVa at Arg 306 is phospholipid-dependent. Upon APC cleavage of FVa at Arg 306, the FVa A2 domain dissociates, resulting in complete loss of FVa procoagulant activity [87].

In addition to inactivation by spontaneous dissociation of its subunits, FVIIIa can also be inactivated by APC. FVIIIa inactivation by APC involves proteolysis at Arg 336 and Arg 562 [88]. Both protein S and procofactor FV act as cofactors to APC in inactivation of FVIIIa [89].

1.2.5 APC inhibition

The half life of APC in plasma is ~30 minutes [90]. The proteolytic function of APC inhibited by protein C inhibitor (PCI), PAI-1 [91], α-1-antitrypsin [92], α-2 macroglobulin and α-2 antiplasmin [93]. APC inhibition by PCI is slow compared with other serpin-protease pairs [94] and is enhanced ~400-fold by heparin [95]. Basic residues of APC loop 37 are involved in modulating PCI-mediated APC inhibition [96]. In contrast, heparin does not stimulate APC inhibition by α-1-antitrypsin [96]. PAI-1-mediated inhibition of APC proteolytic activity is enhanced ~300-fold by vitronectin, increasing the second order rate constant for inhibition from ~$6x10^2$ $m^{-1}s^{-1}$ to $2x10^5$ $m^{-1}s^{-1}$ [91]. This rate constant is similar to that reported for heparin-stimulated APC inhibition by PCI, raising the possibility that PAI-1 may be at least equal in importance to PCI in relative contribution to APC inhibition in plasma. The same authors postulated that, like PCI, PAI-1 interacts with APC loop 37, because reactivity of a protein C mutant in which three basic residues (Lys-37, Lys-38, Lys-39) were substituted with Pro, Gln and Glu respectively was markedly impaired compared with wild type APC [91].

1.2.6 Protein C glycosylation

Many cells and proteins possess covalently-linked sugar chains (called oligosaccharides or "glycans") which comprise a significant portion of their molecular weight [97, 98]. These glycan moieties modulate diverse biological roles, including cell-cell and cell-matrix interactions, protein secretion and function [98-100]. Glycans are composed of monosaccharide units linked together [97]. Commonly encountered units include sialic acid, hexoses (including glucose (Glc), galactose (Gal) and mannose (Man), hexosamines, deoxyhexoses (eg fucose (Fuc)), pentoses and uronic acid [98].

Glycans on eukaryotic cells and proteins are classified according to the nature of the attachment site of the sugar. N-linked oligosaccharides are typically covalently linked to an asparagine residue of a polypeptide chain within the consensus sequence Asn-X-Ser/Thr, while O-linked glycans are typically linked to a Ser/Thr residue [97, 98]. N-linked glycan biosynthesis **(Figure 1.6)** begins with a lipid-linked oligosaccharide precursor which is transferred to proteins emerging from the endoplasmic reticulum by the enzyme oligosaccharyltransferase (OST) [98]. This precursor then undergoes a series of modifications catalyzed by glycosidase enzymes, to generate three N-linked glycan subtypes: high-mannose, hybrid and complex. Most secreted and cell surface N-linked glycans (including those on protein C) are of the complex subtype and therefore are highly branched space-occupying structures, typically capped with negatively charged sialic acid residues [98].

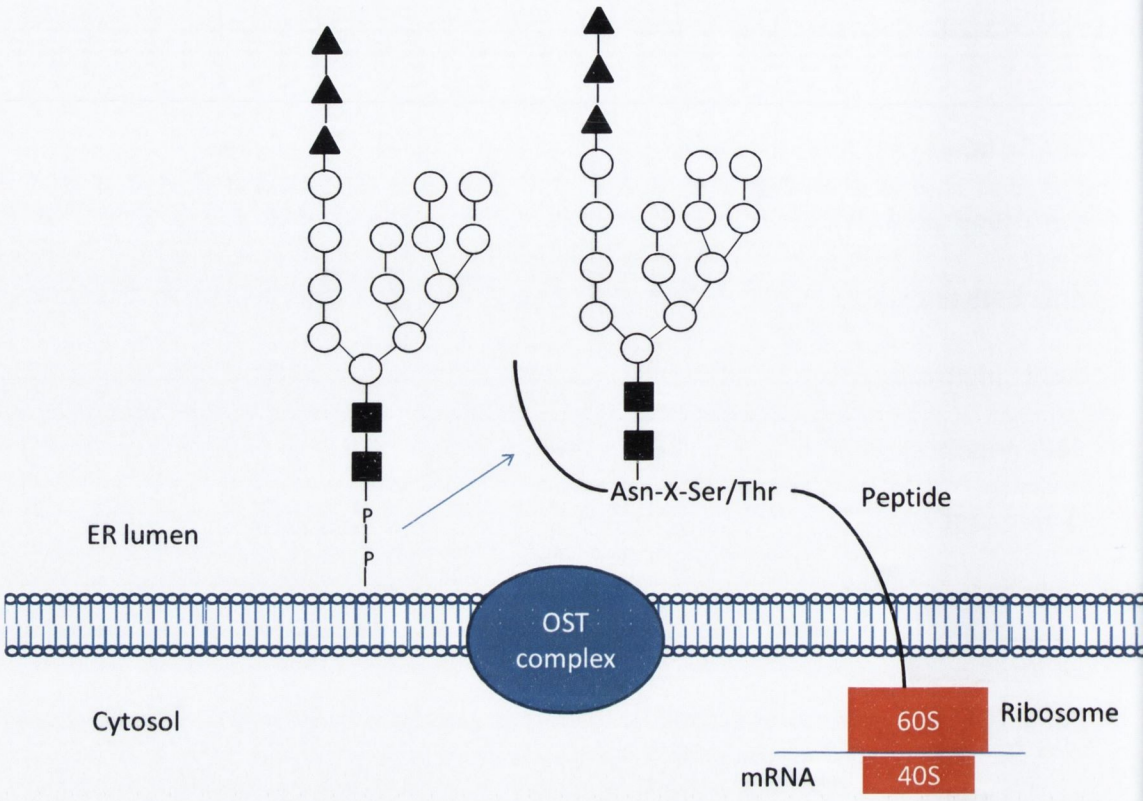


Figure 1.6: Initiation of N-linked glycan biosynthesis

Nascently translated eukaryotic proteins emerging from ribosomes are transferred from the cytosolic compartment into the lumen of the endoplasmic reticulum (ER). Upon entry to the ER, a multisubunit enzyme complex, oligosaccharyltransferase (OST), catalyses transfer of a lipid-linked oligosaccharide precursor to an asparagine (Asn) residue within the typical consensus sequence Asn-X-Ser/Thr of the nascent polypeptide. This oligosaccharide precursor then undergoes a series of processing reactions catalysed by glycosidase enzymes (not shown) to generate mature N-linked glycans. (■, N-acetylglucosamine; ○, Mannose; ▲,Glucose).

The molecular weight of protein C is approximately 23% carbohydrate. [64]. Protein C possesses four sites of N-linked glycosylation, at positions Asn 97, Asn 248, Asn 313 and Asn 329, and no sites of O-linked glycosylation. Asn 97 is located in EGF-1 of the light chain, and the remaining three glycan attachment sites are in the serine protease domain. The glycosylation site at Asn 329 is associated with the unusual consensus sequence Asn-X-Cys rather than Asn-X-Ser/Thr [101]. Protein C exists as the three glycoforms α,β and γ [101]. β protein C was initially thought to represent a proteolytic degradation product of the protein C heavy chain. However it was subsequently confirmed that β protein C is a glycosylation variant of protein C, lacking glycosylation at Asn 329 [102].

Grinnell *et al* generated recombinant protein C mutants lacking individual glycan chains to assess their role in protein C synthesis, secretion and anticoagulant function [101]. The glycosylation site at Asn 248 was shown to regulate intracellular removal of the Lys-Arg dipeptide, as elimination of this glycosylation site resulted in a 3-4 fold increase in the amount of single chain protein C secreted. Removal of the glycosylation site at Asn 329 eliminated expression of the α-protein C glycoform, removal of Asn 97 virtually eliminated total protein C secretion. Absence of glycosylation at Asn 313 resulted in a 3-fold increase in activation by the TM/thrombin complex. Following activation, removal of any heavy chain glycosylation site was shown to increase amidolytic and anticoagulant activity approximately 1.5-fold and 2-2.5 fold respectively. The increases in amidolytic activity of the APC variants lacking Asn 313 and Asn 248 were found to be due to increased K_{cat} while that of the variant

lacking Asn 329 was due to a higher substrate affinity (decreased K_m). No difference in inhibition of APC in plasma was observed for any variant.

McClure *et al* examined protein C glycosylation in the endoplasmic reticulum and Golgi in order to determine in which compartment the rate-limiting step in protein C secretion occurred [103]. HEK 293 cells expressing protein C were treated with enzymes which inhibit successive protein C glycosylation steps in the endoplasmic reticulum. Cells treated with these enzymes exhibited up to 90% reduced protein C secretion, in keeping with the previous work of Grinnell *et al* [101]. In contrast, treatment with enzymes which block glycosylation processing in the Golgi had no effect upon protein C secretion. This implies that glycosylation in the endoplasmic reticulum is a rate-limiting step in protein C secretion. The rate-limiting step was found to occur following transfer of the oligosaccharide core and following γ-carboxylation, but prior to complete carbohydrate processing. Moreover, glycosylation and γ-carboxylation were shown not to be coupled. Inhibition of either did not affect the progress of the other.

A naturally-occurring protein C glycosylation mutation has been described [104] in monochorionic monozygotic twins, one of whom experienced an ileofemoral deep vein thrombosis at the age of 22. Both sisters were compound heterozygous for two protein C mutations. The first, an Asn 329→Thr substitution (protein C N329T), resulted in the absence of plasma α-protein C due to lack of the glycosylation site at Asn 329. Consequently only β-protein C was detectable in each individual's plasma. The second mutation, a Cys 78→Stop substitution, resulted in reduced plasma protein C levels to ~30% of normal. Interestingly, in contrast with the findings of Grinnell *et al*,

the *in vitro* anticoagulant function of plasma immunopurified protein C N329T was impaired compared with plasma wild type protein C, both in plasma and in a purified assay measuring FVa inactivation by the variant APC.

1.2.7 Protective signalling properties of APC

APC administration reduces sepsis-induced death [105, 106] while protein C administration prevents microvascular coagulation in meningococcal sepsis *in vivo* [107, 108]. In addition to its ability to proteolyse FVa /FVIIIa [84, 85], APC has recently been shown to mediate 'cytoprotective' intracellular signalling on multiple cell types. These cytoprotective properties are postulated to mediate the observed survival benefit associated with APC [106] and include anti-inflammatory, anti-apoptotic and endothelial barrier stabilizing functions **(1.2.8.2-4).**

1.2.7.1 Mechanism of APC protective signalling

APC cytoprotective signalling on endothelial cells is mediated primarily by binding of the APC Gla domain to EPCR followed by cleavage of protease activated receptor 1 (PAR1) by the APC active site [109-112]. Alternative mechanisms for APC signalling on different cell types have also been proposed which are EPCR-independent and PAR1-dependent [113] and EPCR and PAR1-independent [114]. These alternative APC signalling pathways have been characterised extensively both *in vitro* **(1.2.7.2)** and *in vivo* **(1.2.8).**

PAR1 is a G-coupled protein heptahelical membrane-associated protein which was initially characterized as a thrombin receptor [115]. Thrombin activates PAR1 by cleavage of the N-terminal PAR1 exodomain between Arg-41 and Ser-42 [115]. This cleavage exposes a new N-terminus, which binds to PAR1 and initiates

transmembrane signalling [115]. During intracellular signalling, PAR1 interacts with members of the $G_{12/13}$, G_q and G_i families of G proteins [116-118]. EPCR-bound APC is also capable of cleaving PAR1 [109] to mediate intracellular signalling **(Figure 1.7)**. EPCR participates in this pathway by coupling PAR1 to G_i [119]. A postulated PAR1-binding APC exosite has recently been identified [120]. In this study two acidic residues (Glu 167 and Glu 170) were identified in the APC serine protease domain which were not conserved in other vitamin K-dependent proteins [67]. Each of these residues was substituted with Ala and two separate APC mutants (E167A and E170A) expressed. While each mutant exhibited similar ability to mediate FVa proteolysis as wild-type APC, they failed to mediate PAR1 cleavage-dependent endothelial barrier-protective, anti-apoptotic and anti-inflammatory functions. Each mutant bound normally to soluble EPCR but failed to cleave an alkaline phosphatase (AP)-PAR1 reporter construct transfected into EA.hy926 cells.

The receptors required for both protein C activation and APC cytoprotective signalling are co-localized in specific endothelial cell domains known as "lipid rafts" [121]. Receptor co-localization is required for APC to signal on endothelial cells [121] and may be essential for *in vivo* PAR1 activation by EPCR-APC.

1.2.7.2 APC anti-inflammatory properties

APC downregulates expression of monocyte proinflammatory cytokines TNF-α [122-124] and interleukins (ILs) 1β, 6 and 8 [124], upregulates expression of monocyte anti-inflammatory cytokine IL-10 [125], inhibits monocyte apoptosis [124] and inhibits expression of leucocyte adhesion molecules in endothelial cells [126].

Exogenous APC administration suppresses secretion of the cytokine TNF-α in rats with lipopolysaccharide (LPS)-induced endotoxaemia [127]. On this basis, it was speculated that APC might modulate monocyte cytokine expression. APC was subsequently shown to inhibit LPS-stimulated TNF-α production by human blood monocytes and cells of the THP-1 monocytic cell line in a concentration-dependent manner [122]. Of note, relatively high APC concentrations (1μg/ml) were required for suppression of TNF-α to be observed. This effect was dependent upon a functional APC active site and was not observed with zymogen protein C. Subsequently Shu *et al* [128] demonstrated saturable binding of fluorescently-labelled APC to a U937 monoblastic cell line. APC binding was inhibited by ~90% in the presence of the mAb RCR-252, which interacts with an EPCR epitope required for protein C binding. Monocyte TF expression can be induced by phorbol 12-myristate 13-acetate (PMA) [129]. Shu *et al* demonstrated a dose- and time- dependent inhibition of TF expression on PMA-stimulated U937 cells upon APC treatment [128]. APC modulation of TF expression was inhibited by RCR-252, demonstrating that APC-EPCR binding is critical in this process.

Using THP-1 cells, White *et al* [123] demonstrated APC-mediated attenuation of LPS-induced translocation of nuclear factor kappa B (NFκB) to the nucleus. Subsequently Joyce *et al* [126] showed that APC modulates the expression of 13 TNF-α-modulated genes in endothelial cells [130]. The profile of these genes was consistent with induction of an anti-inflammatory and anti-apoptotic phenotype. Intercellular adhesion molecule-1 (ICAM-1), E-selectin, vascular cell adhesion molecule-1 (VCAM-1) and the NFκB2 subunit were downregulated, while Bcl-2 and inhibitor of apoptosis (IAP) were upregulated. Moreover, APC was demonstrated to suppress TNF-induced ICAM-1 and VCAM-1 protein expression on endothelial cells in a concentration-dependent manner.

Stephenson *et al* [124] investigated the role of APC in monocyte apoptosis, phagocytosis and cytokine secretion. At high concentrations (60nM), APC was found to inhibit camphothecin-mediated THP-1 cell apoptosis in an EPCR and PAR1-dependent manner. APC also attenuated spontaneous apoptosis of primary human monocytes. Moreover, APC significantly inhibited LPS-stimulated monocyte secretion of interleukin (IL)-1β, IL-6 and IL-8 and to a lesser extent, TNF-α. The same group subsequently showed that APC increases monocyte secretion of proinflammatory cytokine IL-10 [125] in an EPCR and PAR1-dependent manner.

The above studies indicate that the anti-inflammatory effects of APC in various cell types are mediated by EPCR [122, 125, 131] +/- PAR1 [124, 125] dependent signalling, however evidence is emerging that alternative pathways may also be involved. APC-mediated inhibition of TNF signalling may be EPCR-independent [132], while APC-

mediated inhibition of T helper (T_h)- 2 cell cytokine expression in mice was found to be PAR-1 independent [133].

Elphick *et al* [134] noted that the APC catalytic domain possesses an RGD sequence and speculated that it might mediate integrin binding. The authors showed that APC blocks neutrophil adhesion and migration in dishes coated with fibronectin. Blocking monoclonal antibodies against β_1 or β_3 integrins inhibited APC binding to neutrophils in suspension, as did an RGD peptide, suggesting that APC binds to neutrophils through interaction with integrins. In further support of this hypothesis, an APC variant in which the RGD sequence was mutated to RGE (APC-*RGE*) failed to influence neutrophil migration, while the recombinant APC variant S360A, which lacks proteolytic activity [135] inhibited neutrophil migration. The interaction of APC with neutrophils was shown to be EPCR independent, because Gla-domainless APC inhibited neutrophil adhesion and migration almost identically to wild-type APC. Moreover, wild-type APC but not APC-*RGE* inhibited LPS-induced neutrophil recruitment in mouse broncho-alveolar fluid *in vivo*.

The integrin CD11b plays a role in APC-mediated anti-inflammatory signalling in bone marrow derived macrophages [114]. This effect is EPCR-independent but PAR-1 dependent. Moreover, a critical role for the apolipoprotein E receptor 2 (ApoER2) in EPCR/PAR1-independent anti-inflammatory APC signalling has been identified in a monocytic cell line (U937) [113]. In this study, APC bound to soluble ApoER2 (sApoER2) with significantly higher affinity than EPCR (apparent K_d ~30nM, compared with 195nM for sEPCR). ApoER2-dependent APC-mediated anti-inflammatory effects were found to proceed via phosphoinositide 3-kinase (PI3K)/Akt signalling, a pathway

which is well-established to suppress inflammation in endotoxaemic mice [136]. Moreover, very recent published data suggest that APC may inhibit histone-mediated responses to inflammatory challenge by mediating proteolytic histone degradation [137]. In this study, mouse histones were found to be toxic to endothelial cells *in vitro*. This toxicity was reversed by APC. Moreover, mice treated with lethal doses of histones were rescued by APC. Histones were increased in the plasma of baboons treated with lethal doses of E.*coli,* while cleaved histone protein was detected in the plasma of E.*coli*-treated baboons which also received APC. These results suggest that APC-mediated histone proteolysis may represent a novel APC anti-inflammatory mechanism.

1.2.7.3 APC anti-apoptotic properties

Apoptosis, or programmed cell death, can proceed by two separate pathways. The intrinsic pathway of apoptosis is triggered by signals from inside the cell. Cytochrome *c* is released from mitochondria and procaspase-3 is activated. The extrinsic apoptosis pathway is initiated by binding of extracellular mediators to membrane bound receptors. This pathway involves initiator caspase activation but also culminates in activation of procaspase-3.

Joyce *et al* demonstrated by gene expression profiling that APC treatment of HUVECs upregulates antiapoptotic genes Bcl-2 and IAP and downregulates propapoptotic genes calreticulin and testosterone repressed prostatic message-2 (TRMP-2) [126]. In addition, staurosporine-induced apoptosis was inhibited by APC in HUVECs and EA.hy926 cells. APC inhibits p53 expression in hypoxic brain endothelial cells in an EPCR and PAR1-dependent manner, downregulates levels of the pro-apoptotic factor Bax, upregulates levels of the anti-apoptotic factor Bcl-2 and inhibits capase-3 activation [110]. APC has also been shown to protect mouse neurons against apoptosis induced by N-Methyl-D aspartate (NMDA) by inhibiting caspase-3 activation, apoptosis-inducing factor (AIF) translocation to the nucleus and p53 expression [138]. The same authors also showed that APC also inhibits staurosporine-induced apoptosis in mouse neurons by inhibition of caspase-8 (and consequently also caspase-3) activation. Both effects were shown to be dependent upon cleavage of PAR1 and PAR3. Moreover, APC inhibition of staurosporine-induced apoptosis in EA.hy926 cells also proceeds in an EPCR and PAR1-dependent manner which is dependent upon a functional active site [111].

While most data indicates that EPCR binding is a prerequisite for APC-mediated inhibition of apoptosis, there are some exceptions. APC has been shown to inhibit staurosporine-induced apoptosis in human embryonic kidney 293 (HEK 293) cells, which do not express EPCR [126]. APC has also been shown to inhibit TNF-related apoptosis-inducing ligand (TRAIL) expression in HUVECS by stimulating extracellular signal-regulated kinase (ERK) 1/2 phosphorylation in a PAR1-dependent, EPCR-independent manner [132].

1.2.7.4 APC endothelial barrier protective properties.

Increased vascular permeability is one of the hallmarks of sepsis. APC protects the endothelial barrier against thrombin-induced permeability by active site-mediated PAR1 cleavage [112]. PAR1-mediated endothelial barrier protection requires that APC is bound to EPCR and results in sphingosine kinase upregulation and activation, which leads to generation of the bioactive lipid sphingosine-1 phosphate (S1P) [112, 139] and consequent cross-activation of the S1P receptor 1 (S1P1). This activates GTPase Rac-1, leading to cytoskeletal rearrangement and reduced permeability of the endothelial barrier [139] **(Figure 1.7)**. An alternative hypothesis holds that APC-mediated endothelial barrier protection via S1P1 may be PAR1-independent [139]. Finigan *et al* measured APC-induced S1P1 activation in the presence of an EPCR-inhibitory antibody (RCR-252). RCR-252 ablated S1P1 phosphorylation. In contrast, a PAR1-inhibitory antibody failed to significantly reduce APC-induced S1P1 transactivation.

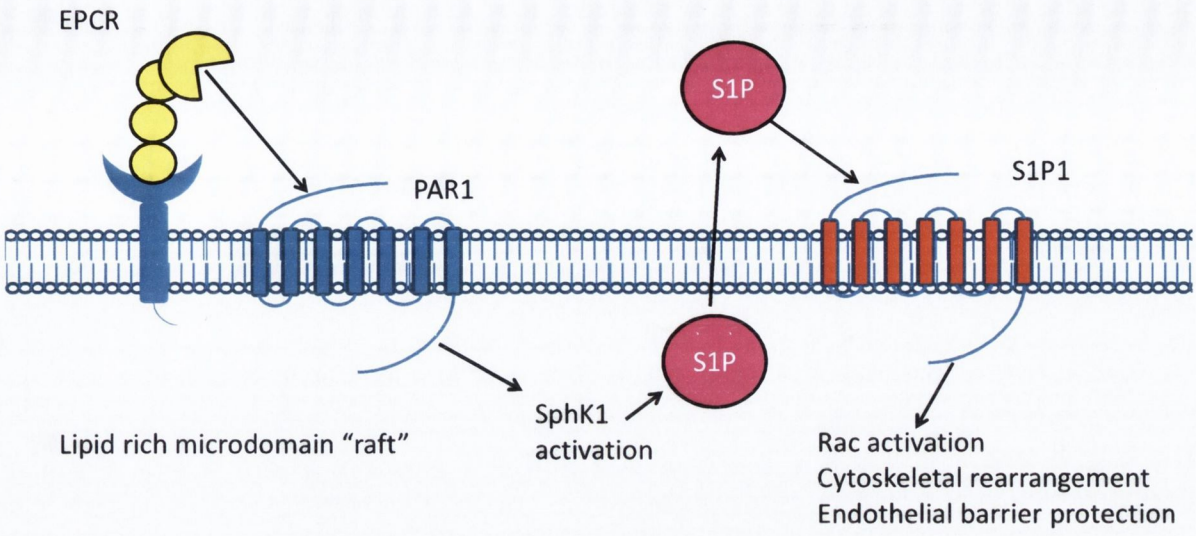


Figure 1.7: Proposed mechanism of APC-mediated endothelial barrier protection

APC bound to EPCR within caveolin-rich lipid rafts binds to, cleaves and activates PAR1. PAR1 activation stimulates sphingosine kinase-1 (SphK1) to generate sphingosine-1-phosphate (S1P) from sphingosine. S1P then activates the sphingosine-1-phosphate receptor 1 (S1P1), which promotes endothelial barrier protection.

Interestingly, occupancy of EPCR by the Gla domain of zymogen protein C or APC results in a switch in thrombin-mediated PAR1 signalling from "barrier disruptive" to "barrier protective" [119], which may help to explain how APC can mediate protective signalling when thrombin is present. Bae *et al* generated a chimaeric prothrombin in which the Gla domain was substituted by that of protein C. Upon activation, the chimaeric zymogen was converted to the PC-Gla/meizothrombin active variant. In contrast to thrombin (which mediated a barrier-disruptive effect on endothelial cells at >50pM), PC-Gla/meizothrombin mediated endothelial barrier protection from ~0.5nM in an EPCR- and PAR 1-dependent manner. Similarly, thrombin exerted a barrier-protective function when co-incubated with the protein C mutant S195A, which lacks a functional active site due to replacement of a member of the active site amino acid triad with Ala. A similar effect was observed in an assay of endothelial cell apoptosis. Collectively, these results suggest that when EPCR is occupied by its natural ligand, cleavage of PAR1 mediates barrier-protective signalling. Based on the results of immunoprecipitation experiments, the authors postulated that EPCR ligation causes it to dissociate from caveolin-1 in lipid rafts and migrate out of the caveolar compartment. This would in turn facilitate PAR1 coupling to G_i protein rather than G_q and/or $G_{12/13}$ and therefore confer barrier-protective, rather than barrier-disruptive responses.

1.2.8 *In vivo* cytoprotective effects mediated by APC.

1.2.8.1 Sepsis

Sepsis is the leading cause of mortality in non-coronary intensive care units, resulting in 40,000-60,000 deaths per year in the United Kingdom alone, and killing 200,000 of the 700,000 patients who develop sepsis in the United States annually [140]. The incidence of sepsis is rising [141], which translates into a massive financial burden, amounting to $17 billion dollars annually in the United States [140] and up to €7 billion annually in Europe. The cost associated with treatment of children with severe sepsis is approximately $2 billion annually in the United States [142].

The molecular basis of the therapeutic efficacy of APC in severe sepsis has been investigated by several groups in wild-type and transgenic mice. In order to address the molecular mechanism underlying APC's protective effect *in vivo,* Kerschen *et al* [143] investigated endotoxaemia mortality reduction in response to APC. Wild type mice were treated with a 20 minute intravenous APC infusion, followed by intraperitoneal lipopolysaccharide (LPS). APC significantly reduced 7-day mortality in response to lethal doses of LPS. The APC active site was shown to be critical for this protective effect, as a non-proteolytic APC variant, APC-*S360A*, did not protect against LPS-induced lethality. In this study, APC demonstrated direct *in vivo* anti-apoptotic and vascular barrier protective function. PAR-1 and EPCR were shown to be critical in mediating APC protection against sepsis-induced lethality, as LPS-induced mortality was not significantly reduced in PAR1- and EPCR- deficient transgenic mice treated with wild-type APC.

In an effort to improve APC therapy in severe sepsis, APC variants have been generated with attenuated anticoagulant function (and consequently reduced potential to cause bleeding side effects). Mosnier *et al* synthesized an APC variant with impaired ability to bind FVa due to mutations in positively charged surface loops which participate in APC-FVa interactions [144]. Five Ala substitutions were made in APC Loop 37 and in the Ca^{2+} binding loop (RR229/230AA and KKK191-193AA). This variant possessed normal EPCR/PAR1-dependent cytoprotective function but severely (>95%) attenuated anticoagulant activity. Moreover, a murine version of this non-anticoagulant APC variant reduced mortality similarly to wild type APC in LPS-treated mice [143].

However, despite recent advances, the molecular determinants which mediate the *in vivo* protective effect of APC remain poorly understood. The observation of Kerschen *et al* that APC administration to EPCR-deficient mice fails to prevent mortality in response to endotoxaemia [143] suggests a key role for EPCR in APC protective signalling *in vivo*. In apparent contrast, however, Cao *et al* [114] demonstrated that Gla-domainless APC, which lacks the ability to bind EPCR, protects against endotoxaemia mortality (albeit less effectively than wild type APC), suggesting that EPCR is not necessary in order for APC to mediate a large proportion of its protective effect. The alternative model proposed by the authors was that APC anti-inflammatory signalling in endotoxaemia is mediated by the integrin CD11b/CD18.

A recent study utilized EPCR/PAR1 bone marrow chimaeric mice in order to further address the molecular determinants of APC protective signalling [145]. Mice were generated which had selective EPCR or PAR1 deficiency affecting vascular or bone

marrow derived immune cells only. Expression of both EPCR and PAR1 on immune cells was found to be critical in order for exogenously administered non-anticoagulant APC to mediate a mortality reduction in response to endotoxaemia. Interestingly, APC reduced mortality in mice with PAR1 deficiency restricted to vascular cells, although the mortality reduction was less than that observed in wild type mice, suggesting that the contribution of PAR1-mediated APC signalling on vascular endothelium to mortality reduction in mice is minor compared with PAR1-mediated signalling on immune cells. Moreover, a specific subset of EPCR-expressing $CD8^+$ splenic dendritic cells were found to mediate PAR1-dependent APC signalling on immune cells. Interestingly, gene expression profiling experiments revealed that some APC-mediated anti-inflammatory effects on dendritic cells may be independent of EPCR and PAR-1. However, the relevance of these results to human sepsis is uncertain, as human EPCR expression has been demonstrated on a variety of immune cells including neutrophils, monocytes, macrophages, eosinophils and natural killer (NK) cells. This is in marked contrast to the restricted EPCR expression on murine immune cells.

The relative contributions of APC signalling on bone marrow derived cells and endothelial barrier protection to its therapeutic role remain unclear. Both of these functions have been demonstrated to play a role in APC cytoprotection *in vivo.* For example, APC-mediated signalling on bone marrow-derived immune cells plays a critical role in protection against sepsis-induced mortality [145], while APC protects from endotoxaemia- induced pulmonary oedema *in vivo* in a PAR1-dependent manner [146]. This demonstrates that EPCR/PAR1-dependent endothelial barrier stabilization

is not only an *in vitro* phenomenon, but is also a key mediator of the protective function of exogenous APC administration in *in vivo* sepsis.

The early observation that APC protected against sepsis-induced death in a primate model [105], along with emerging *in vitro* data suggesting a protective signalling role, led investigators to explore its efficacy in human sepsis **(Table 1.1)**. A phase 3 randomized double-blind multicentre clinical trial of APC in severe sepsis (PROWESS) was conducted in 2001 [106]. In this trial, recombinant human APC (Drotrecogin alfa (activated); DAA) administration was compared with placebo in patients with at least one sepsis-induced organ dysfunction of less than 24 hours duration. DAA was infused at a dose of 24μg/kg/hour for 96 hours in total. A statistically significant difference in 28-day all-cause mortality was observed in patients on treatment versus placebo, with a relative reduction in the risk of death of 19.4% in patients treated with DAA. However, an increased rate of severe bleeding occurred in the DAA-treated group compared with placebo.

On the basis of the PROWESS trial results, DAA was approved by regulatory agencies in November 2001 for use in patients with severe sepsis and a high risk of death, as the risk-benefit profile was most desirable in this subgroup. Interestingly, a randomized trial (ADDRESS) evaluating the use of DAA in patients with a low risk of death demonstrated no difference in 28-day mortality in patients treated with DAA compared with placebo [147]. Again, however, a significant increase in bleeding was observed. Subsequently, a further randomized trial (ENHANCE) demonstrated that earlier commencement of DAA administration enhanced mortality reduction [148].

More recently, the effect of extending DAA treatment beyond the standard 96-hour treatment period was evaluated and found not to influence either vasopressor-dependent hypotension or 28-day mortality [149].

To assess the clinical efficacy of recombinant APC in paediatric sepsis, children with sepsis-induced cardiovascular and respiratory failure were randomly assigned to receive either DAA or placebo in the RESOLVE clinical trial [150]. Because mortality from sepsis is very low in children, the primary endpoint used was a reduction in Composite Time to Complete Organ Failure Resolution (CTCOFR). In contrast to the PROWESS trial [106], no significant difference was observed in either CTCOFR score, 28-day mortality or serious bleeding events. Of note, baseline protein C levels were lower in both groups than were reported in the adult PROWESS trial [106], leading the authors to speculate that higher dosing might be required to observe an improvement in clinical efficacy.

Trial	Study type	Patient population	CTCOFR score	28-day mortality	Severe bleeding during infusion	Severe bleeding during 28 day follow-up.	Other comments
PROWESS [106]	Randomized double-blind placebo-controlled trial	Adults: Severe sepsis	N/A	Treatment 24.7%; placebo 30.8%; p=0.005	Treatment 3.5%; placebo 2.0%; p=0.06	N/A	
ADDRESS [147]	Randomized double-blind placebo-controlled trial	Adults: Severe sepsis and low risk of death**	N/A	Treatment 18.5%; placebo 17%; p=0.34	Treatment 2.4%; placebo 1.2%; p=0.02	Treatment 3.9%; placebo 2.2%; p=0.01	
ENHANCE [148]	Single arm open-label trial	Adults: Severe sepsis. Early vs late initiation of treatment.	N/A	25.3%	3.6%	6.5%	Mortality: 0-24 hrs 22.9%; ≥24 hrs 27.4% p=0.01
RESOLVE [150]	Randomized double-blind placebo-controlled trial	Children with sepsis-induced cardiovascular or respiratory failure	Treatment 6.0 days; placebo 6.0 days; p=0.72	Treatment 17.5%; placebo 17.2%; p=0.93	Treatment 3.8%; placebo 3.4%; p=0.83	Treatment 6.7%; placebo 6.8%; p=0.97	
Dhainaut *et al* [149]	Randomized double-blind placebo-controlled trial	Adults with severe sepsis after 96-hour infusion. **Extended tx ≤72 hrs vs placebo**	N/A	Treatment 39.8%; placebo 32.3%; p=0.283	N/A	N/A	No ↓ in 1° outcome (pressor-dependent hypotension)

Table 1.1: Phase 3 randomized clinical trials of recombinant human APC (DAA) administration in sepsis.

In all trials listed with the exception of Dhainaut *et al* [149], Drotrecogin alfa was infused at a dose of 24μg/kg/hour for 96 hours in total. *Severe sepsis was defined as known or suspected infection AND ≥3 signs of systemic inflammation AND ≥1 organ dysfunction ≤ 24 hrs duration. **APACHE II <25 or single-organ failure.

1.2.8.2 Ischaemic stroke and APC

APC has recently emerged as a potential therapeutic agent in the setting of ischaemic stroke. Cheng *et al* demonstrated that early administration of APC reduced brain infarction volumes when administered to mice after ischaemic stroke [110]. In contrast, reduction in infarction volume of transgenic mice with severe EPCR deficiency treated with APC was only 40% of that seen in wild-type mice. Mice co-treated with APC and PAR1 inhibitory antibodies showed no reduction in infarction volume. Interestingly, low dose (0.04 mg/kg) APC improved motor function without improving cerebral blood flow post ischemic injury, while high dose APC (0.2mg/kg) improved motor function but also increased cerebral blood flow and reduced fibrin deposition. These data suggest that both anticoagulant and cytoprotective APC functions play a role in protecting mice against ischaemic stroke. Interestingly, an APC variant with impaired anticoagulant function reduced infarct volume similarly to wild-type APC and improved neurological score (in contrast to wild-type APC) when administered to mice 5 minutes before transient occlusion of the middle cerebral artery [151].

A later study investigated receptor dependency of APC-mediated neuroprotection, demonstrating that reduction of NMDA-induced brain injury was prevented by APC, but that this APC-mediated protection was greatly reduced when co-administered with anti-PAR1 and anti-PAR3 antibodies and in PAR1 and PAR3-deficient mice [138].

APC's clinical potential in this setting was highlighted by reports that APC reduces cerebral injury induced by tPA (which is used clinically in stroke treatment) in a mouse

stroke model with consequent reduction in neurological deficit [152] and attenuates tPA-induced haemorrhage [153]. Moreover, even late administration of APC post transient brain ischaemia in mice is efficacious, and is independent of infarct volume reduction [154].

1.2.8.3 Other disease models

APC administration has yielded positive results in other neurological conditions besides stroke. APC slows disease progression and extends survival in a mouse model of amyotrophic lateral sclerosis (ALS) [155]. Moreover, early administration of wild-type APC to mice subjected to traumatic brain injury results in decreased lesion volume and improved functional outcome [156], while late administration of either wild-type APC or an APC variant with reduced anticoagulant function was neuroprotective (although interestingly non-anticoagulant APC mediated enhanced neuroprotection compared with wild-type APC) [157]. APC attenuates glomerular and endothelial injury in diabetic mice [158], possesses therapeutic efficacy in a mouse multiple sclerosis model [159] and is protective in a mouse model of inflammatory bowel disease [160].

1.2.9 Conclusion

Given the paucity of evidence supporting the use of recombinant human APC in severe sepsis at its currently licenced dose, and given the increased risk of bleeding associated with its use, the authors of a recent Cochrane updated systematic review advised against promotion of its use in this setting [161]. However, a large body of *in vitro* and *in vivo* data provide strong evidence supporting the ability of APC to mediate protective signalling *in vitro* and improved sepsis survival *in vivo* **(1.2.7; 1.2.8)**. Moreover, a therapeutic role is emerging for APC in settings other than severe sepsis **(1.2.8.3)**. Consequently, the "holy grail" in clinical use of recombinant human APC in severe sepsis is a recombinant APC molecule which has an **enhanced** ability to mediate protective signalling but which has minimal potential to mediate bleeding side effects. While non-anticoagulant APC variants have been described [143, 162], to date no means of enhancing APC protective signalling has been reported.

1.3: AIMS OF THESIS

1.3.1 To investigate the role of glycosylation in APC anticoagulant and cytoprotective signalling function.

1.3.2 To investigate the effect of individual APC N-linked glycan chain removal on APC functions.

1.3.3 To elucidate the molecular mechanism underlying the anticoagulant properties of the heparin-reversal agent protamine sulphate (see introduction in chapter 6).

CHAPTER 2: MATERIALS AND METHODS

2.1: Glycosidase treatment of APC or protein C

To remove all N-linked glycan structures, APC (1μg; Haematologic Technologies Inc. (HTI); Essex Junction, VT) was incubated with N-glycosidase F (PNGase F; 1000U; from *Flavobacterium meningosepticum;* New England Biolabs Inc., Ipswich, MA*)*, 2μL 10 X G7 buffer (500mM sodium phosphate, pH 7.5) and dH_2O (distilled water) in a final reaction volume of 20μl, for one hour at 37°C **(schematic; Figure 2.1)**. Alternatively, in experiments involving protein C deglycosylation, protein C (HTI; 4.3μg) was incubated with PNGase F (375 U) and G7 buffer for four hours. A shorter incubation time (and higher enzyme concentration) was utilized in experiments involving APC to minimize loss of proteolytic activity due to prolonged incubation. To remove both α2-3– and α2-6–linked sialic acid, APC (1μg) was incubated with α2-3,6,8,9 neuraminidase (0.01 U; from *Arthrobacter ureafaciens*; Calbiochem, San Diego, Ca.) in sodium phosphate buffer (pH 6.0; 50mM final concentration in a 20μl reaction volume) for 1 hour at 37°C **(schematic; Figure 2.1)**.

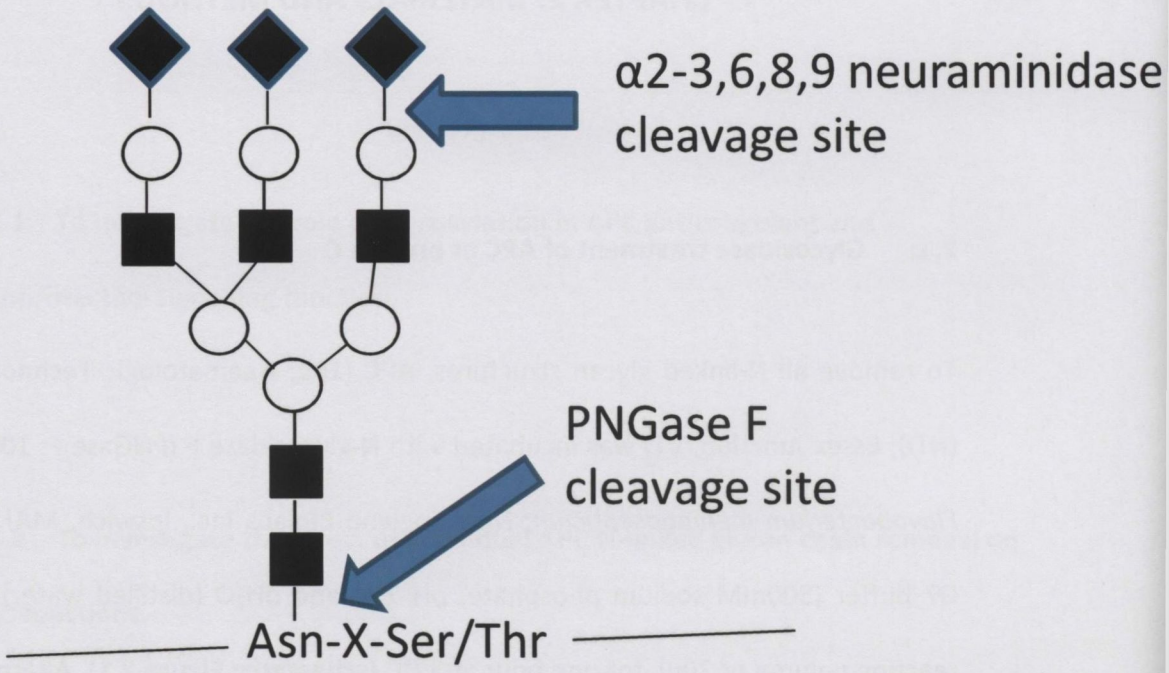


Figure 2.1: Sites of cleavage of glycosidase enzymes

PNGase F cleaves between the innermost GlcNAc and asparagines residues of complex oligosaccharides from N-linked glycoproteins, enzymatically removing entire N-linked carbohydrate chains. α2-3,6,8,9 neuraminidase catalyzes the hydrolysis of all non-reducing terminal sialic acid residues from complex glycoproteins. (■, N-acetylglucosamine (GlcNAc); ○, Mannose; ♦, Sialic acid).

2.2: SDS-PAGE and Western blot analysis

Glycosidase-treated plasma and recombinant protein C/APC variants were characterized by sodium dodecyl sulphate- polyacrylamide gel electrophoresis (SDS-PAGE) analysis and Western blotting using anti-protein C and anti-Gla monoclonal antibodies (mAb). 10ng protein C/ APC was diluted in loading buffer **(appendix I)**, then boiled for 7 minutes to denature the protein. Samples were separated by SDS-PAGE on a precast 7.5% polyacrylamide Tris-HCl gel (Bio-Rad, UK) for 90 minutes at 100V, followed by transfer onto a polyvinylidene fluoride (PVDF) membrane at 100V for 1 hour in transfer buffer **(appendix I)**. Following this, the membrane was incubated in milk (5% (w/v) in phosphate buffered saline (PBS)-Tween **(appendix I)**) to block non-specific membrane binding sites. The membrane was then washed in PBS-Tween three times for 5 minutes. To detect protein C/APC, the membrane was incubated with a sheep polyclonal anti-protein C antibody diluted in 5% blocking buffer for one hour. The membrane was washed as before and then incubated with a horseradish peroxidise (HRP)-conjugated anti-sheep IgG polyclonal antibody diluted in 5% blocking buffer for 40 minutes then washed again. In order to detect protein bands, the membrane was incubated for one minute with Amersham™ ECL™ Plus detection reagents (GE Healthcare LifeSciences; Buckinghamshire, UK). Excess reagent was removed and the membrane was exposed to photographic film for 5-30 seconds. The photographic film was then developed and the bands representing protein C were visualized.

2.3: Total carbohydrate detection

Total carbohydrate detection was performed using the Amersham™ ECL™ glycoprotein detection kit (GE Healthcare). Using this kit, carbohydrate groups are labelled with biotin and then detected with streptavidin-HRP. Using this approach, carbohydrate groups are oxidised with sodium metaperiodate to generate aldehyde groups which can react with biotin hydrazide, enabling detection. APC and PNGase F-treated APC (500ng) were subjected to SDS-PAGE on a 7.5% Tris-HCL gel and transferred onto a PVDF membrane **(2.2)**. Protein-bound carbohydrate moieties were oxidised to aldehydes by incubation with 10mM (final concentration) sodium metaperiodate in 100mM acetate buffer (pH 5.5; **appendix I**) for 20 minutes in the dark at room temperature. Next, the membrane was washed three times in PBS **(appendix I)** for 10 minutes for each wash. 4µl 0.125 mM biotin hydrazide (25pM final concentration) dissolved in 20ml of 100mM acetate buffer (pH 5.5) was added to the membrane for one hour and then washed as before. Next, the membrane was incubated with 5% blocking buffer for 60 minutes followed by washing again. Finally, the membrane was incubated for 30 minutes with 20 ml of a 1/6000 dilution of streptavidin- HRP in PBS followed by washing in PBS and detection of protein bands **(2.2)**.

In addition, the Pro-Q Emerald 300® glycoprotein stain (Invitrogen) was utilized to detect total carbohydrate groups. Using this kit, carbohydrate detection is based upon a similar principle to the Amersham™ ECL™ glycoprotein detection kit (GE Healthcare) but has greater sensitivity for carbohydrate detection. Using this kit, carbohydrate

groups are oxidised with periodate to generate aldehyde groups. These aldehyde groups react with the Pro-Q Emerald 300® glycoprotein stain (an extrinsic fluorophore, or fluorescent dye), so that carbohydrate groups emit a bright green fluorescent signal. APC/PNGase F-treated APC (100ng) were subjected to SDS-PAGE on a 7.5% Tris-HCL gel **(2.2)**. The gel was fixed by incubation with 100ml 50% (v/v) methanol/5% (v/v) acetic acid for 30 minutes twice. The membrane was then washed three times (10 minutes each) in 100ml 3% (v/v) glacial acetic acid. Carbohydrate oxidation was achieved using 25 ml 10mM periodate, which was incubated with the membrane for 30 minutes, then washed. Carbohydrate moieties were detected with Pro-Q Emerald 300® glycoprotein stain (Invitrogen) which was added to the membrane, and incubated in the dark for 90 minutes. The membrane was then washed, and fluorescent-labelled bands visualized using a 300nm ultraviolet transilluminator.

2.4: Sialic acid detection

The Amersham™ ECL™ glycoprotein detection kit (GE Healthcare; **2.3**) was utilized to detect sialic acid residues specifically, rather than total carbohydrate groups. Low periodate concentrations specifically oxidise sialic acid residues with minimal oxidation elsewhere in the glycan moiety [163]. Two terminal sialic acid carbon atoms are selectively cleaved upon peridodate exposure [163]. The key protocol modifications required to achieve specific sialic acid oxidation are the use of a lower concentration of sodium metaperiodate (1mM rather than 10mM), and performance of this oxidation step on ice. APC/neuraminidase-treated APC (500ng) were subjected to SDS-PAGE on a 7.5% Tris-HCL gel **(2.2)** and transferred onto a PVDF membrane. Sialic acid moieties were oxidised to aldehydes by incubation of the membrane with 1 mM sodium metaperiodate (pH 5.5) in 100mM acetate buffer for 20 minutes in the dark. This reaction was performed on ice. All subsequent steps were performed as in **(2.3)**, except that a higher final concentration of biotin hydrazide (10nM rather than 0.025 nM) was used to label oxidised sialic acid moieties.

2.5: Activation of protein C variants using Protac

Protein C variants were activated using Protac, a snake venom isolated from Akigstrodon Contortrix. Protein C (5μg/ml) was incubated in 50mM Tris-HCl (pH 7.4), 100mM NaCl and 0.25U Protac (HYPHEN BioMed, Neuville-Sur-Oise, France) in a total volume of 1ml for one hour at 37°C.

2.6: Determination of amidolytic activity of recombinant APC preparations.

The catalytic activity of each APC preparation was measured by determining steady-state hydrolysis by APC (17.5nM) of the APC-specific chromogenic substrate BIOPHEN CS-21(66) (28.3-2000 μg/ml) in 20mM Tris-HCl (TBS, pH 7.5), 100mM NaCl, 2.5mM $CaCl_2$ and 0.1mg/ml bovine serum albumin (BSA). BIOPHEN CS-21(66) hydrolysis by APC was measured at 405nm at room temperature using a VersaMax® plate reader (Molecular Devices), and the kinetic parameters for each APC preparation determined.

2.7: Protein C activation on the surface of an endothelial cell line.

Purified human protein C, wild type protein C and protein C variants were activated by thrombin on the surface of EA.hy926 cells (kind gift from Dr. C. Edgell, University of North Carolina Chapel Hill, NC [130]). The EA.hy926 line is an immortalised endothelial cell line derived by fusing human umbilical vein endothelial cells with the permanent human cell line A549. EA.hy926 cells ($2x10^5$ cells/ml) were seeded in individual wells of a 96-well plate and grown to confluence over 24 hours. Wells were washed three times in Hank's buffered salt solution (HBSS; **Appendix I**). Protein C (31.2-250nM) in HBSS supplemented with 3mM $CaCl_2$ and 0.6mM $MgCl_2$, 1% (w/v) BSA and 0.1% (w/v) sodium azide, was added to each well. Activation was initiated by addition of thrombin (5.6nM) to each well followed by incubation at 37°C for 30 minutes. The reaction was then stopped with 135nM hirudin (Sigma). APC generation was determined by assessment of APC amidolytic activity in the cell supernatant. 50µl of the supernatant was added to 50µl BIOPHEN CS-21(66) (2mg/ml). The rate of absorbance change was measured at 405nm. The kinetic parameters of each protein C activation were determined according to the Michaelis-Menten equation using Prism® software.

2.8: Assessment of APC Anticoagulant Activity in protein C-Deficient Plasma

APC anticoagulant function in protein C-deficient plasma was assessed using a Fluoroskan Ascent Plate Reader (Thermo Lab System, Helsinki, Finland) in combination with Thrombinoscope software (Thrombinoscope BV, Maastricht, the Netherlands). 80µl plasma were incubated with 20µl platelet-poor plasma (PPP) reagent containing 5pM soluble TF and 4µM phospholipid vesicles (60% phosphatidylcholine, 20% phosphatidylserine and 20% phosphatidylethanolamine) in the presence or absence of APC (2.5-20nM). Thrombin generation was initiated by automatic dispensation of fluorogenic thrombin substrate (Z-Gly-Gly-Arg-AMC.HCl) and 100mM $CaCl_2$ into each well (final concentrations, Z-Gly-Gly-Arg-AMC.HCl, 0.42mM and $CaCl_2$, 16.67mM). Thrombin generation was determined using a thrombin calibration standard. The area under the thrombin generation curve (endogenous thrombin potential, ETP) was measured.

2.9: Preparation of normal platelet poor plasma

Venous blood was collected by sterile venepuncture directly into vacuum tubes containing 0.109 M sodium citrate (blood:citrate; 9:1). Venous blood was collected from ~20 donors. Males and females were equally represented. Donors were of different ethnic backgrounds. Blood was centrifuged at 2000g for 15 minutes at room temperature. Plasma was removed and pooled then re-centrifuged in fresh tubes at >2000g for an additional 10 minutes. Plasma was immediately stored in 1ml aliquots at -80°C.

2.10: Assessment of heparin-stimulated APC inhibition in plasma

To determine the activity of APC in plasma over time, purified APC and PNGase-treated APC (20nM) were incubated with normal platelet-poor plasma **(2.9)** in the presence of heparin (10 U/ml) at 37°C. The presence of heparin stimulates the activity of APC plasma serpin inhibitor PCI [164]. APC amidolytic activity was determined at specific time-points (2.5-20 minutes). This was achieved by assessing the rate of hydrolysis of the APC-specific synthetic chromogenic substrate BIOPHEN CS-21(66) as before. APC half-life was determined by curve fitting using Prism® software.

2.11: Phospholipid preparation

Phospholipids in chloroform solution were purchased from Avanti Polar Lipids Inc, USA and stored at -20°C. Dioleoyl-phosphatidylcholine (DOPC), dioleoyl-phosphatidylethanolamine (DOPE) and dioleoyl-phosphatidylserine (DOPS) were mixed in the ratio 60% DOPC, 20% DOPS and 20% DOPE in brown glass vials. Final phospholipid amount in each vial was 10mg. Chloroform present in the preparations was evaporated under slow flow nitrogen vapour, and the phospholipid mixtures resuspended in ice-cold sterile water to achieve a final concentration of 10mg/ml. Dried phospholipid vesicles were re-suspended and homogenized by vigorously vortex-mixing until a cloudy phospholipid suspension was observed. Unilamellar phospholipid vesicles were prepared by extruding the phospholipid preparations through a 0.1µm polycarbonate membrane 11 times using an Avanti Mini-Extruder (Avanti Polar Lipids Inc). Phospholipid vesicles were stored at 4°C for up to 3-4 days.

2.12: Protein S-independent FVa inactivation by APC variants.

To investigate APC-mediated FVa inactivation, FVa (1nM) was incubated with phospholipid vesicles (20μM; 60% DOPC, 20% DOPS and 20% DOPE) at 37°C in 40mM Tris-HCl, 140mM NaCl, 3mM $CaCl_2$ and 0.3% w/v BSA. FVa proteolysis was initiated by addition of APC (2nM). Aliquots were removed at regular intervals, and added to 1nM FXa, 0.5μM prothrombin and 25μM phospholipids. This prothrombinase reaction was incubated at 37°C for 3 minutes, then stopped by the addition of 5μl ice-cold 0.5M ethylenediaminetetraacetic acid (EDTA). The residual FVa cofactor activity at each time point was determined by the activity of the prothrombinase reaction at each time point. Thrombin was detected by addition of 50μl of each prothrombinase reaction mix to 50μl of a thrombin-specific chromogenic substrate (BIOPHEN CS-01(38); 1mg/ml) and measuring thrombin-dependent colour change at 405nm. Residual FVa activity (%) was determined by comparison with FVa activity observed prior to APC incubation.

2.13: Protein S-dependent FVa inactivation by APC variants

To investigate protein S-stimulated FVa inactivation by APC, FVa (7nM) was incubated with phospholipid vesicles (20μM; 60% DOPC, 20% DOPS and 20% DOPE) and protein S (3.1-50nM) at 37°C in a buffer containing 40mM Tris-HCl, 140mM NaCl, 3mM $CaCl_2$ and 0.3% w/v BSA. FVa proteolysis was initiated by addition of APC (2nM). 2μl aliquots of each mixture were removed after incubation for 2 minutes into 0.75nM FXa, 0.5μM prothrombin and 25μM phospholipids incubated at 37°C. This prothrombinase reaction was incubated for 3 minutes, then stopped by the addition of 5μl ice-cold 0.5M EDTA. The residual FVa cofactor activity at each time point was determined by the activity of the prothrombinase reaction at each time point. Thrombin present was detected by addition of 50μl of each prothrombinase reaction mix to 50μl of a thrombin-specific chromogenic substrate (BIOPHEN CS-01(38); 1mg/ml) and measuring thrombin-dependent colour change at 405nm. Residual FVa activity (%) was determined by comparison with FVa activity observed prior to APC incubation.

2.14: Measurement of APC-mediated endothelial barrier protection.

EA.hy926 cells were grown to confluence on polycarbonate membrane transwells (Costar, 3 μM pore size, 12-mm diameter) and incubated with APC (0.63-20nM; all final concentrations) in the presence of 3mM $CaCl_2$ and 0.6mM $MgCl_2$- supplemented serum-free Dulbecco's Modified Eagle Medium (DMEM). After 3 hours, EA.hy926 cells were treated with 5nM thrombin for 10 minutes. Thrombin was added directly into each APC-treated well without washing. The cells were then washed and incubated with 0.67 mg/ml Evans Blue with 4% BSA. Endothelial barrier permeability was determined by assessment of the increase in absorbance at 650 nm in the outer chamber over time due to transmigration of Evans Blue-BSA. To assess the role of APC-EPCR binding in maintenance of endothelial barrier integrity, supernatant was removed and an anti-EPCR monoclonal antibody (RCR-252) was incubated with the cells for 30 minutes (25μg/ml, final concentration) followed by assessment of BSA-Evans Blue as above. To compare results from multiple assays, permeability (%) was determined using the following equation:

$$P = (X-C)/(F-C)\cdot 100\%$$

Where 'P' is permeability (%), 'X' is the APC-treated OD_{650}, 'C' is the OD_{650} of untreated EAhy926 cells and 'F' is the OD_{650} for thrombin-treated EA.hy926 cells.

2.15: Assessment of APC-mediated protection against endothelial cell apoptosis by TUNEL staining and flow cytometry

During apoptosis, cellular nucleases cause break-up of genomic DNA and exposure of multiple 3'-hyroxyl ends. The enzyme Terminal deoxynucleotidyl Transferase (TdT) catalyzes labelling of these 3'-hydroxyl ends with labelled deoxyuridine triphosphate (dUTP) nucleotides. This process is known as terminal deoxynucleotide transferase nick end labelling (TUNEL).

EA.hy926 cells in a 6-well plate were treated with APC (2.5-20nM) for 3 hours in serum free DMEM supplemented with 3mM $CaCl_2$ and 0.6mM $MgCl_2$. Apoptosis was induced with staurosporine (20μM) for 4 hours. Cells were washed with PBS, then made non-adherent by addition of 0.5 ml 0.25% trypsin/EDTA per well. Cells were fixed by suspending in 1% paraformaldehyde in PBS (pH 7.4) on ice for 1 hour at a density of 1-2 $x10^6$ cells/ml. Fixed EA.hy926 cells were then washed in PBS and permeabilized by incubation with 70% ice-cold ethanol for 30 minutes. Cells were stored in 70% ethanol at -20°C. Fixed cells were washed again and labelled with bromolated dUTP (Br-dUTP) for one hour at 37°C. Cells were washed again, then incubated with a fluorescein-labelled anti-Br-dU monoclonal antibody and stored in darkness for 30 minutes at room temperature. Br-dUTP labelling reflects the number of apoptotic cells [165]. Non-apoptotic cells do not incorporate significant amounts of Br-dUTP due to the lack of exposed 3' hydroxyl DNA ends. Total cellular DNA was detected by incubation with propidium iodide (PI) / RNase A. PI is a fluorescent molecule which binds to DNA by intercalation. RNA binding was inhibited by addition of RNAase. PI was capable of entering cells due to prior permeabilization with 70% ethanol. Apoptotic cells (stained

with PI and anti-Br-dU) and non-apoptotic cells (stained with PI only) were detected by flow cytometry as separate populations. Apoptotic cells were expressed as a percentage of total cells.

2.16: Assessment of APC-mediated protection against apoptosis by measurement of *Bax* and *Bcl-2* mRNA expression.

During apoptosis, relative gene expression of pro-apoptotic *Bax* increases, while that of anti-apoptotic *Bcl-2* decreases [166, 167]. APC pretreatment attenuates the increase and decrease in *Bax* and *Bcl-2* expression respectively [110]. Confluent EA.hy926 cells in 6-well plates were pre-treated with APC or PBS for 4 hours. EA.hy926 cell apoptosis was then induced by incubation with staurosporine (20μM) for 4 hours to induce apoptosis. Control cells were treated with PBS instead of staurosporine. Staurosporine-treated cells were trypsinized, pelleted by centrifugation at 500g for 5 minutes and RNA extracted using the RNeasy Mini kit (Qiagen). Briefly, cells were disrupted by adding 350μl buffer RLT and homogenized by vortexing for 5 minutes. 1 volume of 70% ethanol was added to the homogenized lysate and mixed. The sample was placed in an RNeasy spin column in a 2ml collection tube and centrifuged at >8000g for 2 minutes. The flowthrough was discarded. The spin column was washed by addition of 700μl buffer RW1 followed by centrifugation for 15 seconds then 500μl ethanol-based buffer RPE followed by centrifugation for 15 seconds. The spin column was dried fully by addition of a further 500μl buffer RPE followed by centrifugation for 2 minutes. To elute RNA, the spin column was placed in a new 1.5 ml RNA-free collection tube and 30μl RNA-free dH_2O added, followed by centrifugation for 1 minute.

Two step Real Time Reverse Transcription Polymerase Chain Reaction (Real Time RT-PCR)

Step 1: Reverse transcription

Prior to assessment of *Bax* and *Bcl-2* mRNA expression by Real Time PCR, it was first necessary to convert RNA to DNA. To achieve this, total RNA was converted to single-stranded cDNA by the enzyme Reverse Transcriptase using the High Capacity cDNA Reverse Transcription kit (Applied Biosystems). First, 2X Reverse Transcription (RT) Master Mix was prepared on ice as outlined in **Table 2.1**.

Component	Volume (µl)
10X RT buffer	2.0
25X dNTP mix (100mM)	0.8
10X RT random primers	2.0
RNAase inhibitor	1.0
Multiscribe™ Reverse Transcriptase	1.0
Nuclease-free H_20	3.2
Total volume per reaction	10

Table 2.1: Components of 2X Reverse Transcription Master Mix using the High Capacity cDNA reverse transcription kit (Applied Biosystems).

10µl RNA sample was added to 10µl of 2X RT Master Mix and gently mixed. In order to perform reverse transcription, thermal cycling was performed as outlined in **Table 2.2**. cDNA generated was quantified using the NanoDrop 2000 microvolume spectrophotometer (Thermo Scientific).

	Step 1	Step 2	Step 3	Step 4
Temperature (°C)	25	37	85	4
Time (minutes)	10	120	5	∞

Table 2.2: Thermal cycling parameters for reverse transcription by PCR.

Random primers anneal to RNA at 25°C (approx. 5°C below primer melting temperature). Primers are extended by the enzyme reverse transcriptase, which functions optimally at 37°C. Maximal yield from reverse transcription is at 37°C for 120 minutes. Heating to 85°C inactivates the reverse transcriptase enzyme.

Step2: Real Time PCR

During replication of single-strand cDNA by PCR, repeated temperature cycles were utilized. First, DNA was melted at high temperature (~95°C). Next, specific short oligonucleotide primers were allowed to anneal to cDNA. These primers were of complementary sequence to the region to be amplified. The temperature selected for this cycle was ~ 5° below primer melting temperature. This cycle was followed by DNA replication by primer extension, catalyzed by heat-stable DNA polymerase, with optimal activity at ~60-70°C. *Bax and Bcl-2* gene expression was quantified by Real Time PCR using Taqman probes, oligonucleotides with a fluorescent reporter dye attached to the 5' end and a quencher attached to the 3' end (Applied Biosystems). Taqman probes specific to *Bax* (Hs00180269_m1), *Bcl-2* (Hs00153350_m1) and *β-actin* (Hs99999903_m1) were utilized. These probes specifically annealed during PCR to a region of their corresponding cDNA sequences. DNA polymerase replicated the template to which the probe was bound during PCR. The 5' nuclease activity of the DNA polymerase cleaved the probe during this process, releasing the fluorescent reporter dye and decoupling it from the 3' attached quencher. During PCR therefore, the amount of fluorescence generated by probe cleavage exponentially increased, in a manner which was proportional to the amount of probe cleavage.

To each reaction well of a MicroAmp optical 96 well plate (Applied Biosystems) were added 25µl Taqman™ 2X Universal PCR Mastermix, 70ng sample cDNA, Taqman probe specific to either *Bax, Bcl-2 or β-actin* (250nM final concentration) and dH_2O, in a final reaction volume of 50µl. During PCR, initial temperature cycling steps were performed. First, the reaction was maintained at 50°C for 2 minutes to activate AmpErase™ Uracil N-glycosylase (UNG), an enzyme which prevents the amplification

of carry-over RNA in the PCR reaction by removing any incorporated uracil. Then, the temperature was increased to 95°C for 10 minutes to activate DNA polymerase. These initial steps were followed by 40 PCR cycles, consisting of 95°C for 15 seconds (to melt DNA) then 60°C for 60 seconds (for annealing of Taqman primers and extension).

PCR product quantification was performed by the C_t (comparative threshold) method. C_t values of genes of interest (proapoptotic *Bax* and anti-apoptotic *Bcl-2*) from APC/staurosporine samples were measured automatically by the Applied Biosystems 7500 real time PCR system instrument. C_t values were compared with samples treated with staurosporine alone or PBS (negative control) and in each case, normalized to the housekeeping gene *β-actin.* The value of $\mathbf{2}^{-\Delta\Delta CT}$ was calculated for *Bax* and *Bcl-2* in each sample, where

$$\Delta CT = CT \text{ (gene of interest)} - CT \text{ (}\beta\text{-actin)}.$$

$$\Delta\Delta CT = \Delta CT \text{ (stauroporine-treated sample)} - \Delta CT \text{ (calibrator)}$$

The ratio of $\mathbf{2}^{-\Delta\Delta CT}$ values for *bax* and *bcl-2* (*bax/bcl-2* ratio) were calculated. Each well was replicated at least three times. Experiments were performed in triplicate and plotted as a percentage of the mean staurosporine-treated *Bax/Bcl-2* ratio (100% apoptosis).

2.17: Measurement of APC-mediated protection against apoptosis: Apopercentage® assay

Uptake of an apoptosis-specific pink dye by EA.hy926 cells was assessed using the APO*Percentage*® kit (Biocolor). Phosphatidylserine phospholipids are usually confined to the inner cell membrane leaflet, but during apoptosis, phosphatidylserine transfers to the outer cell membrane leaflet, permitting intracellular uptake of APO*Percentage* dye.

Confluent EA.hy926 cells were treated with APC (0.625-20nM) for 3 hours in serum-free DMEM supplemented with 3mM $CaCl_2$ and 0.6mM $MgCl_2$, then treated with staurosporine (20μM) for 3.5 hours. Upon completion of this period, 100μl DMEM containing 10μl APO*Percentage* dye and staurosporine (20μM) was added to each well for 45 minutes. Cells were then washed to remove non-bound dye and APO*percentage* dye uptake was quantified by conversion of digital photograph images into pixel counts with Adobe™ Photoshop™ software. Average pixel counts were based on analysis of at least three images per well. Results are expressed as a ratio of pixel counts for APC-treated wells/ staurosporine-treated wells.

2.18: Generation of protein C mutants

2.18.1: Human protein C mammalian expression vector

In order to generate vectors for stable expression of recombinant protein C variants, DNA plasmids encoding human protein C with putative N-linked glycosylation site mutations were prepared. The vector used as a template for site-directed mutagenesis was a double-stranded DNA plasmid, pRc/CMV/PC cDNA [164] (kind gift of Professor Björn Dahlbäck, University of Lund, Sweden) **(Figure 2.2)**. This plasmid includes the full-length human protein C cDNA sequence (cloned between *Hind III and Xba I* restriction endonuclease sites), the f1 origin of replication, which permits propagation in *E.coli,* CMV and SV40 promoters to enhance expression of the inserted protein C gene, and resistance genes for ampicillin and neomycin for selection in bacterial and mammalian cell cultures respectively.

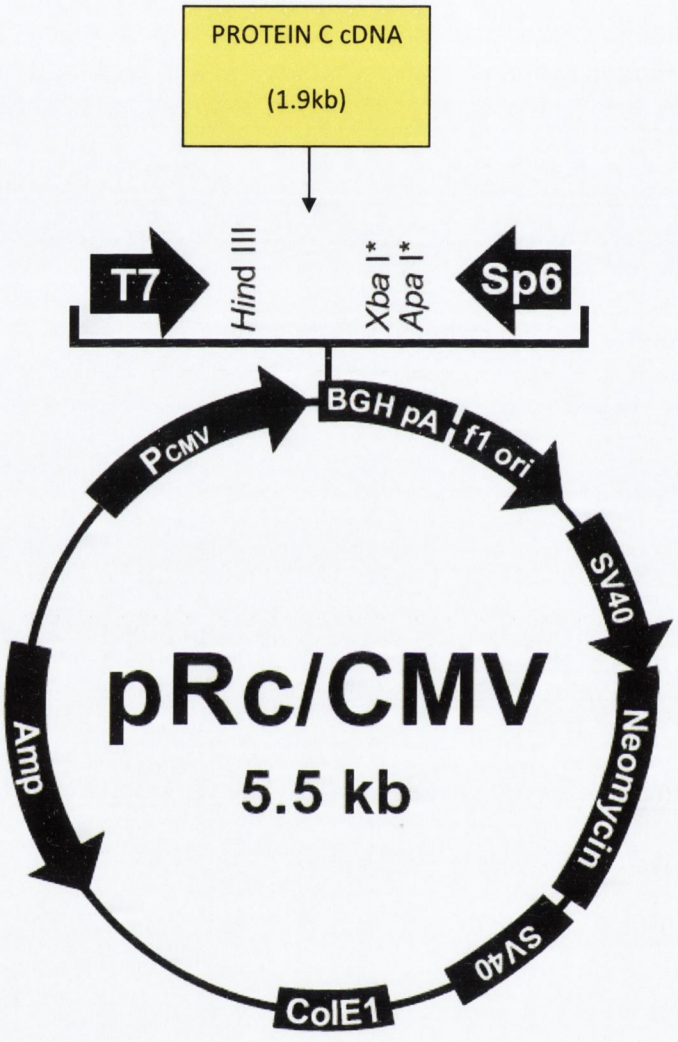


Figure 2.2: The pRc/CMV/Protein C cDNA vector

2.18.2: Site-directed mutagenesis of pRc/CMV/PC plasmid

The QuickChange Site-Directed Mutagenesis Kit (Stratagene, USA) was utilized to generate protein C glycosylation site mutants. Forward and reverse primers encoding each desired nucleotide base change ("mutagenic primers") were synthesized **(Appendix II)**. Primers contained ~30 bases, corresponding to the protein C nucleic acid sequence encoding 5 amino acids upstream of the desired AAC (Asn) to CAA (Gln) amino acid change and continuing for the sequence of 5 amino acids downstream of the desired substitution. Mutagenic primers were used to direct replication of both plasmid strands by polymerase chain reaction using the QuickChange Site-Directed Mutagenesis kit according to manufacturer's instructions. 50ng pRc/CMV/PC, 125ng each of sense and antisense oligonucleotide primers for each desired mutation, 1µl dNTP mix, 5µl 10X reaction buffer and 2.5 U (1µl) of *Pfu Turbo* DNA polymerase were incubated with dH_2O in a final reaction volume of 50µl **(Table 2.3)**. Mutagenesis PCR cycling was performed using a GeneAmp PCR System 2700 (Applied Biosystems, UK). In this procedure, parent plasmid was denatured to create single-stranded DNA. Next, the reaction was cooled to 5°C below primer melting temperature to allow mutagenic primers to anneal to the complementary sequence on each corresponding strand of the denatured parent vector. The primers were extended using the high-fidelity DNA polymerase (*PfuTurbo)* in a buffer containing deoxynucleoside triphosphates (dNTPs). This enabled synthesis of plasmids incorporating the new mutation. Finally, parent plasmid DNA was removed from the PCR reaction mix by incubation of the 50µl reaction mixture with 1µl (20 U) of the restriction enzyme *DpnI* for 1 hour at 37°C.

DpnI digests plasmid DNA containing methylated and hemimethylated DNA, which is present on the parent plasmid but not newly synthesized mutant DNA.

Segment	Temperature (°C)	Time (seconds)	Number of cycles
1 (Denaturation)	95	30	1
2 (Denaturation)	95	30	15
(Primer annealing)	55	60	
(Extension)	68	480 (1 min/kb primer)	

Table 2.3: PCR thermal cycling parameters for protein C mutagenesis

2.18.3: Agarose gel electrophoresis

DNA fragments were separated by size using agarose gel electrophoresis. Agarose (1% w/v) was heated in Tris/Borate/EDTA (TBE) buffer **(Appendix I)** for 1 minute in a microwave oven. Once cooled, ethidium bromide (5µg/ml) was added, which binds DNA and fluoresces upon exposure to ultraviolet light. After ~15 minutes at room temperature the agarose gel polymerized and DNA samples added to individual wells. Electrophoresis was performed at 75 V for ~30 minutes to facilitate DNA band separation. Ethidium bromide-labelled DNA bands were visualized by illumination with a UV lamp.

2.18.4: Luria-Bertani (LB) agar plate preparation

LB agar (Sigma; **appendix I**) was dissolved in water according to manufacturer's instructions and autoclaved. LB agar was microwaved briefly to make soluble then cooled to <60°C and ampicillin (100µg/ml) was added (LB-Amp agar). ~30 ml agar was poured into each $10cm^2$ dish and allowed to solidify.

2.18.5: DNA transformation into NovaBlue Singles® competent *E.coli* cells.

In order to increase the quantity of mutant vectors, *DpnI*-treated mutant plasmid DNA was transformed into NovaBlue Singles® competent *E.coli* cells (Novagen) as per manufacturer's instructions. Competent bacterial cells replicate recombinant plasmid DNA along with host organism DNA, greatly amplifying the mutagenic vector copy number. 50µl aliquots of competent cells were thawed on ice. 2µl of *DpnI*-treated DNA was added to each aliquot followed by incubation on ice for 5 minutes. Cells were "heat-shocked" by incubation at 42°C for 30 seconds to facilitate transfer of plasmid DNA across the competent *E.coli* cell membrane. 250µL super optimal broth with catabolite repression (SOC) medium **(appendix I)** was preheated to 37°C then added to each competent cell/plasmid reaction and gently mixed. 25µL of each preparation was spread onto LB-Amp agar plates and allowed to grow overnight.

2.18.6: Preparation of plasmid minipreps

Plasmid minipreps were prepared using the QIAprep® Spin Miniprep Kit (QIAGEN, UK). Transformed *E.coli* colonies growing on LB-Amp agar plates were picked and inoculated into 5ml starter cultures of LB broth **(appendix I)** inoculated with ampicillin (100μg/ml). Starter cultures were incubated for 15 hours at 37°C with vigorous shaking. Bacterial cells were harvested by centrifugation at >8000 rpm for 5 minutes at room temperature in a table-top microcentrifuge to form a cell pellet. The supernatant was discarded and the cell pellet resuspended in 250μl Buffer P1 in a microcentrifuge tube. Buffer P1 is a resuspension solution that facilitates dispersion of a pellet into single cells. 250μl alkaline lysis Buffer P2 was added to induce cell lysis and the tube inverted 4-6 times gently to mix contents. 350μl of acidic Buffer N3 were added to neutralize the alkaline cell lysate and the tube was immediately inverted 4-6 times. N3 buffer is a high salt buffer that also causes precipitation of cellular proteins, resulting in separation of proteins from DNA. The neutralized cell lysate was centrifuged at 17900g for 10 minutes to form a white pellet. The supernatant (containing plasmid DNA) was pipetted onto a QIAprep spin column (which binds DNA) and centrifuged at 17900g for 1 minute. The flow-through was discarded and the column washed using Buffer PB then centrifuged again for 1 minute. Buffer PB is a DNA wash buffer that washes away any remaining proteins, such as cellular DNAases. The column was then washed in the same way with 0.75ml Buffer PE. PE is another DNA wash buffer that washes away any traces of the other buffers. Buffer PE contains ethanol and induces DNA precipitation on the spin column membrane while washing away water soluble molecules. The flowthrough was discarded after each washing

step. The column was centrifuged again at 17900g for another 1 minute to remove residual wash buffer. In order to elute plasmid DNA, the column was placed in a clean microcentrifuge tube. 50µl Elution Buffer (EB; 10 mM Tris·Cl, pH 8.5) was applied and the column allowed to stand at room temperature for 10 minutes, then centrifuged at 17900g for a further 1 minute. Buffer EB, due to its low salt content, releases DNA from the spin column membrane. The eluted purified plasmid DNA was visualized by agarose gel electrophoresis **(2.18.3)**.

Nucleic acid quantification

Plasmid DNA was quantified using the NanoDrop 2000 microvolume spectrophotometer (Thermo Scientific), which holds 1µl of sample without needing a containment device such as a cuvette. The sample is held in place between two optical surfaces which define light pathlength in a vertical orientation. The device transmits light from a Xenon lamp through the sample via an optical fibre. Absorbance is measured at 300 and 700 nm. There is a linear relationship between absorbance and nucleic acid concentration, which is automatically calculated by the instrument. Prior to use, the optical surfaces were cleaned by pipetting 1µl of dH_2O onto the lower surface, closing the lever arm, then opening it and wiping both surfaces with a laboratory wipe. The NanoDrop software was opened and "nucleic acids" module selected. Initialization was performed by placing 1µl of dH_2O on the lower optical surface and selecting "initialize" on the NanoDrop software. A "blank" measurement was performed first, using 1µl of dH_2O. This "blank" measurement was subtracted automatically from subsequent readings. 1µl of sample was then loaded, the lever arm closed and DNA concentration read.

The presence of each introduced mutation was confirmed by sequencing with multiple sequencing primers **(appendix II)**, which were used to sequence the entire protein C cDNA.

2.19: Recombinant protein C expression

2.19.1: Cell culture

Cell lines were grown in humidified incubators at 37°C in an atmosphere containing 5% CO_2. Cell culture was performed in a class II laminar flow cabinet. Human Embryonic Kidney (HEK) 293 cells were utilized for recombinant protein C expression, as this cell line has been shown to be capable of protein C expression and post-translational modification [168]. HEK 293 cells were grown in Minimal Essential Medium Eagle (MEM; Sigma) supplemented with 1U/ml penicillin, 0.1mg/ml streptomycin (Sigma), 2mM L-glutamine (Sigma), Foetal Calf Serum (FCS). In addition, Vitamin K (10mg/ml) was added to facilitate γ-carboxylation of recombinant protein C variants.

2.19.2: Stable transfection of mammalian cell line

HEK 293 cells were seeded at 2 x 10^5 cells/35mm^2 well and grown in a 6 well plate until ~60-80% confluent. 4µg plasmid DNA was diluted in 250µl OptiMEM. The transfection reagent lipofectamine (10µl; 2mg/ml solution) was also diluted an equal volume of OptiMEM. Each DNA and transfection reagent mixture was incubated for 5 minutes then combined and incubated at room temperature for a further 20 minutes. The HEK 293 cells were washed. The plasmid/lipofectamine-containing mixture was added to cells in 1.5ml OptiMEM (final volume 2 ml). After 4 hours, cells were washed and the growth media changed back to MEM-α as above. Upon reaching confluency (~24-48 hours), cells were trypsinized and re-suspended in growth medium containing the selective agent geneticin sulphate (G418; a neomycin analogue; 500µg/ml). Cells were plated in 10cm^2 dishes and grown in the presence of G418-containing media. After ~14 days, untransfected HEK293 cells died as a result of G418 treatment. Transfected cells formed colonies at this time point and ~20 colonies per transfection were picked. Picked colonies were seeded into individual wells of a 96-well plate and allowed to reach confluency, whereupon they were assessed for protein C expression.

2.19.3: Protein C ELISA

A human protein C ELISA was established in order to assess protein C concentration. 96-well plates (Maxisorp Nunc, UK) were coated with 25µg/ml polyclonal sheep anti-human protein C antibody (Haematologic Technologies Inc.) diluted in a 50mM $Na_2CO_3/NaHCO_3$ buffer (pH 9.6; **appendix I**). Wells were washed three times with TBS/0.05% Tween 20 (TBS-T) and blocked with 2% bovine serum albumin (BSA) in TBS for 2 hours at room temperature, then washed again. All samples were prepared in TBS-T containing 0.02% BSA and were added to wells in duplicate for one hour at room temperature. Protein C bound to each well was detected using a horseradish peroxidise (HRP)-conjugated polyclonal sheep anti-protein C antibody (10µg/ml) followed by detection buffer (33.3mM $C_6H_8O_7$, 67mM Na_2HPO_4 (pH 5), 0.666µg/ml o-phenylenediamine (OPD), 0.0004% (v/v) hydrogen peroxide). Absorbance was measured at 492nm as before.

2.19.4: Partial purification of recombinant protein C variants

High-expressing protein C colonies as determined by protein C ELISA were expanded until they reached full confluence in a multisurface cell vessel (1L; HYPERflask™; Corning). Upon reaching confluency, growth medium was replaced with 1L serum-free OptiMEM containing vitamin K (10μg/ml). After 3 days, growth medium was collected and concentrated to 50ml by filtration using a Pellicon™ XL tangential flow filter device (Millipore). In normal flow filtration (NFF), the direction of fluid flow and of applied pressure are both at 90° to the membrane. In contrast, tangential flow filtration (TFF) devices pump fluid parallel to the filter membrane surface, while pressure is applied at 90° to the direction of fluid flow and to the membrane. Particles greater than the membrane pore size are prevented from passing through. In NFF, particles accumulate at the membrane surface. In contrast, during TFF, retained particles do not accumulate at the membrane surface. Instead, they are swept along by the tangential flow, enhancing the efficiency of the filtration process. Concentration is achieved because excess fluid travels across the filtration membrane into the waste compartment. In this manner, media was concentrated prior to partial protein C purification.

Protein C purification was then performed using a Fast Performance Liquid Chromatography (FPLC) system (GE Healthcare). Concentrated recombinant protein C samples in media (50 ml) were first desalted using the 50ml Hi Prep 26/10 desalting column (GE Healthcare) with an FPLC system, to accomplish buffer exchange into 50mM Tris and 150mM NaCl, pH 7.4 ("FPLC running buffer"). The HiTrap™ desalting column is packed with the gel filtration medium Sephadex™ G25 superfine, based on

cross-linked dextran beads. Protein samples are filtered and salts retained on the column, emerging later from the column. Thus, proteins are exchanged into FPLC running buffer.

Recombinant protein C was partially purified by "pseudo-affinity" chromatography. This procedure is based upon the principle that correctly γ-carboxylated protein C is negatively charged, and will therefore bind to a positively charged resin. To achieve this, a 5ml HiTrap Q HP sepharose anion exchange column (GE Healthcare) was used. In this column, anionic functional groups are covalently attached to the gel matrix via stable ether linkages. A HiTrap™ Q HP column was attached to the FPLC and equilibrated with 5 column volumes (25ml) FPLC running buffer to remove preservatives. Equilibration with 5 column volumes of 50mM Tris, 150mM NaCl, 1M NaCl (pH 7.4; elution buffer) was then performed, to remove any protein bound to the column, followed by a further 5 column volumes of FPLC running buffer. The recombinant protein C sample was manually injected into the FPLC superloop and then automatically injected into the HiTrap™ Q HP column at 1ml/min. Protein C molecules bound to the column were eluted using a gradient of a second buffer containing 50mM Tris, 150mM NaCl and 30mM $CaCl_2$ (pH 7.4; buffer B). This step is based upon the principle that Ca^{2+} in the buffer binds with high affinity to γ-carboxylated protein C, releasing it from the column. This high affinity binding reflects a high level of γ-carboxylation [168]. A concentration gradient of Ca^{2+} (0-30mM) was applied to the column containing bound protein C. The amount of protein eluted was maximal at ~10mM Ca^{2+}. Eluted protein C was collected in 1ml fractions and pooled. These pooled fractions were subsequently concentrated into a final volume of ~1.5 ml.

This was achieved by loading the sample, as before, onto a 5ml HiTrap™ Q HP column equilibrated with FPLC running buffer but this time eluting with 50mM Tris, 150mM NaCl, 1M NaCl (pH 7.4). All protein C was rapidly eluted in a single peak on the UV spectrophotometer output graph, corresponding to a volume of ~1.5ml. 0.5ml fractions were collected and those corresponding to the elution peak were collected. The concentrated protein C sample was subsequently exchanged into FPLC running buffer using a 5ml HiTrap™ desalting column.

2.20: Assessment of protein C binding to soluble EPCR

Protein C-soluble EPCR (sEPCR) binding affinity was characterized by Surface Plasmon Resonance (SPR) using a dual flowcell BIAcore® X biosensor system (BIAcore®, Sweden). SPR is based upon the principle that light excites surface plasmons which propagate parallel to a metal surface. Surface plasmons are electromagnetic waves. Their oscillation is altered by changes to the metal surface, such as by adsorption of molecules to this surface. SPR changes are measured and reflect the amount of a substance which is bound to the surface. The BIAcore® sensor chip surface consists of glass coated with a thin layer of gold, modified with a carboxymethylated dextran layer. The dextran layer provides a hydrophilic environment for attached molecules, preventing them from denaturation. 10μg/ml monoclonal anti-EPCR antibody, RCR-2 (kind gift of Dr. K. Fukudome, Saga Medical School) was covalently immobilized on a carboxymethylated dextran (CM5) sensor chip (BIAcore®) using amine coupling chemistry. RCR-2 was selected as a capture antibody because it does not inhibit APC binding to EPCR. To covalently immobilize RCR-2, carboxymethyl groups on the sensor chip surface were modified using N-hydroxysuccinimide (NHS) and 1-Ethyl-3-[3-dimethylaminopropyl]carbodiimide hydrochloride (EDC). EDC reacts with carboxyl (or carboxymethyl) groups to form an amine-reactive intermediate. This intermediate is unstable, because if it does not encounter an amine, it hydrolyzes and regenerates the carboxyl group. However, in the presence of NHS, EDC converts carboxyl groups to stable amine-reactive NHS esters. These ester groups then react with amines and other nucleophilic groups on the antibody ligand RCR-2, forming covalent bonds. Using this technique, RCR-2 was permanently immobilized onto the surface of the two flow

cells (test and reference) of the sensor chip. Soluble EPCR (sEPCR) was dialysed into HBS-P buffer (100mM HEPES, pH 7.4, 150mM NaCl) and bound to the test flow cell via RCR-2. PC-*N329Q* (31.25–1000nM) was sequentially injected over both flow cells at a flow rate of 10µl/min for 60 seconds. APC-EPCR binding was dissociated using HBS-EP buffer (HBS-P, but containing 3mM EDTA; BIAcore) The RCR-2 surface was regenerated with 10µl of 10mM glycine-HCl (pH 2).

2.21: Measurement of thrombin generation and tail bleeding time in mice

BALB/c mice, aged 6-8 weeks were weighed and anaesthetized with midazolam and etorphine hydrochloride. Protamine sulphate was administered intravenously followed 90 seconds later by transection of the tail tip. The tail was loosely suspended in PBS at 37˚C and time taken for complete cessation of tail bleeding recorded. To assess the effect of protamine on *in vivo* thrombin generation, mice were exsanguinated at specific time points following intravenous protamine administration. Blood was collected into citrate phosphate buffer (Sigma) and plasma collected by centrifugation at 1500g for 20 minutes. Thrombin generation was initiated by addition of 20µL HemosIL APTT lyophilized silica reagent and 100mM $CaCl_2$ and was assessed using a Fluoroskan Ascent Plate reader in combination with Thrombinoscope software **(2.28)**.

2.22: Activated partial thromboplastin time (APTT) and prothrombin time (PT) measurement

Normal platelet poor plasma was prepared (2.9) and APTT and PT measured using the fully automated ACL TOP® coagulometer (Beckman Coulter Inc., Galway, Ireland) using HemosIL APTT lyophilized silica reagent and PT-fibrinogen HS plus reagent respectively (Instrumentation Laboratory, Lexington, MA).

2.23: Characterization of APC-mediated FVIIIa proteolysis in the presence of protamine sulphate

To determine whether protamine enhancement of APC anticoagulant activity was mediated by increased rate of FVIIIa proteolysis a previously characterized APC-resistant FVIII double mutant (R336Q/R562Q) (APCR-FVIII) was utilized (kind gift of Dr Vince Jenkins, National Centre for Hereditary Coagulation Disorders, St James's Hospital, Dublin 8 [169]).

FVIII-deficient plasma (Technoclone GmbH, Vienna, Austria) was supplemented with either B-domainless wild-type FVIII (wt-FVII) or APCR-FVIII (both 1.0 U/ml). Thrombin generation was then initiated with 5pM TF, 4μM phospholipid vesicles (PC:PS:PE 60%:20%:20%) and $CaCl_2$, and ETP determined. Subsequently, the anticoagulant effect of protamine alone (3μg/ml), APC alone (10nM) or protamine in the presence of APC were determined for wt-FVIII and the APCR-FVIII variant as before.

2.24: Determination of rate of FV activation

FV activation was determined using a method previously described by Safa *et al* [170]. Briefly, purified FV (100nM final concentration) was incubated with purified α-thrombin (1nM final concentration) in 100mM NaCl, 20mM HEPES (pH7.5), 5mM $CaCl_2$ and 0.2mg/mL BSA, or with purified FXa (final concentration 20nM) and phospholipid vesicles (final concentration, 80μM). At specific time intervals, aliquots were removed and diluted in 100nM NaCl and 20nM Tris-HCl (pH 7.5) to stop FV activation. The time course of FV activation was immediately quantified using FV-deficient plasma in a standard PT -based clotting assay.

CHAPTER 3: FUNCTIONAL EFFECT OF MODIFYING ACTIVATED PROTEIN C GLYCOSYLATION BY TREATMENT WITH SPECIFIC GLYCOSIDASES

3.1: Digestion of APC with PNGase F results in removal of N-linked glycan residues.

APC N-linked glycan modification may be achieved by enzymatic treatment with specific glycosidases or by elimination of glycosylation sites by site-directed mutagenesis. PNGase F removes all N-linked glycans residues by cleaving between the innermost GlcNAc and asparagine residues of oligosaccharides from N-linked glycoproteins. In order to assess the functional effect of complete APC N-linked glycan removal using PNGase F, it was first necessary to demonstrate that glycan groups had been successfully removed by this method.

APC or PNGase F-treated APC (APC-*DesGly*) were subjected to SDS-PAGE and Western blotting with a horse anti-protein C polyclonal antibody. Untreated APC migrated as a double band **(Figure 3.1 A)**. The molecular weight of each band was ~58 and 53 kDa respectively. These two bands have previously been designated α and β [168]. APC-*DesGly* migrated as a triple band, with molecular weights of ~53, 45 and 40 kDa respectively. The position of the top band corresponded to that of β-protein C **(Figure 3.1 A)**.

Attached carbohydrate moieties were also detected by Western blotting. After transferring to a PVDF membrane, carbohydrate groups were oxidised to aldehydes by

incubation of the membrane with 10mM sodium metaperiodate. Aldehydes were labelled with biotin hydrazide and detected with streptavidin-HRP. As expected, a dark band representing untreated APC was detected, demonstrating the presence of carbohydrate moieties. In contrast, the band corresponding to APC-*DesGly* was extremely faint and of a lower molecular weight than the APC band **(Figure 3.1 B)**, indicating that carbohydrate moieties had been removed. This was confirmed by subjecting APC or APC-DesGly to SDS-PAGE followed by specific carbohydrate detection with the Pro-Q Emerald® glycoprotein stain **(Figure 3.1 C)**. The band corresponding to APC-DesGly was not visible under UV light, again indicating that carbohydrate moieties had been removed.

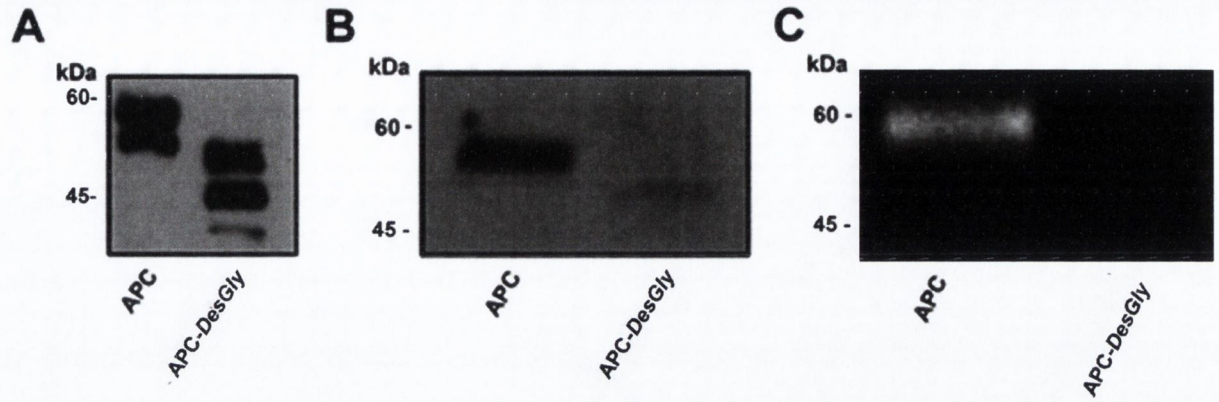


Figure 3.1: Removal of N-linked glycans from APC by enzymatic digestion with PNGase F.

APC (1µg) was incubated with PNGase F (1000 U) at 37°C for 1 hour. ***(A)*** APC or APC-*DesGly* (10ng) were subjected to SDS-PAGE on a 7.5% polyacrylamide Tris-HCl gel under non-reducing conditions. Western blotting was then performed in which APC was detected using a horse polyclonal anti-protein C antibody followed by a HRP-conjugated anti-horse IgG polyclonal antibody. ***(B)*** APC or APC-*DesGly* (500ng) were subjected to SDS-PAGE on a 7.5% polyacrylamide Tris-HCl gel and transferred onto a PVDF membrane. Carbohydrate moieties were oxidised to aldehydes by incubation of the membrane with 10mM sodium metaperiodate for 20 minutes and detected by incubation with a solution of 4µl 0.125 mM biotin hydrazide dissolved in 20ml of 100mM acetate buffer (ph 5.5) followed by streptavidin-HRP. ***(C)*** APC or APC-*DesGly* (100ng) were subjected to SDS-PAGE on a 7.5% polyacrylamide Tris-HCl gel. Carbohydrate moieties were oxidised by incubating the gel with periodic acid and detected by gel treatment with Pro-Q Emerald 300® glycoprotein stain followed by visualization under UV light.

3.2: PNGase F treatment of APC does not affect active site amidolytic activity.

The APC serine protease domain contains a catalytic triad of amino acids (His-57, Asp-102, Ser-195) that mediate substrate proteolysis. BIOPHEN CS-21(66) is a synthetic tripeptide chromogenic substrate (p-Glu-Pro-Arg-pNA.HCl) cleaved specifically by the APC active site. In order to determine whether removal of N-linked glycan moieties influences APC active site function, the rate of BIOPHEN CS-21(66) hydrolysis by APC or APC-*DesGly* was measured as an indicator of APC amidolytic function **(Figure 3.2)**. Amidolytic activity of untreated APC was measured at specific time points during a 7 hour incubation at 37° C with PNGase F **(Figure 3.2 A)**. Activity was found to decrease in a time-dependent manner to a minimum of 66 ±2.1 %. There was no significant difference between the activities of APC and APC-*DesGly* at each time point. The rate of BIOPHEN CS-21(66) (28.3-905 μg/ml) hydrolysis by APC and APC-*DesGly* was also measured. BIOPHEN CS-21(66) hydrolysis by APC increased in a concentration-dependent manner. No significant difference was observed in the rate of hydrolysis of APC or APC-*DesGly* at any BIOPHEN CS-21(66) concentration.

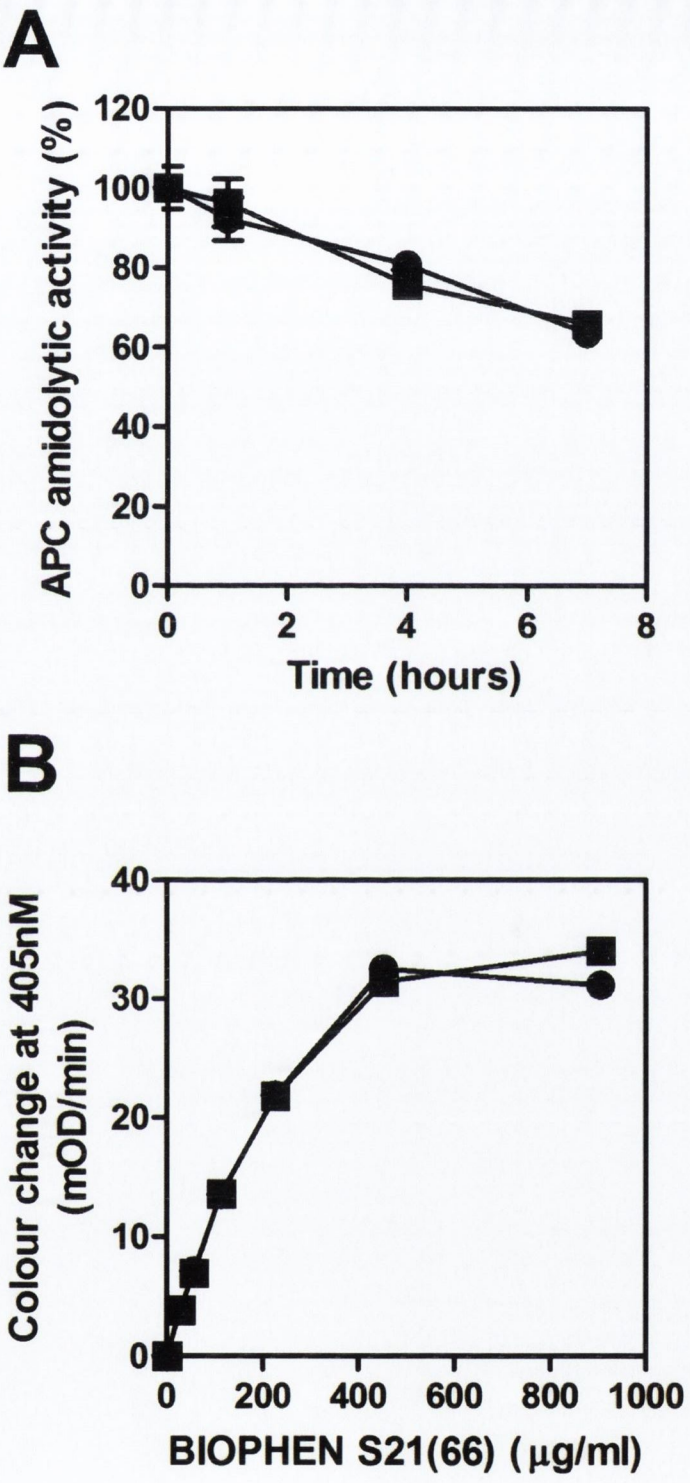

A
APC amidolytic activity (%)
120
100
80
60
40
20
0
0
2
4
6
8
Time (hours)
B
Colour change at 405nM (mOD/min)
40
30
20
10
0
0
200
400
600
800
1000
BIOPHEN S21(66) (µg/ml)

Figure 3.2: Chromogenic substrate hydrolysis by APC-*DesGly*.

(A) APC (1µg) was incubated with PNGase F (1000 U) at 37°C for 7 hours. Amidolytic activity of APC (●) or APC-*DesGly* (■; both 17.5nM) was determined by measuring the rate of hydrolysis of the APC-specific synthetic chromogenic substrate BIOPHEN CS-21(66) (2mg/ml) at 405nm. The reaction was carried out at room temperature in a buffer containing 100mM NaCl and 20mM Tris-HCl (pH 7.5) with 2.5mM $CaCl_2$ and 0.1mg/ml BSA. APC amidolytic activity was expressed as a percentage of APC activity measured prior to PNGase F incubation. ***(B)*** Hydrolysis by APC (●) or APC-*DesGly* (■) of Biophen CS21-(66) chromogenic substrate (28.3-905 µg/ml) was measured as above. All experiments were performed in triplicate. Results are expressed as mean ± standard error of the mean (SEM).

3.3: PNGase F treatment of protein C does not influence EPCR-dependent protein C activation on the surface of EA.hy926 cells.

An assay measuring protein C activation on the surface of EA.hy926 cells was used to assess the influence of removal of protein C N-linked glycans on activation by thrombin. APC generation was measured by determining the rate of cleavage of a chromogenic APC substrate **(Figure 3.3)**. The rate of untreated protein C (31.2-250nM) activation by thrombin increased in a concentration-dependent manner. The K_m for activation of untreated protein C was found to be 95±12 nM. No significant difference was observed between this and the K_m for APC-*DesGly* activation (77±9 nM).

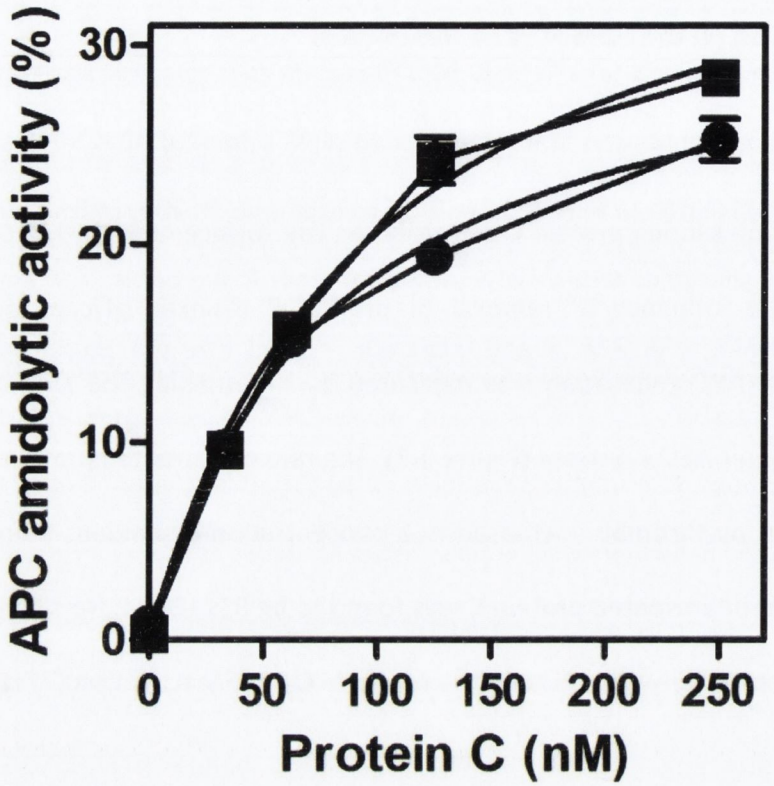


Figure 3.3: Activation of protein C-*DesGly* on the surface of endothelial cells.

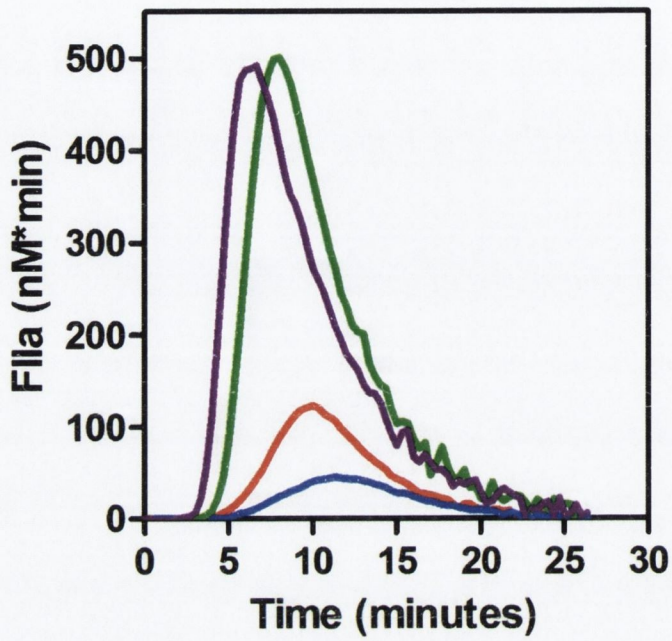
(A) Protein C activation on the surface of EA.hy926 cells was assessed. Protein C (4.3 µg) was incubated with PNGase F (375 U) at 37°C for 4 hours. Protein C (●) or protein C-*DesGly* (■; both 31.2-250nM) in HBSS with 3mM $CaCl_2$ and 0.6mM $MgCl_2$ were incubated in each well at 37°C. Protein C activation was initiated with thrombin (5.6nM) for 30 minutes. The reaction was stopped with hirudin (135nM). Protein C activation was measured by hydrolysis of APC chromogenic substrate BIOPHEN CS-21(66) (2mg/ml) as before. All experiments were performed in triplicate. Results are expressed as mean ± SEM.

3.4: PNGase treatment of APC results in enhanced anticoagulant function.

Recombinant APC variants lacking protease domain glycosylation sites have been shown to prolong plasma clotting times more than equivalent concentrations of wild-type APC [101]. In order to more fully characterize the effect of N-linked glycan removal on APC anticoagulant fuction, a TF-initiated thrombin generation assay in protein C-deficient plasma was utilized (2.8) **(Figure 3.4)**. Initiation of coagulation with 5 pM soluble TF and $CaCl_2$ (16.67mM final concentration) resulted in a rapid increase in thrombin generation **(Figure 3.4 A)**. As expected, APC (10nM) attenuated thrombin generation, reducing peak thrombin generated by ~3.8-fold. However, an identical concentration of APC-*DesGly* exhibited enhanced ability to attenuate thrombin generation in comparison with untreated APC. A similar PNGase concentration to that introduced by 10nM APC-*DesGly* had no effect upon thrombin generation.

In order to determine the magnitude of the enhanced anticoagulant effect observed following removal of APC N-linked glycans with PNGase, the area under a graph of thrombin generated over time (ETP) was measured **(Figure 3.4 B)**. As expected, APC (2.5-20nM) produced a concentration-dependent anticoagulant effect in protein C-deficient plasma. At 5nM APC, ETP was attenuated to 47±4.2% of its value prior to APC treatment. An identical concentration of APC-*DesGly* attenuated ETP to 27±1.4%, representing a 1.7-fold gain in anticoagulant function in response to N-linked glycan removal. A significant gain in anticoagulant function was observed at all concentrations of APC-*DesGly* compared with untreated APC.

A


500
400
300
200
100
0
FIIa (nM*min)
0
5
10
15
20
25
30
Time (minutes)

B

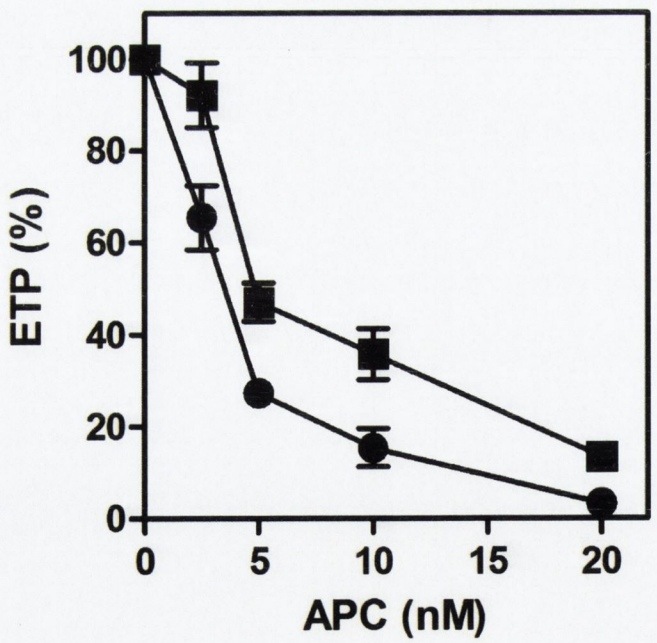

100
80
60
40
20
0
ETP (%)
0
5
10
15
20
APC (nM)

Figure 3.4: Anticoagulant function of APC-*DesGly*.

(A) The anticoagulant activity of APC (*red*) or APC-*DesGly* (*blue*; both 10nM) was assessed in protein C-deficient plasma using a thrombin generation assay. Plasma was incubated with phospholipid vesicles (4μM; 60% phosphatidylcholine, 20% phosphatidylserine and 20% phosphatidylethanolamine) in the presence and absence of APC. Thrombin generation was initiated with 5pM sTF and 100mM $CaCl_2$ and measured by comparing rate of fluorogenic substrate hydrolysis to a thrombin standard. (Protein C-deficient plasma; *green*, plasma with 1160 U/ml PNGase; *purple*. ***(B)*** APC (■) and APC-*DesGly* (●; 2.5-20nM) were incubated with protein C-deficient plasma. Thrombin generation was initiated as outlined above, and endogenous thrombin potential (ETP) (which represents area under a graph of thrombin generation) was calculated. All experiments were performed in triplicate.

3.5: PNGase treatment of APC does not influence its rate of inactivation in normal pooled plasma.

APC is inhibited in plasma by serpins protein C inhibitor (PCI) and α-1 antitrypsin. Inhibition is stimulated by heparin [171]. In order to determine whether the observed gain in anticoagulant function following APC deglycosylation is mediated by enhanced inactivation by inhibitors, APC or APC-*DesGly* were incubated in plasma for one hour and APC activity (% of amidolytic activity measured prior to plasma incubation) was measured. APC and APC-*DesGly* were rapidly inhibited in a time-dependent manner. No significant difference was observed between the half-lives of APC (2.0 minutes; 95% confidence interval 1.33-3.9) or APC-*DesGly* (3.5 minutes; 95% confidence interval 2.16-9.3) **(Figure 3.5)**.

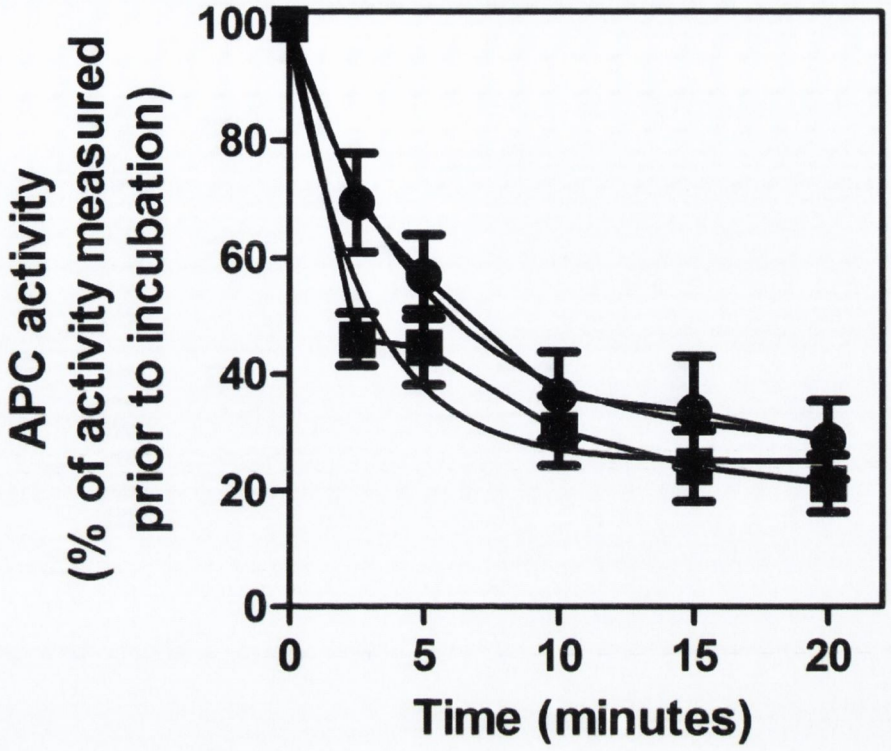


Figure 3.5: Inhibition of APC-*DesGly* in normal plasma.

The activity of APC (●) or APC-*DesGly* (■; both 20nM) was determined upon incubation with normal platelet-poor pooled plasma in the presence of heparin (10 U/ml) at 37°C. APC activity was determined by measuring rate of hydrolysis of the APC-specific synthetic chromogenic substrate BIOPHEN CS-21(66) as before. Experiment was performed in triplicate. Results are expressed as mean ± SEM.

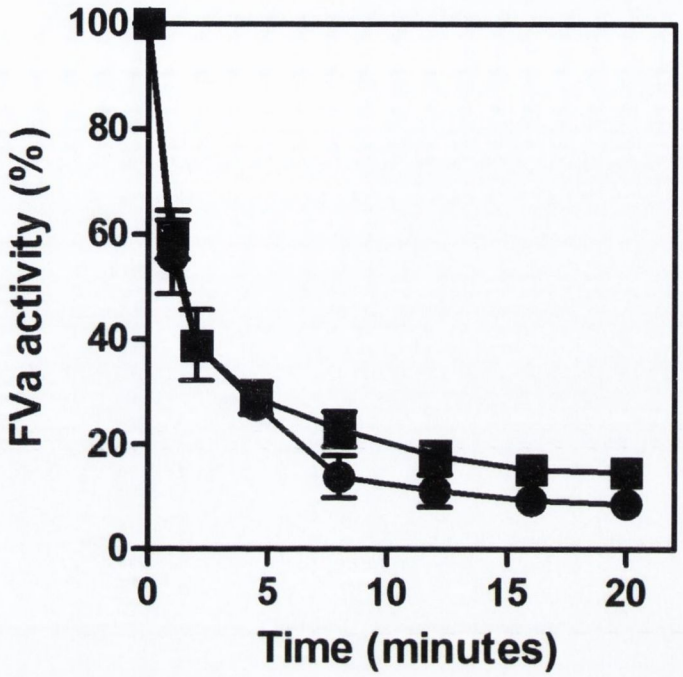
3.6: Enhancement of APC anticoagulant function by PNGase treatment is not mediated by increased rate of substrate proteolysis.

To assess whether FVa proteolysis is affected by N-linked glycan removal, an assay measuring APC-mediated FVa proteolysis in the presence and absence of protein S was performed **(Figure 3.6)**. In the absence of protein S, both APC and APC-*DesGly* (2nM) proteolysed FVa in a time-dependent manner **(Figure 3.6 A)**. 50% FVa proteolysis was observed after 2 minutes in the presence of both APC and APC-*DesGly*. No significant difference was observed in the rate of FVa proteolysis by APC or APC-*DesGly* at any time point.

In a modification of this assay **(Figure 3.6 B)**, protein S (3.1-50nM) stimulated FVa proteolysis by APC (2nM) in a concentration-dependent manner. No significant difference was observed at any protein S concentration between APC and APC-*DesGly* mediated FVa proteolysis.

Collectively, these data show that N-linked glycan removal from APC does not modulate rate of FVa proteolysis, and that the observed enhancement in anticoagulant function is mediated by an alternative mechanism.

A


100
80
60
40
20
0
FVa activity (%)
0
5
10
15
20
Time (minutes)

B

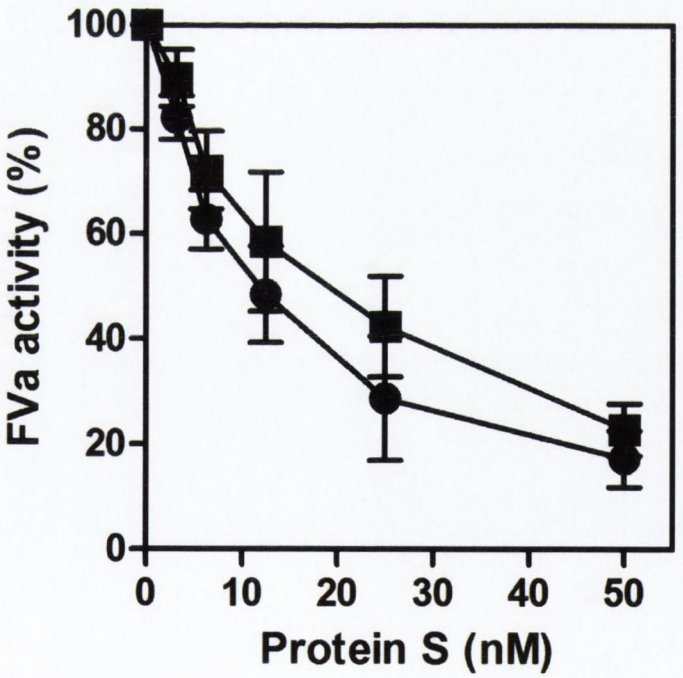

100
80
60
40
20
0
FVa activity (%)
0
10
20
30
40
50
Protein S (nM)

Figure 3.6: FVa proteolysis by APC-*DesGly*.

(A) FVa (1nM) was incubated with phospholipid vesicles (20μM; 60% dioleoyl-phosphatidylcholine (DOPC), 20% dioleoyl-phosphatidylserine (DOPS) and 20% dioleoyl-phosphatidylethanolamine (DOPE)) at 37°C in a buffer containing 40mM Tris-HCl, 140mM NaCl, 3mM $CaCl_2$ and 0.3% w/v BSA. FVa proteolysis was initiated by addition of APC (●) or APC-*DesGly* (■; 2nM). Timed aliquots were removed into a prothrombinase mixture containing 1nM FXa, 500nM prothrombin and 25μM phospholipids as above. Each prothrombinase reaction was stopped after 3 minutes by addition of 5μl ice-cold 0.5M EDTA. FVa activity was determined at each time point by adding 50μl of each prothrombinase reaction mix to 50μl of a thrombin-specific chromogenic substrate (BIOPHEN CS-01(38); 1mg/ml) and measuring thrombin-dependent colour change at 405nm. ***(B)*** FVa (7nM) was incubated with phospholipid vesicles (20μM; 60% DOPC, 20% DOPS and 20% DOPE) and protein S (3.1-50nM) at 37°C as above. FVa proteolysis was initiated by addition of APC (●) or APC-*DesGly* (■; 2nM). Aliquots were removed into a prothrombinase reaction mixture containing 0.75nM FXa, 500nM prothrombin and 25μM phospholipids as above. Each second reaction was stopped after 3 minutes by addition of ice-cold 0.5M EDTA and FVa activity determined as above. All experiments were performed in triplicate. Results are expressed as mean ± SEM.

3.7: PNGase treatment of APC results in enhanced EPCR/PAR1-dependent endothelial barrier protection

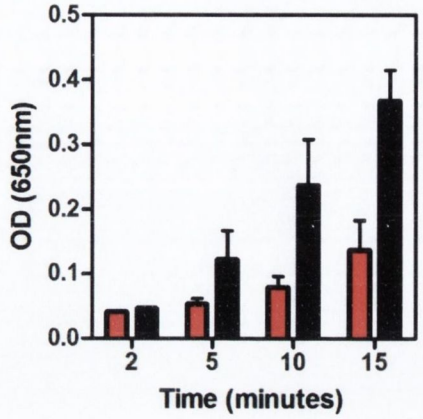
In order to assess the effect of N-linked glycan removal upon APC-mediated cytoprotective function, endothelial cell barrier permeability was assessed. In this assay, APC protects against thrombin-induced permeability in an EPCR and PAR-1 dependent manner. Thrombin was associated with a time-dependent increase in endothelial cell barrier permeability **(Figure 3.7 A)**, determined by measuring OD at 650 nm of aliquots from the outer chamber of a two-chamber compartment separated by a layer of EA.hy926 cells following application of Evans blue dye to the inner chamber. At 15 minutes, OD at 650 nm of non- thrombin treated and thrombin treated wells was 0.37±0.05 and 0.14±0.05 respectively.

As expected, pre-incubation with APC (10nM) protected cells against thrombin induced permeability **(Figure 3.6 B)**. Permeability was reduced to 59±7% of thrombin-treated wells in the presence of APC (10nM). Remarkably, an identical concentration of APC-*DesGly* resulted in greatly enhanced protection against thrombin-induced permeability compared with untreated APC. APC-*DesGly* reduced permeability to 26±4% of thrombin-treated wells. The protective effect of both APC and APC-*DesGly* was ablated by the presence of the function blocking anti-EPCR antibody, RCR-252, indicating that the enhanced signalling effect is dependent upon EPCR binding by APC. Neither PNGase F nor Protac had any effect upon endothelial permeability at concentrations used in this assay.

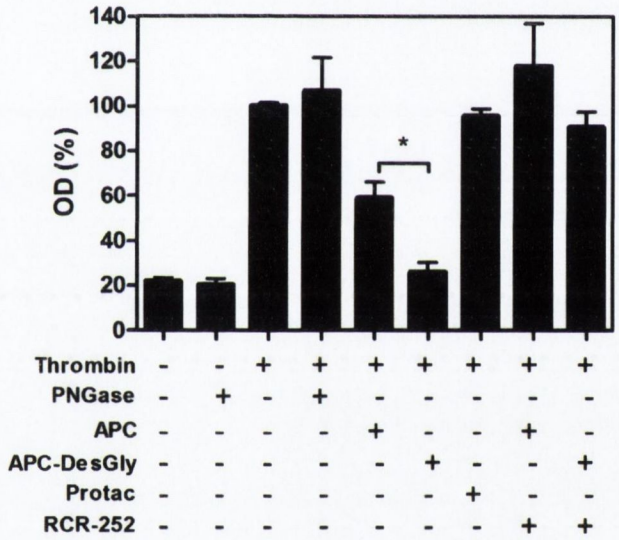
In order to further characterize the magnitude of the enhanced protective effect against thrombin-induced permeability observed upon PNGase treatment, cells were

pre-incubated with APC or APC-*DesGly* (1.25-20nM) **(Figure 3.7 C)**. As expected, APC mediated a concentration-dependent protection against thrombin-induced permeability. However, APC-*DesGly* (2.5-20nM) was associated with significantly enhanced protection. Half-maximal protection was observed at 9.85nM APC and 1.71nM APC-*DesGly* respectively, representing an approximately six-fold enhanced protective effect.

A


0.5
0.4
0.3
0.2
0.1
0.0
OD (650nm)
2
5
10
15
Time (minutes)

B


140
120
100
80
60
40
20
0
OD (%)
*
Thrombin - - + + + + + + +
PNGase - + - + - - - - -
APC - - - - + - - + -
APC-DesGly - - - - - + - - +
Protac - - - - - - + - -
RCR-252 - - - - - - - + +

C

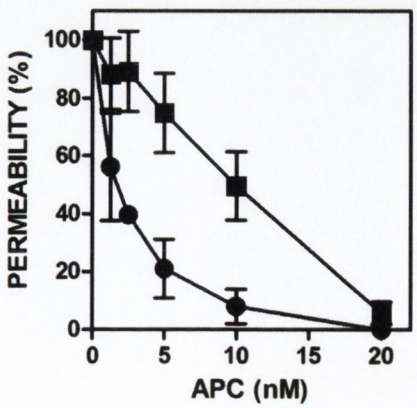

100
80
60
40
20
0
PERMEABILITY (%)
0
5
10
15
20
APC (nM)

Figure 3.7: EPCR/PAR-1 dependent endothelial barrier protective function of APC-*DesGly*.

(A) EA.hy926 cells were grown to confluence on polycarbonate membrane permeable supports (3μM pore size, 12 mm diameter) and treated with thrombin (5nM) for 10 minutes. The cells were then washed and incubated with 0.67 mg/ml Evans Blue with 4% BSA. Evans Blue-BSA transmigration into the outer chamber is dependent upon endothelial barrier permeability and was determined by measuring absorbance at 650 nm of outer chamber aliquots. (No thrombin; *pink*, thrombin (5nM); *black*). ***(B)*** Confluent EA.hy926 cells were treated with APC or APC-*DesGly* (both 10nM); in the presence and absence of the monoclonal anti-EPCR antibody RCR-252 (25μg/ml) for 3 hours in serum-free media supplemented with 3mM $CaCl_2$ and 0.6mM $MgCl_2$ prior to thrombin treatment. In additional control wells, cells were treated with PNGase (105 U/ml) or Protac (0.065 IU/ml) for three hours in place of APC. Permeability was determined (2.14). ***(C)*** Endothelial permeability was measured with APC (●) or APC-*DesGly* (■; both 1.25-20nM) as described in **2.14**. All experiments were performed in triplicate. Results are expressed as mean ± SEM.

3.8: Assessment of endothelial cell apoptosis by TUNEL staining and flow cytometry.

In order to investigate the effect of APC N-linked glycan removal upon EPCR/PAR 1-dependent anti-apoptotic signalling, staurosporine-induced endothelial cell apoptosis in EA.hy926 cells treated with APC was assessed **(2.15)**. TUNEL staining was performed upon fixed cells and the percentage of apoptotic cells was quantified by flow cytometry **(Figure 3.8)**. Negative control wells (EA.hy926 cells incubated for 7 hours in serum-free media) were found to have an apoptosis rate of 27±3.5% as determined by flow cytometry. In contrast, staurosporine (20μM)-treated wells were determined to have 68±3.8% apoptotic cells. This difference was found to be statistically significant ($p<0.05$). Pre-incubation of EA.hy926 cells with APC (2.5-20nM) for 3 hours prior to staurosporine treatment for 4 hours resulted in a dose-dependent reduction in the percentage of apoptotic cells. At 20nM APC, a statistically significant decrease in apoptosis rate was observed compared with cells treated with staurosporine alone ($p<0.05$). At this APC concentration, 40%±5 apoptotic cells were detected.

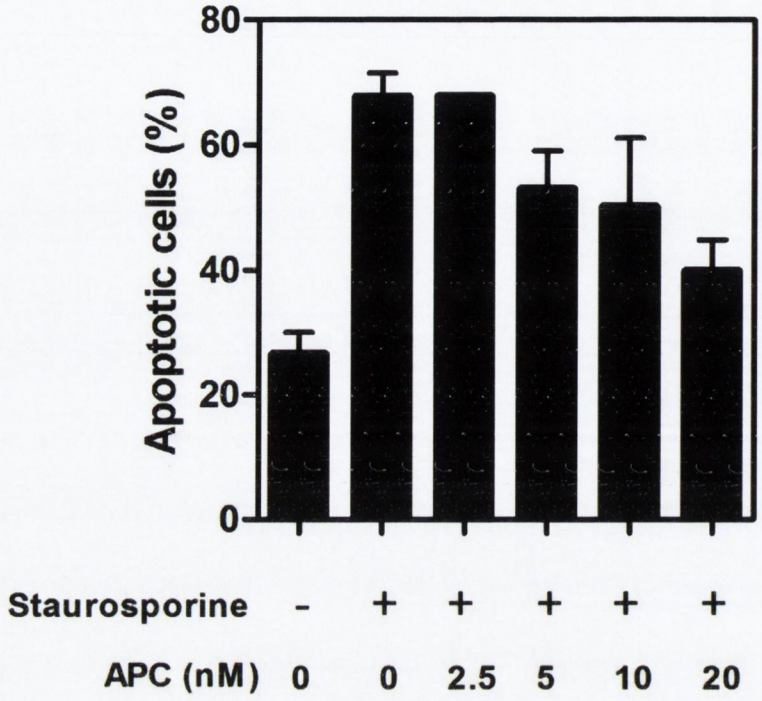


Figure 3.8: Assessment of endothelial cell apoptosis by flow cytometry

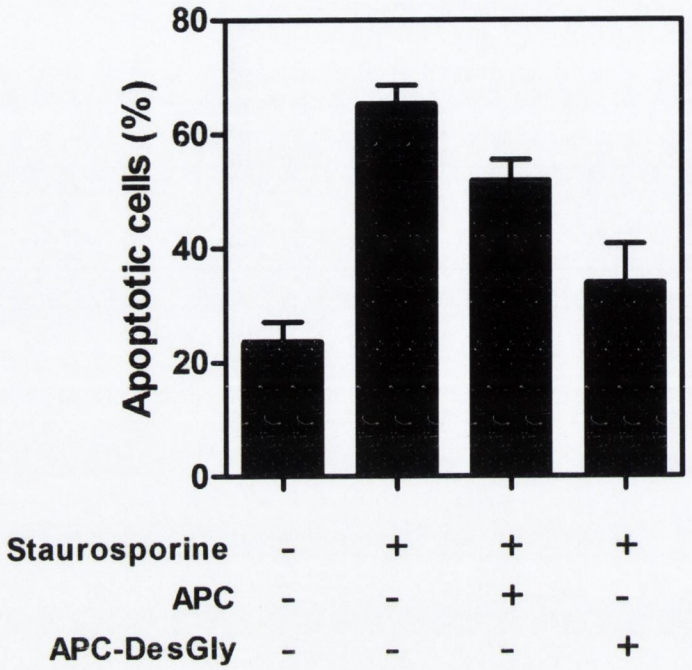
EA.hy926 cells in 6-well plates were treated with APC (2.5-20nM) for 3 hours **(2.15)**. Apoptosis was then induced by incubation with staurosporine (20μM) for 4 hours. Cells were trypsinized and fixed by incubation with 1% paraformaldehyde in PBS (pH 7.4) on ice followed by 70% ice-cold ethanol. Fixed cells were incubated with bromolated dUTP (Br-dUTP) (APO-BRDU, Phoenix Flow Systems, San Diego) followed by a fluoroscein labelled anti-Br-dU monoclonal antibody to detect apoptotic cells. Total cellular DNA was then detected by incubation with propidium iodide (PI) / RNase A. Apoptotic cells (stained with PI and anti-Br-dU) and non-apoptotic cells (stained with PI only) were detected by flow cytometry as separate populations. Apoptotic cells were expressed as a percentage of total cells. All experiments were performed in triplicate. Results are expressed as mean ± SEM.

3.9: PNGase treatment of APC results in improved protective signalling against staurosporine-induced apoptosis.

Having established an assay to measure staurosporine-induced apoptosis in endothelial cells by flow cytometry, this assay was utilized to investigate the effect of N-linked glycan removal upon EPCR/PAR 1-dependent anti-apoptotic signalling by APC. In an assay of staurosporine-induced apoptosis measured by TUNEL staining with flow cytometry detection **(Figure 3.9 A) (2.15)**, APC (5nM) resulted in a 13.4±3.8% reduction in apoptotic cells compared with staurosporine-treated wells. An identical concentration of APC-*DesGly* resulted in a decrease in the observed percentage of apopotic cells (absolute apoptosis rate 33.9±7% compared with 51.8±4% in APC-treated wells), however this difference did not reach statistical significance.

In order to further characterize the effect of N-linked glycan removal upon APC anti-apoptotic function in endothelial cells, an assay of pro/anti-apoptotic gene expression in response to staurosporine-induced apoptosis was utilized **(2.16) (Figure 3.9 B)**. As expected, staurosporine increased *Bax/Bcl-2* gene expression ratio relative to β-actin, as measured by RT-PCR. APC-*DesGly* demonstrated ~ 2 fold enhanced anti-apoptotic signalling compared with an identical concentration of APC ($p<0.05$).

A


80
60
40
20
0
Apoptotic cells (%)
Staurosporine - + + +
APC - - + -
APC-DesGly - - - +

B

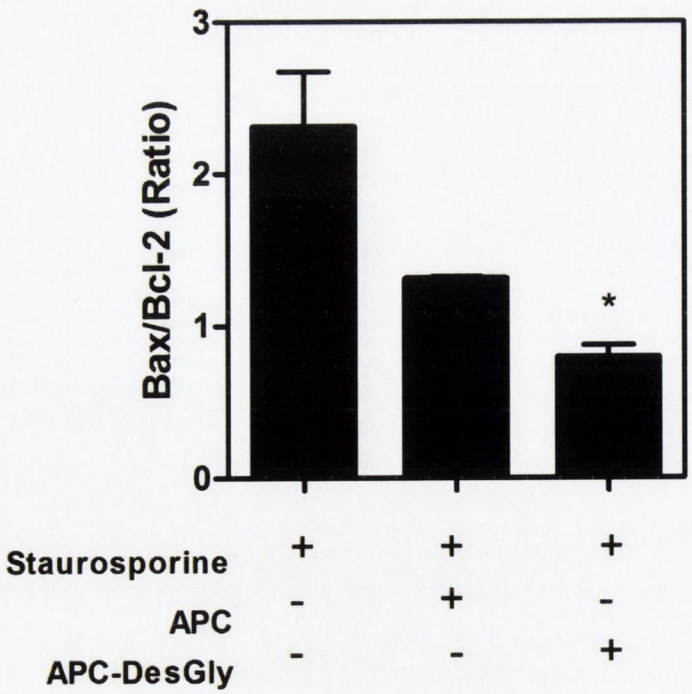

3
2
1
0
Bax/Bcl-2 (Ratio)
*
Staurosporine + + +
APC - + -
APC-DesGly - - +

Figure 3.9: Inhibition of staurosporine-induced apoptosis on EA.hy926 cells by APC-*DesGly*.

EA.hy926 cells were treated with APC or APC-*DesGly* for 3 hours **(2.15)**. Apoptosis was induced by incubation with staurosporine (20μM) for 4 hours. ***(A)*** The percentage of apoptotic cells following treatment with APC (5nM) then staurosporine was measured by flow cytometry using TUNEL staining **(2.15)**. ***(B)*** Following APC (10nM) and staurosporine treatment, cells were trypsinized and RNA extracted **(2.16)**. Reverse transcription followed by RT-PCR was performed using *Bax*, *Bcl-2* and *β-actin* Taqman® gene expression assays (Applied Biosystems). Apoptosis was measured by determining the *Bax/Bcl2* ratio (relative to β-actin) for APC treated cells and plotting it as a percentage of the mean staurosporine-treated *Bax/Bcl-2* ratio (100% apoptosis). (* $P<0.05$, unpaired 2-tailed student's *t* test performed). All experiments were performed in triplicate. Results are expressed as mean ± SEM.

3.10: α2-3,6,8,9 neuraminidase treatment of APC has no effect upon amidolytic or anticoagulant activity.

Having demonstrated that complete N-linked glycan removal influences APC anticoagulant function, the effect of removing negatively charged sialic acid residues from APC (1μg) by digestion with α2-3,6,8,9 neuraminidase (0.01U) was investigated. Following enzymatic digestion with neuraminidase, APC and neuraminidase-treated APC (*Asialo*-APC) were characterized by SDS-PAGE and western blotting with terminal sialic acid labelling **(Figure 3.10 A)**. The latter was achieved by limited oxidation of carbohydrate groups to generate terminal aldehyde moieties using sodium metaperiodate (10mM) followed by labelling of aldehydes with biotin hydrazide and detection with streptavidin-HRP. A clear band was visualised in the lane containing untreated APC, indicating the presence of sialic acid groups. In contrast, the band representing *Asialo*-APC was not visible, demonstrating that sialic acid moieties had been removed.

In order to investigate the effect of sialic acid removal on APC amidolytic activity, rate of hydrolysis of the APC chromogenic substrate, BIOPHEN CS-21(66), was measured **(Figure 3.10 B)**. No significant difference was observed between the Vmax (mOD/min) measured for BIOPHEN CS-21(66) hydrolysis by untreated APC and *Asialo*-APC (both 17.5nM; Vmax 18.5±1.2 and 18.6±0.3 respectively).

To determine whether sialic acid removal influences APC anticoagulant function, a TF-initiated thrombin generation assay in protein C-deficient plasma was utilized **(2.8)** **(Figure 3.10 C and D)**. Initiation of coagulation with 5 pM soluble TF and 16.67mM

$CaCl_2$ resulted in a rapid increase in thrombin generation **(Figure 3.10 C)**. As expected, APC (10nM) attenuated thrombin generation. An identical concentration of *Asialo*-APC attenuated thrombin generation similarly to untreated APC. In order to quantify the anticoagulant effect observed in the presence of APC and *Asialo-APC*, ETP was measured **(Figure 3.10 D)**. In the presence of APC and *Asialo*-APC (both 10nM), ETP was attenuated to 27±9.5 and 36±6 % respectively. Collectively, these data indicate that sialic acid removal from APC does not influence amidolytic or anticoagulant function.

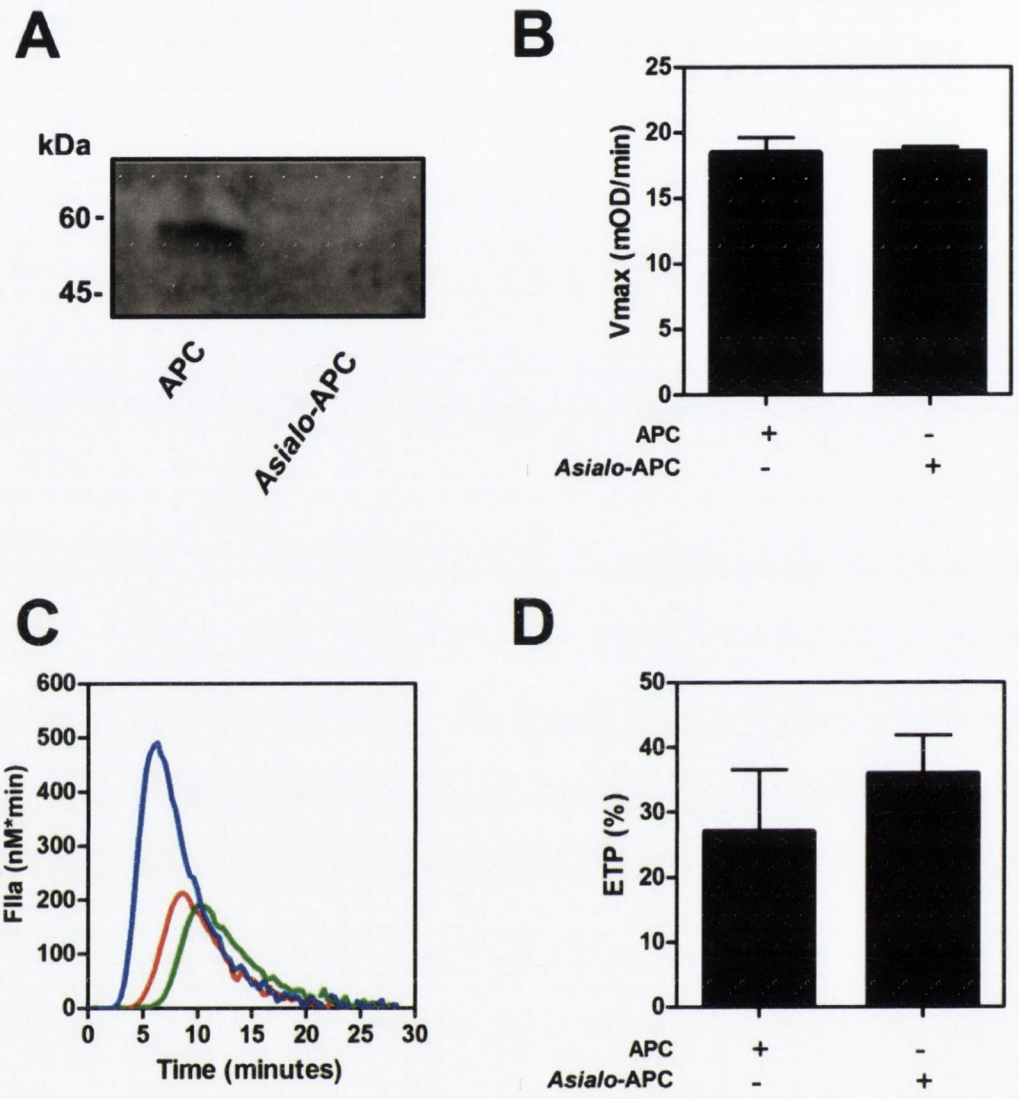

A
kDa
60-
45-
APC
Asialo-APC
B
Vmax (mOD/min)
25
20
15
10
5
0
APC + -
Asialo-APC - +
C
FIIa (nM*min)
600
500
400
300
200
100
0
0 5 10 15 20 25 30
Time (minutes)
D
ETP (%)
50
40
30
20
10
0
APC + -
Asialo-APC - +

Figure 3.10: Sialic acid removal from APC by enzymatic digestion with α2-3,6,8,9 neuraminidase.

APC (1μg) was incubated with neuraminidase isolated from arthrobacter ureafaciens (0.01 U) for 1 hour in order to remove terminal sialic acid residues. ***(A)*** APC or *Asialo*-APC (500ng) were subjected to SDS-PAGE on a 7.5% polyacrylamide Tris-HCl gel and transferred onto a PVDF membrane. Terminal sialic acid moieties were oxidised to aldehydes by incubation of the membrane with 10mM sodium metaperiodate for 20 minutes in darkness on ice and detected by incubation with a solution of 4μl 5.0 mM biotin hydrazide dissolved in 20ml of 100mM acetate buffer (ph 5.5) followed by streptavidin-HRP. ***(B)*** Amidolytic activity of APC or *Asialo*-APC (both 17.5 nM) was determined by measuring the rate of hydrolysis of the APC-specific synthetic chromogenic substrate BIOPHEN CS-21(66) (2mg/ml) at 405nm as before. ***(C)*** The anticoagulant activity of APC (*red*) or *Asialo*-APC (*green*; both 10nM) was assessed in protein C-deficient plasma (blue) using a thrombin generation assay (2.8) ***(D)*** APC and AsialoAPC were incubated with protein C-deficient plasma. Thrombin generation was initiated as above and ETP calculated **(2.8)**.

3.11: Removal of sialic acid moieties from APC does not affect EPCR and PAR-dependent barrier protective properties.

Having demonstrated enhanced APC endothelial barrier protection following removal of total N-linked glycans, it was hypothesized that removal of terminal sialic acid moieties might also influence APC signalling. An assay of endothelial barrier permeability **(2.14)** was utilized to measure the influence of sialic acid removal upon APC-mediated EPCR/PAR1-dependent endothelial barrier protective properties **(Figure 3.11)**. As expected, both APC and *Asialo*-APC mediated a concentration-dependent protection against thrombin-induced permeability. No significant difference was observed between APC or *Asialo*-APC mediated endothelial barrier protection at any concentration measured.

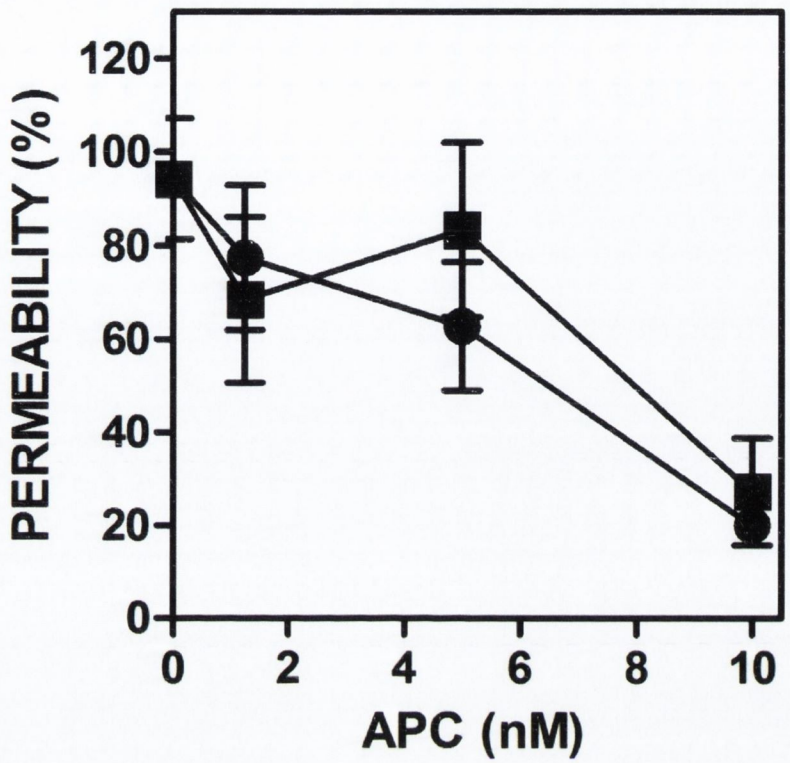


Figure 3.11: EPCR/PAR-1 dependent endothelial barrier protective function of *Asialo*-APC.

(A) APC (●) and *Asialo*-APC (■; both 1.25-10nM) were incubated with EA.hy926 cells grown on polycarbonate membrane permeable supports for 3 hours in serum free media supplemented with 3mM $CaCl_2$ and 0.6mM $MgCl_2$. Permeability was determined **(2.14)**. All experiments were performed in triplicate. Results are expressed as mean ± SEM.

CHAPTER 4: MODIFICATION OF ACTIVATED PROTEIN C GLYCOSYLATION BY SITE-DIRECTED MUTAGENESIS

4.1: Generation of recombinant protein C cDNA glycosylation site variants.

In order to generate recombinant protein C N-linked glycosylation site variants, four vectors encoding mutant human protein C were created by site-directed mutagenesis of a plasmid encoding wild type human protein C (pRc/CMV/PC). Each mutation generated a mutant protein C cDNA that encodes one of four *N*-linked glycosylation sites (Asn-97, Asn-248, Asn-313 and Asn-329) **(2.18.2).** Pairs of mutagenic oligonucleotide primers encoding asparagine (*N*) to glutamine (*Q*) substitutions were prepared **(Appendix II.I)** and used to create protein C cDNA mutants via PCR site-directed mutagenesis **(Figure 4.1 A)**. Mutant plasmids were transformed into competent NovaBlue Singles® *E. coli* cells and isolated using a plasmid miniprep kit. The presence of the introduced mutation and absence of aberrant base changes was confirmed by sequencing the entire PC cDNA in each preparation. DNA preparations corresponding to each protein C mutant were used to transfect HEK 293 cells.

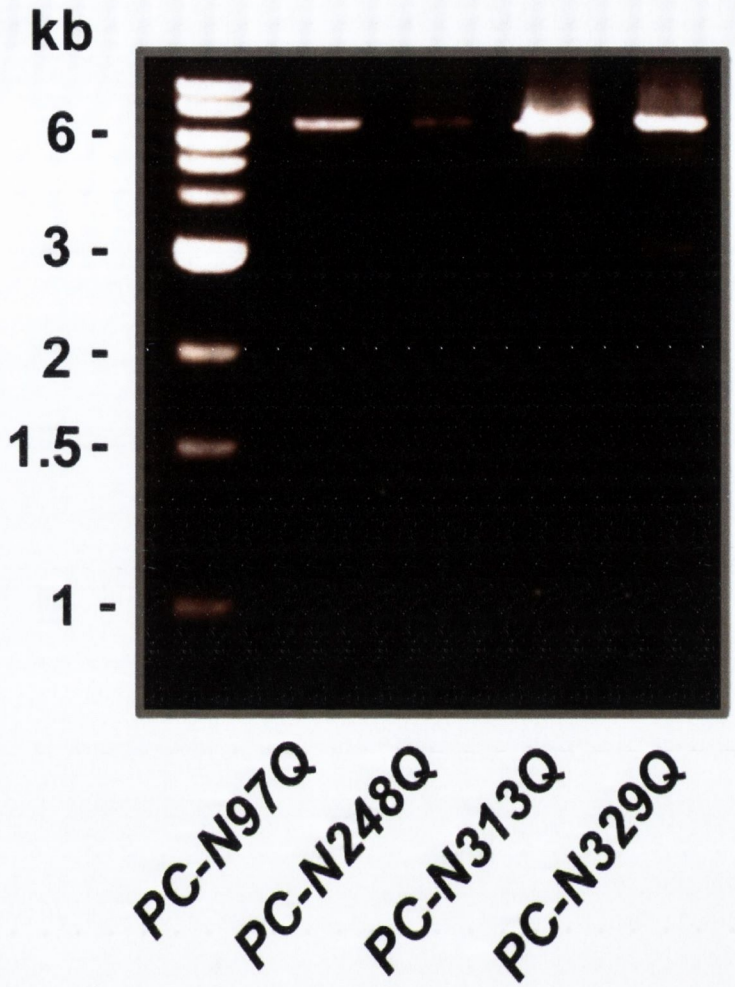


Figure 4.1: Generation of recombinant N-linked glycan variants of a protein C cDNA plasmid.

Oligonucleotide primers were synthesized for mutagenesis of WT-protein C in the pRc/CMV vector to variants N97Q, N313Q, N248Q and N329Q **(2.18.2)**. This was achieved by polymerase chain reaction (PCR) using the QuickChange® site-directed mutagenesis kit (Stratagene). Replicant vectors containing protein C glycosylation site mutations were generated. Mutagenesis products were subjected to electrophoresis at 75 V for 30 minutes on a 1% agarose gel containing 5µg/ml ethidium bromide. DNA bands were visualised using a UV lightbox and photographed.

4.2: Stable expression of recombinant protein C *N*-linked glycosylation site variants.

Plasmids encoding wild-type protein C and individual protein C glycosylation site variants and were used to transfect HEK 293 cells **(2.19.2)**. The pRc/CMV/PC cDNA plasmid contains a neomycin-resistance gene for selection using G418 sulphate **(2.18.1)**, a neomycin analogue. Neomycin caused cell death in ~14 days in untransfected cells. Colonies arising from transfection with each plasmid were picked **(2.19.2)**. A protein C ELISA **(2.19.3)** was used to measure the concentration of protein C in growth media from each colony. Wild-type protein C and variants *N248Q, N313Q* and *N329Q* were expressed between 0.7-1.2 μg/ml per day. Interestingly, despite repeated efforts, no protein expression was detected from HEK-293 cells transfected with the pRC/CMV/PC-*N97Q* vector, confirming that N-linked glycosylation at this site is critical for protein C processing and expression [101].

HEK-293 cells expressing recombinant wild type and variant protein C were expanded, then incubated with serum-free conditioned media for 3-5 days in the presence of Vitamin K_1. At this point, medium was collected. Each recombinant protein C was concentrated to 50ml by filtration using a Pellicon™ XL tangential flow filter device (Millipore) and purified using anion-exchange chromatography **(2.19.4)**. Partial purification of protein C variants was then performed. First, concentrated medium was desalted by buffer exchange into 20mM Tris-HCl (pH 7.4) containing 150mM NaCl using a Fast Performance Liquid Chromatography (FPLC) system (GE Healthcare). Next, γ-carboxylated protein C was partially purified by passing desalted medium over a 5ml HiTrap Q HP sepharose anion exchange column (GE Healthcare) and eluting against a

0-30mM $CaCl_2$ gradient. Calcium-eluted fractions were collected. Concentration was achieved by eluting against 1M NaCl. Samples were again desalted by buffer exchange into 20mM Tris-HCl (pH 7.4) containing 150mM NaCl. This procedure increased the concentration of recombinant protein C variants ~ 50-60 fold, and resulted in fully γ-carboxylated recombinant protein C.

Upon isolation, each recombinant wild type and variant protein C was characterized by reducing 7.5% SDS-PAGE followed by then Western blotting **(Figure 4.2)**. Recombinant protein C was detected using a sheep anti-protein C polyclonal antibody **(Figure 4.2 A)**. Wild type protein C heavy chain migrated at ~35 kDa. Its two bands represent protein C heavy chain glycoforms α and β [101]. The molecular weight of each recombinant protein C N-linked glycan variant band was reduced by 5-10 kDa compared with wild-type protein C. Each protein C variant band was represented by a single major band, probably due to loss of an individual N-linked glycan chain. A second faint band was observed in the protein C *N248Q* preparation. This likely represents protein C lacking glycosylation at positions 248 and 329 (due to the introduced *N248Q* mutation in naturally occurring β protein C). Interestingly no second faint band was visualized in the protein C *N313Q* preparation, perhaps due to the detection limit of the technique. To assess γ-carboxylation of each recombinant protein C, wild type and variant protein C were immunoblotted using an anti-Gla antibody that recognises the presence of Gla amino acids in the absence of Ca^{2+} ions [172]. As expected, bands of equivalent density were observed for both wild type and variant protein C, indicating normal γ-carboxylation in each protein C preparation **(Figure 4.2 B)**. As samples were reduced, all bands were of equal molecular weight, as

Gla residues are present in the protein C light chain, while N-linked glycosylation alterations had been introduced in the protein C heavy chain.

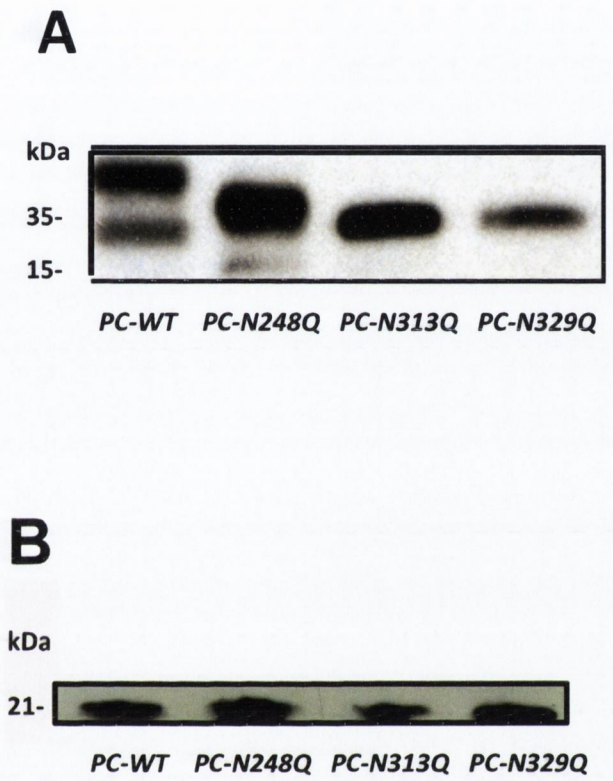


Figure 4.2: Characterization of recombinant protein C *N*-linked glycan variants by SDS-PAGE/Western blotting.

Wild type and recombinant protein C variants (*PC-N248Q, PC-N313Q, PC-N329Q*) were reduced using β-mercaptoethanol and subjected to 7.5% SDS-PAGE. Western blotting was performed, in which each protein C variant was detected using either ***(A)*** a polyclonal sheep anti-protein C antibody or ***(B)*** a polyclonal antibody specific to protein C Gla residues.

4.3: Anticoagulant function of protein C variants generated by site-directed mutagenesis of protein C heavy chain *N*-linked glycan attachment sites.

To determine whether removal of individual N-linked glycan chains influences anticoagulant function, wild type and variant zymogen protein C preparations were activated with Protac **(2.5)**. In order to characterize the effect of individual N-linked glycan chain removal on APC anticoagulant fuction, the anticoagulant activity of each recombinant APC preparation was assessed in a TF-initiated thrombin generation assay using protein C-deficient plasma **(2.8)**. As expected, wild type APC (2.5-10nM) produced a concentration-dependent attenuation of thrombin generation **(Figure 4.3)**, resulting in reduction in thrombin generation to 38±2%. This degree of anticoagulant activity is similar to that described previously in our laboratory, confirming the structural and functional integrity of the recombinant APC. While minor differences in anticoagulant activity were observed between wild type APC and APC-*N329Q*, these differences did not reach statistical significance. APC-*N248Q* and APC-*N313Q* possessed mildly decreased anticoagulant activity compared with wild type APC. At 5nM, wild type APC resulted in attenuation of thrombin generation to 57±3. Identical concentrations of APC-*N248Q* and APC-*N313Q* reduced thrombin generation to 75±0.3% and 76±2% respectively; $p<0.05$.

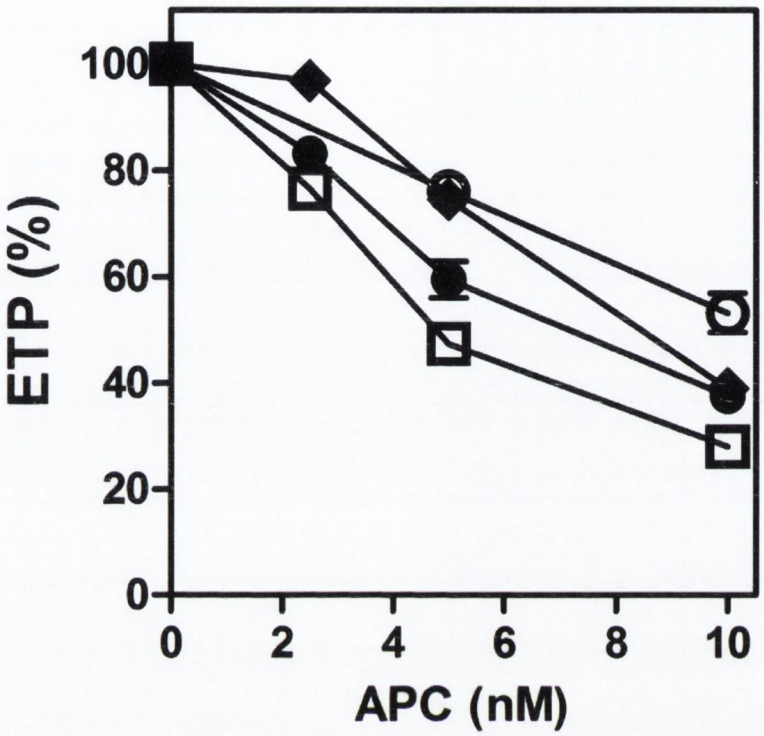


Figure 4.3: APC anticoagulant function following removal of protein C *N*-linked glycan attachment sites at Asn-248, Asn-313 or Asn-329 by glutamine substitution.

Each recombinant protein C variant was activated by Protac (0.2 IU/ml) in a buffer containing 50mM Tris-HCl and 100mM NaCl (pH 7.4). The anticoagulant function of each recombinant APC variant (1.25-10 nM) in protein C-deficient plasma was assessed by performing a thrombin generation assay with ETP determination as before. (Wild type APC, ●; APC-*N248Q*, ○; APC-*N313Q*, ◆; APC-*N329Q*, □). All experiments were performed in triplicate. Results are expressed as mean ± SEM.

4.4 Site-directed mutagenesis at Asn-329 results in enhanced endothelial cell barrier-protection.

To investigate whether specific *N*-linked glycan chains modulate the endothelial cell barrier-protective properties of APC, each APC variant was characterized using an in-house assay developed to characterize these properties. Pre-incubation with either wild type APC and or variants protected against thrombin-induced permeability in an assay of endothelial barrier integrity. APC-*N329Q* significantly enhanced endothelial barrier integrity at lower APC concentrations compared to wild type APC **(Figure 4.4 A)**. Maximal endothelial barrier protection was achieved by APC-*N329Q* at 1.25nM (10.4±4.7%; $p<0.005$ compared with wild type APC). The same concentration of wild type APC had minimal effect upon thrombin-induced endothelial cell barrier permeability, exhibiting 79±13 % less leakage than EA.hy926 cells treated with thrombin alone. In contrast, APC-*N248Q* and APC-*N313Q* had equivalent endothelial cell barrier protective activity to that of wild type APC **(Figure 4.4 B)**.

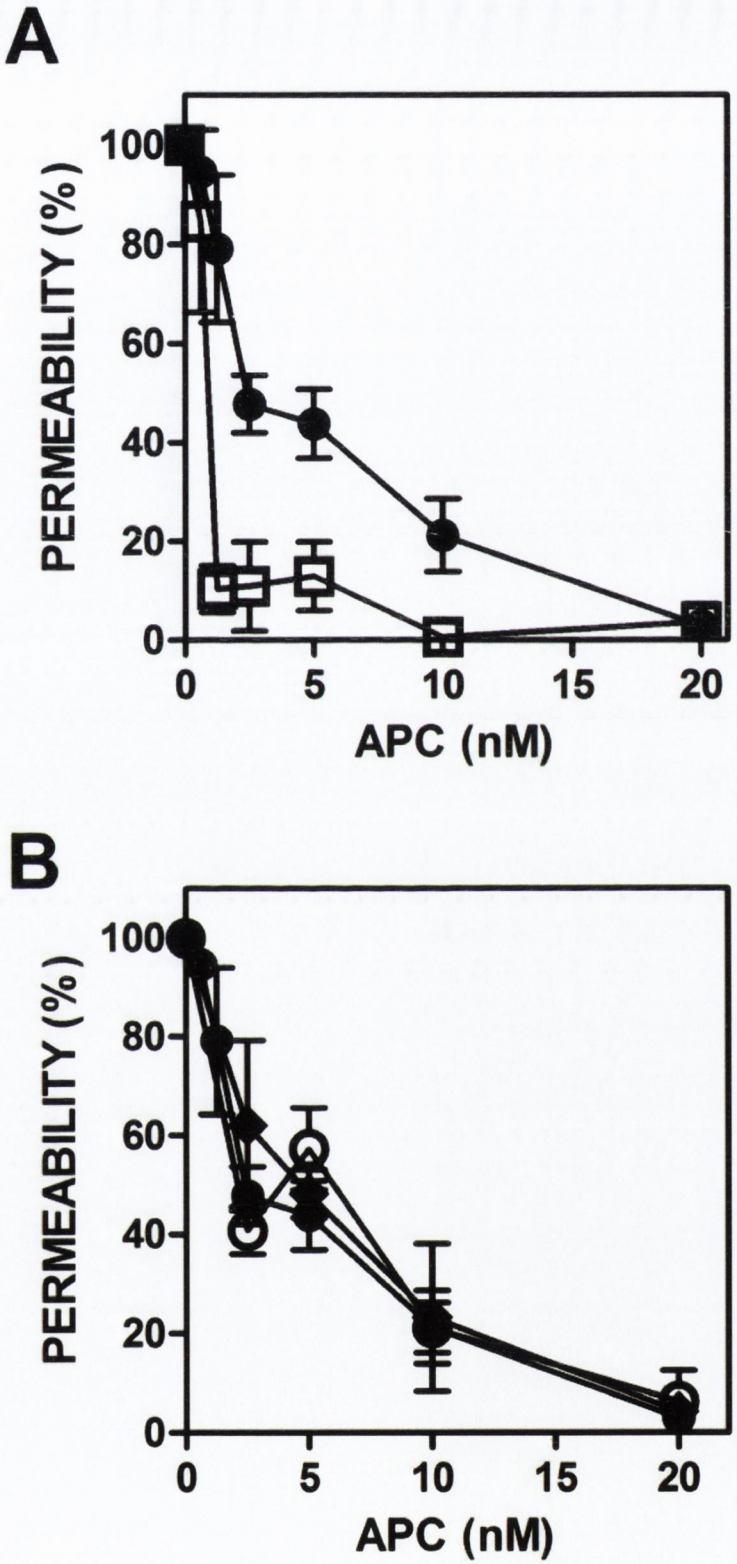

A
PERMEABILITY (%)
100
80
60
40
20
0
0
5
10
15
20
APC (nM)
B
PERMEABILITY (%)
100
80
60
40
20
0
0
5
10
15
20
APC (nM)

Figure 4.4: Site-directed mutagenesis at Asn-329 results in enhanced endothelial cell barrier-protection.

Protection against thrombin-induced endothelial permeability was measured with each recombinant APC variant (1.25-20nM) 2.14. ***(A)*** APC-WT, ●; APC-*N329Q*, □. ***(B)*** APC-WT, ●; APC-*N248Q*,○; APC-*N313Q*, ◆. All experiments were performed in triplicate. Results are expressed as mean ± SEM.

4.5 Characterizing modulation of staurosporine-induced endothelial cell apoptosis by recombinant APC *N*-linked glycan variants using an assay of apoptosis-specific dye uptake.

In order to investigate the effect of specific N-linked glycan chain removal upon EPCR/PAR1-dependent anti-apoptotic signalling by APC, staurosporine-induced endothelial cell apoptosis in EA.hy926 cells treated with APC was assessed **(2.17)**. An assay measuring cellular uptake of phosphatidylserine-specific pink dye in response to staurosporine treatment of EA.hy926 cells was utilized. EA.hy926 cells not treated with staurosporine did not take up apoptosis-specific dye, confirming that the cells were healthy prior to treatment **(Figure 4.5 A)**. Staurosporine-treated EA.hy926 cells, however, accumulated dye in almost all cells visualized. At low APC concentrations, wild type APC and APC-N248Q were unable to prevent apoptosis **(Figure 4.5 A)**. APC-*N248Q* and APC-*N313Q* exhibited improved anti-apoptotic activity compared to wild type APC, but the degree of enhanced protection failed to reach statistical significance. APC-*N329Q*, however, ablated apoptosis-specific dye accumulation at the lowest APC concentration tested (0.625nM). Similar protection was only seen upon treatment with 20nM wild type APC **(Figure 4.5 B)**.

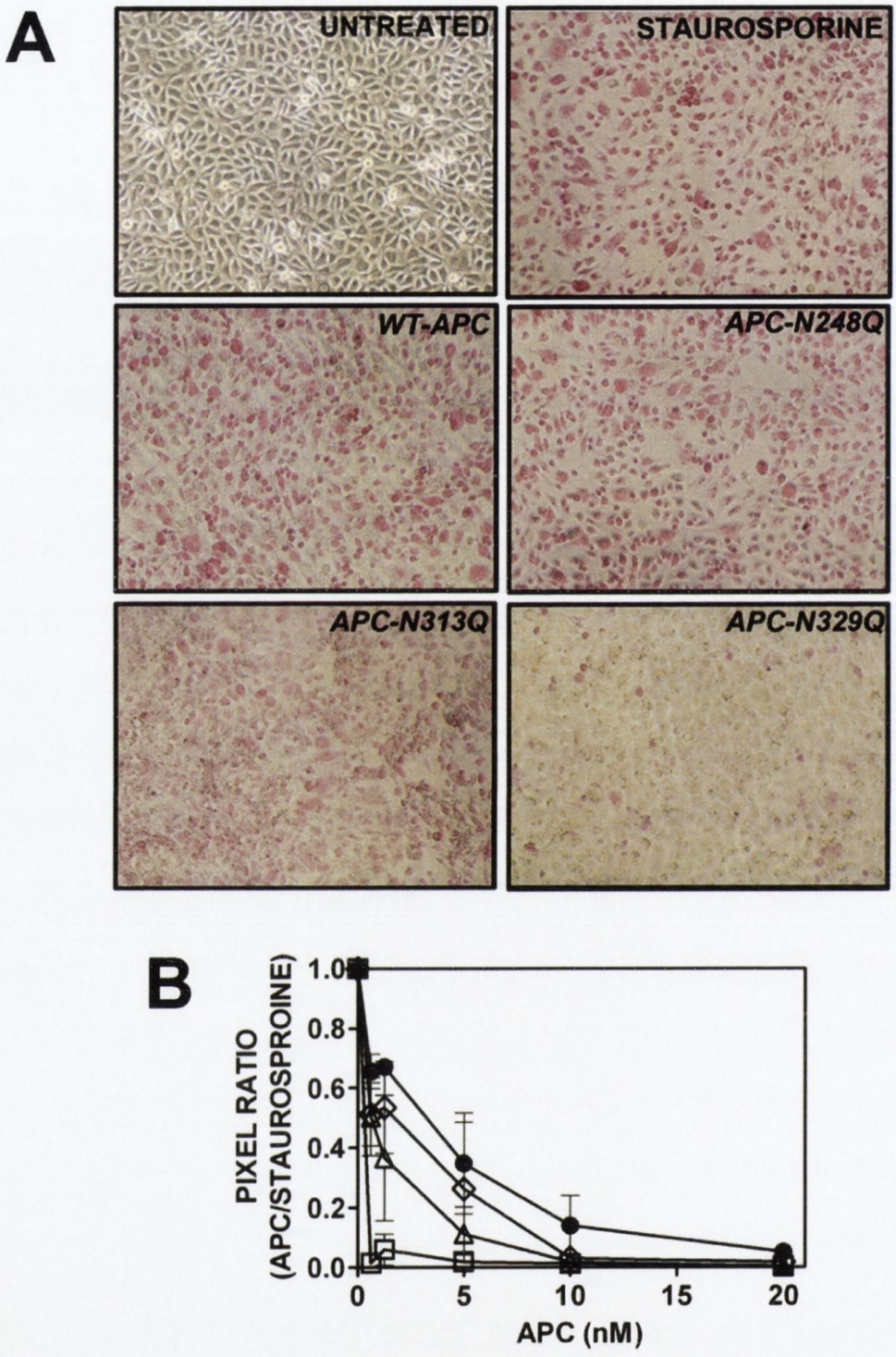

A
UNTREATED
STAUROSPORINE
WT-APC
APC-N248Q
APC-N313Q
APC-N329Q
B
PIXEL RATIO
(APC/STAUROSPROINE)
1.0
0.8
0.6
0.4
0.2
0.0
0
5
10
15
20
APC (nM)

Figure 4.5: Inhibition of endothelial cell apoptosis by recombinant APC *N*-linked glycan variants in an assay measuring uptake of an apoptosis-specific dye.

Confluent EA.hy926 cells seeded in a 96-well plate were treated with APC (0.625-20nM) for 3 hours in serum-free media supplemented with 3mM $CaCl_2$ and 0.6mM $MgCl_2$. Cells were then treated with staurosporine (20μM) in 100μl DMEM. After 3.5 hours, 100μl fresh DMEM containing 10μl APO*Percentage* dye and staurosporine (20μM) was added to each well for 45 minutes, followed by washing twice with PBS. ***(A)*** Cells were visualized by light microscopy and photographed. (Untreated/staurosporine-treated EA.hy926 cells, *top panels;* wild type/ variant APC (1.25 nM), *middle and bottom panels*). Images are representative of three independent experiments. ***(B)*** Uptake of APO*percentage* dye was quantified by converting digital photograph images into pixel counts using Adobe™ Photoshop™ software according to manufacturer's instructions. Average pixel counts were based on analysis of at least three images per well. (Wild type APC, ●; APC-*N248Q*, ◊; APC-*N313Q*, Δ; APC-*N329Q*, □; 0.625-20nM). All experiments were performed in triplicate.

4.6 Characterizing modulation of staurosporine-induced endothelial cell apoptosis by recombinant APC N-linked glycan variants using an assay of pro- and anti-apoptotic gene expression.

Induction of apoptosis results in modulation of pro- and anti- apoptotic gene expression. APC has previously been shown to inhibit apoptosis by reducing expression of proapoptotic gene *Bax* and increasing expression of antiapoptotic gene *Bcl-2* [110]. To further characterize anti-apoptotic signalling properties of each APC *N*-linked glycan variant, pro/anti-apoptotic gene expression in response to staurosporine-induced apoptosis was assessed by RT-PCR **(2.16)**. The expression of pro-apoptotic gene *Bax* and anti-apoptotic gene *Bcl-2* were examined and normalized to the housekeeping gene *β-actin*. The ratio of the change in gene expression of *Bax* and *Bcl-2* relative to *β-actin* is therefore a measure of cellular apoptosis. Wild type APC (5nM) did not significantly inhibit staurosporine-induced *Bax/Bcl-2* gene expression ratio relative to *β-actin*, as measured by RT-PCR, compared with staurosporine-treated cells alone. *Bax/Bcl-2* gene expression ratio measured with staurosporine alone (2.3±0.37) and with wild type APC (5nM; 2.26±0.22) were determined **(Figure 4.6)**. APC-*N329Q* exhibited enhanced protection against staurosporine-induced endothelial cell apoptosis compared with wild-type APC. In contrast to wild type APC, APC-*N329Q* (5nM) significantly reduced the staurosporine-induced *Bax/Bcl-2* gene expression ratio by 43% (1.31±0.2) compared with wild type APC.

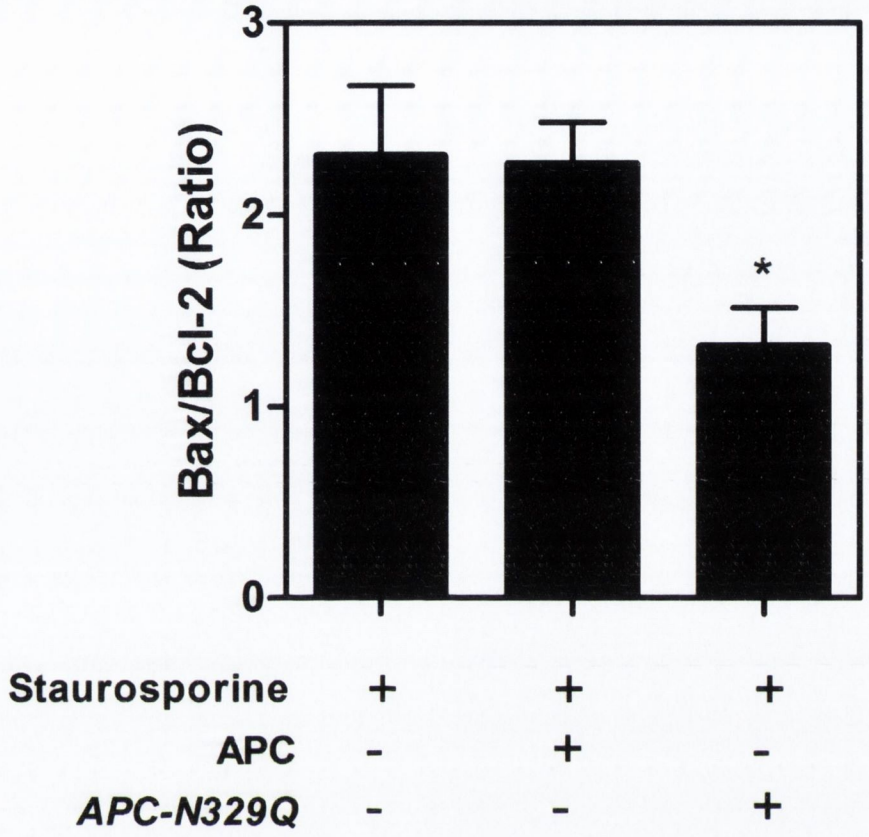


Figure 4.6: Modulation of endothelial cell apoptosis by recombinant APC *N*-linked glycan variants using an assay of pro- and anti-apoptotic gene expression.

Ability of wild type APC and APC-*N329Q* (both 5nM) to protect against staurosporine-induced apoptosis was determined. Apoptosis was determined by the *bax/bcl-2* ratio analysis (relative to β-actin) using RT-PCR. All experiments were performed in triplicate. Results are expressed as percentage of the mean ± SEM of staurosporine-treated *bax/bcl-2* ratio (100% apoptosis). (* $P<0.05$, unpaired 2-tailed student's *t* test performed).

4.7 EPCR affinity of protein C-*N329Q*

APC binding to EPCR is required for PAR1 activation and subsequent barrier protective and anti-apoptotic signalling **(1.2.8)**. To determine whether enhanced affinity for EPCR was the cause of the improved cytoprotective activity of APC-*N329Q*, PC-*N329Q* affinity for sEPCR was assessed by surface plasmon resonance using a technique previously established by our group for determination of PC-sEPCR binding affinity [162]. PC-*N329Q* (3.125-1000nM) was bound to a sEPCR surface and found to bind with a K_D of ~193nM **(Figure 4.7)**, which is similar to the K_D reported previously for binding of wild type PC to sEPCR [77, 173]. Therefore, the enhanced cytoprotective function of APC-*N329Q* is not due to improved affinity for EPCR.

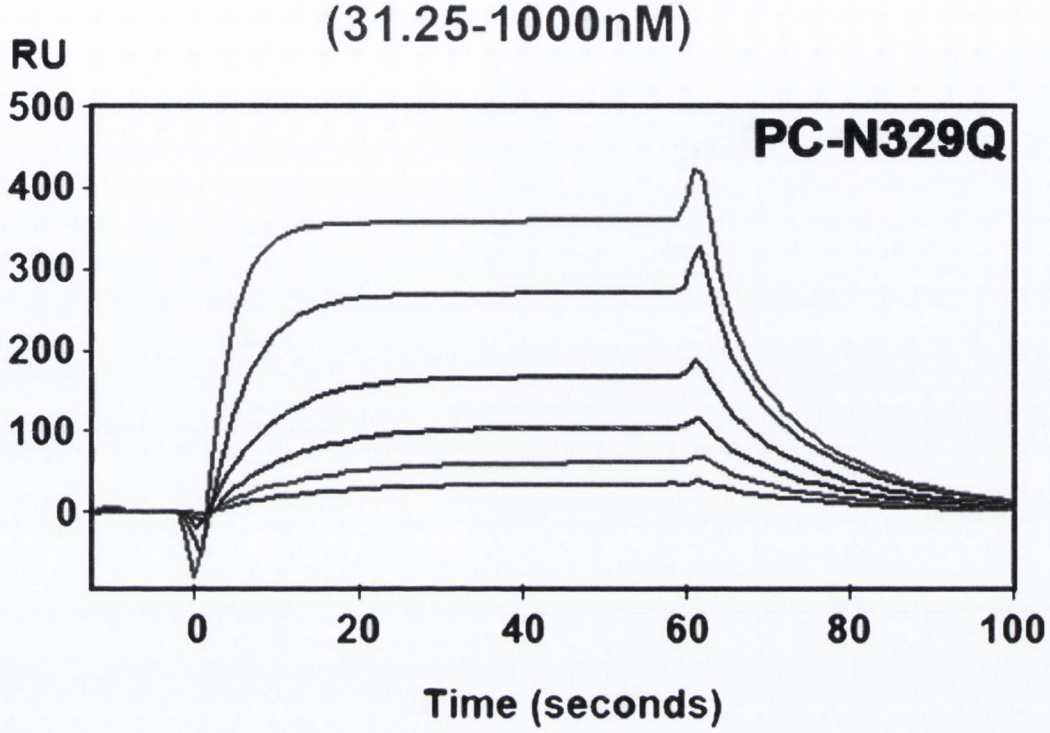


Figure 4.7: Affinity of protein C-*N329Q* for sEPCR.

Protein C-sEPCR binding affinity was determined by surface plasmon resonance. Monoclonal anti-EPCR antibody, RCR-2 (10μg/ml) was immobilized by amine coupling to both flow cells of a CM5 sensor chip. Soluble EPCR (sEPCR) was dialysed into HBS-P buffer (100mM HEPES, pH 7.4, 150mM NaCl) and bound to the test flow cell via RCR-2. RCR-2 was immobilized on the reference flow cell to detect non-specific binding. PC-*N329Q* (31.25–1000nM) was sequentially injected over both flow cells at a flow rate of 10μl/min for 60 seconds. APC-EPCR binding was dissociated using HBS-EP buffer (HBS-P, but containing 3mM EDTA; BIAcore) The RCR-2 surface was regenerated with 10μl of 10mM glycine-HCl (pH 2).

4.8: Enzymatic removal of *N*-linked glycans from a non-anticoagulant recombinant APC variant results in enhancement of EPCR-dependent, PAR-1 mediated cytoprotective signalling.

To determine whether enzymatic deglycosylation would result in enhanced cytoprotective function of non-anticoagulant APC, a recombinant non-anticoagulant APC variant (APC-*L38D*) that is not enhanced by the presence of protein S but signals normally via EPCR/PAR1 [162] was incubated with PNGase F **(2.1)** to remove all *N*-linked glycan moieties (APC-*L38D-DesGly*). APC-*L38D* and APC-*L38D-DesGly* were characterized by non-reducing 7.5% SDS-PAGE/Western blot analysis. The molecular weight of APC-*L38D-DesGly* was reduced by ~10kDa, reflective of complete *N*-linked glycan removal **(Figure 4.8 A)**. The cytoprotective function of APC-*L38D-DesGly* was assessed by an endothelial barrier permeability assay. APC-*L38D-DesGly* (1.25-10nM) exhibited enhanced protection of EA.hy926 cells against thrombin-induced permeability compared with APC-*L38D* at each concentration tested **(Figure 4.8 B)**. Therefore, APC-*L38D-DesGly* possesses improved EPCR/PAR1-dependent signalling function on endothelial cells.

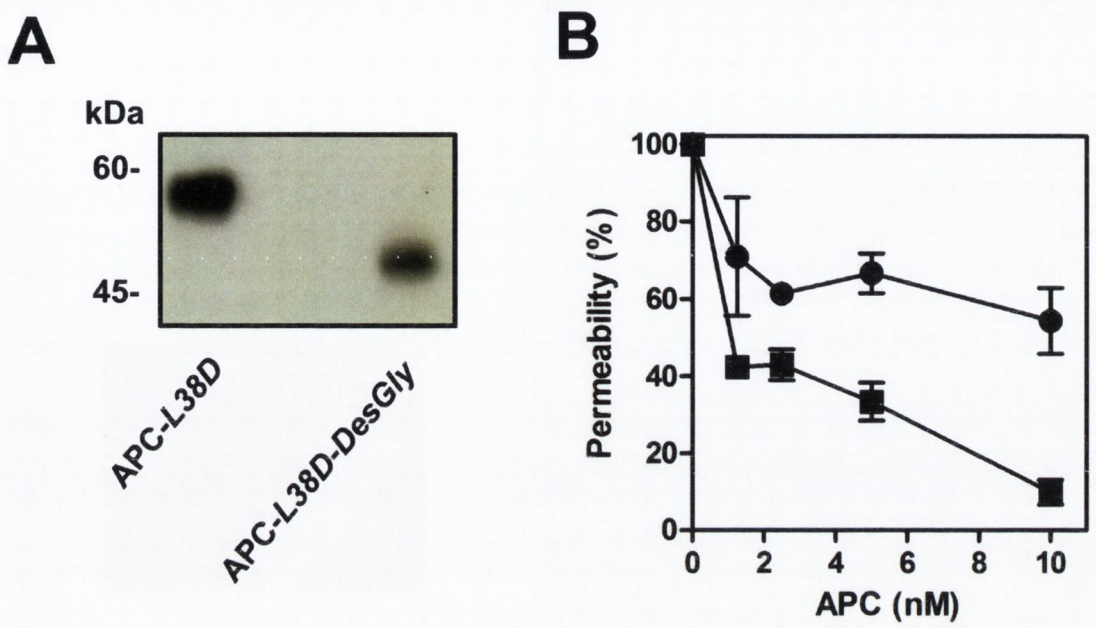


Figure 4.8: Enzymatic deglycosylation of non-anticoagulant APC variant APC-*L38D* with PNGase F enhances APC-L38D-mediated endothelial cell barrier protection.

PC-*L38D*, was deglycosylated with PNGase F and activated with Protac **(2.5)**. ***(A)*** APC-*L38D* or APC-*L38D-DesGly* (20ng) was subjected to SDS-PAGE (7.5%). Western blotting was performed, in which each APC variant was detected with a polyclonal sheep anti-protein C antibody and a HRP-conjugated anti-sheep secondary antibody. ***(B)*** Endothelial barrier permeability was assessed in the presence of APC-*L38D* (●) and APC-*L38D-DesGly* (■; 1.25-10nM) for 3 hours in serum-free media supplemented with 3mM $CaCl_2$ and 0.6mM $MgCl_2$ followed by incubation with 5nM thrombin. Endothelial barrier permeability was assessed by leakage of Evans Blue-BSA through a confluent suspension layer of EA.hy926 cells, as before. All experiments were performed in triplicate. Results are expressed as mean ± SEM.

4.9: A recombinant non-anticoagulant APC variant lacking a glycan attachment site at Asn *329* due to glutamine substitution (APC-*L38D/N329Q).*

From the experiments described, it was hypothesized that glutamine substitution of this glycan attachment site in combination with *L38D* substitution might result in a recombinant APC molecule possessing enhanced cytoprotective, but minimal anticoagulant properties. In order to address this, a pRc/CMV plasmid encoding *PC-L38D* cDNA was used as a template for site-directed mutagenesis. An asparagine→glutamine substitution was introduced at amino acid position 329, followed by expression, purification and activation using Protac **(2.5)** of the resultant protein C variant PC-*L38D/N329Q.* Anticoagulant function of APC-*L38D/N329Q* was assessed in a thrombin generation assay using protein C-deficient plasma. In contrast to wild type APC, APC-*L38D/N329Q* (20nM) produced no anticoagulant effect **(Figure 4.9).**

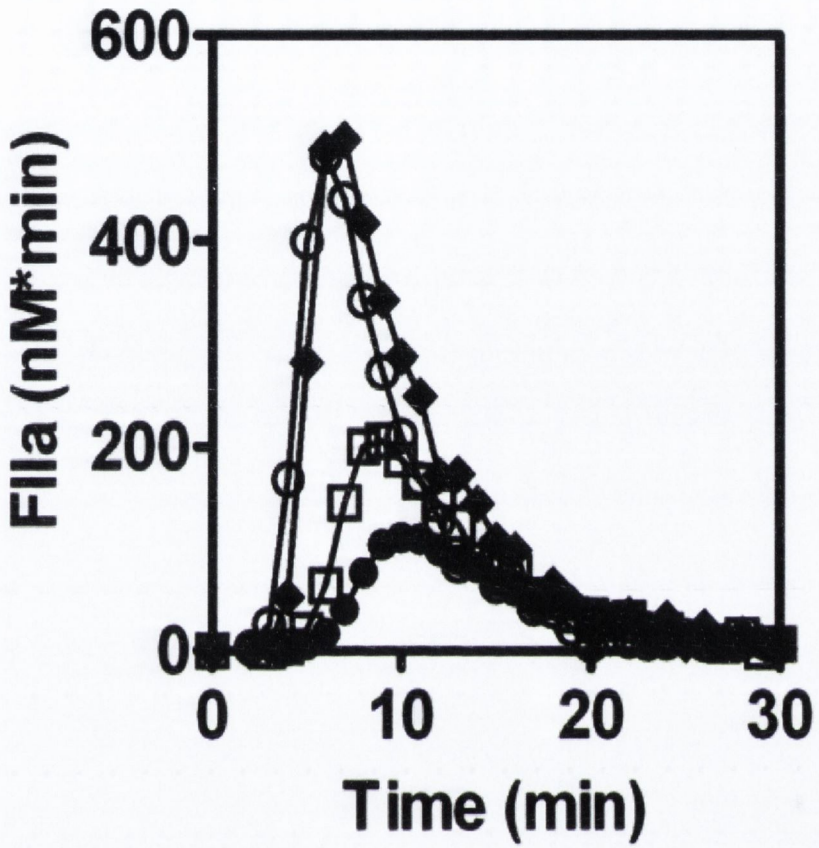


Figure 4.9: Assessment of anticoagulant function of APC-*L38D/N329Q*

Following activation of PC variants with Protac **(2.5)**, thrombin generation in protein C-deficient plasma was assessed in the presence of wild type APC and APC-*L38D/N329Q*. Thrombin generation (nM*min) was initiated with PPP reagent and $CaCl_2$ as before, and ETP (%, thrombin generation in absence of APC) determined. (No APC, ○; wild type APC (5nM), □; wild type APC (10nM), ●; APC-*L38D/N329Q* (20nM),

4.10: APC-*L38D/N329Q* exhibits enhanced endothelial barrier protective function.

APC-*L38D/N329Q* was found to possess greatly enhanced EPCR/PAR1-dependent endothelial protective signalling function compared with wild-type APC: 1.25 nM APC-*L38D/N329Q* reduced thrombin-induced endothelial barrier permeability by 72% compared with permeability observed in the absence of APC, while the same concentration of wild type APC only reduced permeability by 15 %. This represents a 5-fold enhancement of endothelial barrier protective function **(Figure 4.10)**.

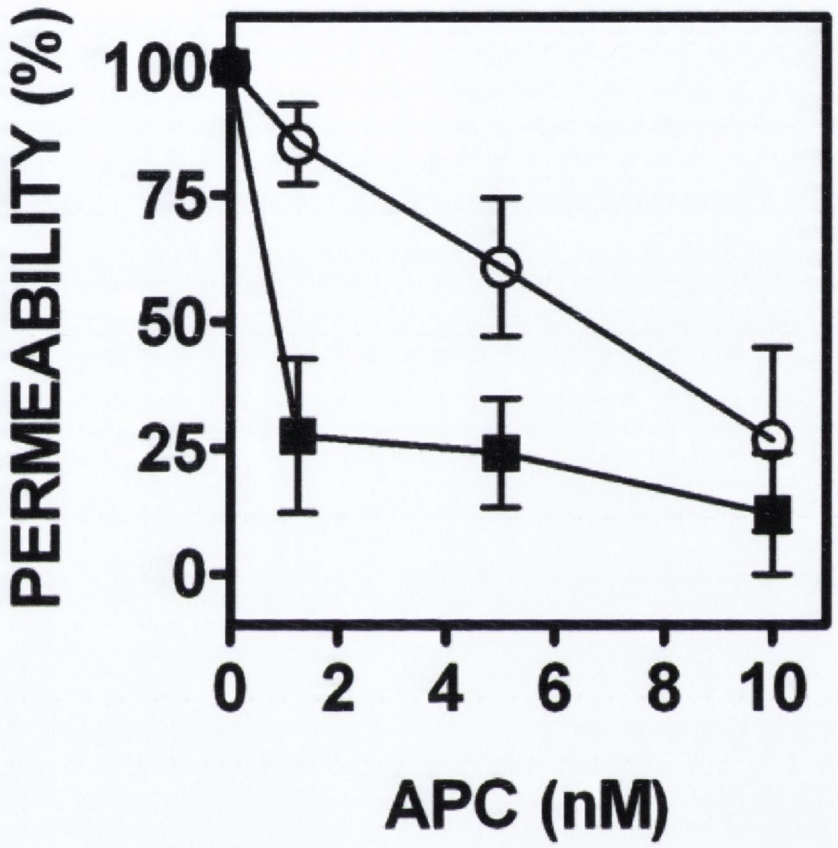


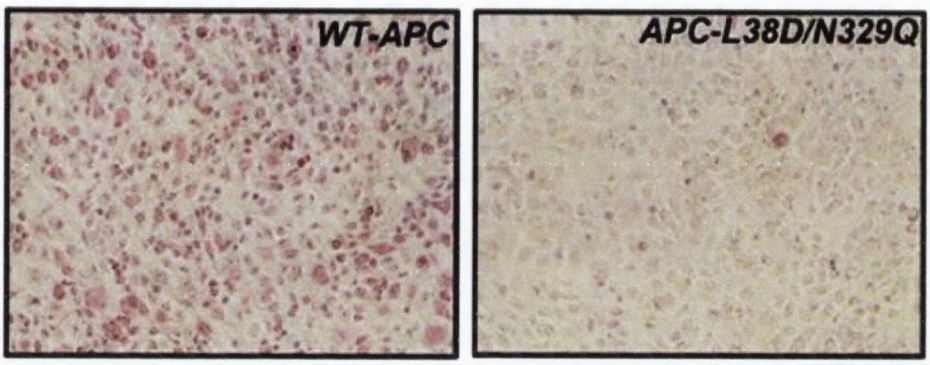
Figure 4.10: APC-*L38D/N329Q* possesses enhanced endothelial barrier protective function.

EPCR/PAR1-dependent endothelial cell barrier protection by APC-*L38D/N329Q* is more potent than wild type APC. An endothelial barrier permeability assay using EA.hy926 cells were performed in the presence of wild type APC (○) or APC-*L38D/N329Q* (■; 1.25-10nM) prior to thrombin treatment. Permeability is expressed as a percentage of total thrombin-induced endothelial cell barrier permeability. All experiments were performed in triplicate. Results are expressed as mean ± SEM.

4.11: APC-*L38D/N329Q* exhibits enhanced anti-apoptotic function

in an assay measuring staurosporine-induced endothelial cell apoptosis **(2.17)**, pretreatment with wild-type APC resulted in concentration-dependent protection against apoptosis. APC-*L38D/N329Q* demonstrated enhanced protection against EA.hy926 cell apoptosis compared with wild-type APC **(Figure 4.11 A and B)**. While maximal protection against apoptosis was only achieved with 20nM wild type APC, the same protective effect was observed with only 0.625 nM APC-*L38D/N329Q*, suggesting that this variant is ~30 fold more effective in protecting against endothelial cell apoptosis.

A


WT-APC
APC-L38D/N329Q

B

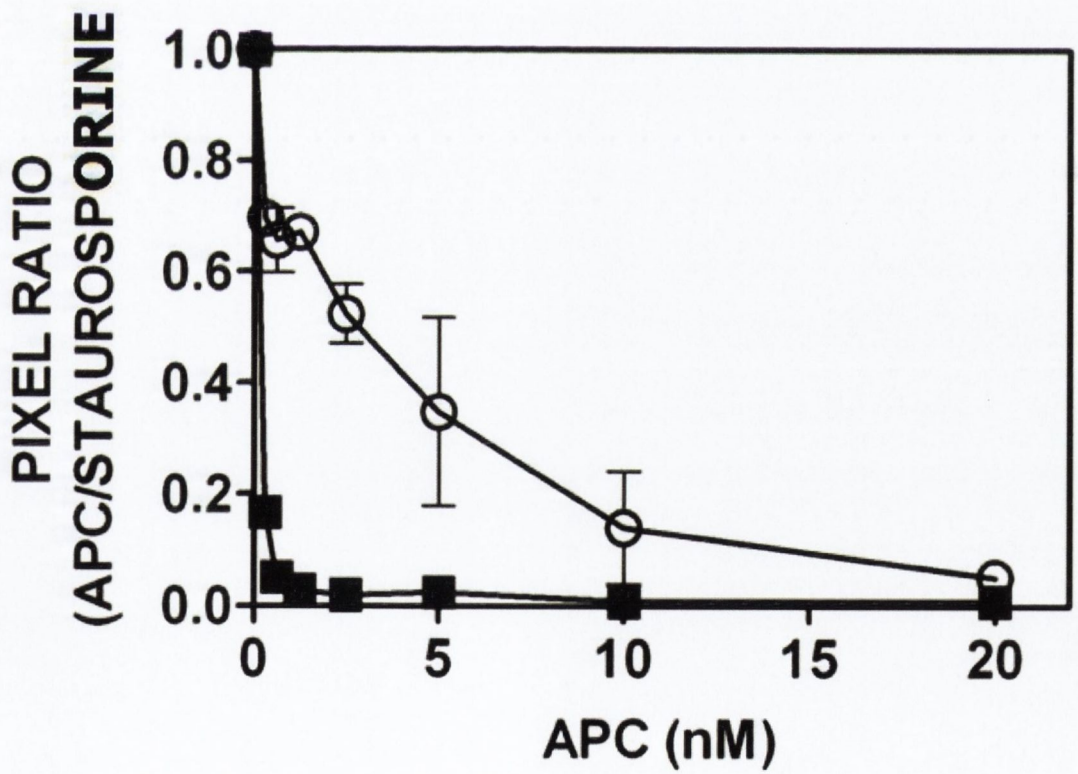

PIXEL RATIO
(APC/STAUROSPORINE
1.0
0.8
0.6
0.4
0.2
0.0
0
5
10
15
20
APC (nM)

Figure 4.11: APC-*L38D/N329Q* exhibits enhanced endothelial anti-apoptotic function.

Confluent EA.hy926 cells were treated with APC (0.625-20nM) for 3 hours in serum-free media supplemented with 3mM $CaCl_2$ and 0.6mM $MgCl_2$. Cells were then treated with staurosporine (20μM) in 100μl DMEM. After 3.5 hours, 100μl fresh DMEM containing 10μl APO*Percentage* dye and staurosporine (20μM) was added to each well for 45 minutes, followed by washing twice with PBS. ***(A)*** Cells were visualized by light microscopy and photographed. (Wild type APC, *left panel;* APC-*L38D/N329Q, right panel;* both 1.25 nM). Images are representative of three independent experiments. ***(B)*** Uptake of APO*percentage* dye was quantified by converting digital photograph images into pixel counts using Adobe™ Photoshop™ software according to manufacturer's instructions. Average pixel counts were based on analysis of at least three images per well. (Wild type APC, ○; APC-*L38D/N329Q*, ■; 0.625-20nM). All experiments were performed in triplicate.

CHAPTER 5: DISCUSSION OF RESULTS DESCRIBED IN CHAPTERS 3 AND 4

5.1 ROLE OF GLYCOSYLATION IN PROTEIN FUNCTION

Glycosylation of membrane signalling receptors and soluble ligands is frequently encountered as a mechanism of functional regulation, and can influence many aspects of signal transduction, including ligand recognition and affinity [174], intracellular trafficking and receptor activation **(1.2.6)** [100, 175]. Moreover, many proteins naturally exist as two or more glycoforms, and in some cases enhanced functional properties are observed with one naturally ocurring glycoform compared with the other [176]. It was therefore hypothesized that APC N-linked glycans might modulate anticoagulant and signalling properties.

5.2 ROLE OF APC GLYCOSYLATION IN ANTICOAGULANT FUNCTION AND IN SIGNALLING FUNCTION EFFICIENCY ON ENDOTHELIAL CELLS

In results described in Chapters 3 and 4, the functional consequences of APC glycosylation modification were determined. Complete removal of APC N-linked glycans was shown to enhance EPCR and PAR1-dependent endothelial barrier-protective and anti-apoptotic properties. These properties have been postulated to contribute to the *in vivo* protective effects of APC in murine models of sepsis **(1.2.8)**. Moreover, Asn-329 was identified as a critical modulator of APC cytoprotective function, as specific removal of the N-linked glycan attachment site at Asn-329 by site-directed mutagenesis resulted in similar enhancement in endothelial cell barrier-protective and anti-apopotic properties to that observed upon enzymatic digestion of all N-linked glycan moieties.

5.2.1 Role of N-linked glycans in modulating APC amidolytic function

The APC serine protease domain contains a catalytic triad of amino acids (His 57, Asp 102, Ser 195) that mediate substrate proteolysis [67]. Complex N-linked glycans are large space-occupying structures that can modulate protein function due to steric hindrance [97]. However, in our hands, APC amidolytic activity was unaffected by enzymatic N-linked glycan removal **(Figure 3.2)**, indicating that N-linked glycans do not modulate APC active site substrate cleavage. These findings are in contrast to those of Grinnell *et al* [101], who demonstrated mild (1.4-1.8-fold) increases in amidolytic activity upon removal of individual APC protease domain glycosylation sites. APC N-linked glycans are not located close to the active site **(Figure 5.1)**. Consequently, it is unclear how removal of individual protease domain glycosylation sites influenced cleavage of a small chromogenic substrate.

5.2.2 Role of N-linked glycans in modulating protein C activation

Protein C activation by thrombin was also found to be unaffected by N-linked glycan removal in an assay measuring protein C activation on the surface of EA.hy926 cells **(Figure 3.3)**. Grinnell *et al* also demonstrated identical rates of activation of wild type protein C, protein C-*N248Q* and protein C-*N329Q* using a cell-free assay of protein C activation by the thrombin-TM complex [101]. Interestingly, activation of protein C-*N313Q* was enhanced 3-fold compared with wild type protein C in this study. It is likely that differences in the assays used in that study compared with the current study are responsible for this apparent difference. EA.hy926 cells express EPCR, which enhances protein C activation **(1.2.3)**. Consequently, differences observed in the rate of protein C activation using a cell-free assay in the absence of cell surface EPCR may not be relevant during physiological protein C activation on the cell surface in the presence of EPCR. Correct orientation of APC by EPCR on the cell surface may render insignificant any enhancement in protein C activation observed in solution.

5.2.3 Role of N-linked glycans in modulating APC anticoagulant function

In keeping with the findings of Grinnell *et al*, APC anticoagulant function was enhanced upon N-linked glycan removal **(Figure 3.4)**. Possible mechanisms underlying this observed effect were explored, including APC inactivation by plasma inhibitors **(Figure 3.5)** and FVa proteolysis in the presence and absence of the APC cofactor, protein S **(Figure 3.6)**. Neither was significantly influenced by complete APC deglycosylation. Therefore, the precise molecular mechanism underlying the enhancement of APC anticoagulant activity following N-linked glycan removal remains incompletely understood. Interestingly, removal of terminal sialic acid residues from APC using neuraminidase **(Figure 3.10)** did not affect APC anticoagulant function, in contrast to complete N-linked glycan removal. A possible interpretation for these findings is that removal of terminal negative charge alone is insufficient to mediate enhancement of APC anticoagulant activity. Rather, removal of entire glycan moieties is necessary. Consequently, enhancement of anticoagulant activity is likely to be mediated by the absence of large structural groups.

In the current study, a small (up to 2-fold) gain in anticoagulant function was observed with APC-*DesGly* in a plasma thrombin generation assay **(Figure 3.4)**. Similarly, in a previous study, removal of any APC protease domain glycan attachment site was found to result in a ~2-fold gain in APC anticoagulant function in an APTT assay [101]. However in contrast, removal of individual sites of N-linked glycan attachment in the APC protease domain in the current study did not result in enhanced anticoagulant function in a thrombin generation assay **(Figure 4.3)**. Rather, APC-*N248Q* and APC-

N313Q exhibited mildly reduced anticoagulant function compared with wild-type APC. The anticoagulant function of APC-*N329Q* was identical to that of wild type APC.

It is possible that some of the differences observed between the results of Grinnell *et al* [101] and the current study may be due to differences in the type of plasma coagulation assay used. While Grinnell *et al* studied anticoagulant function of APC glycan variants in an APTT assay, a thrombin generation assay was used in the current study. Moreover, there is an apparent discrepancy in the current study between APC anticoagulant function following complete enzymatic deglycosylation and following removal of individual glycan chains. This discrepancy also remains poorly understood. It is possible that removal of individual N-linked glycan attachment sites could mediate a significant gain in anticoagulant function when combined. Unfortunately, some of these discrepancies remain unexplained.

5.2.4 Role of N-linked glycans in modulating APC cytoprotective function

In contrast, removal of N-linked glycans resulted in a remarkable gain in EPCR-dependent, PAR1- mediated cytoprotective function. An approximately six-fold gain in endothelial barrier protective function was observed upon N-linked glycan removal by PNGase F treatment **(Figure 3.7 C)**. This effect was found to require EPCR binding, as an EPCR-blocking antibody entirely ablated the barrier-protective function of both APC and APC-*DesGly* **(Figure 3.7 B)**. N-linked glycan removal from APC also resulted in a two-fold improved ability to protect against staurosporine-induced apoptosis measured by TUNEL staining **(Figure 3.9 A)** and in an RT-PCR based assay measuring relative gene expression of *Bax/Bcl-2* **(Figure 3.9 B)**. In contrast, removal of terminal sialic acid residues did not affect APC cytoprotective function in an APC endothelial barrier protection assay **(Figure 3.11)**. This suggests that removal of APC N-linked glycans modulates APC cytoprotective function by removing glycan moieties that sterically hinder APC substrate or cofactor access, rather than negative charge.

The gain in APC endothelial barrier protective function mediated by complete N-linked glycan removal was found to be wholly replicated by isolated removal of an individual N-linked glycan attachment site Asn 329 **(Figure 4.4 A)**. In contrast, removal of N-linked glycans at Asn 313 and Asn 248 had no sigificant effect upon endothelial barrier protective function **(Figure 4.4 B)**. Consequently, the N-linked glycan site at Asn 329 is a critical modulator of APC signalling on endothelial cells. APC-*N329Q* impaired thrombin-induced endothelial barrier permeability up to 6-fold more efficiently than wild type APC. APC-*N329Q* also inhibited staurosporine-induced endothelial cell apoptosis at ~30-fold lower APC concentration than wild type APC **(Figure 4.5)**.

Similarly, a PNGase F-treated non-anticoagulant APC variant (APC-*L38D-DesGly;* **Figure 4.8**) and an APC variant with no anticoagulant activity but lacking the N-linked glycan chain at Asn 329 due to site-directed mutagenesis (APC-*L38D-N329Q;* **Figures 4.10 and 4.11**) were found to also possess enhanced endothelial cell barrier-protective and anti-apoptotic functions compared with wild type APC. These variants represent the first description of APC variants with enhanced "cytoprotective" function and attenuated anticoagulant function.

The detailed molecular mechanism for the increased cytoprotective signalling function of APC-*N329Q* also remains incompletely elucidated. The N-linked glycan attachment site at Asn 329 is in the APC serine protease domain [67]. This N-linked glycan consensus sequence is higly conserved across mammalian species **(Figure 5.1 A)**, suggesting a critical functional role for this glycan . Two acidic APC residues (Glu 167 and Glu 170) in the APC 162 helix have recently been shown to play an important role in specific PAR1 recognition [120]. Residues in the 162 helix also facilitate binding of other coagulation proteases to specific cofactors [177, 178]. A space-occupying model of Gla domainless APC was constructed using PyMOL software, on which this putative PAR1 binding exosite and the heavy chain N-linked glycan attachment sites were mapped. Critically, in this model, the Asn 329 glycosylation site was found to be located in close proximity to the proposed PAR1 binding exosite **(Figure 5.1 B)**. APC-mediated endothelial barrier protective and anti-apoptotic functions are dependent upon PAR1 interaction and subsequent cleavage. Therefore, it is possible that APC/PAR1 interaction is "shielded" by the Asn 329 glycan chain. This mechanism may regulate access of PAR1 to its exosite-binding region on APC and therefore modulate

APC- PAR1 binding and/or rate of cleavage. The complex N-linked glycan chain at APC Asn 329 may therefore inhibit the rate at which EPCR-dependent, PAR1 mediated activation occurs. Intriguingly, Soto *et al* have recently reported that N-linked glycan moieties in the second extracellular loop of PAR1 modulate thrombin-induced signalling [174]. Mutants lacking N-linked glycosylation sites in the second PAR1 extracellular loop (ECL2) were found to mediate enhanced G protein-mediated thrombin signalling. The rate of cleavage of these PAR1 ECL2 mutants was unchanged. The authors have speculated that the observed enhancement in signalling responses could be due to ligand interactions which stabilize an active receptor confirmation. Whether PAR1 glycans modulate APC-mediated signalling is unknown. Extrapolating the conclusions of Soto *et al* to the current study, it is possible that the enhancement of PAR1-mediated APC protective signalling demonstrated upon removal of the glycosylation site at Asn 329 may also be mediated by enhanced ligand-receptor binding, rather than an enhanced rate of PAR1 cleavage.

It is also possible that an alternative mechanism to improved PAR1 interaction mediates the observed enhancement in the anti-apoptotic effects observed with APC-*N329Q*. All *in vitro* reports to date implicate EPCR and PAR1 in the barrier protective and anti-apoptotic properties of APC [110-112, 138, 139]. However, other receptors have recently been shown to be involved in mediating APC's anti-inflammatory properties; including ApoER-2 [113] and Mac-1 [114]. Glycosylation at Asn-313 or Asn-248 could potentially modulate interaction of APC with these novel receptors, possibly contributing to the minor enhancements of anti-apoptotic function observed with APC-*N248Q* and APC-*N313Q*.

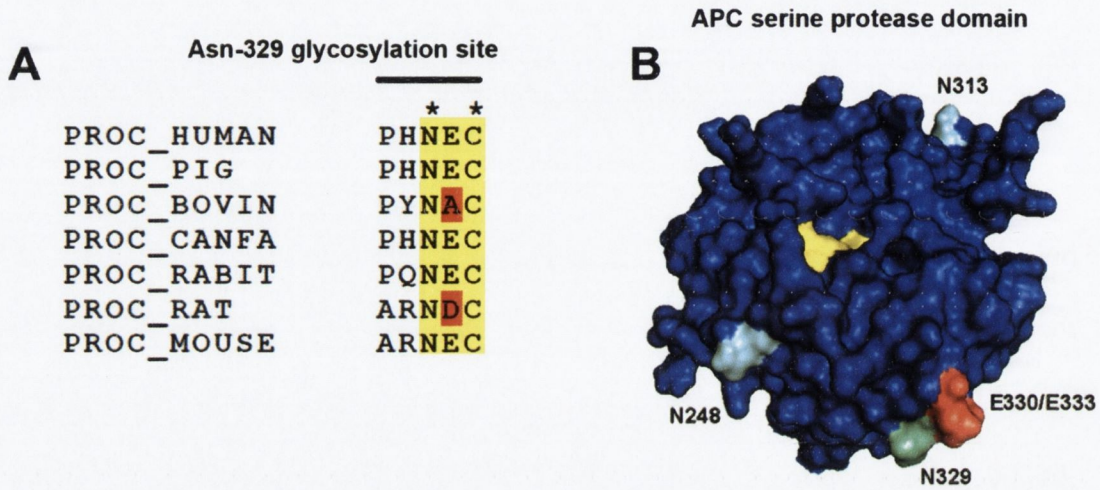


Figure 5.1: The N-linked glycan at Asn-329 is conserved and proximal to a PAR1 binding exosite on APC.

(A) Amino acid alignment of known protein C amino acid sequences indicates conservation of the unusual N-X-C N-linked glycan attachment site in known mammalian protein C amino acid sequences. ***(B)*** N-linked glycosylation occurs at 3 sites (Asn 248, Asn 313 and Asn 329; *turquoise*) on the protein C/APC serine protease domain (*blue*). The Asn 329 glycan attachment site that regulates APC cytoprotective signaling is situated next to two amino acid residues (Glu 330/Glu 333; *red*) that are essential for PAR1 cleavage by APC. The APC catalytic triad (His 211, Asp 257, Ser 360; *yellow*) is indicated. Model generated based upon Gla domainless APC crystal structure (1AUT) using PYMOL molecular visualization software.

5.3 β-APC LACKS GLYCOSYLATION AT ASN-329 AND MAY REPRESENT A PHYSIOLOGICAL MEANS OF MODULATING APC CYTOPROTECTIVE FUNCTION

Approximately 30% of plasma protein C typically exists as β protein C (which lacks the glycan chain at Asn-*329* [102]). Interestingly, plasma levels of this naturally occurring glycoform can vary. The rate of protein C synthesis, for example, influences the proportion of protein C glycosylated at Asn 329 [102]. The Asn 329 glycosylation site possesses the unusual consensus sequence Asn-X-Cys, which differs from the typical glycosylation consensus sequence, Asn-X-Ser/Thr. It is postulated that the free sulfhydryl group of a cysteine residue can substitute for the hydroxyl group of a threonine or serine residue in recognition by a glycosylation site binding protein but that it does so less efficiently [179]. Furthermore, protein disulfide isomerase (PDI) catalyses the formation of a disulfide bond between Cys 331 and Cys 345. This has lead to previous speculation that during slower protein synthesis, Asn 329 is available for glycosylation for longer before Cys 345 also enters the lumen of the endoplasmic reticulum and forms a disulfide bond with Cys 331, while in contrast, during rapid protein synthesis, Cys 331 becomes linked by this disulfide bond before it can participate in Asn 329 glycosylation [102].

Naturally occurring glycoforms are a means of endogenous regulation of protein function. For example, the naturally ocurring "β" AT glycoform is only partially glycosylated at Asn-135 (located near the heparin binding site), and exhibits enhanced heparin binding compared with the α glycoform [176]. The consensus sequence

(1.2.6) Asn-X-Ser is less efficiently glycosylated than Asn-X-Thr, and inefficient core glycosylation at Asn-135 of AT "β" has been shown to be due to the Asn-X-Ser glycosylation consensus sequence at this site, as AT mutants with Asn-X-Thr at this site express only α glycoform [176]. All three other AT glycosylation sites have the consensus sequence Asn-X-Thr. Given the critical role now demonstrated for Asn 329 in modulation of APC cytoprotective function, it is tempting to speculate that Asn 329 glycosylation status *in vivo,* like that of AT [176], represents a means of natural modulation of APC protective function.

5.4 RATIONALE FOR GENERATING RECOMBINANT APC VARIANTS WITH ENHANCED CYTOPROTECTIVE PROPERTIES AND REDUCED ANTICOAGULANT FUNCTION

Sepsis is the leading cause of mortality in non-coronary intensive care units, resulting in 40,000-60,000 deaths per year in the United Kingdom alone, and killing 200,000 of the 700,000 patients who develop sepsis in the United States annually [140]. In severe sepsis, reduced plasma concentrations of protein C can occur and may be associated with an increased morbidity and mortality [106, 180]. Bernard *et al* found ~80% of patients with severe sepsis to have reduced baseline protein C levels. Fijnvandraat *et al* reported protein C deficiency in 5% of survivors of meningococcal septic shock and 23% of non-survivors, respectively ($p<0.0001$). Moreover, the same authors showed that protein C deficiency is associated with larger skin lesions. APC administration improves survival in severe sepsis [106] and is approved by the FDA for use in this setting. Moreover, in 2003 critical care and infectious disease experts from 11 international organizations compiled management guidelines for severe sepsis and septic shock as part of the "Surviving Sepsis Campaign", advocating the use of recombinant APC for patients with severe sepsis and a high risk of death, along with standard management [181]. However APC administration is associated with an increased risk of severe bleeding [106, 147]. Consequently, intensive care physicians are frequently reluctant to administer recombinant APC to septic patients, even in those fulfilling standard criteria for its use. Concerns regarding the clinical use of recombinant APC are reflected in a recent systematic review published by the Cochrane Collaboration, advocating against its use in patients with severe sepsis [161].

To address these concerns, "second generation" recombinant APC variants have been designed, which have similar "cytoprotective function" to wild type APC but significantly attenuated anticoagulant properties [144, 162, 182]. Mosnier *et al* [144] generated and characterized a recombinant APC variant with defective FVa substrate recogition due to mutation of its FVa-binding exosite, while in this laboratory an APC variant with impaired protein S cofactor function has been expressed [162]. Bae *et al* engineered an APC variant in which a disulfide bond was introduced which stabilized the Ca^{2+}-binding loop 70-80, with virtual ablation of anticoagulant function [182]. However, previous to this study, no recombinant non-anticoagulant APC variant had been designed that possessed enhanced cytoprotective signalling function. The recombinant variant described in this study, APC-*L38D/N329Q,* represents the first example of an APC molecule with enhanced cytoprotective function but attenuated anticoagulant function.

5.6 CONCLUSION

APC N-linked glycosylation plays a critical role in regulation of APC cytoprotective function, and the N-linked glycan moiety at Asn-329 in the APC serine protease domain has been identified as a key modulator of N-linked glycan-regulated, EPCR/PAR1-dependent cytoprotective signalling on endothelial cells. Moreover, novel APC variants have been generated which possess markedly attenuated anticoagulant function but enhanced cytoprotective function compared with APC. These novel recombinant variants represent a potential novel approach to improving the therapeutic potential of recombinant APC therapy in sepsis.

CHAPTER 6: PROTAMINE SULPHATE ENHANCES APC ANTICOAGULANT PROPERTIES AND DOWNREGULATES THROMBIN GENERATION BY INHIBITING FACTOR V ACTIVATION

6.1 INTRODUCTION

6.1.1 Work leading up to this chapter.

Platelet factor 4 (PF4) has been shown to inhibit APC-mediated anticoagulant function in plasma [183]. In work performed to characterize the molecular mechanism of this effect, it was demonstrated that another positively charged small molecule, protamine sulphate, greatly enhanced APC anticoagulant function. Protamine, which is widely used clinically to reverse anticoagulant properties of heparin **(1.1.5)**, is known to possess intrinsic anticoagulant properties **(6.1.3)**. Consequently it was hypothesized that the observation that protamine enhances APC's anticoagulant function could be utilized to elucidate the molecular mechanism underlying protamine's anticoagulant properties.

6.1.2 Protamine structure and function

In clinical practice, reversal of heparin-induced anticoagulation **(section 1.1.5)** is achieved with protamine sulphate. Protamine sulphate which is used therapeutically is a small (5kDa) positively charged polypeptide produced in salmon sperm that binds negatively-charged proteins and in particular, heparin [184]. Protamines are one of a group of basic nuclear proteins that package DNA in the sperm of a variety of species, replacing histones in the final stages of spermatid maturation [185]. They are short polypeptides, consisting of 50-110 amino acids and are all highly basic, with an arginine content of up to 70% [185]. Protamines are closely related to histones and are hypothesized to have evolved from H1 histones [186]. All vertebrate protamines contain multiple domains consisting of multiple basic residues, which bind the protamine molecule to DNA. In addition, protamines possess several serine and threonine residues which are potential phosphorylation sites [185].

6.1.3 Clinical use of protamine sulphate in reversal of systemic heparinization

Heparin and protamine form a complex which is rapidly cleared by the reticuloendothelial system [187]. For this reason, protamine has been used for over three decades to reverse heparin-induced anticoagulation *in vivo*. Given the long history of protamine use, it is used by clinicians as the treatment of choice for those patients who develop bleeding complications while on unfractionated heparin (UFH) [188, 189]. Protamine is also administered routinely in order to reverse high dose UFH administered during cardiopulmonary bypass and cardiac surgery [190]. In this setting, large doses of heparin are required to avoid catastrophic clotting in the cardiopulmonary bypass circuit. Protamine has been shown in pharmacokinetic studies to be rapidly cleared from human plasma, with a half-life of about 7.4 minutes. Consequently, repeated dosing is frequently necessary [191, 192]. Despite its useful therapeutic properties, protamine sulphate causes many unwanted side effects, including pulmonary and systemic hypotension [184]. Interestingly, *in vitro* and *in vivo* studies have also demonstrated that protamine is associated with anticoagulant properties **(6.1.4 and 6.1.5)**.

6.1.4 *In vitro* anticoagulant properties of protamine sulphate

Carr *et al* investigated the effects of excess protamine following heparin reversal in plasma [193]. Protamine was demonstrated to prolong plasma activated partial thromboplastin time (APTT), inhibit platelet function and decrease clot elastic modulus. Griffin *et al* also noted a protamine-induced APTT prolongation and also observed that protamine prolonged plasma prothrombin time (PT) [194]. In addition, Griffin *et al* showed that protamine influences platelet activation under conditions of physiological shear stress [194]. The latter was achieved using a near-patient testing device, the Clot Signature Analyzer (CSA™). The CSA™ measures the time required for a platelet plug to occlude a puncture in a capillary tube containing flowing unanticoagulated whole blood. In addition, the time taken for this platelet plug to completely obstruct the tube lumen ("clotting time") is recorded. Both parameters were prolonged by protamine. *Ex-vivo* spiking of normal pooled plasma with protamine sulphate also resulted in a significant reduction in tissue factor (TF)-initiated thromboelastography [195]. Specifically, the clot initiation time was prolonged by protamine. In addition, the clot propagation rate and clot strength were attenuated. These effects were concentration-dependent.

The Activated Clotting Time (ACT) is a clotting assay commonly used as a near- patient test during and after cardiothoracic surgery to guide heparin dosing and reversal. Weight-based heparin dosing does not always result in a reliable degree of anticoagulation, as individuals may respond differently to a fixed heparin dose [196]. A linear relationship exists between plasma heparin concentration and ACT. A prolonged ACT following a cardiothoracic procedure may represent inadequate reversal of

heparin. However, protamine can also influence the ACT, leading to difficulties in its interpretation as a simple surrogate marker of plasma heparin concentration. Mochizuki *et al* demonstrated that excess protamine, when added to heparinized platelet-rich plasma obtained from patients following cardiopulmonary bypass, resulted in significant dose-dependent ACT prolongations [197]. This effect occurred in the presence of protamine: heparin ratios of ≥ 1.3: 1 and was not observed in the presence of recombinant PF4. At a similar protamine: heparin ratio, significant reductions in ADP-induced platelet aggregation were also observed. The ACT used in near-patient testing is a whole-blood assay and is therefore sensitive to platelet and coagulation-mediated anticoagulant effects. As protamine mediates both, its potential to prolong the ACT *in vivo* is particularly important. Administration of further doses of protamine to "correct" a prolonged ACT mediated by excess protamine rather than heparin could potentially be deleterious.

6.1.5 *In vivo* anticoagulant properties of protamine sulphate

Following the administration of protamine sulphate to dogs, Kresowik *et al* observed dose-dependent ACT and APTT prolongations, thrombocytopoenia and inhibition of ADP-induced platelet aggregation [198]. In this study, four doses of protamine, ranging from 1.5 mg/kg to 15.0 mg/kg, were administered either alone, or following administration of 150 IU/kg of heparin. In both groups, significant prolongations of ACT were observed following administration of ≥ 3mg/kg protamine. Significant APTT prolongation and thrombocytopoenia were only observed at very high protamine doses (15mg/kg) in heparinised dogs, while these effects were seen at much lower protamine doses in the absence of heparin. Significant reduction in ADP-induced platelet aggregation occurred at ≥ 6mg/kg in dogs receiving prior heparin and at ≥ 3mg/kg with no prior heparin. This study demonstrates that protamine may produce anticoagulant effects *in vivo*. The protamine dose required to mediate an anticoagulant effect is higher following co-administration with heparin. This suggests that "excess protamine" rather than protamine present in complex with heparin mediates these anticoagulant effects.

In keeping with the results of Kresowik *et al,* Worowski *et al* similarly observed significant thrombocytopenia in dogs following protamine administration [199].

In addition to its observed *in vivo* effect in a canine model, protamine has been shown to mediate anticoagulant properties in human subjects. Mittermayr *et al* investigated the effect of protamine on thromboelastometry in patients following cardiopulmonary bypass [200]. Following discontinuation of CPB, patients received a dose of protamine

calculated to reverse the total dose of heparin administered during CPB. Additional protamine (70 IU/kg) was administered to any patient with a prolonged ACT (>10% baseline) and evidence of diffuse bleeding 15 minutes after end of CPB. In addition, thromboelastometry (ROTEM, Pentapharm GmbH, Munich, Germany) was performed on whole citrated blood and anti-factor Xa activity was measured. Additional doses of protamine were found to significantly prolong clotting measurements as measured by thromboelastometry. The vast majority of these samples were shown not to contain detectable heparin, as measured by anti-factor Xa activity.

When large amounts of protamine are administered in excess of the amount required to reverse systemic heparinization, bleeding has been reported, particularly in the setting of cardiothoracic surgery [201-203]. Due to the possible associations of protamine with bleeding complications, as a consequence of its intrinsic anticoagulant effect, current international consensus guidelines recommend that protamine dosing is limited to 1mg of protamine per 100 IU heparin [188, 189].

6.1.6 Molecular mechanisms underlying anticoagulant effects of protamine sulphate

The molecular mechanisms underlying its unwanted clinical anticoagulant side effects have been incompletely understood. Chu *et al* investigated potential modulation by protamine of the extrinsic pathway of blood coagulation and demonstrated significant attenuation of TF-mediated FVII activation [204]. Protamine weakly inhibits adenosine 5'diphosphate-induced platelet aggregation [197] and attenuates VWF binding to platelet GP1b [205] however these effects are only observed at very high plasma concentrations which are rarely encountered *in vivo*. Collectively, these results demonstrate that the precise molecular mechanism underlying the anticoagulant effect of protamine sulphate has been unknown. However, the recent observation that protamine sulphate, unlike PF4, enhances the anticoagulant properties of APC in a thrombin generation assay [183] has led to the work reported in Chapter 5, the aim of which was to elucidate the mechanism underlying protamine's anticoagulant properties.

6.2 RESULTS

6.2.1 Protamine sulphate prolongs normal pooled plasma clotting times.

The anticoagulant effect of protamine sulphate on *in vitro* standard clotting times was determined. Incubation of protamine (10-120µg/ml) with normal pooled platelet-poor human plasma resulted in dose-dependent APTT **(Figure 6.1 A)** and PT **(Figure 6.1 B)** prolongations: Incubation of plasma with protamine at concentrations of 60 and 120µg/ml resulted in 7.3 and 8.4-fold APTT prolongations and PT prolongations of 0.4 and 0.5-fold respectively ($p<0.05$).

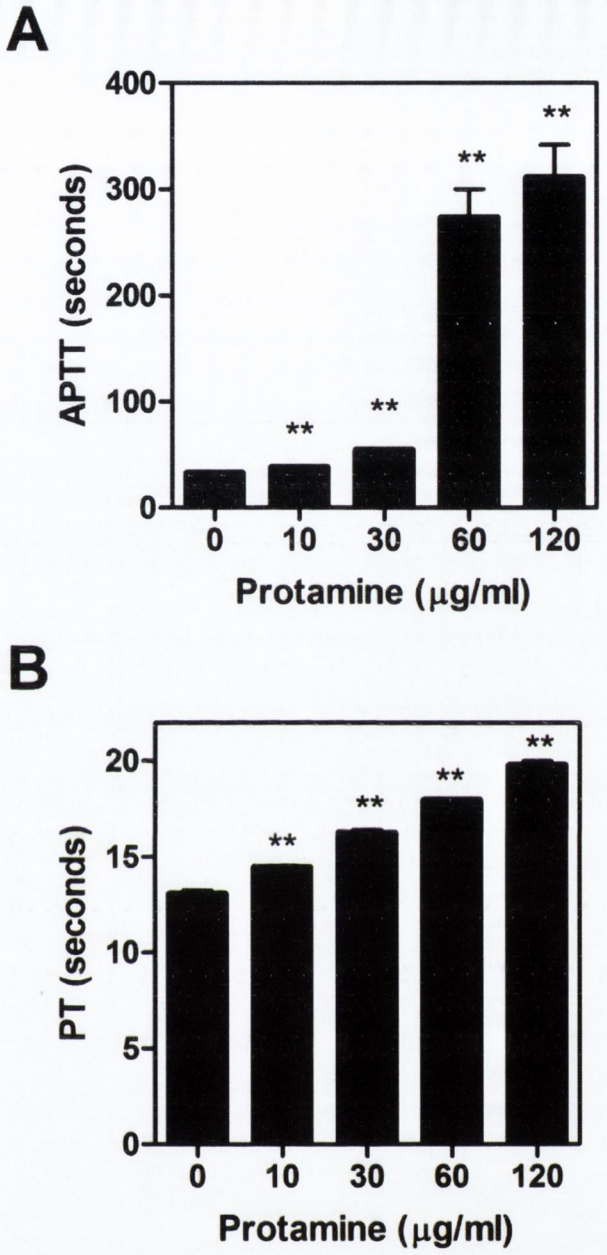


Figure 6.1: Protamine prolongs clotting time of normal pooled plasma *in vitro.*

Protamine sulphate (10-120μg/ml) was incubated with plasma at 37° and APTT ***(A)*** and PT ***(B)*** were measured using the automated ACL TOP coagulometer (Beckman Coulter). All experiments were performed in triplicate. Results are expressed as mean ± SEM. (**P<0.01; unpaired 2-tailed *t* tests performed).

6.2.2 Protamine sulphate attenuates TF-initiated thrombin generation in normal platelet-poor plasma.

In order to further characterize the *in vitro* anticoagulant effect associated with protamine sulphate, an assay measuring TF-initiated thrombin generation in normal platelet-poor plasma was utilized **(2.8)**. In this assay, stimulation of thrombin generation with TF resulted in a rapid time-dependent increase in thrombin generation following a lag of ~2 minutes. The rate of thrombin generated reached a peak at ~4 minutes followed by an expected phase of rapid inhibition. Protamine (3 and 30μg/ml) dose-dependently attenuated thrombin generation. At the higher concentration of 30μg/ml, protamine dramatically altered the shape of the thrombin generation curve **(Figure 6.2)**.

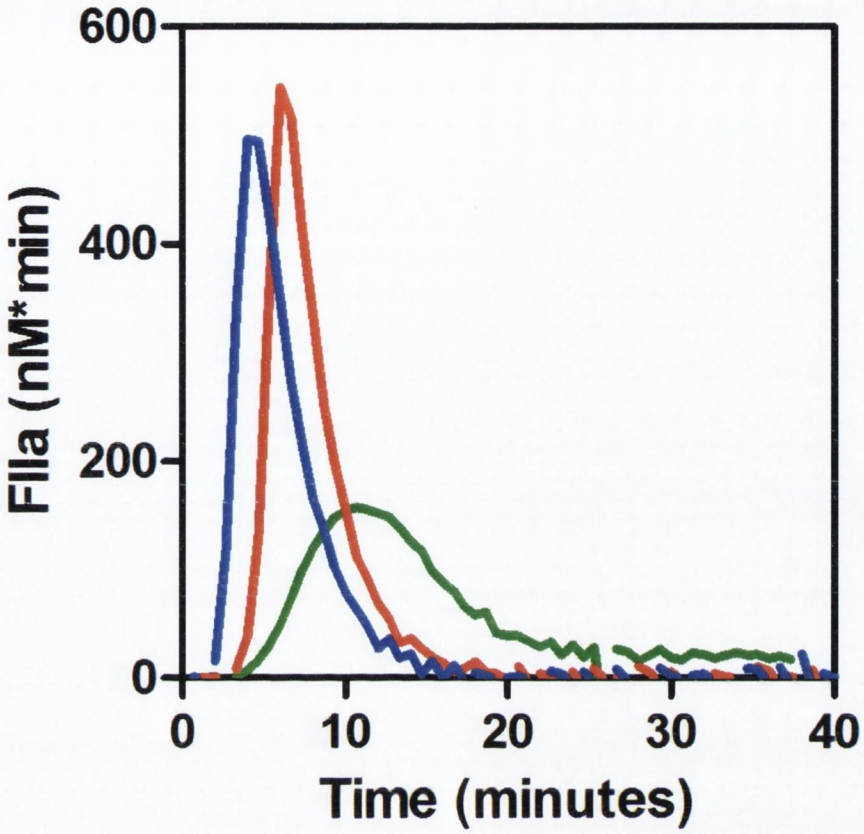


Figure 6.2: Protamine inhibits TF-initiated thrombin generation in normal plasma.

Normal pooled plasma was incubated in the absence (*blue*) or presence of protamine sulphate (3μg/ml, *red;* or 30μg/ml, *green,* respectively) and thrombin generation initiated with 5pM TF, 4μM phospholipid vesicles and 6.67 mM $CaCl_2$ as described previously **(2.8)**. All experiments were performed in triplicate.

6.2.3 Protamine sulphate alters specific parameters of a TF-initiated thrombin generation curve in normal platelet-poor plasma.

Analysis of individual graph parameters identified significant dose-dependent reductions of endogenous thrombin potential (ETP) and peak thrombin in the presence of protamine (3-80μg/ml): Following incubation with protamine sulphate at 30 and 60μg/ml respectively, ETP was attenuated to 58.7±7.2% and 58.5±12% of normal plasma ETP ($p<0.05$), while peak thrombin was reduced from 486±39 nM to 119±21 nM and 122±27 nM ($p<0.001$). In contrast, time to peak thrombin (TTP) and lagtime were significantly prolonged **(Figure 5.3)**: Incubation with protamine sulphate at 30 and 60μg/ml respectively resulted in a TTP prolongation from 4.5±0.2 minutes to 11.1±0.4 and 14.5±0.2 minutes ($p<0.001$) and a lagtime prolongation from 2.4±0.1 minutes to 5±0.1 and 6.4±0.1 minutes respectively ($p<0.001$).

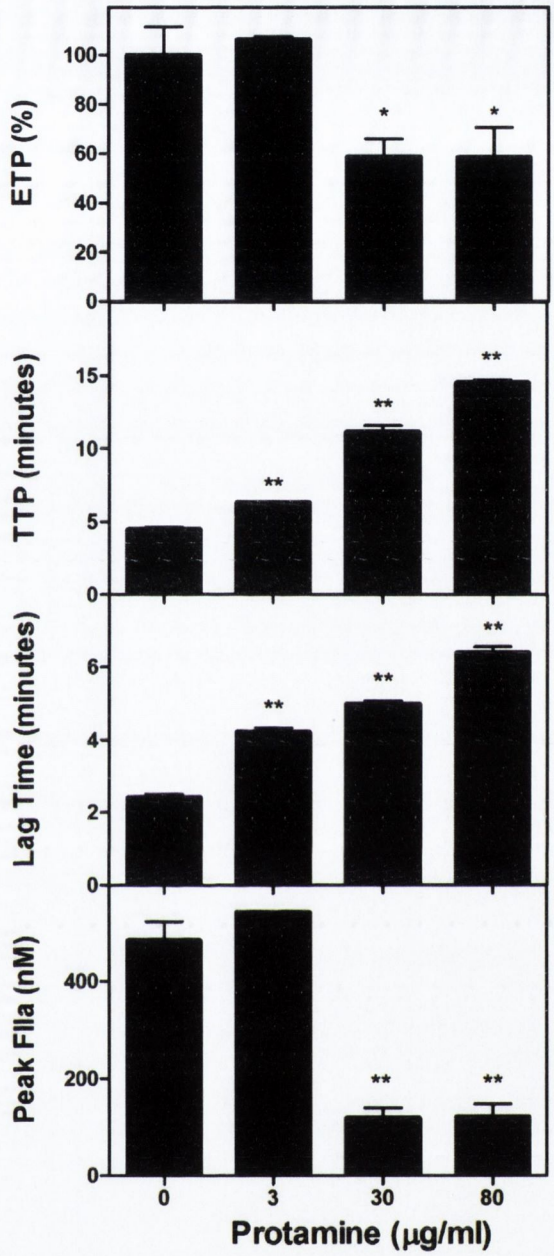


Figure 6.3: Protamine inhibits specific thrombin generation curve parameters in normal plasma.

ETP (%), time to peak FIIa (TTP), time to commencement of FIIa generation curve (lag time) and peak FIIa generated were measured in the presence of protamine sulphate (3-80 µg/ml). All experiments were performed in triplicate. Results are expressed as mean ± SEM.

6.2.4 Anticoagulant effects of protamine sulphate following reversal of heparin-induced anticoagulation.

Randomized clinical trials have suggested that administration of protamine in excess of the amount required to fully reverse heparin is associated with bleeding complications [202]. Having demonstrated that protamine produces direct *in vitro* anticoagulant effects, it was consequently hypothesized that protamine could also mediate anticoagulant effects when present in excess following heparin reversal *in vitro*. A thrombin generation assay **(2.8)** was utilized to investigate the anti/procoagulant effect of increasing concentrations of protamine (1.25-80μg/ml) on plasma ETP in the presence of therapeutic doses of unfractionated heparin (UFH; 0.3 or 1.0 IU/ml). As expected, thrombin generation was not detected in plasma incubated with either concentration of UFH in the absence of protamine **(Figure 6.4)**. At lower protamine concentrations, ETP was progressively returned to that of normal pooled plasma (100%), indicating reversal of heparin-induced anticoagulation. 5μg/ml and 30μg/ml protamine were required to fully reverse the *in vitro* anticoagulant effect of 0.3 IU/ml and 1.0 IU/ml of UFH respectively. When protamine was present in excess however, a dose-dependent anticoagulant effect was observed, such that ETP was progressively reduced to a minimum of and 57±9% of normal plasma ETP with 0.3 IU/ml and 1.0 IU/ml UFH respectively.

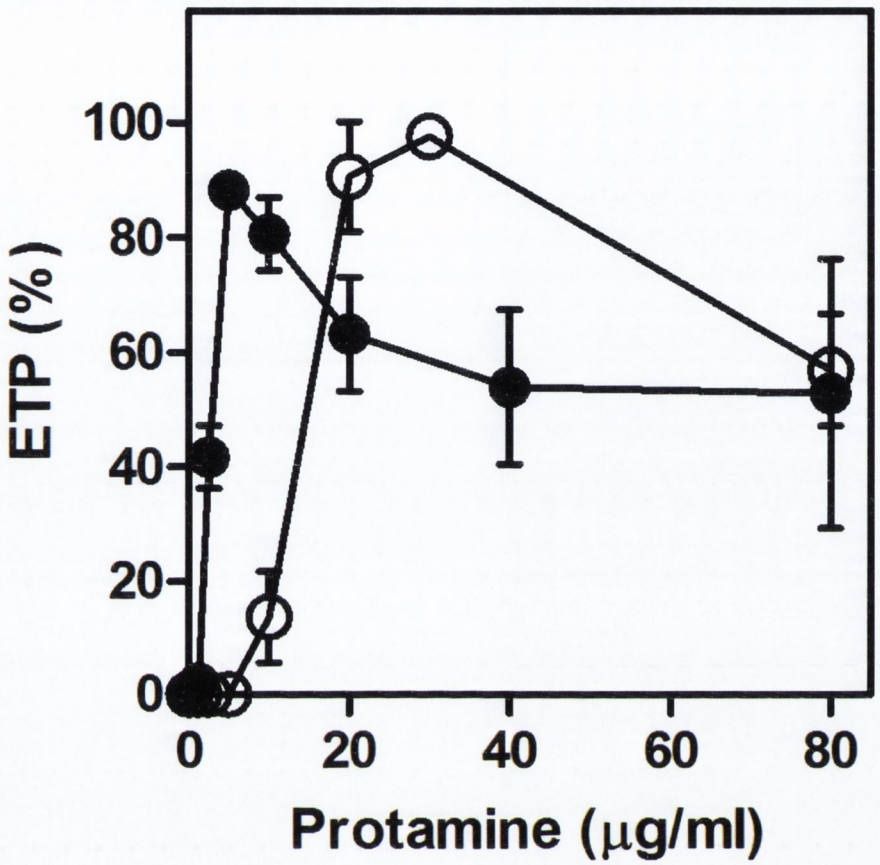


Figure 6.4: Protamine inhibits thrombin generation in heparinised normal pooled plasma when it is present at a higher concentration than is required for full reversal of heparin.

Protamine sulphate (1.25-80μg/ml) was incubated with normal pooled plasma containing 0.3 IU/ml (●) or 1.0 IU/ml (○) unfractionated heparin. Thrombin generation was initiated with TF **(2.8)** and ETP (%) calculated. All experiments were performed in triplicate. Results are expressed as mean ± SEM.

6.2.5 Anticoagulant effects of protamine sulphate following reversal of low molecular weight heparin (LMWH)

While anticoagulant effects were also observed when protamine was in excess following reversal of LMWH, the magnitude of the effect differed depending on the LMWH used **(Figure 6.5)**. Following reversal of Tinzaparin®, ETP initially reached 92±0.1% of normal plasma ETP. Subsequently, ETP was reduced to a minimum of 78±0.3% normal plasma ETP. In contrast, during enoxaparin reversal, ETP reached a maximum of 78±6% normal plasma ETP, followed by a striking dose-dependent ETP attenuation to a minimum of only 20±2%.

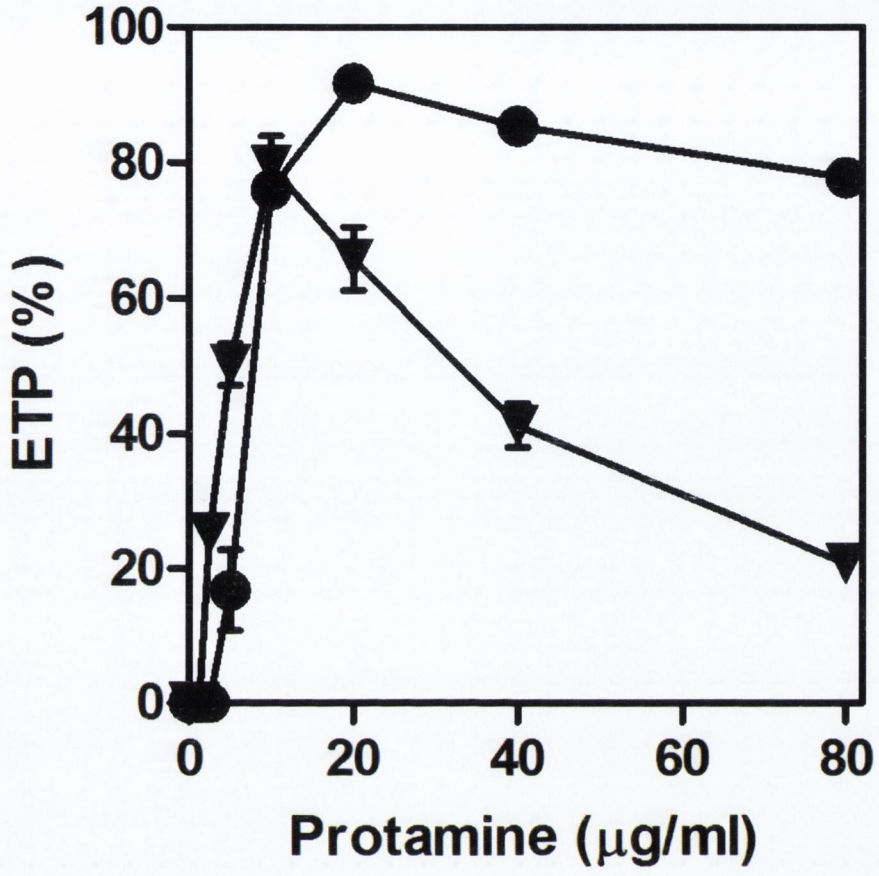


Figure 6.5: Excess protamine inhibits thrombin generation in normal pooled plasma containing LWMH.

Protamine sulphate (1.25-80μg/ml) was incubated with normal pooled plasma containing 1.0 IU/ml LMWH tinzaparin® (●) or enoxaparin® (▼). Thrombin generation was initiated with TF **(2.8)** and ETP (%) calculated. All experiments were performed in triplicate. Results are expressed as mean ± SEM.

6.2.6 Protamine sulphate enhances APC-mediated APTT prolongation in normal pooled plasma.

APC attenuates thrombin generation by specific proteolysis of procoagulant cofactors FVa and FVIIIa [84, 85]. FVa proteolysis by APC is impaired by another cationic polypeptide, platelet factor 4 (PF4) [206]. It was therefore hypothesized that protamine sulphate, by virtue of its cationicity, might similarly impair APC-mediated anticoagulant function. In a standard APTT assay, APC (1.25-20nM) produced a dose-dependent APTT prolongation, as expected. Unlike PF4, protamine (30μg/ml) enhanced the anticoagulant effect of APC in this assay **(Figure 6.6)**. APTT prolongation observed in the presence of both APC (1.25-20nM) and protamine sulphate was greater than the additive effect of each alone: plasma incubation with either APC (20nM) or protamine sulphate (30μg/ml) resulted in 180±9% and 67±3% APTT prolongations respectively, while incubation with both agents resulted in a 530±37% APTT prolongation.

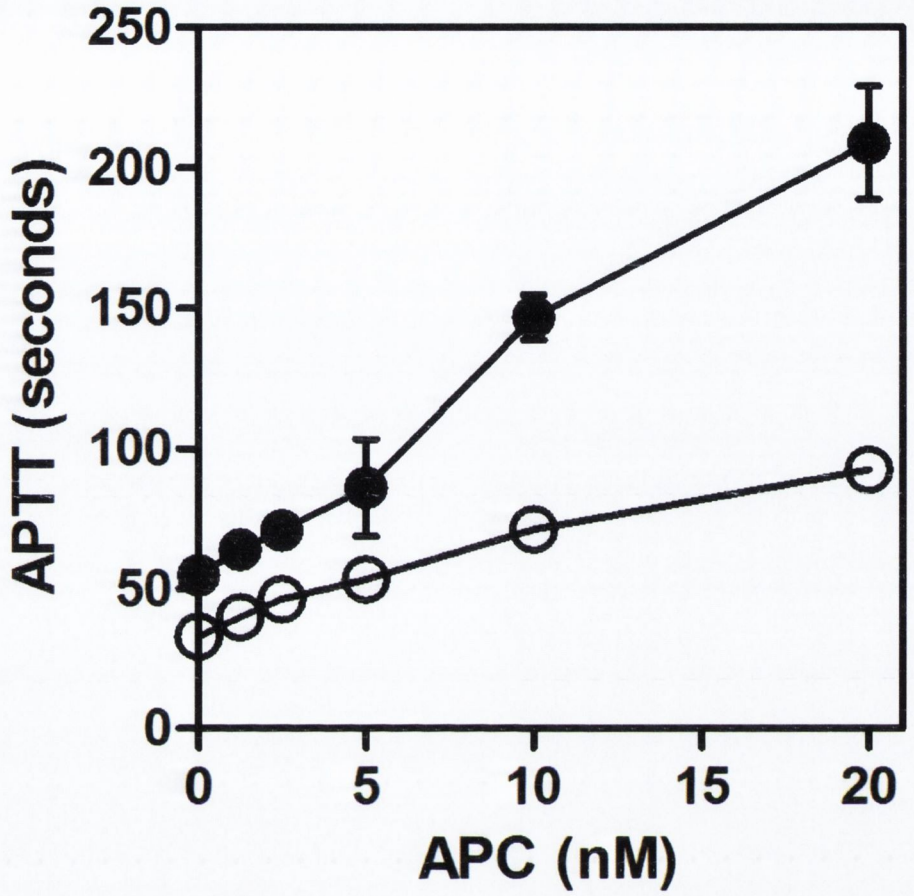


Figure 6.6: Plasma APTT prolongation by APC is enhanced by protamine sulphate.

APC (1.25-20nM) was incubated with normal pooled plasma in the presence (●) and absence (○) of protamine sulphate (30μg/ml). APTT was measured **(2.22)**. All experiments were performed in triplicate. Results are expressed as mean ± SEM.

6.2.7 Protamine sulphate enhances APC-mediated APTT prolongation in normal pooled plasma.

1nM APC resulted in only minimal attenuation of TF-induced thrombin generation in normal plasma. Co-incubation with 30μg/ml protamine sulphate virtually ablated thrombin generation **(Figure 6.7)**.

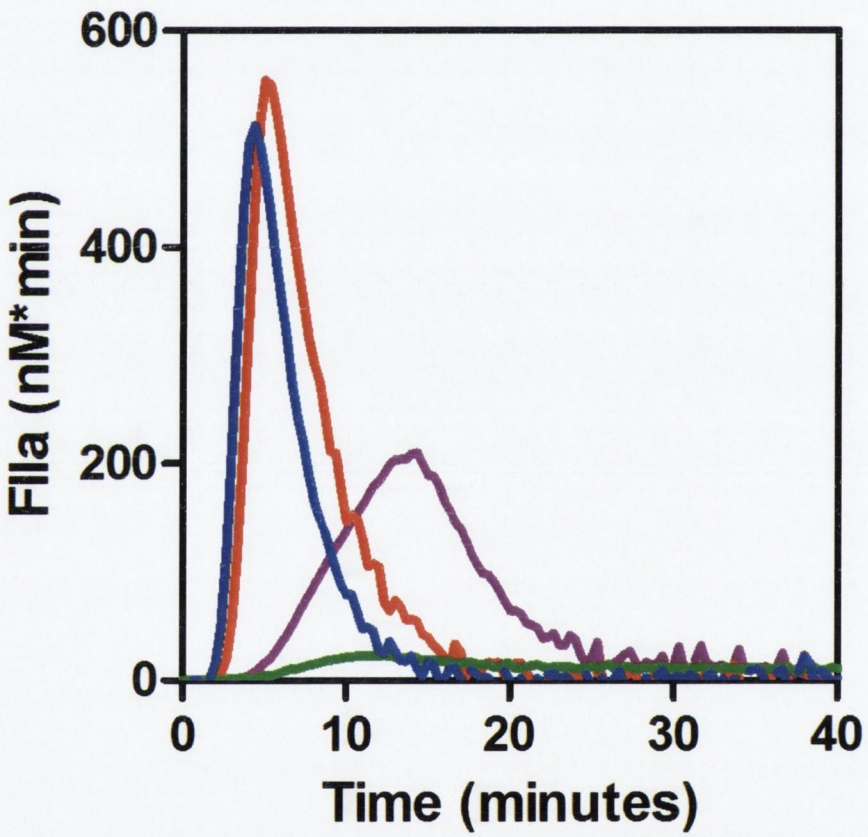


Figure 6.7: APC-mediated attenuation of thrombin generation is enhanced by protamine.

Thrombin generation was initiated with TF **(2.8)** in normal pooled plasma (*blue*) incubated with APC (1nM, *red*); protamine sulphate (30μg/ml, *purple*); or both (*green*). All experiments were performed in triplicate.

6.2.8 Protamine sulphate enhances APC-mediated attenuation of thrombin generation in heparinized normal pooled plasma.

A similar co-operative effect between APC and protamine was observed following *in vitro* reversal of UFH (1.0 IU/ml)-induced anticoagulation in normal plasma **(Figure 6.8)**. In the absence of APC, excess protamine attenuated ETP in a concentration-dependent fashion to a minimium of 57±9.8% of normal plasma ETP, as expected. In contrast, in the presence of APC (1nM), excess protamine (40 μg/ml) ablated thrombin generation.

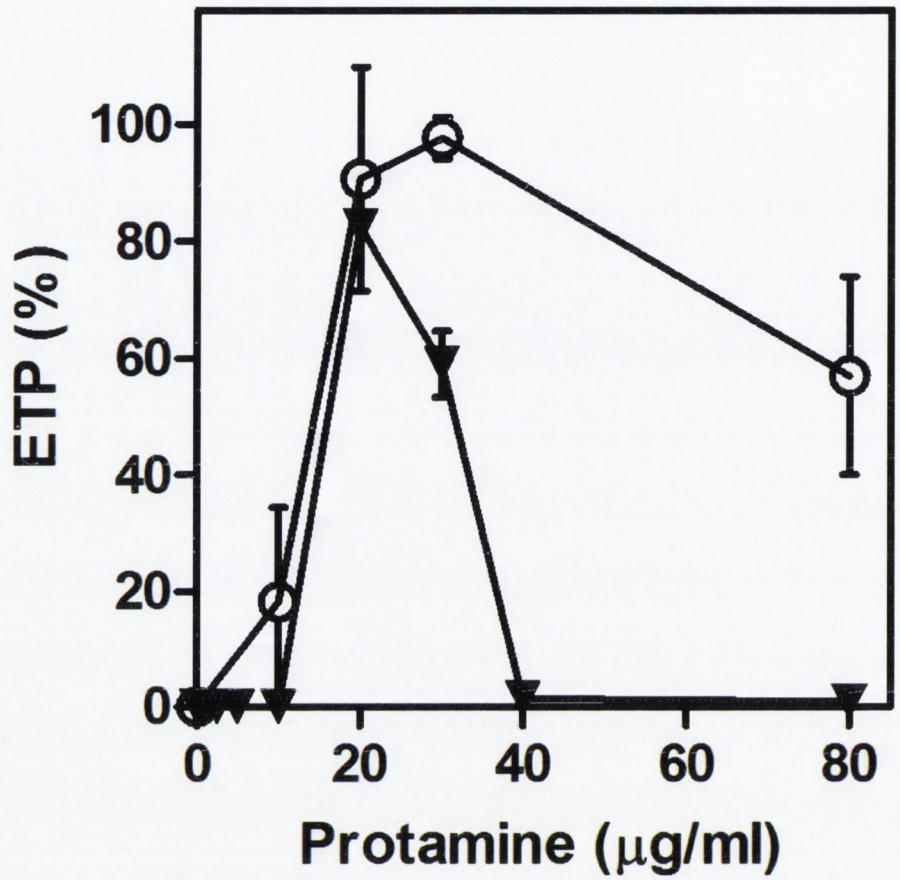


Figure 6.8: Excess protamine enhances the anticoagulant effect of APC in heparinised plasma.

Thrombin generation was initiated in normal pooled plasma incubated with 1.0 IU/ml unfractionated heparin and protamine sulphate (0.2-80μg/ml) in the presence (▼) and absence (○) of APC (1nM) and ETP (%) calculated. All experiments were performed in triplicate. Results are expressed as mean ± SEM.

6.2.9 Protamine sulphate does not enhance the anticoagulant effect of APC by influencing rate of FVa proteolysis.

Having identified a novel co-operative anticoagulant effect between protamine sulphate and APC, it was hypothesized that the mechanism underlying this co-operative effect might be enhancement of APC substrate proteolysis. To investigate the effect of protamine upon APC-mediated FVa proteolysis, an assay measuring rate of FVa inactivation in a purified system **(2.12)** was utilized. In this assay, APC (8nM)-mediated proteolysis of FVa (4nM) in the presence of phospholipids vesicles (PC:PS:PE 60%:20%:20%) was observed as expected over a 20-minute timecourse. No significant difference in rate of FVa proteolysis by APC was observed in the presence or absence of protamine sulphate **(Figure 6.9)**.

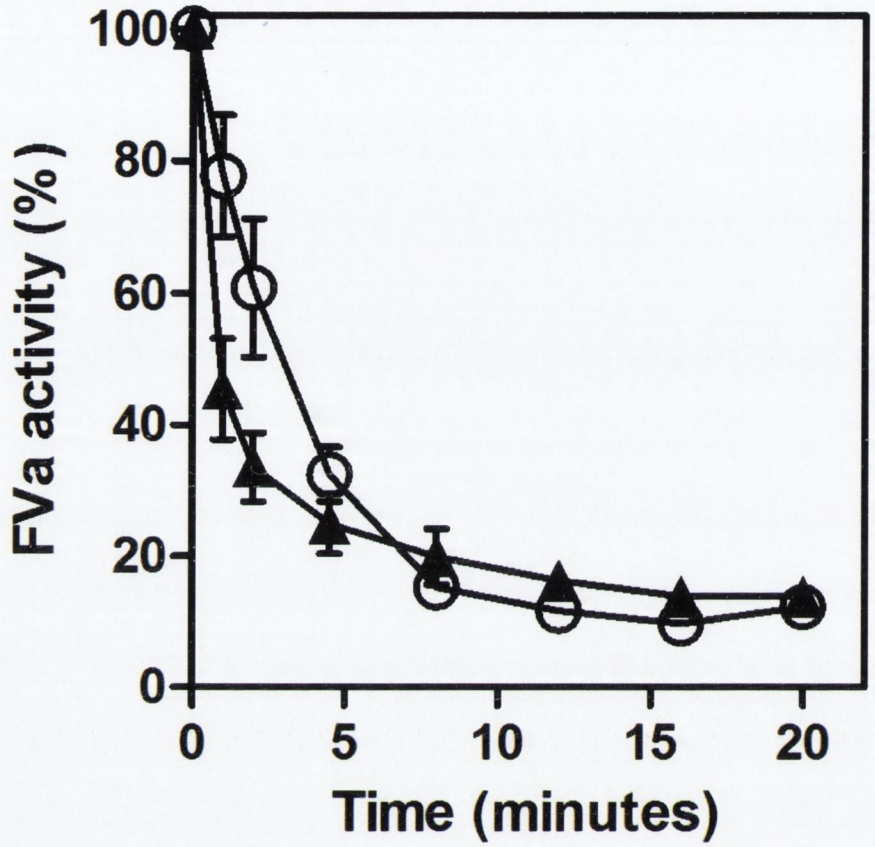


Figure 6.9: Enhancement by protamine of the anticoagulant effect of APC is not mediated by enhanced FVa hydrolysis.

The rate of FVa proteolysis by APC in the presence (○) and absence (▲) of protamine sulphate (3μg/ml) was measured **(2.12)**. All experiments were performed in triplicate. Results are expressed as mean ± SEM.

6.2.10 Protamine sulphate does not enhance the anticoagulant effect of APC by influencing rate of FVIIIa proteolysis.

To determine whether the co-operative effect of APC and protamine is instead mediated by enhancement of FVIIIa proteolysis, a thrombin generation assay using FVIII-deficient plasma supplemented with the APC-resistant recombinant FVIII variant, *R336Q/R562Q* [169] was utilized **(Figure 6.10)**. This assay was devised based upon the premise that if the APC/protamine co-operative anticoagulant effect were mediated primarily by enhanced FVIIIa proteolysis, then no co-operative effect should be observed in the presence of this APC-resistant FVIII variant. ETP of FVIII-deficient plasma supplemented with normal plasma concentration (1.0 IU/ml) of wild-type FVIII or FVIII-*R336Q/R562Q* was identical. In the absence of APC, protamine (3μg/ml) did not significantly attenuate the ETP of FVIII-deficient plasma supplemented with wild-type FVIII or FVIII-*R336Q/R562Q* (p=0.16; both 1.0 IU/ml). This result is in keeping with similar experiments performed at this protamine concentration in normal pooled plasma **(Figure 6.2)**. No significant difference was observed in APC-mediated enhancement of protamine sulphate's anticoagulant effect in FVIII-deficient plasma supplemented with normal levels (1.0 IU/ml) of either wild type FVIII or FVIII-*R336Q/R562Q*: ETP was attenuated to 11.6±4.3 % and 3.4±1.6% (compared with FVIII-deficient plasma supplemented with 1.0 IU/ml FVIII) respectively in the presence of both APC and protamine. Inability of APC to proteolyse FVIII did not ablate protamine sulphate's enhancement of APC-mediated anticoagulation, demonstrating that this phenomenon is not mediated by enhanced FVIIIa proteolysis.

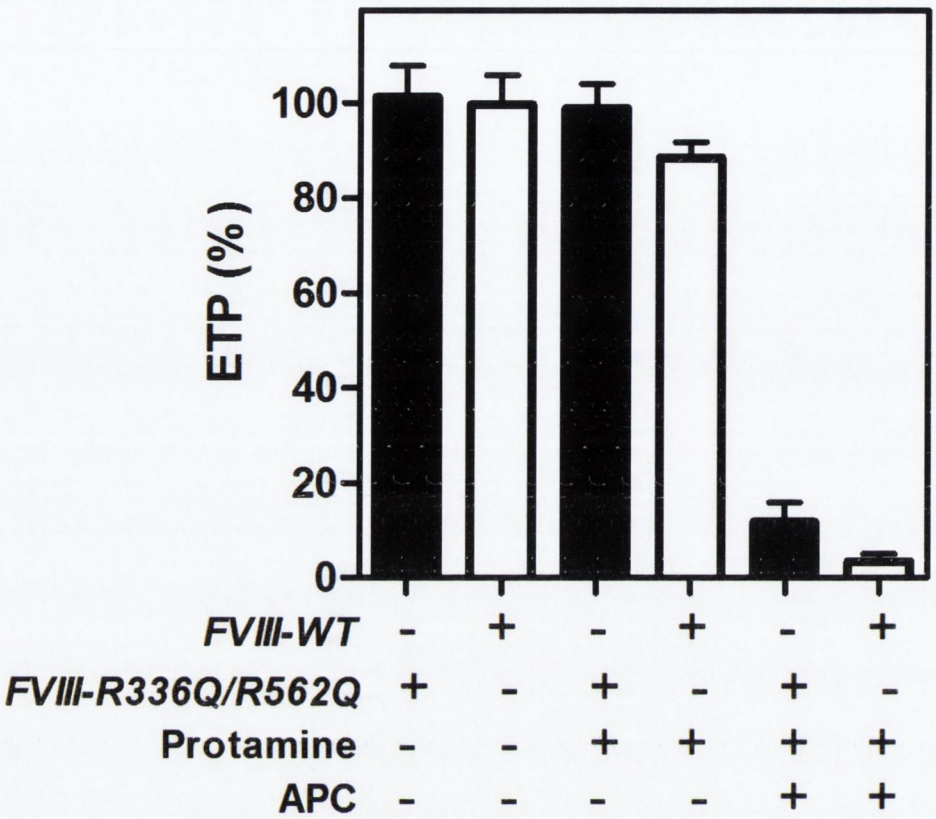


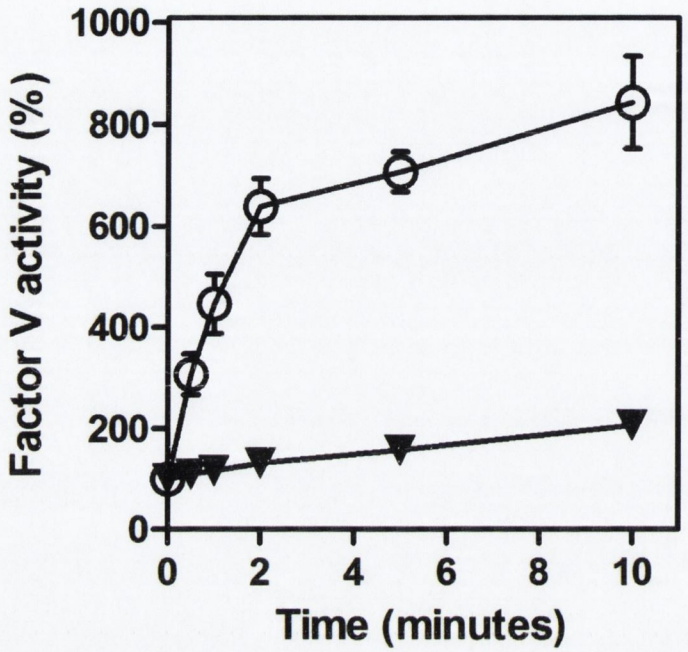
Figure 6.10: Enhancement by protamine of the anticoagulant effect of APC is not mediated by enhanced FVIIIa hydrolysis.

FVIII-deficient plasma (Technoclone®) was incubated with normal plasma concentration (1.0 IU/ml) of wild-type recombinant FVIII, or an APC-resistant FVIII variant, *FVIII-R336Q/R562Q*. Thrombin generation was initiated by TF as described previously **(2.8)** and ETP calculated in the presence and absence of protamine (3μg/ml), APC (10nM) or both. All experiments were performed in triplicate. Results are expressed as mean ± SEM.

6.2.11 Protamine sulphate inhibits thrombin -mediated activation of coagulation factor V.

It was hypothesized that protamine sulphate might influence the generation of the principal APC substrate, FVa. In order to address this, an assay measuring activation of coagulation factor V by thrombin or by FXa was established **(2.24)**. As anticipated, thrombin activated coagulation FV, resulting in a rapid increase in FV activity **(Figure 6.11 A)**. Protamine sulphate at pharmacological concentration (50μg/ml) entirely ablated thrombin-mediated FV activation. 50% inhibition of thrombin-mediated FV activation by protamine sulphate (0.25-12.5μg/ml) was observed at only 0.8μg/ml **(Figure 6.11 B)**. Given that peak plasma concentrations of protamine can reach 50μg/ml after a 50mg bolus dose [192], the clinical relevance of this effect is likely to be significant.

A


Factor V activity (%)
1000
800
600
400
200
0
0
2
4
6
8
10
Time (minutes)

B

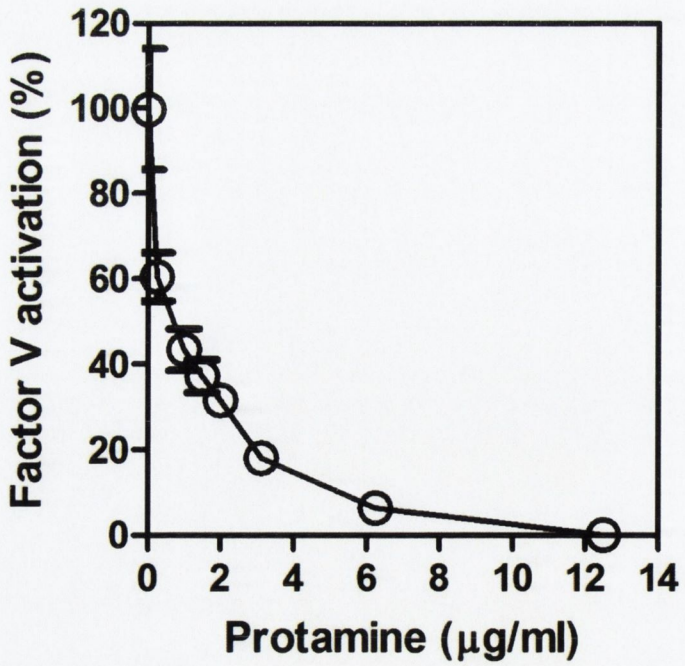

Factor V activation (%)
120
100
80
60
40
20
0
0
2
4
6
8
10
12
14
Protamine (µg/ml)

Figure 6.11: Protamine inhibits activation of coagulation factor V by thrombin.

(A) Factor V (100nM) was incubated with thrombin (0.1nM) at 37°C in a buffer containing 100mM NaCl, 5mM $CaCl_2$, 20mM HEPES (pH 7.5) and 0.2mg/ml BSA in the presence (▼) and absence (○) of protamine sulphate (50µg/ml). Timed aliquots (5µl) were removed and diluted 20-fold in a buffer containing 100mM NaCl and 20mM Tris-HCl (pH 7.5). 50µl of each diluted aliquot was immediately incubated with 50µl FV-deficient plasma (Instrumentation Laboratories®) at 37°C, followed by PT measurement **(2.22)**. Factor V activity (%) of each aliquot was determined by comparison to a standard curve of known FV activity. ***(B)*** The same assay was used to measure FV activity following incubation of factor V (100nM) with thrombin (0.1nM) at 37°C for 60 seconds in the presence of protamine (0.25-12.5µg/ml). Factor V activation represents percentage of FV activity measured following incubation for 60 seconds in the absence of protamine. All experiments were performed in triplicate. Results are expressed as mean ± SEM.

6.2.12 Protamine sulphate inhibits FXa- mediated activation of coagulation factor V.

While physiological FV activation is mediated principally by thrombin, FXa also contributes to FV activation [207]. Interestingly, FV activation by FXa was also ablated in the presence of protamine (50μg/ml; **Figure 6.12**).

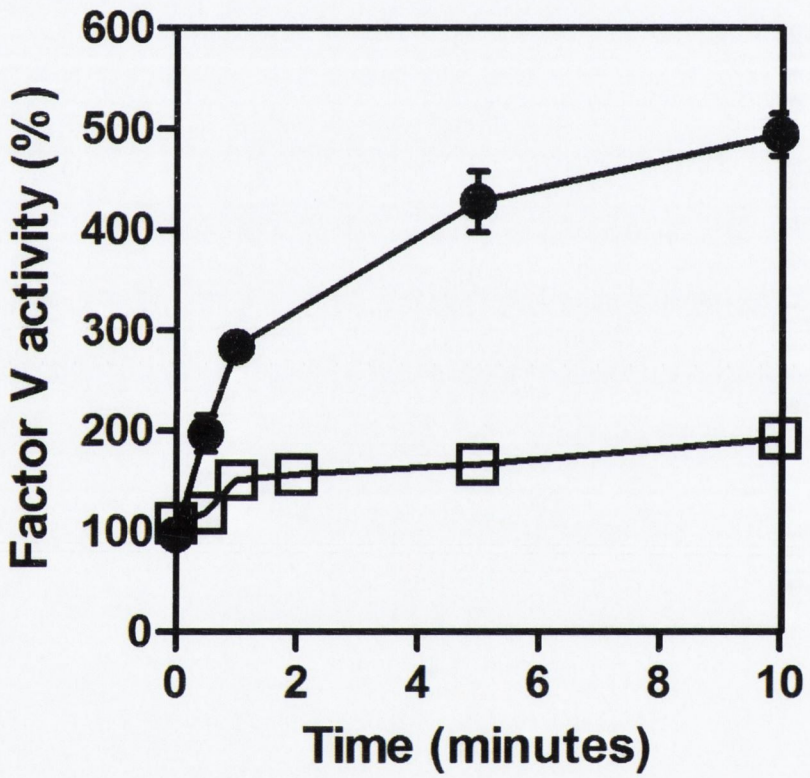


Figure 6.12: Protamine inhibits activation of coagulation factor V by Xa.

Factor V activation by FXa was measured by incubation of Factor V (100nM) with FXa (20nM) and phospholipid vesicles (80μM; 60% phosphatidylcholine, 20% phosphatidylserine and 20% phosphatidylethanolamine) in the presence (□) and absence (●) of protamine sulphate (50μg/ml). FV activity (%) was determined **(2.24)**. All experiments were performed in triplicate. Results are expressed as mean ± SEM.

6.2.13 Preactivation of FV greatly reduces the anticoagulant effect of protamine in plasma.

In order to determine the relative contribution of protamine-mediated inhibition of FV activation to its entire observed anticoagulant effect in plasma, a thrombin generation assay was utilized in which either FV or FVa (both 2.5-20nM) were incubated with FV-deficient plasma in the presence and absence of protamine sulphate (30μg/ml). ETP of FV-deficient plasma supplemented with FV at normal plasma concentration (20nM) was defined as 100% **(Figure 6.13 A)** and was associated with a normal thrombin generation curve (not shown). FV-deficient plasma supported thrombin generation likely due to the presence of residual FV, however ETP was greatly reduced (by ~80%) compared with normal plasma. Pre-incubation with FV (2.5-20nM) resulted in a rapid restoration of thrombin generation to normal: in the presence of even 2.5nM FV, ETP had returned to 87±0.9% of ETP measured in FV-deficient plasma supplemented with normal plasma FV concentration (20nM). In the presence of protamine sulphate (30μg/ml), ETP was significantly attenuated at each FV concentration, reaching a maximum of only 29±3% at 20nM FV ($p<0.001$ compared with FV-deficient plasma supplemented with 20nM FV in the absence of protamine). In contrast, pre-incubation of FV-deficient plasma with FVa (0.1-20nM) resulted in a rapid resoration of thrombin generation both in the absence and presence of protamine sulphate **(Figure 6.13 B)**. Interestingly, a minimal, non-significant, residual ETP attenuation was observed at each FVa concentration in the presence of protamine (~7% at 20nM FVa, $p=0.3$).

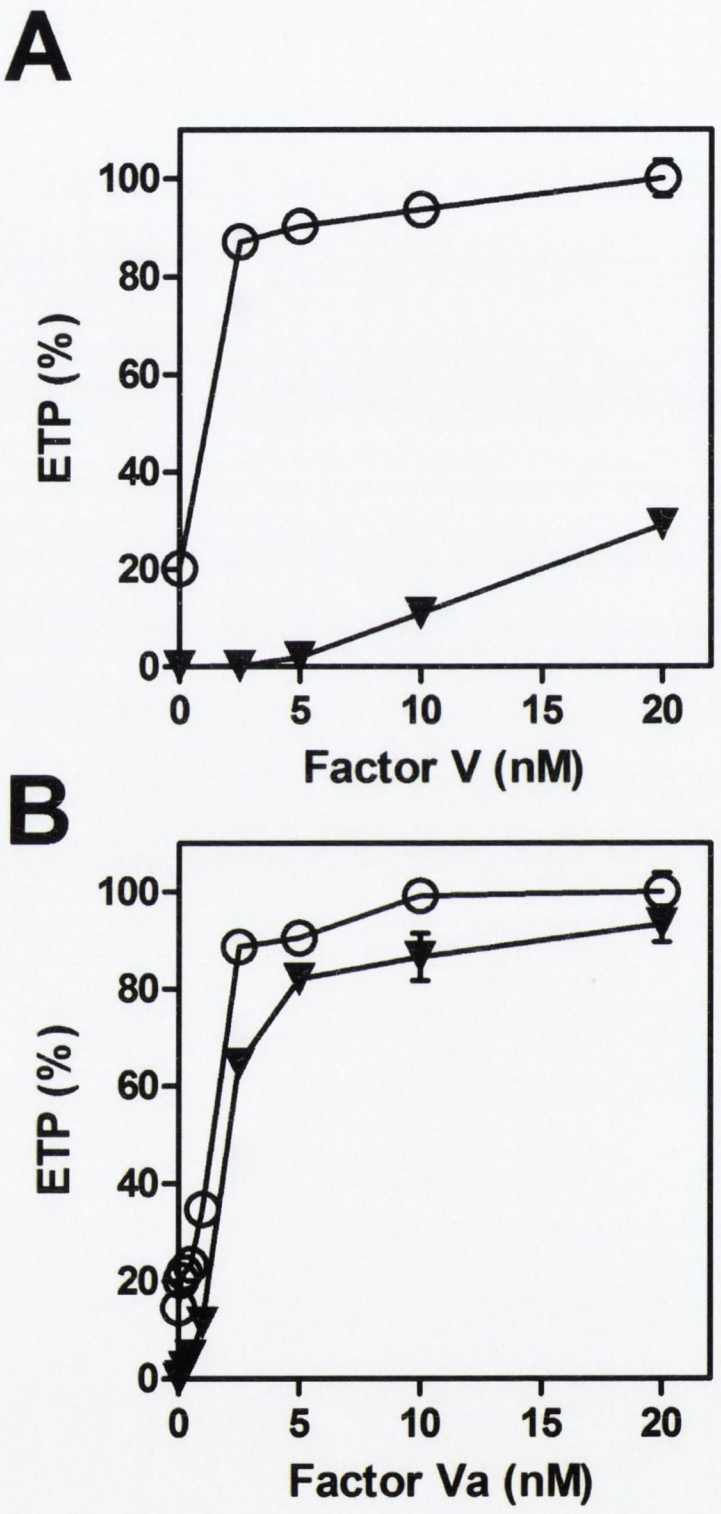

A
100
80
60
40
20
0
ETP (%)
0
5
10
15
20
Factor V (nM)
B
100
80
60
40
20
0
ETP (%)
0
5
10
15
20
Factor Va (nM)

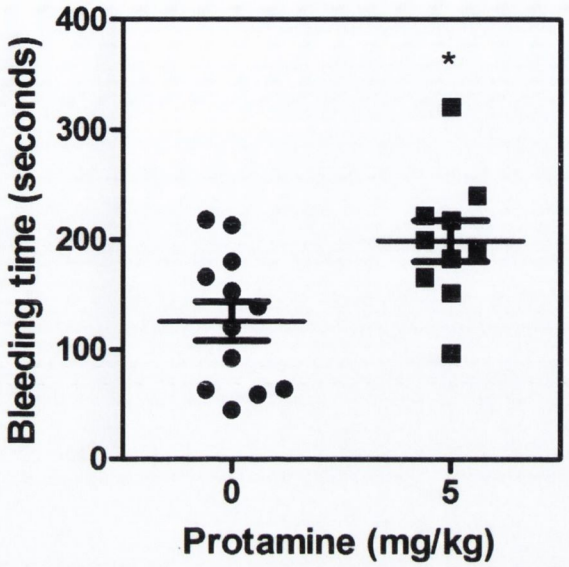
Figure 6.13: The anticoagulant effect of protamine is greatly reduced by preactivation of FV to FVa.

FV-deficient plasma (HemosIL®) was supplemented with ***(A)*** factor V (2.5-20nM) or ***(B)*** factor Va (0.1-20nM) in the presence (▼) or absence (○) of protamine sulphate (30μg/ml). Thrombin generation was initiated with TF **(2.8)**, and ETP calculated. All experiments were performed in triplicate. Results are expressed as mean ± SEM.

6.2.14: Characterization of *in vivo* anticoagulant properties of protamine sulphate.

Typical plasma protamine concentrations following a single 50mg bolus can reach 50µg/ml [192]. However in practice, particularly following cardiopulmonary bypass, higher and repeated doses are frequently administered. Consequently, dosing levels in excess of 5mg/kg are frequently encountered [200]. In order to investigate the anticoagulant effects associated with protamine sulphate *in vivo*, BALB/c mice were injected with either protamine sulphate (5mg/kg) or phosphate buffered saline **(2.21).** Protamine administration resulted in a significant prolongation of bleeding time **(Figure 6.14 A)**, from 126±18 to 199±19 seconds ($p<0.05$), but only a minimal (14±5%, $p<0.05$) reduction in TF-induced plasma thrombin generation **(Figure 6.14 B)**.

A


Bleeding time (seconds)
400
300
200
100
0
*
0
5
Protamine (mg/kg)

B

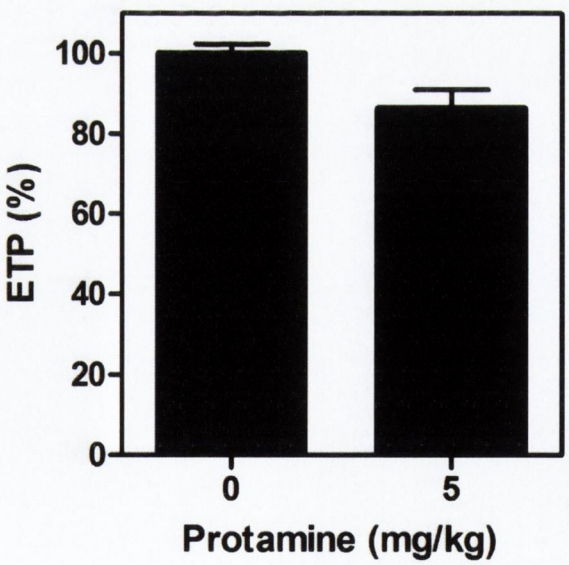

ETP (%)
100
80
60
40
20
0
0
5
Protamine (mg/kg)

Figure 6.13: Protamine prolongs bleeding time *in vivo*.

(A) BALB/c mice, aged 6-8 weeks, were weighed and anaesthetized with midazolam and etorphine hydrochloride. 50µl protamine sulphate (5mg/kg) or phosphate buffered saline (PBS), was administered intravenously. After 90 seconds tail tip transaction was performed. The tail was suspended in PBS (37°C) and time taken for complete cessation of bleeding recorded. ***(B)*** Protamine sulphate (5mg/kg) or PBS were administered intravenously to a separate group of mice. Mice were exsanguinated 1.5 minutes after protamine administration. Murine plasma was incubated with 4µM phospholipids and thrombin generation initiated with 5pM sTF and 100mM $CaCl_2$ as described previously **(2.8)**. Endogenous thrombin potential (ETP; %) was calculated as before. All experiments were performed in triplicate. Results are expressed as mean ± SEM. (*P<0.05; unpaired 2-tailed *t* test performed.

6.3 DISCUSSION

Protamine sulphate is widely used during reversal of heparin anticoagulation and is itself paradoxically associated with anticoagulant properties, which have been associated with increased blood loss after cardiothoracic surgery involving cardiopulmonary bypass [202, 203]. While some attempts had previously been made to elucidate the molecular mechanisms underlying this clinically relevant anticoagulant effect, they remained poorly understood. I hypothesized that the observed unexpected enhancement of APC-mediated anticoagulation by protamine sulphate could provide novel insights into the molecular mechanism underlying the anticoagulant effect of protamine itself.

Protamine sulphate has been used for decades as the treatment of choice in reversal of heparin-induced anticoagulation. One of its most frequent indications is reversal of systemic anticoagulation used during cardiopulmonary bypass (CBP) procedures. In this setting, protamine has been postulated to increase post-operative blood loss [202, 203]. In a prospective study, 254 patients who received UFH during CPB were randomized to have heparin neutralized by either a fixed dose of protamine (0.8 mg per mg total UFH) or a calculated protamine dose based upon residual plasma heparin concentration [202]. Lower total protamine doses (which were observed in the latter group) resulted in reduced perioperative blood loss and reduced requirement for platelet, fresh frozen plasma and cryoprecipitate transfusion in the perioperative period, leading authors to advocate minimization of postoperative protamine use, using the algorithm which bases protamine dosing on measured residual plasma heparin concentration [202]. In another prospective randomized trial, reduced

protamine dosing was similarly associated with decreased mediastinal blood loss [203].

In this chapter the molecular mechanisms underlying these clinically significant anticoagulant properties of protamine sulphate were sought, using the observation that protamine enhances APC-mediated anticoagulant properties as a basis for further investigation. Protamine was shown to prolong both APTT and PT of normal plasma *in vitro* **(Figure 6.1)**. Consequently it was hypothesized that the anticoagulant effect of protamine might be mediated by an effect upon the common pathway. Moreover, protamine significantly attenuated TF-initiated thrombin generation **(Figures 6.2 and 6.3)**. ETP attenuation to 58.7±7.2% of normal plasma ETP ($p<0.05$) was observed following incubation with protamine sulphate at the clinically relevant plasma concentration of 30μg/ml [192]. Attenuation of thrombin generation was also observed when protamine was present in excess in plasma anticoagulated with UFH **(Figure 6.4)**. Several thrombin generation curve parameters were influenced by protamine, including ETP, lag time to initiation of thrombin generation, time to peak thrombin, and peak thrombin. While plasma levels of many factors, including FV, FVII, TFPI, free protein S and fibrinogen have been shown to modulate the lag time to initiation of thrombin generation [208, 209], FV uniquely possesses the ability to influence several parameters simultaneously [209]. Collectively these results led to speculation that modulation of either proteolysis or activation of procoagulant FV could mediate anticoagulant properties of protamine sulphate.

A profound anticoagulant co-operative effect was demonstrated between protamine sulphate and APC in APTT and thrombin generation assays **(Figures 6.6, 6.7 and 6.8)**.

The anticoagulant effect of APC is mediated by proteolysis of FVa [84] and FVIIIa [85]. However, the anticoagulant effect of protamine was not found to be mediated by enhanced proteolysis of either FVa or FVIIIa **(Figures 6.9 and 6.10)**. Consequently, it was hypothesized that the co-operative effect of protamine and APC might be mediated by inhibition of substrate generation. Procofactor V is activated early in the coagulation process by thrombin by limited cleavage at Arg-709, Arg-1018 and Arg-1545 [210]. FVa associates with FXa on negatively charged phospholipid membrane surfaces, where it plays a critical cofactor role in the prothrombinase complex. A 300,000-fold increase in the rate of FXa-catalyzed conversion of prothrombin to thrombin is observed in the presence of FVa [39]. Protamine was found to significantly attenuate activation of FV by thrombin and by FXa **(Figures 6.11 and 6.12)**. Previous studies have postulated alternative mechanisms for the anticoagulant effect of protamine sulphate [197, 204]. However, protamine only minimally attenuated thrombin generation in plasma containing pre-activated FVa rather than procofactor V **(Figure 6.13)**, suggesting that the majority of the anticoagulant effect of protamine sulphate may in fact be attributed to specific inhibition of FV activation, with other reported effects playing a relatively minor role.

in keeping with previous studies [198], protamine was initially confirmed to be associated with *in vivo* anticoagulant properties, resulting in a significant prolongation of tail bleeding time in mice **(Figure 6.14 A).** Interestingly, TF-induced plasma thrombin generation was only minimally reduced *in vivo* **(Figure 6.14 B)**, possibly reflecting the well-recognized ability of protamine to interact with and bind to negatively charged cell surface proteoglycans, which may limit its bioavailability [211].

Future work will focus upon elucidating the precise molecular mechanism underlying protamine-mediated inhibition of FV activation. Given that FV activation by both thrombin and FXa was found to be inhibited by protamine, it is likely that protamine forms an inhibitory complex with FV. Due to a high arginine content, protamine is highly cationic. Interestingly, six procofactor FV tyrosine residues undergo post-translational modification by addition of negatively charged sulphate groups [212]. Five of these residues are located at the C-terminal end of the heavy chain and in the 150-kDa activation peptide, in close proximity to sites of thrombin cleavage [212]. Consequently, it is possible that positively charged protamine sulphate binds to this region, inhibits interaction of thrombin with procofactor FV and modulates its rate of activation. Several recent studies have demonstrated conversely that anionic molecules have the opposite effect to cationic protamine on FV activation [213-215]. AV513, a sulphated proteoglycan derived from plants, increases thrombin generation by enhancing FV activation [215]. Similarly, Smith *et al* found that negatively charged platelet polyphosphate also mediates procoagulant activity by the same mechanism [213].

These findings have important clinical implications. The ACT assay is universally used for monitoring of anticoagulation induced by UFH in the setting of cardiac surgery and to monitor UFH reversal with protamine postoperatively [190], while the APTT assay is routinely used to monitor efficacy of heparin reversal in most other clinical situations. The finding that protamine inhibits FV activation, prolonging plasma clotting times including APTT, is of critical importance in this situation. Administration of excessive protamine doses prolongs plasma clotting time. A clinician interpreting this result may

infer that the prolonged clotting time is due to the presence of residual heparin and administer further protamine doses, therefore further prolonging plasma clotting times and possibly causing bleeding complications. Moreover, the observation that protamine produces a co-operative anticoagulant effect with APC by inhibiting FV activation could theoretically result in bleeding complications in patients receiving doses of protamine to reverse heparin in order to facilitate administration of recombinant APC. To date no such cases have been reported.

Finally, these results raise potential concerns in relation to the use of protamine to reverse LMWH-induced anticoagulant. Protamine was more effective in reversing the anticoagulant activity of LMWH with low anti-FXa: anti-IIa activity ratios (Fig 6.3 B). The anti-FXa: anti-IIa ratio of LMWH Tinzaparin® is 2:1. In contrast, that of Enoxaparin® is 3:1. Perhaps more significantly, however, the anticoagulant effect of excess protamine following reversal of LMWH was found to vary depending upon the type of LMWH being reversed (Fig 6.3 B). In the presence of LMWH Tinzaparin®, excess protamine was found to result in a mild dose-dependent ETP reduction however the maximum reduction observed was only to 78% of normal. However, in plasma containing LMWH Enoxaparin®, higher doses of protamine resulted in a significant anticoagulant effect. Maximal ETP reduction was to 21% of normal. This effect may reflect residual anti-FXa activity, coupled with an inhibitory effect of excess free protamine on FV activation.

In conclusion, protamine sulphate exerts an anticoagulant effect in plasma by inhibiting activation of procoagulant cofactor FV by thrombin and by FXa. This finding

is of significant potential clinical importance. Adequately powered clinical studies will be required to define consequences of excess protamine in clinical heparin reversal.

REFERENCES

1. Furie, B. and B.C. Furie, *Mechanisms of thrombus formation.* N Engl J Med, 2008. **359**(9): p. 938-49.
2. Andrews, R.K. and M.C. Berndt, *Platelet adhesion: a game of catch and release.* J Clin Invest, 2008. **118**(9): p. 3009-11.
3. Sadler, J.E., *Biochemistry and genetics of von Willebrand factor.* Annu Rev Biochem, 1998. **67**: p. 395-424.
4. Ruggeri, Z.M., *Von Willebrand factor, platelets and endothelial cell interactions.* J Thromb Haemost, 2003. **1**(7): p. 1335-42.
5. Kramer, R.H., K.G. Vogel, and G.L. Nicolson, *Solubilization and degradation of subendothelial matrix glycoproteins and proteoglycans by metastatic tumor cells.* J Biol Chem, 1982. **257**(5): p. 2678-86.
6. Lenting, P.J., et al., *Regulation of von Willebrand factor-platelet interactions.* Thromb Haemost, 2010. **104**(3): p. 449-55.
7. Moroi, M., et al., *A patient with platelets deficient in glycoprotein VI that lack both collagen-induced aggregation and adhesion.* J Clin Invest, 1989. **84**(5): p. 1440-5.
8. Dubois, C., et al., *Glycoprotein VI-dependent and -independent pathways of thrombus formation in vivo.* Blood, 2006. **107**(10): p. 3902-6.
9. Nieswandt, B. and S.P. Watson, *Platelet-collagen interaction: is GPVI the central receptor?* Blood, 2003. **102**(2): p. 449-61.
10. Nieuwenhuis, H.K., et al., *Human blood platelets showing no response to collagen fail to express surface glycoprotein Ia.* Nature, 1985. **318**(6045): p. 470-2.
11. Kehrel, B., *Platelet receptors for collagens.* Platelets, 1995. **6**(1): p. 11-6.
12. Jung, S.M. and M. Moroi, *Signal-transducing mechanisms involved in activation of the platelet collagen receptor integrin alpha(2)beta(1).* J Biol Chem, 2000. **275**(11): p. 8016-26.
13. Atkinson, B.T., G.E. Jarvis, and S.P. Watson, *Activation of GPVI by collagen is regulated by alpha2beta1 and secondary mediators.* J Thromb Haemost, 2003. **1**(6): p. 1278-87.
14. Mackman, N., R.E. Tilley, and N.S. Key, *Role of the extrinsic pathway of blood coagulation in hemostasis and thrombosis.* Arterioscler Thromb Vasc Biol, 2007. **27**(8): p. 1687-93.
15. Fleck, R.A., et al., *Localization of human tissue factor antigen by immunostaining with monospecific, polyclonal anti-human tissue factor antibody.* Thromb Res, 1990. **59**(2): p. 421-37.
16. Drake, T.A., J.H. Morrissey, and T.S. Edgington, *Selective cellular expression of tissue factor in human tissues. Implications for disorders of hemostasis and thrombosis.* Am J Pathol, 1989. **134**(5): p. 1087-97.
17. Egorina, E.M., et al., *Intracellular and surface distribution of monocyte tissue factor: application to intersubject variability.* Arterioscler Thromb Vasc Biol, 2005. **25**(7): p. 1493-8.
18. Taylor, F.B., Jr., et al., *Lethal E. coli septic shock is prevented by blocking tissue factor with monoclonal antibody.* Circ Shock, 1991. **33**(3): p. 127-34.
19. Pawlinski, R., et al., *Role of tissue factor and protease-activated receptors in a mouse model of endotoxemia.* Blood, 2004. **103**(4): p. 1342-7.
20. Parry, G.C. and N. Mackman, *Transcriptional regulation of tissue factor expression in human endothelial cells.* Arterioscler Thromb Vasc Biol, 1995. **15**(5): p. 612-21.
21. Shibamiya, A., et al., *A key role for Toll-like receptor-3 in disrupting the hemostasis balance on endothelial cells.* Blood, 2009. **113**(3): p. 714-22.

22. Kelley, R.F., et al., *Analysis of the factor VIIa binding site on human tissue factor: effects of tissue factor mutations on the kinetics and thermodynamics of binding.* Biochemistry, 1995. **34**(33): p. 10383-92.
23. Morrissey, J.H., et al., *Quantitation of activated factor VII levels in plasma using a tissue factor mutant selectively deficient in promoting factor VII activation.* Blood, 1993. **81**(3): p. 734-44.
24. Ruf, W. and T.S. Edgington, *Structural biology of tissue factor, the initiator of thrombogenesis in vivo.* FASEB J, 1994. **8**(6): p. 385-90.
25. Dickinson, C.D. and W. Ruf, *Active site modification of factor VIIa affects interactions of the protease domain with tissue factor.* J Biol Chem, 1997. **272**(32): p. 19875-9.
26. Wildgoose, P., et al., *The role of phospholipids and the factor VII Gla-domain in the interaction of factor VII with tissue factor.* Thromb Haemost, 1992. **67**(6): p. 679-85.
27. Mann, K.G., S. Butenas, and K. Brummel, *The dynamics of thrombin formation.* Arterioscler Thromb Vasc Biol, 2003. **23**(1): p. 17-25.
28. Crawley, J.T. and D.A. Lane, *The haemostatic role of tissue factor pathway inhibitor.* Arterioscler Thromb Vasc Biol, 2008. **28**(2): p. 233-42.
29. Wun, T.C., et al., *Cloning and characterization of a cDNA coding for the lipoprotein-associated coagulation inhibitor shows that it consists of three tandem Kunitz-type inhibitory domains.* J Biol Chem, 1988. **263**(13): p. 6001-4.
30. Girard, T.J., et al., *Functional significance of the Kunitz-type inhibitory domains of lipoprotein-associated coagulation inhibitor.* Nature, 1989. **338**(6215): p. 518-20.
31. Piro, O. and G.J. Broze, Jr., *Role for the Kunitz-3 domain of tissue factor pathway inhibitor-alpha in cell surface binding.* Circulation, 2004. **110**(23): p. 3567-72.
32. Baugh, R.J., G.J. Broze, Jr., and S. Krishnaswamy, *Regulation of extrinsic pathway factor Xa formation by tissue factor pathway inhibitor.* J Biol Chem, 1998. **273**(8): p. 4378-86.
33. Hackeng, T.M., et al., *Protein S stimulates inhibition of the tissue factor pathway by tissue factor pathway inhibitor.* Proc Natl Acad Sci U S A, 2006. **103**(9): p. 3106-11.
34. Ragni, M.V., et al., *Comparison of bleeding tendency, factor XI coagulant activity, and factor XI antigen in 25 factor XI-deficient kindreds.* Blood, 1985. **65**(3): p. 719-24.
35. Pieters, J., T. Lindhout, and H.C. Hemker, *In situ-generated thrombin is the only enzyme that effectively activates factor VIII and factor V in thromboplastin-activated plasma.* Blood, 1989. **74**(3): p. 1021-4.
36. Brummel, K.E., et al., *Thrombin functions during tissue factor-induced blood coagulation.* Blood, 2002. **100**(1): p. 148-52.
37. Suttie, J.W. and C.M. Jackson, *Prothrombin structure, activation, and biosynthesis.* Physiol Rev, 1977. **57**(1): p. 1-70.
38. Rosing, J., et al., *The role of phospholipids and factor Va in the prothrombinase complex.* J Biol Chem, 1980. **255**(1): p. 274-83.
39. Nesheim, M.E., J.B. Taswell, and K.G. Mann, *The contribution of bovine Factor V and Factor Va to the activity of prothrombinase.* J Biol Chem, 1979. **254**(21): p. 10952-62.
40. Shen, B.W., et al., *The tertiary structure and domain organization of coagulation factor VIII.* Blood, 2008. **111**(3): p. 1240-7.
41. van Dieijen, G., et al., *The role of phospholipid and factor VIIIa in the activation of bovine factor X.* J Biol Chem, 1981. **256**(7): p. 3433-42.
42. Foster, P.A., et al., *A major factor VIII binding domain resides within the amino-terminal 272 amino acid residues of von Willebrand factor.* J Biol Chem, 1987. **262**(18): p. 8443-6.
43. Ahmad, S.S., R. Rawala-Sheikh, and P.N. Walsh, *Components and assembly of the factor X activating complex.* Semin Thromb Hemost, 1992. **18**(3): p. 311-23.

44. Ariens, R.A., et al., *Role of factor XIII in fibrin clot formation and effects of genetic polymorphisms.* Blood, 2002. **100**(3): p. 743-54.
45. Spraggon, G., S.J. Everse, and R.F. Doolittle, *Crystal structures of fragment D from human fibrinogen and its crosslinked counterpart from fibrin.* Nature, 1997. **389**(6650): p. 455-62.
46. Holvoet, P., H.R. Lijnen, and D. Collen, *A monoclonal antibody specific for Lys-plasminogen. Application to the study of the activation pathways of plasminogen in vivo.* J Biol Chem, 1985. **260**(22): p. 12106-11.
47. Cesarman-Maus, G. and K.A. Hajjar, *Molecular mechanisms of fibrinolysis.* Br J Haematol, 2005. **129**(3): p. 307-21.
48. Rau, J.C., et al., *Serpins in thrombosis, hemostasis and fibrinolysis.* J Thromb Haemost, 2007. **5 Suppl 1**: p. 102-15.
49. Zwaal, R.F., P. Comfurius, and E.M. Bevers, *Lipid-protein interactions in blood coagulation.* Biochim Biophys Acta, 1998. **1376**(3): p. 433-53.
50. McDonald, J.F., et al., *Comparison of naturally occurring vitamin K-dependent proteins: correlation of amino acid sequences and membrane binding properties suggests a membrane contact site.* Biochemistry, 1997. **36**(17): p. 5120-7.
51. Villoutreix, B.O., et al., *Three-dimensional model of the SHBG-like region of anticoagulant protein S: new structure-function insights.* Proteins, 2001. **43**(2): p. 203-16.
52. Broze, G.J., Jr. and J.P. Miletich, *Human Protein Z.* J Clin Invest, 1984. **73**(4): p. 933-8.
53. Sejima, H., et al., *Primary structure of vitamin K-dependent human protein Z.* Biochem Biophys Res Commun, 1990. **171**(2): p. 661-8.
54. Ichinose, A., et al., *Amino acid sequence of human protein Z, a vitamin K-dependent plasma glycoprotein.* Biochem Biophys Res Commun, 1990. **172**(3): p. 1139-44.
55. Han, X., R. Fiehler, and G.J. Broze, Jr., *Characterization of the protein Z-dependent protease inhibitor.* Blood, 2000. **96**(9): p. 3049-55.
56. Stenflo, J., et al., *Vitamin K dependent modifications of glutamic acid residues in prothrombin.* Proc Natl Acad Sci U S A, 1974. **71**(7): p. 2730-3.
57. Nelsestuen, G.L., T.H. Zytkovicz, and J.B. Howard, *The mode of action of vitamin K. Identification of gamma-carboxyglutamic acid as a component of prothrombin.* J Biol Chem, 1974. **249**(19): p. 6347-50.
58. Dementiev, A., et al., *The ternary complex of antithrombin-anhydrothrombin-heparin reveals the basis of inhibitor specificity.* Nat Struct Mol Biol, 2004. **11**(9): p. 863-7.
59. Abildgaard, U., *Highly purified antithrombin 3 with heparin cofactor activity prepared by disc electrophoresis.* Scand J Clin Lab Invest, 1968. **21**(1): p. 89-91.
60. Lindahl, U., et al., *Structure of the antithrombin-binding site in heparin.* Proc Natl Acad Sci U S A, 1979. **76**(7): p. 3198-202.
61. Choay, J., et al., *Structural studies on a biologically active hexasaccharide obtained from heparin.* Ann N Y Acad Sci, 1981. **370**: p. 644-9.
62. Foster, D.C., S. Yoshitake, and E.W. Davie, *The nucleotide sequence of the gene for human protein C.* Proc Natl Acad Sci U S A, 1985. **82**(14): p. 4673-7.
63. Beckmann, R.J., et al., *The structure and evolution of a 461 amino acid human protein C precursor and its messenger RNA, based upon the DNA sequence of cloned human liver cDNAs.* Nucleic Acids Res, 1985. **13**(14): p. 5233-47.
64. Kisiel, W., *Human plasma protein C: isolation, characterization, and mechanism of activation by alpha-thrombin.* J Clin Invest, 1979. **64**(3): p. 761-9.
65. Stearns-Kurosawa, D.J., et al., *The endothelial cell protein C receptor augments protein C activation by the thrombin-thrombomodulin complex.* Proc Natl Acad Sci U S A, 1996. **93**(19): p. 10212-6.

66. Stenflo, J., et al., *Epidermal growth factor-like domains in the vitamin K-dependent clotting factors. Some structure-function relationships.* Ann N Y Acad Sci, 1991. **614**: p. 11-29.
67. Mather, T., et al., *The 2.8 A crystal structure of Gla-domainless activated protein C.* EMBO J, 1996. **15**(24): p. 6822-31.
68. Bode, W. and R. Huber, *Natural protein proteinase inhibitors and their interaction with proteinases.* Eur J Biochem, 1992. **204**(2): p. 433-51.
69. Gale, A.J., A. Tsavaler, and J.H. Griffin, *Molecular characterization of an extended binding site for coagulation factor Va in the positive exosite of activated protein C.* J Biol Chem, 2002. **277**(32): p. 28836-40.
70. Fukudome, K. and C.T. Esmon, *Identification, cloning, and regulation of a novel endothelial cell protein C/activated protein C receptor.* J Biol Chem, 1994. **269**(42): p. 26486-91.
71. Simmonds, R.E. and D.A. Lane, *Structural and functional implications of the intron/exon organization of the human endothelial cell protein C/activated protein C receptor (EPCR) gene: comparison with the structure of CD1/major histocompatibility complex alpha1 and alpha2 domains.* Blood, 1999. **94**(2): p. 632-41.
72. Laszik, Z., et al., *Human protein C receptor is present primarily on endothelium of large blood vessels: implications for the control of the protein C pathway.* Circulation, 1997. **96**(10): p. 3633-40.
73. Oganesyan, V., et al., *The crystal structure of the endothelial protein C receptor and a bound phospholipid.* J Biol Chem, 2002. **277**(28): p. 24851-4.
74. Barral, D.C. and M.B. Brenner, *CD1 antigen presentation: how it works.* Nat Rev Immunol, 2007. **7**(12): p. 929-41.
75. Esmon, C.T., *The endothelial cell protein C receptor.* Thromb Haemost, 2000. **83**(5): p. 639-43.
76. Nayak, R.C., et al., *Endothelial cell protein C receptor cellular localization and trafficking: potential functional implications.* Blood, 2009. **114**(9): p. 1974-86.
77. Preston, R.J., et al., *Multifunctional specificity of the protein C/activated protein C Gla domain.* J Biol Chem, 2006. **281**(39): p. 28850-7.
78. Esmon, C.T., *Thrombomodulin as a model of molecular mechanisms that modulate protease specificity and function at the vessel surface.* FASEB J, 1995. **9**(10): p. 946-55.
79. Yang, L. and A.R. Rezaie, *The fourth epidermal growth factor-like domain of thrombomodulin interacts with the basic exosite of protein C.* J Biol Chem, 2003. **278**(12): p. 10484-90.
80. Knobe, K.E., et al., *Probing the activation of protein C by the thrombin-thrombomodulin complex using structural analysis, site-directed mutagenesis, and computer modeling.* Proteins, 1999. **35**(2): p. 218-34.
81. Gerlitz, B. and B.W. Grinnell, *Mutation of protease domain residues Lys37-39 in human protein C inhibits activation by the thrombomodulin-thrombin complex without affecting activation by free thrombin.* J Biol Chem, 1996. **271**(37): p. 22285-8.
82. Dahlback, B. and B.O. Villoutreix, *Regulation of blood coagulation by the protein C anticoagulant pathway: novel insights into structure-function relationships and molecular recognition.* Arterioscler Thromb Vasc Biol, 2005. **25**(7): p. 1311-20.
83. Taylor, F.B., Jr., et al., *Endothelial cell protein C receptor plays an important role in protein C activation in vivo.* Blood, 2001. **97**(6): p. 1685-8.
84. Walker, F.J., P.W. Sexton, and C.T. Esmon, *The inhibition of blood coagulation by activated Protein C through the selective inactivation of activated Factor V.* Biochim Biophys Acta, 1979. **571**(2): p. 333-42.

85. Fay, P.J., T.M. Smudzin, and F.J. Walker, *Activated protein C-catalyzed inactivation of human factor VIII and factor VIIIa. Identification of cleavage sites and correlation of proteolysis with cofactor activity.* J Biol Chem, 1991. **266**(30): p. 20139-45.
86. Nicolaes, G.A., et al., *Peptide bond cleavages and loss of functional activity during inactivation of factor Va and factor VaR506Q by activated protein C.* J Biol Chem, 1995. **270**(36): p. 21158-66.
87. Mann, K.G., et al., *Activated protein C cleavage of factor Va leads to dissociation of the A2 domain.* J Biol Chem, 1997. **272**(33): p. 20678-83.
88. Fay, P.J., *Regulation of factor VIIIa in the intrinsic factor Xase.* Thromb Haemost, 1999. **82**(2): p. 193-200.
89. Varadi, K., et al., *Factor V enhances the cofactor function of protein S in the APC-mediated inactivation of factor VIII: influence of the factor VR506Q mutation.* Thromb Haemost, 1996. **76**(2): p. 208-14.
90. Gruber, A. and J.H. Griffin, *Direct detection of activated protein C in blood from human subjects.* Blood, 1992. **79**(9): p. 2340-8.
91. Rezaie, A.R., *Vitronectin functions as a cofactor for rapid inhibition of activated protein C by plasminogen activator inhibitor-1. Implications for the mechanism of profibrinolytic action of activated protein C.* J Biol Chem, 2001. **276**(19): p. 15567-70.
92. Heeb, M.J. and J.H. Griffin, *Physiologic inhibition of human activated protein C by alpha 1-antitrypsin.* J Biol Chem, 1988. **263**(24): p. 11613-6.
93. Heeb, M.J., A. Gruber, and J.H. Griffin, *Identification of divalent metal ion-dependent inhibition of activated protein C by alpha 2-macroglobulin and alpha 2-antiplasmin in blood and comparisons to inhibition of factor Xa, thrombin, and plasmin.* J Biol Chem, 1991. **266**(26): p. 17606-12.
94. Hermans, J.M. and S.R. Stone, *Interaction of activated protein C with serpins.* Biochem J, 1993. **295 (Pt 1)**: p. 239-45.
95. Shen, L., B.O. Villoutreix, and B. Dahlback, *Involvement of Lys 62(217) and Lys 63(218) of human anticoagulant protein C in heparin stimulation of inhibition by the protein C inhibitor.* Thromb Haemost, 1999. **82**(1): p. 72-9.
96. Glasscock, L.N., et al., *Basic residues in the 37-loop of activated protein C modulate inhibition by protein C inhibitor but not by alpha(1)-antitrypsin.* Biochim Biophys Acta, 2003. **1649**(1): p. 106-17.
97. Spiro, R.G., *Protein glycosylation: nature, distribution, enzymatic formation, and disease implications of glycopeptide bonds.* Glycobiology, 2002. **12**(4): p. 43R-56R.
98. Helenius, A. and M. Aebi, *Intracellular functions of N-linked glycans.* Science, 2001. **291**(5512): p. 2364-9.
99. Marth, J.D. and P.K. Grewal, *Mammalian glycosylation in immunity.* Nat Rev Immunol, 2008. **8**(11): p. 874-87.
100. Moloney, D.J., et al., *Fringe is a glycosyltransferase that modifies Notch.* Nature, 2000. **406**(6794): p. 369-75.
101. Grinnell, B.W., J.D. Walls, and B. Gerlitz, *Glycosylation of human protein C affects its secretion, processing, functional activities, and activation by thrombin.* J Biol Chem, 1991. **266**(15): p. 9778-85.
102. Miletich, J.P. and G.J. Broze, Jr., *Beta protein C is not glycosylated at asparagine 329. The rate of translation may influence the frequency of usage at asparagine-X-cysteine sites.* J Biol Chem, 1990. **265**(19): p. 11397-404.
103. McClure, D.B., J.D. Walls, and B.W. Grinnell, *Post-translational processing events in the secretion pathway of human protein C, a complex vitamin K-dependent antithrombotic factor.* J Biol Chem, 1992. **267**(27): p. 19710-7.
104. Simioni, P., et al., *Compound heterozygous protein C deficiency resulting in the presence of only the beta-form of protein C in plasma.* Blood, 1996. **88**(6): p. 2101-8.

105. Taylor, F.B., Jr., et al., *Protein C prevents the coagulopathic and lethal effects of Escherichia coli infusion in the baboon.* J Clin Invest, 1987. **79**(3): p. 918-25.
106. Bernard, G.R., et al., *Efficacy and safety of recombinant human activated protein C for severe sepsis.* N Engl J Med, 2001. **344**(10): p. 699-709.
107. Smith, O.P., et al., *Use of protein-C concentrate, heparin, and haemodiafiltration in meningococcus-induced purpura fulminans.* Lancet, 1997. **350**(9091): p. 1590-3.
108. White, B., et al., *An open-label study of the role of adjuvant hemostatic support with protein C replacement therapy in purpura fulminans-associated meningococcemia.* Blood, 2000. **96**(12): p. 3719-24.
109. Riewald, M., et al., *Activation of endothelial cell protease activated receptor 1 by the protein C pathway.* Science, 2002. **296**(5574): p. 1880-2.
110. Cheng, T., et al., *Activated protein C blocks p53-mediated apoptosis in ischemic human brain endothelium and is neuroprotective.* Nat Med, 2003. **9**(3): p. 338-42.
111. Mosnier, L.O. and J.H. Griffin, *Inhibition of staurosporine-induced apoptosis of endothelial cells by activated protein C requires protease-activated receptor-1 and endothelial cell protein C receptor.* Biochem J, 2003. **373**(Pt 1): p. 65-70.
112. Feistritzer, C. and M. Riewald, *Endothelial barrier protection by activated protein C through PAR1-dependent sphingosine 1-phosphate receptor-1 crossactivation.* Blood, 2005. **105**(8): p. 3178-84.
113. Yang, X.V., et al., *Activated protein C ligation of ApoER2 (LRP8) causes Dab1-dependent signaling in U937 cells.* Proc Natl Acad Sci U S A, 2009. **106**(1): p. 274-9.
114. Cao, C., et al., *The efficacy of activated protein C in murine endotoxemia is dependent on integrin CD11b.* J Clin Invest, 2010. **120**(6): p. 1971-80.
115. Vu, T.K., et al., *Molecular cloning of a functional thrombin receptor reveals a novel proteolytic mechanism of receptor activation.* Cell, 1991. **64**(6): p. 1057-68.
116. Hung, D.T., et al., *The cloned platelet thrombin receptor couples to at least two distinct effectors to stimulate phosphoinositide hydrolysis and inhibit adenylyl cyclase.* J Biol Chem, 1992. **267**(29): p. 20831-4.
117. Offermanns, S., et al., *G proteins of the G12 family are activated via thromboxane A2 and thrombin receptors in human platelets.* Proc Natl Acad Sci U S A, 1994. **91**(2): p. 504-8.
118. Barr, A.J., L.F. Brass, and D.R. Manning, *Reconstitution of receptors and GTP-binding regulatory proteins (G proteins) in Sf9 cells. A direct evaluation of selectivity in receptor.G protein coupling.* J Biol Chem, 1997. **272**(4): p. 2223-9.
119. Bae, J.S., et al., *The ligand occupancy of endothelial protein C receptor switches the protease-activated receptor 1-dependent signaling specificity of thrombin from a permeability-enhancing to a barrier-protective response in endothelial cells.* Blood, 2007. **110**(12): p. 3909-16.
120. Yang, L., et al., *Identification of a specific exosite on activated protein C for interaction with protease-activated receptor 1.* J Biol Chem, 2007. **282**(35): p. 25493-500.
121. Bae, J.S., L. Yang, and A.R. Rezaie, *Receptors of the protein C activation and activated protein C signaling pathways are colocalized in lipid rafts of endothelial cells.* Proc Natl Acad Sci U S A, 2007. **104**(8): p. 2867-72.
122. Grey, S.T., Tsuchida, A., Hau, H., Orthner, C.L., Salem, H.H., Hancock, W.W., *Selective inhibitory effects of the anticoagulant activated protein C on the responses of human mononuclear phagocytes to LPS, IFN-gamma or phorbol ester.* J Immunol, 1994. **1994**(153): p. 3664-72.
123. White, B., et al., *Activated protein C inhibits lipopolysaccharide-induced nuclear translocation of nuclear factor kappaB (NF-kappaB) and tumour necrosis factor alpha (TNF-alpha) production in the THP-1 monocytic cell line.* Br J Haematol, 2000. **110**(1): p. 130-4.

124. Stephenson, D.A., et al., *Modulation of monocyte function by activated protein C, a natural anticoagulant.* J Immunol, 2006. **177**(4): p. 2115-22.
125. Toltl, L.J., S. Beaudin, and P.C. Liaw, *Activated protein C up-regulates IL-10 and inhibits tissue factor in blood monocytes.* J Immunol, 2008. **181**(3): p. 2165-73.
126. Joyce, D.E., et al., *Gene expression profile of antithrombotic protein c defines new mechanisms modulating inflammation and apoptosis.* J Biol Chem, 2001. **276**(14): p. 11199-203.
127. Hancock, W.W., Salem, H.H., *Activated protein C (APC) blocks endotoxin-induced renal injury: reduction in cytokine expression, endothelial activation, fibrin deposition and cellular infiltration.* J Am Soc Nephrol, 1993. **4:605 (Abstr)**.
128. Shu, F., Kobayashi, H., Fukudome, K., Tsuneyoshi, N., Kimoto, M., Terao, T., *Activated protein C suppresses tissue factor expression on U937 cells in the endothelial protein C receptor-dependent manner.* FEBS letters, 2000. **477**: p. 208-212.
129. Ternisien, C., et al., *Protein tyrosine kinase activation is required for LPS and PMA induction of tissue factor mRNA in human blood monocytes.* Thromb Haemost, 1995. **73**(3): p. 413-20.
130. Edgell, C.J., C.C. McDonald, and J.B. Graham, *Permanent cell line expressing human factor VIII-related antigen established by hybridization.* Proc Natl Acad Sci U S A, 1983. **80**(12): p. 3734-7.
131. Feistritzer, C., et al., *Endothelial protein C receptor-dependent inhibition of human eosinophil chemotaxis by protein C.* J Allergy Clin Immunol, 2003. **112**(2): p. 375-81.
132. O'Brien, L.A., et al., *Activated protein C decreases tumor necrosis factor related apoptosis-inducing ligand by an EPCR- independent mechanism involving Egr-1/Erk-1/2 activation.* Arterioscler Thromb Vasc Biol, 2007. **27**(12): p. 2634-41.
133. Yuda, H., et al., *Activated protein C inhibits bronchial hyperresponsiveness and Th2 cytokine expression in mice.* Blood, 2004. **103**(6): p. 2196-204.
134. Elphick, G.F., et al., *Recombinant human activated protein C inhibits integrin-mediated neutrophil migration.* Blood, 2009. **113**(17): p. 4078-85.
135. Gale, A.J., et al., *Nonenzymatic anticoagulant activity of the mutant serine protease Ser360Ala-activated protein C mediated by factor Va.* Protein Sci, 1997. **6**(1): p. 132-40.
136. Schabbauer, G., et al., *PI3K-Akt pathway suppresses coagulation and inflammation in endotoxemic mice.* Arterioscler Thromb Vasc Biol, 2004. **24**(10): p. 1963-9.
137. Xu, J., et al., *Extracellular histones are major mediators of death in sepsis.* Nat Med, 2009. **15**(11): p. 1318-21.
138. Guo, H., et al., *Activated protein C prevents neuronal apoptosis via protease activated receptors 1 and 3.* Neuron, 2004. **41**(4): p. 563-72.
139. Finigan, J.H., et al., *Activated protein C mediates novel lung endothelial barrier enhancement: role of sphingosine 1-phosphate receptor transactivation.* J Biol Chem, 2005. **280**(17): p. 17286-93.
140. Angus, D.C., et al., *Epidemiology of severe sepsis in the United States: analysis of incidence, outcome, and associated costs of care.* Crit Care Med, 2001. **29**(7): p. 1303-10.
141. Martin, G.S., et al., *The epidemiology of sepsis in the United States from 1979 through 2000.* N Engl J Med, 2003. **348**(16): p. 1546-54.
142. Watson, R.S., et al., *The epidemiology of severe sepsis in children in the United States.* Am J Respir Crit Care Med, 2003. **167**(5): p. 695-701.
143. Kerschen, E.J., et al., *Endotoxemia and sepsis mortality reduction by non-anticoagulant activated protein C.* J Exp Med, 2007. **204**(10): p. 2439-48.
144. Mosnier, L.O., et al., *Activated protein C variants with normal cytoprotective but reduced anticoagulant activity.* Blood, 2004. **104**(6): p. 1740-4.

145. Kerschen, E., et al., *Activated protein C targets CD8+ dendritic cells to reduce the mortality of endotoxemia in mice.* J Clin Invest, 2010. **120**(9): p. 3167-78.
146. Schuepbach, R.A., et al., *Protection of vascular barrier integrity by activated protein C in murine models depends on protease-activated receptor-1.* Thromb Haemost, 2009. **101**(4): p. 724-33.
147. Abraham, E., et al., *Drotrecogin alfa (activated) for adults with severe sepsis and a low risk of death.* N Engl J Med, 2005. **353**(13): p. 1332-41.
148. Vincent, J.L., et al., *Drotrecogin alfa (activated) treatment in severe sepsis from the global open-label trial ENHANCE: further evidence for survival and safety and implications for early treatment.* Crit Care Med, 2005. **33**(10): p. 2266-77.
149. Dhainaut, J.F., et al., *Extended drotrecogin alfa (activated) treatment in patients with prolonged septic shock.* Intensive Care Med, 2009. **35**(7): p. 1187-95.
150. Nadel, S., et al., *Drotrecogin alfa (activated) in children with severe sepsis: a multicentre phase III randomised controlled trial.* Lancet, 2007. **369**(9564): p. 836-43.
151. Wang, Y., et al., *Differential neuroprotection and risk for bleeding from activated protein C with varying degrees of anticoagulant activity.* Stroke, 2009. **40**(5): p. 1864-9.
152. Liu, D., et al., *Tissue plasminogen activator neurovascular toxicity is controlled by activated protein C.* Nat Med, 2004. **10**(12): p. 1379-83.
153. Cheng, T., et al., *Activated protein C inhibits tissue plasminogen activator-induced brain hemorrhage.* Nat Med, 2006. **12**(11): p. 1278-85.
154. Thiyagarajan, M., et al., *Activated protein C promotes neovascularization and neurogenesis in postischemic brain via protease-activated receptor 1.* J Neurosci, 2008. **28**(48): p. 12788-97.
155. Zhong, Z., et al., *Activated protein C therapy slows ALS-like disease in mice by transcriptionally inhibiting SOD1 in motor neurons and microglia cells.* J Clin Invest, 2009. **119**(11): p. 3437-49.
156. Petraglia, A.L., et al., *Activated protein C is neuroprotective and mediates new blood vessel formation and neurogenesis after controlled cortical impact.* Neurosurgery, 2010. **66**(1): p. 165-71; discussion 171-2.
157. Walker, C.T., et al., *Activated protein C analog with reduced anticoagulant activity improves functional recovery and reduces bleeding risk following controlled cortical impact.* Brain Res, 2010. **1347**: p. 125-31.
158. Isermann, B., et al., *Activated protein C protects against diabetic nephropathy by inhibiting endothelial and podocyte apoptosis.* Nat Med, 2007. **13**(11): p. 1349-58.
159. Han, M.H., et al., *Proteomic analysis of active multiple sclerosis lesions reveals therapeutic targets.* Nature, 2008. **451**(7182): p. 1076-81.
160. Scaldaferri, F., et al., *Crucial role of the protein C pathway in governing microvascular inflammation in inflammatory bowel disease.* J Clin Invest, 2007. **117**(7): p. 1951-60.
161. Marti-Carvajal, A.J., et al., *Human recombinant activated protein C for severe sepsis.* Cochrane Database Syst Rev, 2011. **4**: p. CD004388.
162. Harmon, S., et al., *Dissociation of activated protein C functions by elimination of protein S cofactor enhancement.* J Biol Chem, 2008. **283**(45): p. 30531-9.
163. Van Lenten, L. and G. Ashwell, *Studies on the chemical and enzymatic modification of glycoproteins. A general method for the tritiation of sialic acid-containing glycoproteins.* J Biol Chem, 1971. **246**(6): p. 1889-94.
164. Shen, L., et al., *Enhancing the activity of protein C by mutagenesis to improve the membrane-binding site: studies related to proline-10.* Biochemistry, 1997. **36**(51): p. 16025-31.
165. Li, X. and Z. Darzynkiewicz, *Labelling DNA strand breaks with BrdUTP. Detection of apoptosis and cell proliferation.* Cell Prolif, 1995. **28**(11): p. 571-9.

166. Kimura, M., et al., *Orphan G protein-coupled receptor, GPR41, induces apoptosis via a p53/Bax pathway during ischemic hypoxia and reoxygenation.* J Biol Chem, 2001. **276**(28): p. 26453-60.
167. Miyashita, T., et al., *Tumor suppressor p53 is a regulator of bcl-2 and bax gene expression in vitro and in vivo.* Oncogene, 1994. **9**(6): p. 1799-805.
168. Yan, S.C., et al., *Characterization and novel purification of recombinant human protein C from three mammalian cell lines.* Biotechnology (N Y), 1990. **8**(7): p. 655-61.
169. Varfaj, F., H. Wakabayashi, and P.J. Fay, *Residues surrounding Arg336 and Arg562 contribute to the disparate rates of proteolysis of factor VIIIa catalyzed by activated protein C.* J Biol Chem, 2007. **282**(28): p. 20264-72.
170. Safa, O., et al., *Factor VIIa/tissue factor generates a form of factor V with unchanged specific activity, resistance to activation by thrombin, and increased sensitivity to activated protein C.* Biochemistry, 1999. **38**(6): p. 1829-37.
171. Pratt, C.W. and F.C. Church, *Heparin binding to protein C inhibitor.* J Biol Chem, 1992. **267**(13): p. 8789-94.
172. Brown, M.A., et al., *Identification and purification of vitamin K-dependent proteins and peptides with monoclonal antibodies specific for gamma -carboxyglutamyl (Gla) residues.* J Biol Chem, 2000. **275**(26): p. 19795-802.
173. Preston, R.J., et al., *Selective modulation of protein C affinity for EPCR and phospholipids by Gla domain mutation.* Febs J, 2005. **272**(1): p. 97-108.
174. Soto, A.G. and J. Trejo, *N-linked glycosylation of protease-activated receptor-1 second extracellular loop: a critical determinant for ligand-induced receptor activation and internalization.* J Biol Chem, 2010. **285**(24): p. 18781-93.
175. Compton, S.J., et al., *Glycosylation of human proteinase-activated receptor-2 (hPAR2): role in cell surface expression and signalling.* Biochem J, 2002. **368**(Pt 2): p. 495-505.
176. Picard, V., E. Ersdal-Badju, and S.C. Bock, *Partial glycosylation of antithrombin III asparagine-135 is caused by the serine in the third position of its N-glycosylation consensus sequence and is responsible for production of the beta-antithrombin III isoform with enhanced heparin affinity.* Biochemistry, 1995. **34**(26): p. 8433-40.
177. Dickinson, C.D., C.R. Kelly, and W. Ruf, *Identification of surface residues mediating tissue factor binding and catalytic function of the serine protease factor VIIa.* Proc Natl Acad Sci U S A, 1996. **93**(25): p. 14379-84.
178. Rezaie, A.R., *Identification of basic residues in the heparin-binding exosite of factor Xa critical for heparin and factor Va binding.* J Biol Chem, 2000. **275**(5): p. 3320-7.
179. Bause, E. and G. Legler, *The role of the hydroxy amino acid in the triplet sequence Asn-Xaa-Thr(Ser) for the N-glycosylation step during glycoprotein biosynthesis.* Biochem J, 1981. **195**(3): p. 639-44.
180. Fijnvandraat, K., et al., *Coagulation activation and tissue necrosis in meningococcal septic shock: severely reduced protein C levels predict a high mortality.* Thromb Haemost, 1995. **73**(1): p. 15-20.
181. Dellinger, R.P., et al., *Surviving Sepsis Campaign guidelines for management of severe sepsis and septic shock.* Intensive Care Med, 2004. **30**(4): p. 536-55.
182. Bae, J.S., et al., *Engineering a disulfide bond to stabilize the calcium-binding loop of activated protein C eliminates its anticoagulant but not its protective signaling properties.* J Biol Chem, 2007. **282**(12): p. 9251-9.
183. Preston, R.J., et al., *Platelet factor 4 impairs the anticoagulant activity of activated protein C.* J Biol Chem, 2009. **284**(9): p. 5869-75.
184. Horrow, J.C., *Protamine: a review of its toxicity.* Anesth Analg, 1985. **64**(3): p. 348-61.
185. Balhorn, R., *The protamine family of sperm nuclear proteins.* Genome Biol, 2007. **8**(9): p. 227.

186. Lewis, J.D., et al., *Histone H1 and the origin of protamines.* Proc Natl Acad Sci U S A, 2004. **101**(12): p. 4148-52.
187. Carr, J.A. and N. Silverman, *The heparin-protamine interaction. A review.* J Cardiovasc Surg (Torino), 1999. **40**(5): p. 659-66.
188. Baglin, T., et al., *Guidelines on the use and monitoring of heparin.* Br J Haematol, 2006. **133**(1): p. 19-34.
189. Hirsh, J., et al., *Parenteral anticoagulants: American College of Chest Physicians Evidence-Based Clinical Practice Guidelines (8th Edition).* Chest, 2008. **133**(6 Suppl): p. 141S-159S.
190. Dunning, J., et al., *Guideline on antiplatelet and anticoagulation management in cardiac surgery.* Eur J Cardiothorac Surg, 2008. **34**(1): p. 73-92.
191. Butterworth, J., et al., *Rapid disappearance of protamine in adults undergoing cardiac operation with cardiopulmonary bypass.* Ann Thorac Surg, 2002. **74**(5): p. 1589-95.
192. Butterworth, J., et al., *The pharmacokinetics and cardiovascular effects of a single intravenous dose of protamine in normal volunteers.* Anesth Analg, 2002. **94**(3): p. 514-22; table of contents.
193. Carr, M.E., Jr. and S.L. Carr, *At high heparin concentrations, protamine concentrations which reverse heparin anticoagulant effects are insufficient to reverse heparin anti-platelet effects.* Thromb Res, 1994. **75**(6): p. 617-30.
194. Griffin, M.J., et al., *The effects of heparin, protamine, and heparin/protamine reversal on platelet function under conditions of arterial shear stress.* Anesth Analg, 2001. **93**(1): p. 20-7.
195. Nielsen, V.G., *Protamine enhances fibrinolysis by decreasing clot strength: role of tissue factor-initiated thrombin generation.* Ann Thorac Surg, 2006. **81**(5): p. 1720-7.
196. Esposito, R.A., et al., *Heparin resistance during cardiopulmonary bypass. The role of heparin pretreatment.* J Thorac Cardiovasc Surg, 1983. **85**(3): p. 346-53.
197. Mochizuki, T., et al., *Protamine reversal of heparin affects platelet aggregation and activated clotting time after cardiopulmonary bypass.* Anesth Analg, 1998. **87**(4): p. 781-5.
198. Kresowik, T.F., et al., *Anticoagulant effects of protamine sulfate in a canine model.* J Surg Res, 1988. **45**(1): p. 8-14.
199. Worowski, K., S. Glowinski, and Z. Skrzydlewski, *The effect of basic proteins on the haemostatic system of the dog.* Haematologia (Budap), 1978. **12**(1-4): p. 165-8.
200. Mittermayr, M., et al., *Detection of protamine and heparin after termination of cardiopulmonary bypass by thrombelastometry (ROTEM): results of a pilot study.* Anesth Analg, 2009. **108**(3): p. 743-50.
201. McLaughlin, K.E. and J. Dunning, *In patients post cardiac surgery do high doses of protamine cause increased bleeding?* Interact Cardiovasc Thorac Surg, 2003. **2**(4): p. 424-6.
202. Despotis, G.J., et al., *The impact of heparin concentration and activated clotting time monitoring on blood conservation. A prospective, randomized evaluation in patients undergoing cardiac operation.* J Thorac Cardiovasc Surg, 1995. **110**(1): p. 46-54.
203. Jobes, D.R., G.L. Aitken, and G.W. Shaffer, *Increased accuracy and precision of heparin and protamine dosing reduces blood loss and transfusion in patients undergoing primary cardiac operations.* J Thorac Cardiovasc Surg, 1995. **110**(1): p. 36-45.
204. Chu, A.J., et al., *Protamine inhibits tissue factor-initiated extrinsic coagulation.* Br J Haematol, 2001. **115**(2): p. 392-9.
205. Barstad, R.M., et al., *Protamine sulphate inhibits platelet membrane glycoprotein Ib-von Willebrand factor activity.* Thromb Haemost, 2000. **83**(2): p. 334-7.
206. Preston, R.J., et al., *Platelet factor 4 impairs the anticoagulant activity of activated protein C.* J Biol Chem, 2009. **284**(9): p. 5869-75.

207. Orfeo, T., et al., *The factor V activation paradox.* J Biol Chem, 2004. **279**(19): p. 19580-91.
208. Dielis, A.W., et al., *Coagulation factors and the protein C system as determinants of thrombin generation in a normal population.* J Thromb Haemost, 2008. **6**(1): p. 125-31.
209. Allen, G.A., et al., *Impact of procoagulant concentration on rate, peak and total thrombin generation in a model system.* J Thromb Haemost, 2004. **2**(3): p. 402-13.
210. Suzuki, K., B. Dahlback, and J. Stenflo, *Thrombin-catalyzed activation of human coagulation factor V.* J Biol Chem, 1982. **257**(11): p. 6556-64.
211. Sarafanov, A.G., et al., *Cell surface heparan sulfate proteoglycans participate in factor VIII catabolism mediated by low density lipoprotein receptor-related protein.* J Biol Chem, 2001. **276**(15): p. 11970-9.
212. Hortin, G.L., *Sulfation of tyrosine residues in coagulation factor V.* Blood, 1990. **76**(5): p. 946-52.
213. Smith, S.A., et al., *Polyphosphate modulates blood coagulation and fibrinolysis.* Proc Natl Acad Sci U S A, 2006. **103**(4): p. 903-8.
214. Smith, S.A. and J.H. Morrissey, *Heparin is procoagulant in the absence of antithrombin.* Thromb Haemost, 2008. **100**(1): p. 160-2.
215. Liu, T., et al., *Improved coagulation in bleeding disorders by Non-Anticoagulant Sulfated Polysaccharides (NASP).* Thromb Haemost, 2006. **95**(1): p. 68-76.

APPENDICES

APPENDIX I: COMPOSITION OF BUFFERS

10 X G7 buffer

500mM sodium phosphate (pH 7.5)

2 X Loading buffer

150mM Tris-HCl (pH 6.8)

20% (v/v) glycerol

4% (w/v) sodium dodecyl sulphate (SDS)

0.125% (w/v) bromophenol blue

Electrophoresis buffer

25mM Tris-HCl (pH 8.3)

192mM glycine

0.1% (w/v) SDS

Transfer buffer

25mM Tris-HCl (pH 8.3)

192mM glycine

20% (v/v) methanol

200 mM sodium acetate

27.21 g of sodium acetate trihydrate in 1 litre of distilled water.

200 mM acetic acid

2 ml of glacial acetic acid

172 ml of distilled water.

200 mM acetate buffer

220 ml of 200 mM sodium acetate + 30 ml of 200 mM acetic acid (pH 5.5).

100 mM acetate buffer

Dilute 200 mM acetate buffer 1:1 with distilled water.

10 mM sodium metaperiodate reagent

(For total carbohydrate labelling on the membrane)

43 mg dissolved in 20 ml of 100 mM acetate buffer. Prepare freshly just before use.

1 mM sodium metaperiodate reagent

(For preferential sialic acid labelling on the membrane)

Dilute 10 mM sodium metaperiodate 1 in 10 with 100 mM acetate buffer. Prepare freshly just before use.

10 X APC amidolytic assay buffer

1M NaCl

0.2M Tris-HCl (TBS, pH 7.5)

25mM $CaCl_2$

ELISA coating buffer

50mM Na_2CO_3 (1.7 g/L)

50mM $NaHCO_3$ (2.86 g/L)

ELISA detection buffer

33.3mM $C_6H_8O_7$

67mM Na_2HPO_4 (pH 5)

0.666µg/ml o-phenylenediamine (OPD)

0.0004% (v/v) H_2O_2

LB broth

1% (w/v) tryptone

0.5% (w/v) yeast extract

1% (w/v) NaCl

LB Agar

1% (w/v) tryptone

0.5% (w/v) yeast extract

1% (w/v) NaCl

1% (w/v) bacto-agar

10 X TBE buffer

0.89M Tris-borate (pH 8.3), 20mM EDTA.

Phosphate-buffered saline (PBS) buffer

Dissolve 5 tablets PBS (Sigma) in 1L dH_2O.

PBS-Tween buffer

Dissolve 5 tablets PBS (Sigma) + 0.1% Tween-20 (Sigma) in 1L dH_2O.

Hank's buffered salt solution (HBSS) buffer composition

0.137 M NaCl

5.4 mM KCl

0.25 mM Na_2HPO_4

0.44 mM KH_2PO_4

1.3 mM $CaCl_2$

1.0 mM $MgSO_4$

4.2 mM $NaHCO_3$

FPLC running buffer

50mM Tris (2.54 g/L Trizma HCl; 0.47 g/L Trizma base)

150mM NaCl (8.76 g/L)

pH 7.4

SOC medium

0.5% w/v yeast extract

2% tryptone

10 mM NaCl

2.5 mM KCl

10 mM MgCl2

10 mM MgSO4

20 mM Glucose

APPENDIX II: OLIGONUCLEOTIDE PRIMER SEQUENCES

II.I Oligonucleotide mutagenic primer sequences

Primer ID	Sequence 5'→3'
PC_N97Q_Sense	GAG GTG AGC TTC CTC **CAA** TGC TCG GAC AAC
PC_N97Q_Antisense	GTT GTC CAG CGA GCA **TTG** GAG GAA GCT CAC CTC
PC_N248Q_Sense	GTC TTC GTC CAC CCC **CAA** TAC AGC AAG AGC ACC
PC_N248Q_Antisense	GGT GCT CTT GCT GTA **TTG** GGG GTG GAC GAA GAC
PC_N313Q_Sense	GGA GGC CAA GAG A**CA A**CG CAC CTT CGT CCT C
PC_N313Q_Antisense	GAG GAC GAA GGT GCG **TTG** TCT CTT GGC CTC C
PC_N329Q_Sense	CCC GTG GTC CCG CAC **CAA** GAG TGC AGC GAG GTC
PC_N329Q_Antisense	GAC CTC GCT GCA CTC **TTG** GTG CGG GAC CAC GGG

II.II Oligonucleotide sequencing primers

Primer ID	Sequence 5′ →3′
Sequencingprimer1 (Sequences "sense" DNA strand commencing at nucleotide 860 in protein C cDNA)	ATG GAT GAG TCC AAG AAG
Sequencingprimer2 (Sequences "sense" DNA strand commencing at nucleotide 480 in protein C cDNA)	GCC AGC CTG TGC TGC GGG
Sequencingprimer 3 (Sequences "antisense" DNA strand commencing at nucleotide corresponding to 710 in "sense" DNA strand)	CTC AAA GAA GAA GCT GG

ACCEPTED FOR PUBLICATION

Supplemental Material can be found at:
http://www.jbc.org/content/suppl/2010/11/02/M110.159475.DC1.html

THE JOURNAL OF BIOLOGICAL CHEMISTRY VOL. 286, NO. 2, pp. 1323–1330, January 14, 2011
© 2011 by The American Society for Biochemistry and Molecular Biology, Inc. Printed in the U.S.A.

Activated Protein C *N*-Linked Glycans Modulate Cytoprotective Signaling Function on Endothelial Cells*[S]

Received for publication, July 2, 2010, and in revised form, October 22, 2010 Published, JBC Papers in Press, November 2, 2010, DOI 10.1074/jbc.M110.159475

Fionnuala Ní Áinle[‡1], James S. O'Donnell[‡§1,2], Jennifer A. Johnson[‡], Laura Brown[‡], Eimear M. Gleeson[‡], Owen P. Smith[¶], and Roger J. S. Preston[‡]

From the [‡]Haemostasis Research Group, Institute of Molecular Medicine, Trinity College Dublin, Dublin 2, the [§]National Centre for Hereditary Coagulation Disorders, St. James's Hospital, James Street, Dublin 8, and the [¶]Department of Haematology, Our Lady's Children's Hospital, Crumlin, Dublin 12, Ireland

Activated protein C (APC) has potent anticoagulant and anti-inflammatory properties that limit clot formation, inhibit apoptosis, and protect vascular endothelial cell barrier integrity. In this study, the role of *N*-linked glycans in modulating APC endothelial cytoprotective signaling via endothelial cell protein C receptor/protease-activated receptor 1 (PAR1) was investigated. Enzymatic digestion of APC *N*-linked glycans (PNG-APC) decreased the APC concentration required to achieve half-maximal inhibition of thrombin-induced endothelial cell barrier permeability by 6-fold. Furthermore, PNG-APC exhibited increased protection against staurosporine-induced endothelial cell apoptosis when compared with untreated APC. To investigate the specific *N*-linked glycans responsible, recombinant APC variants were generated in which each *N*-linked glycan attachment site was eliminated. Of these, APC-N329Q was up to 5-fold more efficient in protecting endothelial barrier function when compared with wild type APC. Based on these findings, an APC variant (APC-L38D/N329Q) was generated with minimal anticoagulant activity, but 5-fold enhanced endothelial barrier protective function and 30-fold improved anti-apoptotic function when compared with wild type APC. These data highlight the previously unidentified role of APC *N*-linked glycosylation in modulating endothelial cell protein C receptor-dependent cytoprotective signaling via PAR1. Furthermore, our data suggest that plasma β-protein C, characterized by aberrant *N*-linked glycosylation at Asn-329, may be particularly important for maintenance of APC cytoprotective functions *in vivo*.

In response to thrombin generation, zymogen plasma protein C is converted to activated protein C (APC)[3] by the thrombin-thrombomodulin complex on endothelial cells and serves to limit clot development (1). APC attenuates coagulation by proteolytic inactivation of procoagulant-activated cofactors factor Va (FVa) and factor VIIIa (FVIIIa) (2, 3). APC also has important non-anticoagulant properties. APC activates the G protein-coupled thrombin receptor, protease-activated receptor 1 (PAR1), when bound to its prototypic receptor, the endothelial cell protein C receptor (EPCR) (4). PAR1 activation by EPCR-bound APC mediates broad protective cellular benefits. APC inhibits endotoxin-induced secretion of TNF-α by macrophages (5), reduces cellular NFκB activation in endothelial cells (5), and prevents leukocyte adhesion to activated endothelial cells (6). APC also reduces apoptosis by blocking the pro-apoptotic activity of p53 in human brain endothelium (7). Moreover, APC signaling induces stabilization of endothelial cell barrier integrity via sphingosine-1 phosphate release and sphingosine-1 phosphate receptor 1 ($S1P_1$) activation (8, 9). Prevention of vascular leakage by EPCR-bound APC-PAR1-$S1P_1$ activation is a contributory factor in rescuing mice from lipopolysaccharide-induced lethality (10).

The anti-inflammatory and anti-apoptotic properties of APC are of proven therapeutic benefit. APC reduces the relative risk of mortality in individuals with severe sepsis when compared with placebo, and recombinant APC (Xigris®) is licensed for the treatment of severe sepsis (11). Recent evidence suggests that APC anticoagulant activity is not required to reduce mortality in murine models of sepsis (12). Consequently, removal or alteration of APC anticoagulant activity, but retention of the anti-inflammatory activity, has been postulated as a potential method to improve APC therapy (13).

Protein C is secreted from the liver into plasma as a glycoprotein and possesses four *N*-linked glycosylation attachment sites. Of these, three attachment sites (Asn-248, Asn-313, and Asn-329) are located in the protein C/APC serine protease domain, and one is present in the C-terminal EGF domain (Asn-97). The *N*-linked glycans attached to protein C/APC are sialylated bi- or tri-antennary complex structures (14). Interestingly, the Asn-329 glycan attachment site does not possess a typical *N*-linked glycosylation consensus sequence (N*X*(S/T)) but instead utilizes a cysteine residue in place of the serine/threonine amino acid residue (N*X*C) (15). Furthermore, an *N*-linked glycan chain is only attached at Asn-329 in 70–80% plasma protein C (14, 16). The role of each *N*-linked glycan chain in protein C activation and APC anticoagulant

* This work was supported by a Molecular Medicine Ireland Clinician Scientist Fellowship (to F. N. A.), a Science Foundation Ireland (SFI) Starting Investigator Research Grant (to R. J. S. P. and E. M. G.), and SFI PIYRA (J. S. O'D.).

[S] The on-line version of this article (available at http://www.jbc.org) contains supplemental Figs. 1–3.

[1] Both authors contributed equally to this work.

[2] To whom correspondence should be addressed: Haemostasis Research Group, Institute of Molecular Medicine, St. James's Hospital, Trinity College Dublin, Dublin 8, Ireland. Tel.: 353-1-8963260; Fax: 353-1-8963260; E-mail: jodonne@tcd.ie.

[3] The abbreviations used are: APC, activated protein C; EPCR, endothelial cell protein C receptor; PNG-APC, PNGase F-treated APC; PNGase F, *N*-glycosidase F; Z, benzyloxycarbonyl; AMC, 7-amido-4-methylcoumarin; ETP, endogenous thrombin potential.

Downloaded from www.jbc.org at IReL (Trinity College Dublin), on January 17, 2011

activity has been previously investigated. Amino acid substitution of the *N*-linked glycan attachment site at Asn-97 was found to impair *in vitro* protein C secretion from mammalian cells. Furthermore, *N*-linked glycosylation at Asn-248 was found to be important for generation of the protein C disulfide-linked heterodimer (17). The same study showed that individual mutagenesis of each *N*-linked glycosylation attachment site on the APC serine protease domain increases APC generation by the thrombin-thrombomodulin complex and improves anticoagulant activity in a modified activated partial thromboplertin time (APTT) assay (17).

In this study, the role of APC *N*-linked glycans in regulating EPCR-dependent PAR1 signaling on endothelial cells was assessed. Enzymatic removal of *N*-linked glycans significantly enhanced APC endothelial barrier protective and anti-apoptotic functions. *N*-Linked glycosylation at amino acid position Asn-329 was identified as a key regulator of APC-EPCR-PAR1 signaling on endothelial cells. These data indicate that deglycosylated, non-anticoagulant recombinant APC variants may represent a novel tool for treatment of sepsis and other inflammatory diseases.

EXPERIMENTAL PROCEDURES

Materials—Plasma-purified human protein C and thrombin were purchased from Hematologic Technologies Inc. (Essex Junction, VT). PNGase F was purchased from New England Biolabs Inc. (Ipswich, MA). Sheep anti-protein C polyclonal antibody was from Abcam (Cambridgeshire, UK). APC chromogenic substrate BIOPHEN CS-21(66), Protac, and protein C-deficient plasma were from HYPHEN BioMed (Neuville-Sur-Oise, France). Thrombin generation assay reagents (platelet-poor plasma reagent, fluorogenic substrate, thrombin calibration standard) were purchased from Thrombinoscope BV, Maastricht, The Netherlands. EA.hy926 cells were a kind gift from Dr. C. Edgell, University of North Carolina, Chapel Hill, NC (18). Polycarbonate membrane Transwell permeable supports (Costar, 3-μM pore size, 12-mm diameter) were from Millipore (Billerica, MA). Anti-EPCR monoclonal antibody RCR-252 and staurosporine was obtained from Sigma. The RNA extraction kit (RNeasy Mini) was from Qiagen (Hilden, Germany). High capacity cDNA reverse transcription kit and specific primers for *Bax* and *Bcl-2* were purchased from Applied Biosystems Inc. (Foster City, CA). APOPercentage apoptosis kit was purchased from Biocolor (Belfast, Northern Ireland, UK).

Deglycosylation of Protein C by PNGase F Digestion—To remove *N*-linked glycans, plasma-purified and recombinant protein C/APC were incubated with PNGase F and G7 buffer for 4 h at 37 °C, as per manufacturer's instructions. PNGase F-treated protein C was activated with Protac, as described previously (19). Briefly, protein C (5 μg/ml) was incubated with 0.25 units of Protac in 50 mM Tris-HCl (pH 7.4), 100 mM NaCl for 1 h at 37 °C. PNGase F-treated APC was characterized by SDS-PAGE analysis and Western blotting.

Generation of Recombinant Protein C Variants—Recombinant PC variants PC-N97Q, PC-N248Q, PC-N313Q, and PC-N329Q were generated by site-directed mutagenesis, expressed, purified, and characterized as described previously (19). Wild type protein C and protein C variants were activated with Protac as outlined above (19, 20). The concentration of each recombinant APC concentration was determined by active-site titration against a calibration curve generated from the amidolytic activity of APC of known concentration. APC chromogenic substrate cleavage by each recombinant APC preparation was determined as described previously (19).

Assessment of APC Anticoagulant Activity in Protein C-deficient Plasma—APC anticoagulant function in protein C-deficient plasma was assessed using a Fluoroskan Ascent plate reader (Thermo Lab System, Helsinki, Finland) in combination with Thrombinoscope software (Thrombinoscope BV). Briefly, 80 μl of plasma were incubated with 20 μl of platelet-poor plasma reagent containing 5 pM soluble tissue factor and 4 μM phospholipids (60% phosphatidylcholine, 20% phosphatidylserine, and 20% phosphatidylethanolamine) in the presence or absence of APC (2.5–20 nM). Thrombin generation was initiated by automatic dispensation of fluorogenic thrombin substrate (Z-Gly-Gly-Arg-AMC·HCl) and 100 mM $CaCl_2$ into each well (final concentrations, Z-Gly-Gly-Arg-AMC·HCl, 0.42 mM and $CaCl_2$, 16.67 mM). Thrombin generation was determined using a thrombin calibration standard. The area under the thrombin generation curve (endogenous thrombin potential, ETP) was measured. Experiments were performed in triplicate, and data were reported as mean ± S.E.

Measurement of Endothelial Cell Barrier Protection by APC—Endothelial cell barrier permeability was determined as described previously, with minor modifications (20, 21). Briefly, EA.hy926 cells were grown to confluence on polycarbonate membrane Transwell permeable supports (Costar, 3-μM pore size, 12-mm diameter) and incubated with APC (0.63–20 nM; all final concentrations). After 3 h, EA.hy926 cells were treated with 5 nM thrombin in serum-free medium for 10 min. The cells were then washed and incubated with 0.67 mg/ml Evans Blue with 4% bovine serum albumin (BSA; Sigma). Changes in endothelial cell barrier permeability were determined by assessment of the increase in absorbance at 650 nm in the outer chamber over time due to transmigration of Evans Blue-BSA. To assess the role of APC-EPCR binding, supernatant was removed, and an anti-EPCR monoclonal antibody (RCR-252) was incubated with the cells for 30 min (25 μg/ml, final concentration) followed by standard permeability measurement (see above). The same assay was used to evaluate the effect of thrombin (5 nM for 3 h) on permeability of EA.hy926 cells pretreated with a non-enzymatic protein C variant PC-S360A (2.5–10 nM) for 15 min. Experiments were performed in triplicate and plotted as the mean ± S.E. Permeability (percentage) was determined using the following equation

$$P = (X - C)/(F - C) \times 100\% \qquad \text{(Eq. 1)}$$

where P is permeability (percentage), X is the APC-treated OD_{650}, C is the OD_{650} of untreated EAhy926 cells, and F is the OD_{650} for thrombin-treated EA.hy926 cells.

Regulation of Apoptosis-related Gene Expression in Endothelial Cells by APC—Confluent EA.hy926 cells in 6-well plates were pretreated with APC for 4 h. EA.hy926 cell apoptosis was then induced by incubation with staurosporine (20 μM) for 4 h. Staurosporine-treated cells were trypsinized and RNA-extracted using the RNeasy mini kit (Qiagen). Reverse transcription (high capacity cDNA reverse transcription kit, Applied Biosystems) followed by RT-PCR was performed using *Bax* (Hs00180269_m1), *Bcl-2* (Hs00153350_m1), and β-actin (Hs99999903_m1) TaqMan® gene expression assays (Applied Biosystems) in an Applied Biosystems 7500 real time PCR system. Experiments were performed in triplicate and plotted as a percentage of the mean staurosporine-treated *bax/bcl-2* ratio (100% apoptosis).

Determination of APC-mediated Protection of Apoptotic Endothelial Cells—EA.hy926 cells were grown to confluence in a 96-well plate and then treated for 3 h with wild type or variant APC (0.625–20 nM). Apoptosis was then induced by incubation with staurosporine (20 μM) for 4 h. 30 min prior to the end of this incubation period, an apoptosis-specific purple dye (Biocolor) was added to each well. The cells were then washed twice with phosphate-buffered saline and photographed. Apoptosis was quantified by converting digital photograph images into pixel counts using Adobe® Photoshop® software, according to the manufacturer's instructions. Average pixel counts calculated were based on analysis of at least three images per well. Three independent experiments were performed, and data are reported as the "pixel ratio" calculated from the pixel count from each APC-treated well relative to pixels calculated from staurosporine-treated wells.

RESULTS

Deglycosylation of APC by PNGase F—To enable assessment of the role of APC *N*-linked glycans in mediating APC cytoprotective signaling, *N*-linked carbohydrate moieties were removed from APC by enzymatic digestion with PNGase F. Untreated and PNGase F-treated APC (PNG-APC) were characterized by reducing SDS-PAGE analysis and Western blotting using an anti-protein C polyclonal antibody that detects the protein C/APC heavy chain. For wild type APC, a doublet of ~35–40 kDa, corresponding to the heavy chains of the two major APC glycoforms, α and β, was identified (Fig. 1*A*). PNGase F treatment of APC reduced the molecular mass of the APC doublet ~10 kDa (Fig. 1*A*), corresponding to the disappearance of the fully glycosylated APC heavy chain and the formation of lower molecular mass APC glycoforms upon *N*-linked glycan proteolysis (16, 22). In keeping with previous reports, total APC deglycosylation could not be achieved without significant APC degradation and loss of function (16).

A thrombin generation assay using protein C-deficient plasma was used to assess PNG-APC anticoagulant activity. As described previously (17), removal of APC *N*-linked glycans caused a slight increase in plasma APC anticoagulant activity. 5 nM APC reduced the ETP to 47% of the ETP in the absence of APC, whereas an identical concentration of PNG-APC attenuated thrombin generation to 27% of the original ETP (Fig. 1*B*). Increased anticoagulant activity was not associated with increased amidolytic activity, as determined by PNG-APC hydrolysis of a short APC-specific chromogenic substrate (data not shown).

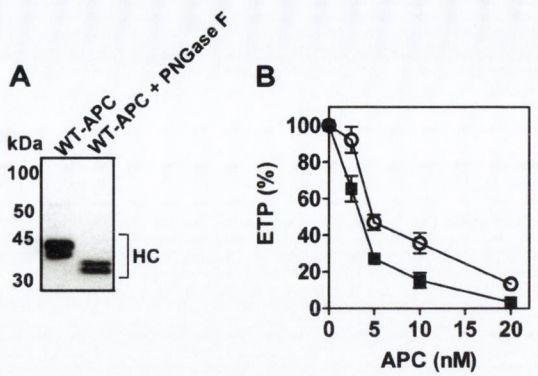


FIGURE 1. **Characterization of PNGase F-treated APC.** *A*, APC and PNGase F-treated APC (PNG-APC, 1 μg) were characterized by 4–15% SDS-PAGE analysis and Western blotting, using a sheep anti-protein C/APC polyclonal antibody that detects the protein C/APC heavy chain (*HC*, shown). *B*, the anticoagulant activity of APC (○) and PNG-APC (■ 2.5–20 nM) was assessed in protein C-deficient plasma by a thrombin generation assay. Thrombin generation was initiated with 5 pM soluble tissue factor and 100 mM $CaCl_2$ and assessed as described under "Experimental Procedures." The percentage of ETP was determined for thrombin generation in the presence and absence of APC, with *100% ETP* defined as ETP in the absence of either APC species.

Enzymatic Removal of N-Linked Glycans Improves APC Protection against Thrombin-induced Endothelial Cell Barrier Permeability and Staurosporine-induced Apoptosis—APC protects the endothelium from thrombin-induced permeability in an EPCR- and PAR1-dependent manner (23). To determine the functional consequences of APC deglycosylation on EPCR-dependent PAR1 signaling, PNG-APC cytoprotective activity (2.5–20 nM) was assessed in a thrombin-induced endothelial cell permeability assay. As expected, preincubation with untreated APC induced a dose-dependent improvement in endothelial cell barrier integrity (Fig. 2*A*). Interestingly, preincubation with PNG-APC maintained barrier integrity at ~6-fold lower concentration than wild type APC. Half-maximal endothelial barrier protection was achieved at 9.85 nM for wild type APC, yet only 1.71 nM PNG-APC was required to achieve the same level of endothelial barrier protection (Fig. 2*A*). The presence of Protac and PNGase F alone had no effect upon thrombin-induced endothelial cell barrier permeability (supplemental Fig. 1).

EPCR occupancy by protein C causes thrombin to exert barrier-protective, rather than barrier-disruptive, intracellular signaling (24). A protein C variant containing an amino acid substitution in the serine protease catalytic triad (PC-S360A) that renders the variant enzymatically inactive was preincubated with EA.hy926 cells in the presence of 5 nM thrombin. As shown previously (24), EPCR occupancy by PC-S360A induced a barrier-protective response upon PAR1 activation by thrombin. PNGase F-treatment of PC-S360A did not affect EPCR occupancy-mediated reversal of thrombin signaling specificity upon PAR1 proteolysis. (data not shown). PNG-APC signaling via PAR1 was completely abolished in the presence of a monoclonal antibody that prevents APC-EPCR binding (RCR-252; Fig. 2*B*). These data indicate that enhanced PNG-APC cytoprotective signaling is dependent on both APC proteolytic activity and EPCR binding.

Downloaded from www.jbc.org at IReL (Trinity College Dublin), on January 17, 2011

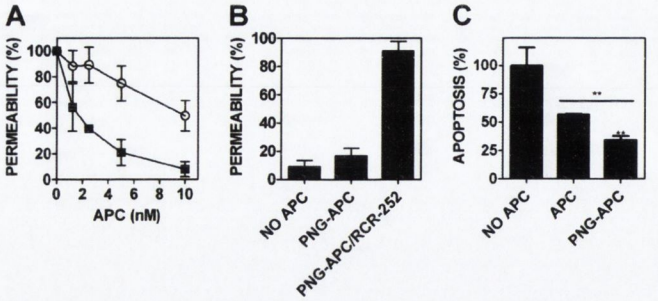


FIGURE 2. **PNGase F-treated APC possesses enhanced endothelial barrier-protective function and up-regulation of anti-apoptotic gene expression.** *A*, the role of APC *N*-linked glycosylation in mediating APC-dependent endothelial cell signaling was assessed in a thrombin-induced endothelial cell barrier permeability assay. EA.hy926 cells were grown to confluence on polycarbonate membrane Transwell permeable supports and then incubated with either APC (○) or PNG-APC (■) (1.25–10 nM). Treated cells were then incubated with 5 nM thrombin for 10 min, and barrier permeability was determined for each APC concentration at 10 min. Endothelial barrier permeability (percentage) was calculated as described under "Experimental Procedures." *B*, to assess the role of EPCR binding in PNGase F-treated APC cytoprotective signaling, EA.hy926 cells were incubated with PNGase F-treated APC and an anti-EPCR monoclonal antibody (RCR-252; 25 μg/ml) to prevent APC-EPCR binding. Thrombin-induced permeability was then assessed as described above. *C*, deglycosylation improves APC anti-apoptotic gene expression in staurosporine-treated endothelial cells. The anti-apoptotic function of PNG-APC was determined by calculation of the ratio of pro- and anti-apoptotic gene expression, using *Bax* and *Bcl-2* expression, respectively. EA.hy926 cells were pretreated with 10 nM APC for 4 h. EA.hy926 cell apoptosis was then induced by staurosporine (20 μM, 4 h). After RNA extraction, RT-PCR was performed using *bax*, *bcl-2*, and β-actin TaqMan® gene expression assays. Experiments were performed in triplicate and plotted as a percentage of the mean staurosporine-treated *bax/bcl-2* ratio (100% apoptosis). **, $p < 0.005$.

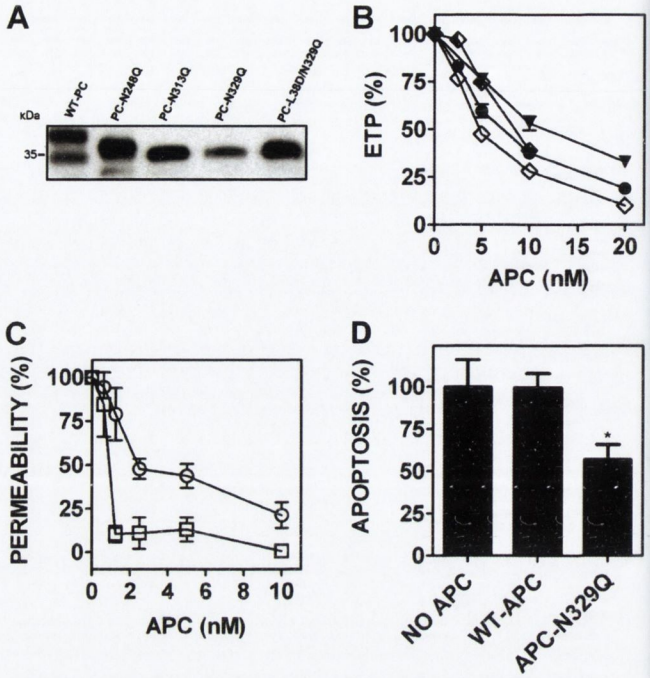


FIGURE 3. **Glutamine substitution of the *N*-linked glycan attachment site at Asn-329 causes enhanced endothelial barrier-protective and anti-apoptotic APC activity.** *A*, each recombinant protein C (wild type protein C, PC-N248Q, PC-N313Q, PC-N329Q, and PC-L38D/N329Q) was reduced using β-mercaptoethanol and assessed by 7.5% SDS-PAGE analysis. The protein C heavy chain was subsequently detected by Western blot using a sheep anti-protein C polyclonal antibody. *B*, the anticoagulant activity of each APC variant was determined by a thrombin generation assay in protein C-deficient plasma (●, wild type APC; ▼, APC-N248Q; ◆, APC-N313Q; ◇, APC-N329Q; all 1.25–20 nM, except APC-N313Q, 1.25–10 nM). *C*, the endothelial barrier-protective properties of wild type APC (○) and APC-N329Q (□; 1.25–10 nM) were determined as described previously. *D*, endothelial cell pro/anti-apoptotic gene expression in the presence of wild type APC and APC-N329Q (both 5 nM) was measured by RT-PCR quantification of the relative expression of *Bax/Bcl-2* mRNA transcripts, as described under "Experimental Procedures." *, $p < 0.05$.

APC-mediated cell signaling inhibits endothelial cell apoptosis in an EPCR-PAR1-dependent manner (7, 23). To examine the role of APC *N*-linked glycans in APC regulation of pro/anti-apoptotic gene expression, the ability of PNG-APC to modulate EA.hy926 cell pro/anti-apoptotic gene expression was assessed by RT-PCR analysis of the *Bax/Bcl-2* ratio in the presence of staurosporine. At identical concentrations (10 nM), PNG-APC was almost twice as effective in reducing staurosporine-induced apoptosis as wild type APC ($p < 0.05$; Fig. 2*C*).

Removal of N-Linked Glycans at Asn-329 Mediates Enhanced Protective APC Signaling—PNGase F treatment of APC enhances the EPCR-PAR1-dependent barrier-protective and anti-apoptotic functions of endothelial cells. However, PNGase F does not completely deglycosylate APC under conditions required to maintain APC function and does not provide information as to the specific *N*-linked glycans that regulate APC endothelial cell signaling function. To map the location of the *N*-linked glycans that regulate APC cytoprotective signaling via EPCR-PAR1, four recombinant APC variants were generated in which each *N*-linked glycosylation attachment site sequence was individually modified to prevent glycan linkage (APC-N97Q, APC-N248Q, APC-N313Q, and APC-N329Q). *N*-Linked glycosylation at Asn-97 on the protein C light chain is critical for protein C secretion in a mammalian cell expression system (17), preventing sufficient expression of this variant for analysis. APC variants APC-N248Q, APC-N313Q, and APC-N329Q were expressed and characterized. Reducing SDS-PAGE/Western blot analysis of each variant was performed prior to activation (Fig. 3*A*). The observed wild type doublet represents the heavy chains of the two major protein C glycoforms, α and β (17). Each protein C *N*-linked glycan variant exhibited a single major band of reduced molecular weight when compared with wild type protein C, corresponding to the loss of an individual *N*-linked glycan. A faint band corresponding to a protein C heavy chain glycoform predicted to possess a single *N*-linked glycan chain at Asn-313 was observed in the PC-N248Q preparation. An additional band of similar molecular weight, corresponding to a protein C glycoform predicted to possess a single *N*-linked glycan at Asn-248, was observed in the PC-N313Q preparation upon blot overexposure (data not shown).

The anticoagulant activity of wild type APC and each glycan variant (2.5–20 nM) was assessed in protein C-deficient plasma using a thrombin generation assay. Each APC variant exhibited comparable anticoagulant activity to that of wild type APC (Fig. 3*B*). To determine whether specific *N*-linked glycan chains modulate EPCR-dependent APC signaling via PAR1 on endothelial cells, the barrier-protective and anti-apoptotic activity of each expressed APC variant was characterized. APC-N248Q and APC-N313Q exhibited similar endothelial cell barrier protection to recombinant wild type

APC (supplemental Fig. 2). In contrast, APC-N329Q was significantly more barrier-protective than wild type APC and achieved maximum protection (~90%) from thrombin-induced endothelial barrier permeability at 1.25 nM APC. The same concentration of wild type APC reduced endothelial barrier leakage by only 21% (Fig. 3*C*). The enhanced activity of APC-N329Q was not due to improved affinity for EPCR as surface plasmon resonance analysis revealed a comparable soluble EPCR affinity as wild type APC (K_D ~193 nM, supplemental Fig. 3) (19, 20, 25, 26). Similarly, 5 nM wild type APC was ineffective in reducing staurosporine-induced apoptotic gene expression in EA.hy926 cells, whereas the same APC-N329Q concentration reduced the *Bax/Bcl-2* ratio by 43% (Fig. 3*D*). The extent of altered pro/anti-apoptotic gene expression mediated by APC-N329Q was comparable with that observed in the presence of an identical PNG-APC concentration. Collectively, these data demonstrate that the enhanced barrier-protective and anti-apoptotic signal transduction of PNG-APC is mediated by specific removal of the *N*-linked glycan at Asn-329.

APC-N329Q Is More Effective than Wild Type APC in Preventing Staurosporine-induced EA.hy926 Cell Apoptosis—The anti-apoptotic role of each APC *N*-linked glycan variant in EA.hy926 cells was further assessed using an assay in which apoptosis was determined by accumulation of an apoptosis-specific dye in staurosporine-treated EA.hy926 cells. Untreated EA.hy926 cells were largely impermeable to the dye, as expected (Fig. 4*A*). In comparison, staurosporine treatment led to widespread purple dye accumulation in EA.hy926 cells (Fig. 4*A*). Wild type and variant APC reduced dye accumulation and therefore endothelial cell apoptosis in a concentration-dependent manner (Fig. 4, *A* and *B*). Interestingly, variants APC-N248Q and APC-N313Q were more protective than wild type APC at all concentrations tested, but this enhanced anti-apoptotic function failed to reach statistical significance (Fig. 4*B*). At 1.25 nM, wild type APC reduced endothelial cell apoptosis by ~30%, as determined by analytical digital photomicroscopy (Fig. 4, *A* and *B*). Remarkably, however, APC-N329Q virtually ablated apoptotic cell dye accumulation at the lowest APC-N329Q concentration tested (0.625 nM). A similar rate of endothelial cell apoptosis inhibition was only observed at 20 nM wild type APC (Fig. 4*B*).

Enzymatic Deglycosylation of Non-anticoagulant Recombinant APC Causes Enhanced PAR1-mediated Protection of Endothelial Cell Barrier Integrity—Non-anticoagulant recombinant APC variants represent a potentially improved recombinant APC therapy for severe sepsis. APC-L38D has similar anti-inflammatory and anti-apoptotic properties to wild type APC but has limited anticoagulant function (25). To examine the functional consequences of APC-L38D deglycosylation, the anticoagulant and barrier-protective signaling properties of PNGase F-treated APC-L38D (PNG-APC-L38D) were examined. Like APC-L38D, PNG-APC-L38D was unable to inhibit thrombin generation in protein C-deficient plasma (data not shown). However, PNG-APC-L38D exhibited improved EPCR-PAR1-dependent barrier-protective function when compared with its glycosylated counterpart at each APC concentration tested (Fig. 5). Enzymatic deglycosylation of non-

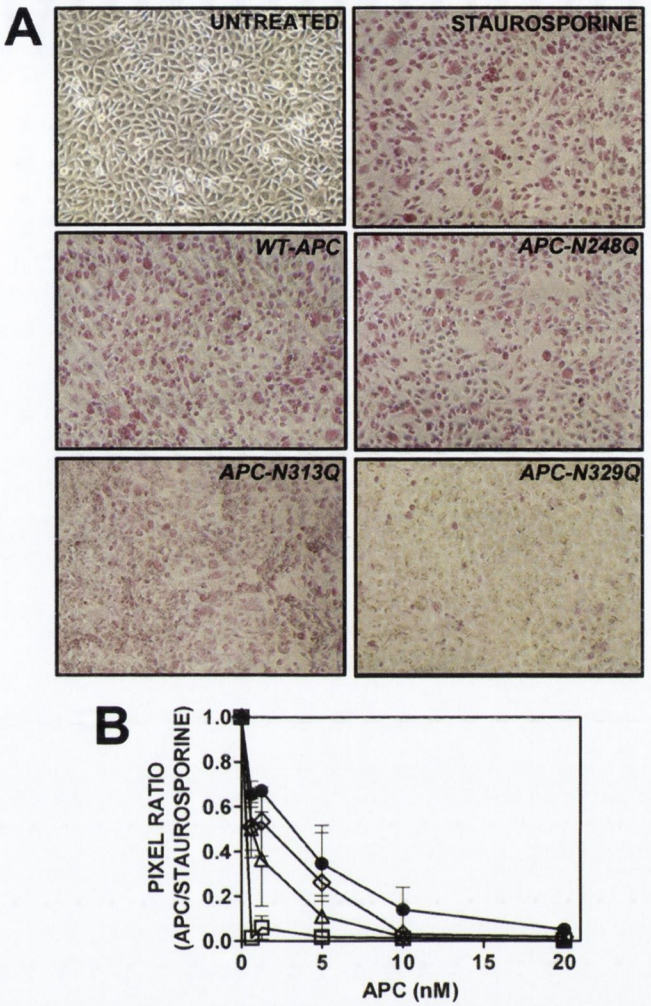


FIGURE 4. **Inhibition of endothelial cell apoptosis by recombinant APC *N*-linked glycan variants.** *A*, endothelial cell apoptosis was measured by accumulation of apoptosis-specific dye (*pink-purple*) in staurosporine-treated EA.hy926 cells following incubation with wild type/variant APC. Untreated/staurosporine-treated EA.hy926 cells (*top panels*) and wild type/variant APC (1.25 nM, *middle* and *bottom panels*) are shown. Images are representative of three independent experiments. *B*, APC concentration-dependent reduction in endothelial cell apoptosis (●, wild type APC; ◇, APC-N248Q; △, APC-N313Q; □, APC-N329Q; 0.625–20 nM). Uptake of apoptosis-specific dye was quantified by converting digital photograph images into pixel counts using Adobe® Photoshop® software according to manufacturer's instructions. Average pixel counts calculated were based on analysis of at least three images per well.

anticoagulant recombinant APC therefore leads to improved APC signaling function via EPCR-PAR1 on endothelial cells.

APC-L38D/N29Q Has Minimal Anticoagulant Activity but Exhibits Enhanced Barrier-protective and Anti-apoptotic Activity on Endothelial Cells—To generate a non-anticoagulant APC variant with improved EPCR-dependent signaling function without glycosidase treatment, a recombinant APC variant was prepared containing the L38D amino acid substitution (to limit anticoagulant function) combined with the N329Q amino acid substitution (to enhance APC-protective signaling). When assessed by SDS-PAGE and Western blotting, this variant migrated as a single band similar to that of APC-N329Q. APC-L38D/N329Q exhibited limited anticoagulant activity in a thrombin

Downloaded from www.jbc.org at IReL (Trinity College Dublin), on January 17, 2011

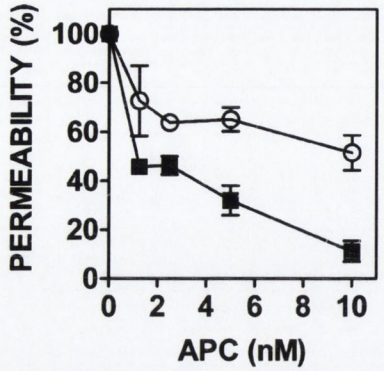


FIGURE 5. **Enzymatic deglycosylation of non-anticoagulant APC variant APC-L38D with PNGase F enhances APC-L38D-mediated endothelial cell barrier protection.** Endothelial cell barrier permeability was assessed in the presence of wild type APC (○) and PNG-APC-L38D (■) (1.25–10 nM) for 3 h prior to incubation with 5 nM thrombin. Endothelial barrier permeability was assessed by leakage of Evans Blue-BSA through the endothelial cell barrier, as described above.

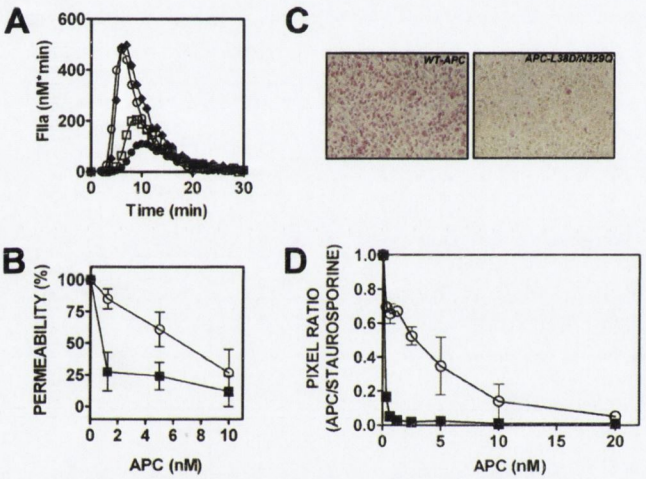


FIGURE 6. **APC-L38D/N329Q possesses no anticoagulant activity in plasma but demonstrates enhanced cytoprotective PAR-1 signaling.** *A*, thrombin generation in protein C-deficient plasma was assessed in the presence of wild type APC and APC-L38D/N329Q. Thrombin generation (*nm* × *min*) was initiated with platelet-poor plasma reagent and $CaCl_2$ as before, and the percentage of ETP (thrombin generation in the absence of APC) was determined. (○, no APC; □, 5 nM wild type APC; ●, 10 nM wild type APC; ◆, 20 nM APC-L38D/N329Q). *B*, EPCR-PAR1-dependent endothelial cell barrier protection by APC-L38D/N329Q is more potent than wild type APC. Barrier permeability assays using EA.hy926 cells were performed in the presence of wild type APC (○) or APC-L38D/N329Q (■; 1.25–10 nM) prior to thrombin treatment. Permeability is expressed as a percentage of total thrombin-induced endothelial cell barrier permeability. *C*, endothelial cell apoptosis was measured by accumulation of apoptosis-specific dye (*pink-purple*) in staurosporine-treated EA.hy926 cells following incubation with wild type APC or APC-L38D/N329Q (1.25 nM). *D*, APC concentration-dependent reduction in endothelial cell apoptosis (○, wild type APC; ■, APC-L38D/N329Q; 0.3125–20 nM).

generation assay using protein C-deficient plasma such that no anticoagulant activity was observed at 20 nM APC-L38D/N329Q (Fig. 6*A*). However, 1.25 nM APC-L38D/N329Q reduced endothelial barrier permeability by 72%, whereas wild type APC only reduced thrombin-induced permeability by 15% at the same APC concentration (Fig. 6*B*). Therefore, despite possessing virtually no anticoagulant activity, APC-L38D/N329Q possesses up to 5-fold enhanced endothelial cell barrier-protective function when compared with wild type APC. Furthermore, when assessed in an endothelial cell apoptosis assay, APC-L38D/N329Q was a significantly better inhibitor of endothelial cell apoptosis than wild type APC (Fig. 6, *C* and *D*). Apoptotic specific dye accumulation in EA.hy926 cells was only completely inhibited at 20 nM wild type APC, whereas the same protective effect was observed at 0.625 nM APC-L38D/N329Q. These data suggest that APC-L38D/N329Q is ~30-fold more effective than wild type APC in preventing staurosporine-induced endothelial cell apoptosis.

DISCUSSION

Reduced protein C plasma concentration is observed in the majority of cases of severe sepsis and is strongly associated with high morbidity and mortality in this setting (11, 27). The anticoagulant activity of APC means that its administration is associated with an increased risk of severe bleeding. To address this, "second generation" recombinant APC variants have been designed that possess limited anticoagulant activity but retain full cytoprotective signaling properties. This was originally demonstrated using an APC variant with defective factor Va substrate recognition and anticoagulant activity but normal cytoprotective function (13). Recombinant APC variants with similar divergent functional activities have since been described in which APC cofactor sensitivity has been abrogated (25) or where engineered disulfide bonds were incorporated into the protease domain to specifically prevent anticoagulant activity (28). To date, no recombinant non-anticoagulant APC variant has been described that also exhibits improved cytoprotective signaling function.

Glycosylation of membrane signaling receptors and soluble ligands is a common mechanism by which signaling networks can be regulated and can influence multiple aspects of signal transduction, including ligand recognition and affinity (29), intracellular trafficking, and receptor activation (30, 31). In this study, the role of *N*-linked glycosylation of APC in modulating EPCR-dependent APC endothelial cell signaling via PAR1 was examined. Enzymatic deglycosylation of APC significantly reduced the APC concentration required to achieve maximum protection against thrombin-induced endothelial cell barrier permeability and apoptosis (Fig. 2). Assessment of recombinant APC variants in which individual *N*-linked glycan attachment sites were removed identified the *N*-linked glycan at Asn-329 as a critical modulator of APC endothelial cell signaling. APC-N329Q impaired thrombin-induced endothelial cell barrier permeability up to 6-fold more efficiently than wild type APC and completely inhibited staurosporine-induced endothelial cell apoptosis at ~30-fold lower APC concentration than wild type APC (Figs. 3 and 4). Similarly, a PNGase F-treated non-anticoagulant APC variant (PNG-L38D-APC) and an APC variant with no anticoagulant activity but specific substitution of the Asn-329 glycan attachment site (APC-L38D/N329Q) displayed similarly enhanced endothelial cell barrier-protective and anti-apoptotic functions when compared with wild type APC (Fig. 6). These novel APC variants are, to our knowledge, the first description of APC variants in which APC anticoagulant function is attenuated, but the cytoprotective anti-inflammatory and anti-apoptotic functions of APC are simultaneously improved.

Plasma protein C is composed of three distinct glycoforms. 55–78% of plasma protein C possesses *N*-linked glycans at each of the four potential *N*-linked glycan attachment sites (α-protein C) (14, 16, 17). 22–45% of plasma protein C is aberrantly glycosylated at Asn-329 and therefore possesses only three *N*-linked glycan chains (β-protein C). The final glycoform (γ-protein C) is *N*-linked-glycosylated at two positions (Asn-97 and Asn-313) and constitutes ~5% of total plasma protein C (16, 17). The molecular basis for partial glycosylation at the Asn-329 *N*-linked glycan attachment site is unknown but is not linked to level of protein C expression as transgenic pigs that display both high and low protein C expression levels exhibit similar protein C glycosylation patterns (14). One possible explanation is that the unusual *NXC* glycan attachment site at Asn-329 is a less favorable substrate for glycosyltransferase processing than the typical N*X*(S/T) site (16).

The *N*-linked glycan attachment site at position Asn-329 is located in the protein C/APC serine protease domain (32) and is conserved across mammalian species (Fig. 6*A*). The importance of *N*-linked glycosylation at this site in regulating APC anticoagulant activity is controversial. In this study, we observed a small increase (up to 2-fold) in anticoagulant activity of PNGase F-treated APC and APC-N329Q variant when added to protein C-deficient plasma and anticoagulant activity determined by attenuation of thrombin generation (Figs. 1 and 3). In agreement with our findings, previous characterization of the APC-N329Q variant found that removal of the Asn-329 *N*-linked glycan enhanced protein C activation by thrombin in the presence of soluble thrombomodulin and increased APC anticoagulant function 2-fold when assessed by APTT assay (17). In contrast, a naturally occurring protein C variant containing the N329T substitution was associated with reduced anticoagulant activity. This variant protein was immunopurified from plasma, and its rate of protein C activation and anticoagulant activity was determined. PC-N329T was found to be activated by thrombin to the same extent as normal protein C, but in its activated form, it exhibited a reduced rate of FVa proteolysis when compared with normal APC (33).

The molecular mechanism(s) for the increased cytoprotective signaling functions of APC-N329Q observed in this study is currently unknown. However, Asn-329 is in close proximity to two amino acids (Glu-330/Glu-333) that form a putative PAR1-binding exosite on the APC protease domain surface (Fig. 7*B*). A previous study found that mutagenesis of this region did not alter APC anticoagulant activity but completely prevented EPCR-dependent APC signaling via PAR1 on endothelial cells (34). Consequently, we hypothesize that the presence of a complex *N*-linked glycan chain at Asn-329 regulates PAR1 access to its exosite-binding region on APC and subsequently inhibits the rate at which EPCR-dependent, APC-mediated PAR1 activation can occur. As such, increased APC-N329Q access to the PAR1-binding exosite facilitates increased PAR1 proteolysis. However, an increased rate of PAR1 activation by its prototypal ligand thrombin is associated with pro-inflammatory, rather than increased anti-inflammatory, downstream endothelial cell signaling. PAR1

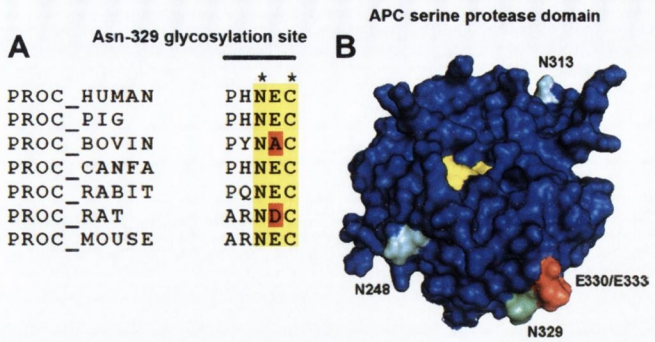


FIGURE 7. **The *N*-linked glycan at Asn-329 is conserved and proximal to a PAR1-binding exosite on APC.** *A*, amino acid alignment of known protein C (*PROC*) amino acid sequences indicates conservation of the unusual *NXC N*-linked glycan attachment site in known mammalian protein C amino acid sequences. *B*, *N*-linked glycosylation occurs at three sites (Asn-248, Asn-313, and Asn-329; *turquoise*) on the protein C/APC serine protease domain (*blue*). The Asn-329 glycan attachment site that regulates APC cytoprotective signaling is situated next to two amino acid residues (Glu-330/Glu-333; *red*) that are essential for PAR1 cleavage by APC (34). The APC catalytic triad (His-211, Asp-257, and Ser-360; *yellow*) is indicated. The model was generated based upon the Gla domainless APC crystal structure (1AUT (32)) using the PyMOL molecular visualization software.

activation by thrombin (10,000-fold more rapid than EPCR-bound APC on endothelial cells (35)) initiates distinct G protein coupling to that of APC-activated PAR1 (G_q and $G_{12/13}$, rather than G_i) (24). Caveolar compartmentalization of PAR1 and/or EPCR occupancy by APC have been proposed as potential mechanisms by which the divergent downstream consequences of PAR1 activation are mediated (24, 36). Interestingly, a meizothrombin chimeric variant containing a protein C/APC Gla domain has also been shown to exhibit significantly faster PAR1 cleavage than APC yet still possesses APC-like barrier-protective functions as a consequence of its ability to bind EPCR (24). This suggests that EPCR binding of PNGase F-treated APC or APC-N329Q is critical for determining protective signaling transduction induced by PAR1 proteolysis on endothelial cells, irrespective of PAR1 activation rate.

The physiological relevance of different plasma protein C glycoforms is not well understood. Interestingly, the zymogen form of the APC-N329Q variant used in this study is predicted to possess a similar glycosylation pattern to that of plasma β-protein C. Our study suggests that once activated, β-protein C may be particularly important for APC cytoprotective function *in vivo*. Furthermore, this implies that β-protein C plasma concentration may be a more reliable marker of endogenous APC anti-inflammatory potential than total plasma protein C concentration. Further studies are underway to assess the influence of β-protein C in mediating cytoprotective activity in the setting of acute inflammatory disease.

In summary, APC *N*-linked glycosylation plays a significant role in the regulation of APC cytoprotective function. In particular, we have identified the *N*-linked glycan moiety attached at amino acid Asn-329 in the APC serine protease domain as a key modulator of *N*-linked glycan-enhanced APC cytoprotective signaling function on endothelial cells. Furthermore, this observation has lead to the generation of recombinant non-anticoagulant APC variants in which the pro-

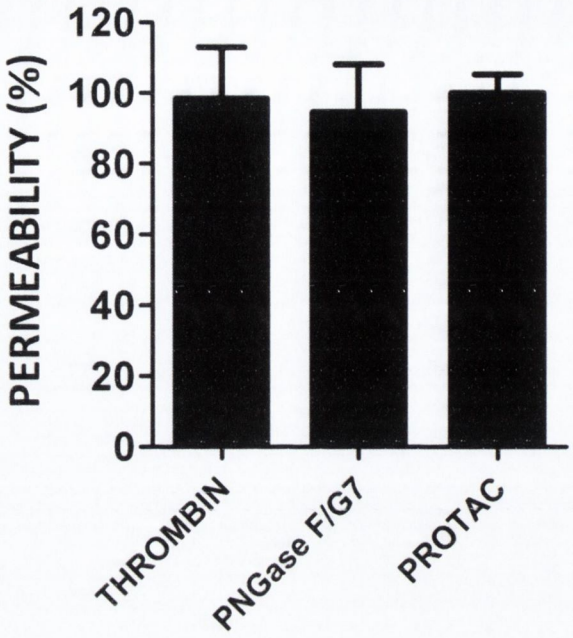
Downloaded from www.jbc.org at IReL (Trinity College Dublin), on January 17, 2011

tective PAR1-mediated signaling capacity is significantly enhanced when compared with wild type APC. The development of such recombinant APC variants represents a novel approach to improve the therapeutic potential of recombinant APC therapy in the treatment of acute and non-resolving inflammatory disease.

Acknowledgment—We thank Bridget-Ann Kenny for technical assistance.

REFERENCES

1. Owen, W. G., and Esmon, C. T. (1981) *J. Biol. Chem.* **256,** 5532–5535
2. Fay, P. J., Smudzin, T. M., and Walker, F. J. (1991) *J. Biol. Chem.* **266,** 20139–20145
3. Walker, F. J., Sexton, P. W., and Esmon, C. T. (1979) *Biochim. Biophys. Acta* **571,** 333–342
4. Riewald, M., Petrovan, R. J., Donner, A., Mueller, B. M., and Ruf, W. (2002) *Science* **296,** 1880–1882
5. White, B., Schmidt, M., Murphy, C., Livingstone, W., O'Toole, D., Lawler, M., O'Neill, L., Kelleher, D., Schwarz, H. P., and Smith, O. P. (2000) *Br. J. Haematol.* **110,** 130–134
6. Iba, T., Kidokoro, A., Fukunaga, M., Nagakari, K., Shirahama, A., and Ida, Y. (2005) *Crit. Care Med.* **33,** 368–372
7. Cheng, T., Liu, D., Griffin, J. H., Fernández, J. A., Castellino, F., Rosen, E. D., Fukudome, K., and Zlokovic, B. V. (2003) *Nat. Med.* **9,** 338–342
8. Feistritzer, C., and Riewald, M. (2005) *Blood* **105,** 3178–3184
9. Finigan, J. H., Dudek, S. M., Singleton, P. A., Chiang, E. T., Jacobson, J. R., Camp, S. M., Ye, S. Q., and Garcia, J. G. (2005) *J. Biol. Chem.* **280,** 17286–17293
10. Niessen, F., Furlan-Freguia, C., Fernández, J. A., Mosnier, L. O., Castellino, F. J., Weiler, H., Rosen, H., Griffin, J. H., and Ruf, W. (2009) *Blood* **113,** 2859–2866
11. Bernard, G. R., Vincent, J. L., Laterre, P. F., LaRosa, S. P., Dhainaut, J. F., Lopez-Rodriguez, A., Steingrub, J. S., Garber, G. E., Helterbrand, J. D., Ely, E. W., and Fisher, C. J., Jr. (2001) *N. Engl. J. Med.* **344,** 699–709
12. Kerschen, E. J., Fernandez, J. A., Cooley, B. C., Yang, X. V., Sood, R., Mosnier, L. O., Castellino, F. J., Mackman, N., Griffin, J. H., and Weiler, H. (2007) *J. Exp. Med.* **204,** 2439–2448
13. Mosnier, L. O., Gale, A. J., Yegneswaran, S., and Griffin, J. H. (2004) *Blood* **104,** 1740–1744
14. Gil, G. C., Velander, W. H., and Van Cott, K. E. (2009) *Proteomics* **9,** 2555–2567
15. Foster, D., and Davie, E. W. (1984) *Proc. Natl. Acad. Sci. U.S.A.* **81,** 4766–4770
16. Miletich, J. P., and Broze, G. J., Jr. (1990) *J. Biol. Chem.* **265,** 11397–11404
17. Grinnell, B. W., Walls, J. D., and Gerlitz, B. (1991) *J. Biol. Chem.* **266,** 9778–9785
18. Edgell, C. J., McDonald, C. C., and Graham, J. B. (1983) *Proc. Natl. Acad. Sci. U.S.A.* **80,** 3734–3737
19. Preston, R. J., Ajzner, E., Razzari, C., Karageorgi, S., Dua, S., Dahlbäck, B., and Lane, D. A. (2006) *J. Biol. Chem.* **281,** 28850–28857
20. Preston, R. J., Villegas-Mendez, A., Sun, Y. H., Hermida, J., Simioni, P., Philippou, H., Dahlbäck, B., and Lane, D. A. (2005) *FEBS. J.* **272,** 97–108
21. Preston, R. J., Tran, S., Johnson, J. A., Ainle, F. N., Harmon, S., White, B., Smith, O. P., Jenkins, P. V., Dahlbäck, B., and O'Donnell, J. S. (2009) *J. Biol. Chem.* **284,** 5869–5875
22. Yan, S. C., Razzano, P., Chao, Y. B., Walls, J. D., Berg, D. T., McClure, D. B., and Grinnell, B. W. (1990) *Biotechnology* **8,** 655–661
23. Mosnier, L. O., and Griffin, J. H. (2003) *Biochem. J.* **373,** 65–70
24. Bae, J. S., Yang, L., Manithody, C., and Rezaie, A. R. (2007) *Blood* **110,** 3909–3916
25. Harmon, S., Preston, R. J., Ainle, F. N., Johnson, J. A., Cunningham, M. S., Smith, O. P., White, B., and O'Donnell, J. S. (2008) *J. Biol. Chem.* **283,** 30531–30539
26. Yang, X. V., Banerjee, Y., Fernández, J. A., Deguchi, H., Xu, X., Mosnier, L. O., Urbanus, R. T., de Groot, P. G., White-Adams, T. C., McCarty, O. J., and Griffin, J. H. (2009) *Proc. Natl. Acad. Sci. U.S.A.* **106,** 274–279
27. Cohen, J., Guyatt, G., Bernard, G. R., Calandra, T., Cook, D., Elbourne, D., Marshall, J., Nunn, A., and Opal, S. (2001) *Crit. Care Med.* **29,** 880–886
28. Bae, J. S., Yang, L., Manithody, C., and Rezaie, A. R. (2007) *J. Biol. Chem.* **282,** 9251–9259
29. Soto, A. G., and Trejo, J. (2010) *J. Biol. Chem.* **285,** 18781–18793
30. Compton, S. J., Sandhu, S., Wijesuriya, S. J., and Hollenberg, M. D. (2002) *Biochem. J.* **368,** 495–505
31. Moloney, D. J., Panin, V. M., Johnston, S. H., Chen, J., Shao, L., Wilson, R., Wang, Y., Stanley, P., Irvine, K. D., Haltiwanger, R. S., and Vogt, T. F. (2000) *Nature* **406,** 369–375
32. Mather, T., Oganessyan, V., Hof, P., Huber, R., Foundling, S., Esmon, C., and Bode, W. (1996) *EMBO J.* **15,** 6822–6831
33. Simioni, P., Kalafatis, M., Millar, D. S., Henderson, S. C., Luni, S., Cooper, D. N., and Girolami, A. (1996) *Blood* **88,** 2101–2108
34. Yang, L., Bae, J. S., Manithody, C., and Rezaie, A. R. (2007) *J. Biol. Chem.* **282,** 25493–25500
35. Ludeman, M. J., Kataoka, H., Srinivasan, Y., Esmon, N. L., Esmon, C. T., and Coughlin, S. R. (2005) *J. Biol. Chem.* **280,** 13122–13128
36. Russo, A., Soh, U. J., Paing, M. M., Arora, P., and Trejo, J. (2009) *Proc. Natl. Acad. Sci. U.S.A.* **106,** 6393–6397



Supplementary Figure 1: PNGase F and Protac do not influence thrombin-induced endothelial cell barrier permeability. Thrombin-induced endothelial cell barrier permeability was determined as described in 'Experimental Procedures'. In this experiment, PNGase F and its buffer G7 or Protac were incubated for 3 hours prior to addition of 5nM thrombin for 10 minutes. Both PNGase/G7 and Protac reagent final concentrations were set to those equivalent to experiments with APC present. Endothelial barrier permeability was detected using Evans Blue-BSA transmigration as described in 'Experimental Procedures'. The data represent experiments performed in triplicate and plotted as the mean ± S.E.M.

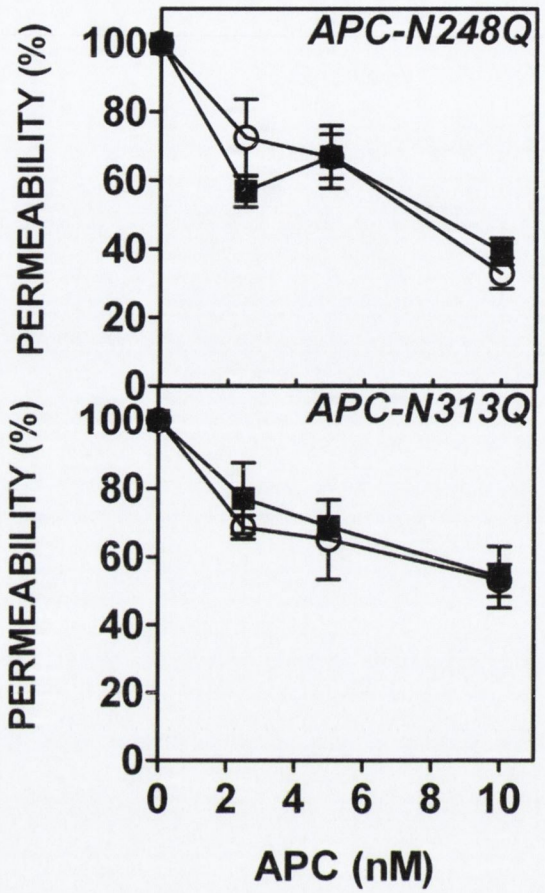
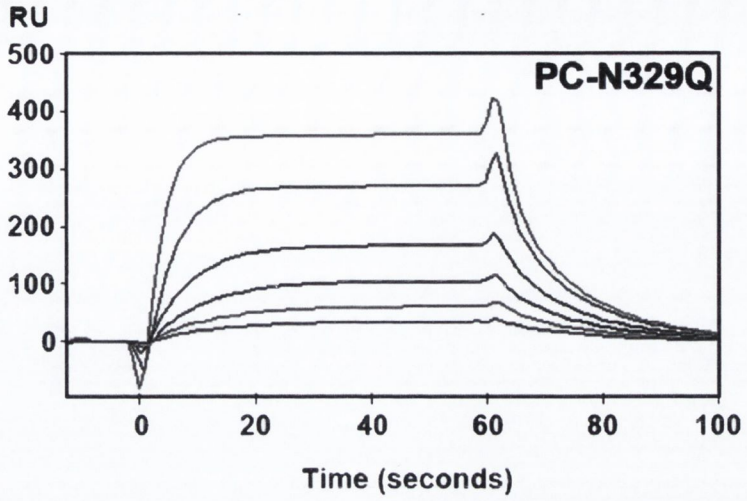


Figure 2: Variants *APC-N248Q* and *APC-N313Q* exhibit comparable endothelial cell barrier protective function to wild type APC: Thrombin-induced endothelial cell barrier permeability was determined as described in 'Experimental Procedures'. EA.hy926 cells were incubated with wild type APC (○), *APC-N248Q* (■; *top panel*) or *APC-N313Q* (■; *bottom panel*) (2-10nM; all final concentrations). After 3 hours, EA.hy926 cells were treated with 5nM thrombin in serum-free media for 10 minutes. The cells were then washed and incubated with 0.67 mg/ml Evans Blue with 4% bovine serum albumin. Changes in endothelial cell barrier permeability were determined by assessment of the increase in absorbance at 650nm in the outer chamber as before.



Supplementary Figure 3: Assessment of *PC-N329Q* Binding to Soluble EPCR. Protein C-sEPCR binding affinity was determined as previously described (19). Briefly, 10 μg/ml monoclonal anti-EPCR antibody, RCR-2 (kind gift of Dr. K. Fukudome, Saga Medical School), was immobilized by amine coupling to both flow cells of a CM5 sensor chip. Soluble EPCR (sEPCR) (19) was dialysed into HBS-P buffer (100mM HEPES, pH 7.4, 150mM NaCl) and bound to the test flow cell via RCR-2. RCR-2 was immobilized on the reference flow cell to detect non-specific binding. *PC-N329Q* (31.25–1000nM) was sequentially injected over both flow cells at a flow rate of 10μl/min for 60 seconds. APC-EPCR binding was dissociated using HBS-EP buffer (HBS-P, but containing 3mM EDTA; BIAcore) The RCR-2 surface was regenerated with 10μl of 10mM glycine-HCl (pH 2).

Protamine sulfate down-regulates thrombin generation by inhibiting factor V activation

Fionnuala Ni Ainle,[1] Roger J. S. Preston,[1] P. Vincent Jenkins,[1] Hendrik J. Nel,[2] Jennifer A. Johnson,[1] Owen P. Smith,[3] Barry White,[4] Padraic G. Fallon,[2] and James S. O'Donnell[1,4]

[1]Haemostasis Research Group, and [2]Inflammation and Immunity Research Group, Institute of Molecular Medicine, St James's Hospital, Trinity College, Dublin; [3]Department of Haematology, Our Lady's Children's Hospital, Dublin; and [4]National Centre for Hereditary Coagulation Disorders, St James's Hospital, Dublin, Republic of Ireland

Protamine sulfate is a positively charged polypeptide widely used to reverse heparin-induced anticoagulation. Paradoxically, prospective randomized trials have shown that protamine administration for heparin neutralization is associated with increased bleeding, particularly after cardiothoracic surgery with cardiopulmonary bypass. The molecular mechanism(s) through which protamine mediates this anticoagulant effect has not been defined. In vivo administration of pharmacologic doses of protamine to BALB/c mice significantly reduced plasma thrombin generation and prolonged tail-bleeding time (from 120 to 199 seconds). Similarly, in pooled normal human plasma, protamine caused significant dose-dependent prolongations of both prothrombin time and activated partial thromboplastin time. Protamine also markedly attenuated tissue factor-initiated thrombin generation in human plasma, causing a significant decrease in endogenous thrombin potential (41% ± 7%). As expected, low-dose protamine effectively reversed the anticoagulant activity of unfractionated heparin in plasma. However, elevated protamine concentrations were associated with progressive dose-dependent reduction in thrombin generation. To assess the mechanism by which protamine mediates down-regulation of thrombin generation, the effect of protamine on factor V activation was assessed. Protamine was found to significantly reduce the rate of factor V activation by both thrombin and factor Xa. Protamine mediates its anticoagulant activity in plasma by down-regulation of thrombin generation via a novel mechanism, specifically inhibition of factor V activation. (Blood. 2009;114: 1658-1665)

Introduction

Protamine sulfate is a 5-kDa cationic polypeptide derived from salmon sperm that can bind negatively charged unfractionated heparin (UFH).[1] Although the mechanisms of the molecular interaction between protamine and heparin are not well defined, this binding serves to neutralize the antithrombin-mediated anticoagulant properties of heparin. Moreover, the resultant protamine-heparin complex is rapidly cleared by the reticuloendothelial system.[2] Consequently, for more than 30 years, protamine has been widely used to reverse the anticoagulant effects of UFH. Protamine is considered the treatment of choice for patients who develop significant bleeding complications while on UFH.[3,4] Furthermore, protamine is routinely administered postoperatively to reverse the high concentrations of UFH required for patients undergoing cardiac surgery and cardiopulmonary bypass (CPB).[5] As a result, estimates suggest that more than 2 million heparinized patients are managed with protamine each year.[2]

Clinical use of protamine is, however, associated with several important adverse side effects, including potentially life-threatening systemic arterial hypotension and pulmonary artery hypertension.[1] Paradoxically, in vitro studies have also suggested that protamine may possess intrinsic anticoagulant properties.[6-8] Administration of excess protamine in the neutralization of UFH has been associated with increased bleeding in clinical settings, particularly after cardiothoracic surgery.[9] Due to concerns regarding the inherent anticoagulant potential of protamine, current consensus guidelines recommend that the dose of protamine is limited to 1 mg protamine per 100 IU heparin.[3,4] However, pharmacokinetic studies have demonstrated that protamine is cleared rapidly from human plasma (half life 7.4 minutes), so that repeated doses may be necessary to prevent rebound heparin anticoagulant effects.[10,11] Animal studies have shown that although protamine fully neutralizes the thrombin-inhibitory activity of low molecular weight heparins (LMWH), it can only partially neutralize their anti–factor Xa (FXa) activities.[12,13] Therefore, the clinical efficacy of protamine for reversing LMWH-induced anticoagulation remains unclear.[4]

Despite the widespread use of protamine in clinical practice, the molecular mechanism(s) underlying its associated intrinsic anticoagulant effect is not clearly defined. Previous studies in which incremental concentrations of protamine (50-300 μg/mL) were added to heparinized patient samples ex vivo demonstrated that heparin anticoagulation was maximally reversed at a protamine to heparin ratio of 1.3:1.[8,14] However, addition of higher protamine: heparin ratios (ie, excess free protamine) resulted in significant prolongation of the activated clotting time (ACT) through an unidentified mechanism.[8] Similarly, ex vivo addition of protamine to normal pooled plasma markedly attenuated tissue factor (TF)–initiated thromboelastography.[15] Protamine significantly increased clot initiation time (R time), decreased the rate of clot propagation

Submitted May 18, 2009; accepted June 10, 2009. Prepublished online as *Blood* First Edition paper, June 16, 2009; DOI 10.1182/blood-2009-05-222109.

Presented in abstract form as an oral presentation at the 50th annual meeting of the American Society of Hematology, San Francisco, CA, December 7, 2009.

The publication costs of this article were defrayed in part by page charge payment. Therefore, and solely to indicate this fact, this article is hereby marked "advertisement" in accordance with 18 USC section 1734.

© 2009 by The American Society of Hematology

(α angle), and diminished clot strength (maximum amplitude) in a concentration-dependent manner. Protamine has also been reported to have a weak inhibitory effect on in vitro platelet aggregation induced by adenosine 5′-diphosphate or collagen.[8] In contrast, platelet factor 4, another cationic molecule that has been used therapeutically to reverse UFH anticoagulation, has no apparent endogenous anticoagulant activity in vitro.[16]

In this study, we sought to characterize the molecular mechanism(s) responsible for the clinically important anticoagulant activity of protamine. We demonstrate that pharmacologic doses of protamine significantly reduce thrombin generation in both murine and human plasma in a concentration-dependent manner. Moreover, although low-dose protamine (< 20 μg/mL) effectively reverses the effects of UFH, increased protamine concentration results in a progressive anticoagulant effect. We further demonstrate that this anticoagulant effect of protamine is mediated via a specific inhibition of factor V (FV) activation by either thrombin or FXa. These new insights into the mechanism of the anticoagulant side effects of protamine will advance the generation of new protamine variants with reduced associated bleeding risk.

Methods

Materials

Protamine sulfate and tinzaparin (Innohep) were obtained from Leo Pharma. Unfractionated heparin, enoxaparin (Clexane), and danaparoid (Orgaran) were from Sigma-Aldrich, Sanofi-Aventis, and Schering-Plough, respectively. BALB/c mice were purchased from Harlan. Animals were housed in a pathogen-free facility using individually ventilated and filtered cages under positive pressure. All animal experiments were performed in compliance with Irish Department of Health and Children regulations and approved by the Trinity College Dublin BioResources ethical review board. Purified human activated protein C (APC), FV, FVa, FXa, and prothrombin were purchased from Haematologic Technologies. Purified human thrombin was obtained from Enzyme Research Laboratories, and phospholipid vesicles were from Avanti Polar Lipids. Synthetic chromogenic substrates BIOPHEN CS-21(66) and BIOPHEN CS-01(38) for APC and thrombin, respectively, were sourced from HYPHEN Biomed. Thrombin generation assay reagents (platelet-poor-plasma reagent, fluorogenic substrate, thrombin calibration standard) were purchased from Thrombinoscope BV. HemosIL FV-deficient plasma was from Instrumentation Laboratory, and factor VIII (FVIII)–deficient plasma from Technoclone. The wild-type FVIII and APC-cleavage–resistant FVIII double-mutant R336Q/R562Q were gifts of Dr Philip Fay (University of Rochester School of Medicine, Rochester, NY).

Measurement of thrombin generation and tail-bleeding time in mice

BALB/c mice, aged 6 to 8 weeks, were weighed and anesthetized with midazolam and etorphine hydrochloride. Protamine sulfate was administered intravenously, followed 90 seconds later by transection of the tail tip. The tail was loosely suspended in PBS at 37°C, and time taken for complete cessation of tail bleeding was recorded. To assess the effect of protamine on in vivo thrombin generation, mice were exsanguinated at specific time points after intravenous protamine administration. Blood was collected into citrate phosphate buffer (Sigma-Aldrich), and plasma was collected by centrifugation at 1500*g* for 20 minutes. Thrombin generation was initiated by addition of 20 μL HemosIL activated partial thromboplastin time (APTT)–lyophilized silica reagent and 100 mM $CaCl_2$, and was assessed using a Fluoroskan Ascent plate reader in combination with Thrombinoscope software, as described below.

APTT and PT measurement

Human plasma was prepared from a pool of normal healthy volunteers. APTT and prothrombin time (PT) were measured using the fully automated ACL TOP coagulometer (Beckman Coulter) using HemosIL APTT-lyophilized silica reagent and PT-fibrinogen HS plus reagent, respectively (Instrumentation Laboratory).

Effect of protamine on thrombin generation in normal human plasma

The anticoagulant function of protamine in normal, platelet-poor, pooled plasma was assessed using a Fluoroskan Ascent plate reader (Thermo Lab System) in combination with Thrombinoscope software (Thrombinoscope BV), as previously described.[17] Briefly, 80 μL of plasma was incubated with 20 μL of platelet-poor-plasma reagent containing 5 pM TF and 4 μM phospholipids (composed of 60% phosphatidylcholine [PC], 20% phosphatidylserine [PS], and 20% phosphatidylethanolamine [PE] in the presence or absence of protamine [3-80 μg/mL; all final concentrations]). Thrombin generation was initiated by automatic dispensation of fluorogenic thrombin substrate (Z-Gly-Gly-Arg-AMC.HCl) and 100 mM $CaCl_2$ into each well (final concentrations, Z-Gly-Gly-Arg-AMC.HCl, 0.42 mM and $CaCl_2$, 16.67 mM). Thrombin generation was determined using a thrombin calibration standard. Measurements were taken at 20-second intervals for 60 minutes, or until thrombin generation was complete. The lag time to start of thrombin generation, peak amount of thrombin generated, time to peak thrombin (TTP), and area under the thrombin generation curve, represented by endogenous thrombin potential (ETP), were measured. Experiments were performed in triplicate, and data were reported as mean plus or minus SEM.

Characterization of APC-mediated FVa proteolysis in the presence of protamine

FVa degradation by APC was assessed, as previously described.[16] A total of 8 nM APC was incubated at 37°C with phospholipid vesicles (PC:PS:PE 60%:20%:20%; Avanti Polar Lipids) and 4 nM FVa (Hematologic Technologies) in the presence and absence of protamine sulfate (3 μg/mL final concentration) in 40 mM Tris-HCl, 140 mM NaCl, 3 mM $CaCl_2$, and 0.3% wt/vol bovine serum albumin (2 nM APC, 19 mM phospholipids, and 1 nM FVa, final concentration). Phospholipid vesicles (PC:PS:PE 60%:20%:20%) were prepared, as described previously.[17] At specified time points, more than 20 minutes, 2-μL aliquots were removed and added to a prothrombinase mixture (25 μM phospholipids, 1 nM FXa, and 0.5 μM prothrombin [Hematologic Technologies], final concentrations) for 3 minutes. Each reaction was stopped using 5 μL ice-cold 0.5 M EDTA (ethylenediaminetetraacetic acid). A total of 100 μL reaction mixture was removed and incubated with 100 μl of 2 mM thrombin chromogenic substrate BIOPHEN CS-01(38) (HYPHEN Biomed) to assess thrombin generation. The rate of chromogenic substrate cleavage was measured at 405 nm using a VERSAmax microplate reader (Molecular Devices). Residual FVa activity was determined by comparison with FVa activity observed before APC incubation, and plotted values represent the mean of at least 3 individual experiments plus or minus SEM.

Characterization of APC-mediated FVIIIa proteolysis in the presence of protamine

To determine whether protamine enhancement of APC anticoagulant activity was mediated through increased rate of FVIIIa proteolysis, we used a previously characterized APC-resistant FVIII double mutant (R336Q/R562Q; APCR-FVIII).[18] FVIII-deficient plasma (Technoclone) was spiked with either B-domainless wild-type FVIII (wt-FVII) or the APCR-FVIII variant (both final concentration 1.0 U/mL [300 ng/mL]). Thrombin generation was then initiated with 5 pM TF, 4 μM phospholipid vesicles (PC:PS:PE 60%:20%:20%), and $CaCl_2$, and ETP was determined. Subsequently, the anticoagulant effect of protamine alone (3 μg/mL), APC alone (10 nM), or protamine in the presence of APC was determined for wt-FVIII and the APCR-FVIII variant, as before.

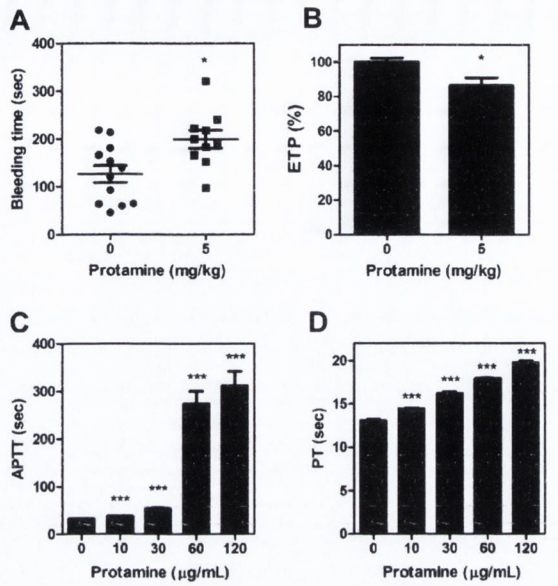


Figure 1. Protamine prolongs in vivo bleeding time and clotting time of normal pooled plasma. BALB/c mice were injected with either phosphate-buffered saline or 5 mg/kg protamine. Tail-bleeding time (A) or, in separate mice, plasma endogenous thrombin potential (B) was measured, as described in "Methods." In addition, the effect of protamine on clotting times of human normal pooled plasma was characterized. Increasing concentrations (10-120 μg/mL) of protamine were titrated into normal pooled plasma, and the effect on plasma APTT (C) and plasma PT (D) was determined. Results described represent the mean ± SEM (*$P < .05$, ***$P < .001$, respectively; unpaired 2-tailed *t* tests performed).

Determination of rate of FV activation in the presence of protamine

The effect of protamine on FV activation was determined using a method previously described by Safa et al.[19] Briefly, purified FV (100 nM final concentration) was incubated with purified α-thrombin (1 nM final concentration) in 100 mM NaCl, 20 mM HEPES (N-2-hydroxyethylpiperazine-N′-2-ethanesulfonic acid; pH 7.5), 5 mM $CaCl_2$, and 0.2 mg/mL bovine serum albumin, or with purified FXa (20 nM final concentration) and phospholipid vesicles (80 μM final concentration). At specific time intervals, aliquots were removed and diluted in 100 nM NaCl and 20 nM Tris-HCl (pH 7.5) to stop FV activation. The time course of FV activation was immediately quantified using FV-deficient plasma in a standard prothrombin-based clotting assay.

Results

Protamine prolongs in vivo bleeding time in mice and has a concentration-dependent anticoagulant effect in plasma

After intravenous administration of a therapeutic protamine dose (50 mg), pharmacokinetic studies have demonstrated typical plasma protamine levels of up to 50 μg/mL.[11] However, in practice, doses exceeding 5 mg/kg are frequently administered.[20] In BALB/c mice, we observed that parenteral protamine (5 mg/kg) administration significantly prolonged tail-bleeding time and attenuated thrombin generation (Figure 1A-B). These findings, which are in keeping with a previous report in which intravenous protamine (1.5 mg/kg) prolonged the ACT and APTT in a canine model,[21] confirm that protamine has in vivo anticoagulant activity. In addition, the presence of protamine in normal pooled human plasma resulted in significant prolongations in the APTT and PT, respectively (Figure 1C-D). Furthermore, again in keeping with previous reports, protamine (5-60 μg/mL) also significantly prolonged human whole blood ACT (data not shown).[8] In contrast, although previous studies demonstrated that protamine can bind fibrinogen,[22] we observed no effect of protamine (final concentration 5-50 μg/mL) on thrombin-clotting time (data not shown).

Calibrated automated thrombography was used to assess the impact of protamine on TF-initiated thrombin generation. In normal plasma, protamine significantly reduced thrombin generation (Figure 2A). Calculation of ETP demonstrated that 30 μg/mL protamine reduced thrombin generation to 59% (± 7%; $P < .05$) of the original ETP before protamine incubation (Figure 2B). Furthermore, at pharmacologic doses, protamine significantly influenced all of the individual parameters assessed during thrombin generation, with significant prolongation of lag time and TTP and a marked decrease in peak thrombin generation (Figure 2B), suggesting that protamine may influence the initiation and propagation phases of coagulation. This inhibition of thrombin generation was not mediated by protamine inhibition of contact activation, as corn trypsin inhibitor, which eliminates the contribution of contact pathway activation to thrombin generation in this system, had no effect on the observed reduction in thrombin generation (data not shown).

Anticoagulant effects of protamine in reversal of heparin-induced anticoagulation

Pharmacologic dose UFH (0.3 U/mL or 1 IU/mL) reduced the ETP such that no thrombin generation was detectable (Figure 3A). Protamine initially reversed the anticoagulant effect of UFH, resulting in a progressive increase in TF-initiated thrombin generation (Figure 3A). However, addition of higher concentrations of protamine to heparinized plasma resulted in a significant progressive reduction in thrombin generation, to a minimum of 54% (± 14%) and 57% (± 10%) of normal plasma ETP for 0.3 and 1.0 IU/mL UFH, respectively (Figure 3A). Similarly, although protamine at low dose (5-20 μg/mL) completely reversed the anticoagulant effect of the LMWH tinzaparin (1.0 U/mL), higher doses of protamine (20-80 μg/mL) were again associated with a significant reduction in ETP (to 78% ± 1%). In contrast, titration of protamine into plasma containing LMWH enoxaparin (1.0 U/mL) failed to fully correct TF-initiated thrombin generation (maximum 80% ± 4%). Moreover, in plasma containing enoxaparin, higher doses of protamine resulted in a more marked anticoagulant effect than that observed with either UFH or tinzaparin, respectively, to 21% (± 2% of normal ETP (Figure 3B).

Anticoagulant effects of APC in plasma are enhanced by protamine

APC down-regulates thrombin generation by inactivation of procoagulant cofactors FVa and FVIIIa. Moreover, we have recently demonstrated that FVa proteolysis by APC can be specifically modulated by another cationic polypeptide, platelet factor 4.[16] Consequently, we hypothesized that the anticoagulant effects of cationic protamine might be mediated through a similar mechanism. As expected, APC (1.25-20 nM) alone caused a concentration-dependent prolongation in APTT (maximum 2.8 ± 0.1-fold prolongation) in normal plasma (Figure 4A). However, the anticoagulant activity of APC on the APTT was markedly enhanced at all concentrations in the presence of protamine (30 μg/mL; Figure 4A). Furthermore, in keeping with the observed APTT findings, pharmacologic doses of protamine also significantly enhanced APC attenuation of TF-initiated thrombin generation. For example, although 1 nM APC alone had minimal effect on thrombin

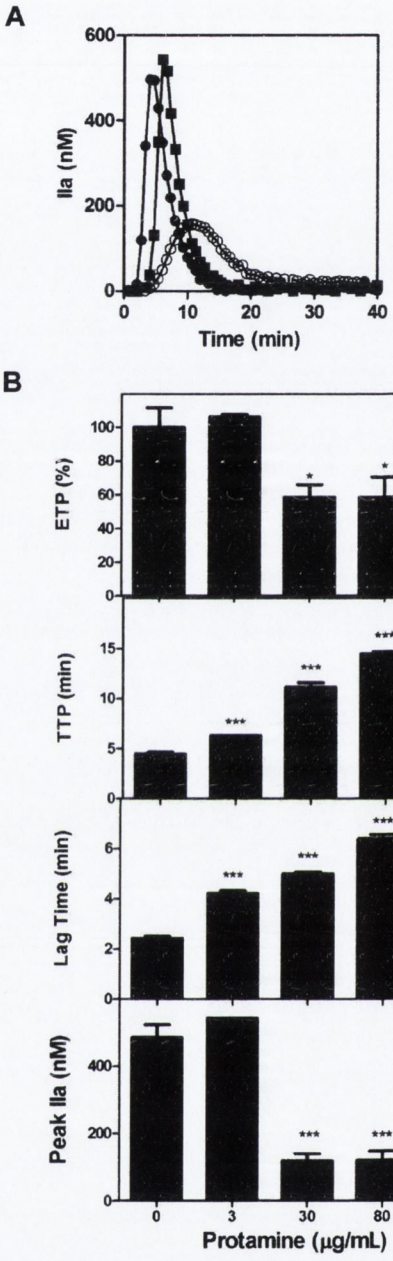


Figure 2. Protamine inhibits TF-initiated thrombin generation in normal plasma. Coagulation was initiated in pooled normal plasma with 5 pM TF, 4 μM phospholipid vesicles (PC:PS:PE 60%:20%:20%), and 6.67 mM $CaCl_2$, and thrombin generation was followed using a fluorogenic substrate, as described in "Methods." (A) Thrombin generation in the absence of protamine (●) was compared with 3 μg/mL (■) and 30 μg/mL (○) of protamine, respectively. (B) The effect of protamine (3-80 μg/mL) on individual thrombin generation curve parameters was determined. Parameters measured (top to bottom) were ETP (% of normal pooled plasma), TTP (minutes), lag time (minutes), and peak thrombin (nM). Unpaired 2-tailed *t* tests were performed to determine significance (***$P < .0001$ compared with plasma in the absence of protamine). All experiments were performed in triplicate. Results are expressed as mean ± SEM.

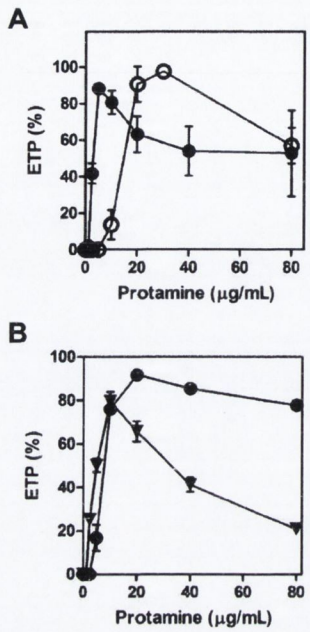


Figure 3. Anticoagulant activity of excess protamine administration during reversal of heparin-induced anticoagulation. (A) Protamine (10-80 μg/mL) was titrated into normal pooled plasma containing 0.3 U/mL (●) or 1.0 U/mL (○) UFH, and TF-initiated thrombin generation was determined as before. (B) The ability of protamine (10-80 μg/mL) to reverse different LMWH preparations of 1.0 U/mL tinzaparin (●) or 1.0 U/mL enoxaparin (▼) was also characterized.

generation, coincubation of the same APC concentration with protamine (30 μg/mL) entirely ablated thrombin generation in normal plasma (Figure 4B). A synergistic anticoagulant interaction between APC and protamine was also observed in heparinized plasma. In the presence of 1 nM APC, the ability of high protamine concentrations to inhibit thrombin generation was markedly enhanced, such that thrombin generation was entirely ablated at 40 μg/mL protamine (Figure 4C).

Protamine does not enhance FVa or FVIIIa proteolysis by APC

To further elucidate the mechanism(s) through which protamine enhances APC anticoagulant activity, the rate of FVa proteolysis in the presence or absence of protamine was determined using a phospholipid-dependent FVa proteolysis time course assay (Figure 5A). In this purified system, the ability of APC to cleave and inactivate procoagulant FVa was not significantly enhanced in the presence of pharmacologic concentrations of protamine. Therefore, to determine whether the anticoagulant activity of protamine was due to enhanced FVIIIa proteolysis by APC, we assessed thrombin generation in FVIII-deficient plasma in the presence of an APC-resistant FVIII variant (R336Q/R562Q).[18] Wild-type or variant FVIII in FVIII-deficient plasma entirely restored ETP to normal plasma levels (Figure 5B). Although low-dose protamine (3 μg/mL) did not significantly reduce ETP, a marked anticoagulant interaction was again observed when protamine was combined with APC (10 nM). Moreover, the synergistic anticoagulant effects of APC in combination with protamine were comparable for wild-type FVIII and for APC-resistant FVIII, suggesting that accelerated FVIIIa proteolysis is not responsible for the enhanced anticoagulant effects of APC in the presence of protamine.

Protamine inhibits activation of FV by α-thrombin and FXa

We further investigated whether protamine enhancement of APC in plasma was due to inhibition of FVa generation. In the presence of pharmacologic concentrations of protamine (50 μg/mL), activation of FV by thrombin (1 nM) was entirely ablated (Figure 6A). Moreover, low concentrations of protamine (0.25-12.5 μg/mL) significantly attenuated FV activation in a dose-dependent manner

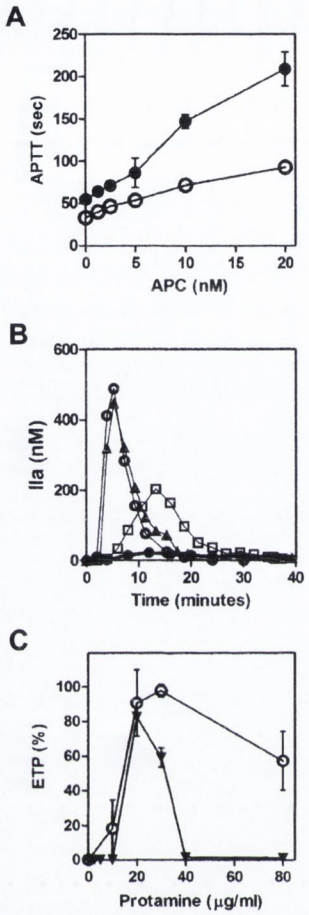


Figure 4. Anticoagulant effects of APC in normal plasma are enhanced by protamine. (A) Increasing concentrations of APC (1.25-20 nM) were added to normal pooled plasma in the presence (●) and absence (○) of 30 μg/mL protamine, and plasma APTT was measured. (B) Thrombin generation in normal pooled plasma (○) was compared with plasma spiked with 1 nM APC (▲) alone, 30 μg/mL protamine (□) alone, or 1 nM APC plus 30 μg/mL protamine (●) in combination. (C) ETP (% of normal pooled plasma) was calculated after titration of protamine (0.2-80 μg/mL) into normal plasma containing 1.0 U/mL UFH and either in the absence (○) or presence (▼) of 1 nM APC.

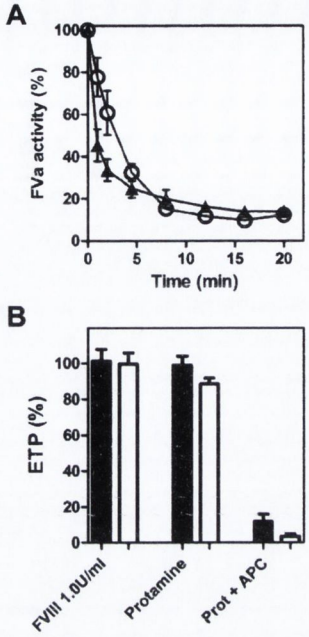


Figure 5. APC-protamine anticoagulant synergy is not mediated by enhanced substrate proteolysis. (A) FVa proteolysis by APC was assessed in both the absence (▲) and presence (○) of 3 μg/mL protamine. Purified FVa (1 nM final concentration) was incubated with phospholipid vesicles (PC:PS:PE, 60%:20%:20%, 20 μM final concentration) in a buffer containing 175 mM NaCl, 3 mM $CaCl_2$, and 25 mM HEPES (pH 7.4) at 37°C. APC (2 nM final concentration) was added to initiate FVa inactivation. At specific time points, aliquots of the reaction mix were added to a separate prothrombinase mixture and thrombin generated was measured, as described in "Methods." (B) To assess FVIIIa proteolysis by APC, thrombin generation was initiated with TF, phospholipid vesicles, and $CaCl_2$ in FVIII-deficient plasma to which 1.0 U/mL wild-type (□) or APC-resistant FVIII R336Q/R562Q (■), respectively, had been added. ETP was determined for each FVIII variant in the presence and absence of protamine (3 μg/mL) and also in the presence of APC (10 nM).

(Figure 6B). The 50% inhibitory concentration for protamine inhibition of FV activation by thrombin was only 0.8 μg/mL. Consequently, this effect is of clear clinical importance, given that peak protamine plasma concentrations can potentially reach 50 μg/mL after a single 50-mg bolus administration.[11] Although physiologic activation of FV is predominantly mediated by thrombin, FXa can also activate FV.[23] Interestingly, however, in the presence of protamine (50 μg/mL), FV activation by FXa (20 nM) was also significantly reduced (Figure 6C).

Preactivation of FV eliminates protamine anticoagulant effect in plasma

Previous studies have suggested that protamine may influence several different procoagulant and anticoagulant reactions in plasma.[6,7,24,25] To determine the relative importance of protamine inhibition of FV activation in mediating the anticoagulant effect of protamine in plasma, increasing concentrations of either FV or FVa (0-20 nM) were titrated into FV-deficient plasma in the presence or absence of protamine (30 μg/mL; Figure 7). In a TF-initiated thrombin generation assay, addition of FV or FVa resulted in a significant increase in thrombin generation (Figure 7A-B). In keeping with our previous findings, protamine (30 μg/mL) significantly inhibited thrombin generation at all concentrations of FV (Figure 7A). However, in the presence of preactivated FVa, the ability of protamine to significantly inhibit thrombin generation was no longer evident (Figure 7B). Cumulatively, these data support the hypothesis that protamine-mediated inhibition of FV activation plays a critical role in mediating its anticoagulant activity in human plasma.

Discussion

Protamine sulfate is widely regarded as the treatment of choice for reversing UFH-induced anticoagulation. However, excessive protamine administration has been associated with anticoagulant activity, and has been implicated in the etiology of perioperative bleeding for many years.[6-8,26] In particular, previous trials have demonstrated that the use of lower doses of protamine for heparin neutralization in patients after CPB resulted in reduced postoperative blood loss.[26-30] In a prospective study, Despotis et al randomized 254 patients requiring CPB to heparin neutralization with either a fixed dose of protamine (0.8 mg of protamine per mg total UFH), or a titrated protamine dosing based upon residual plasma heparin concentration.[28] Although patients in the titrated protamine dosing arm of the study received lower doses of protamine, they developed fewer bleeding complications and required significantly

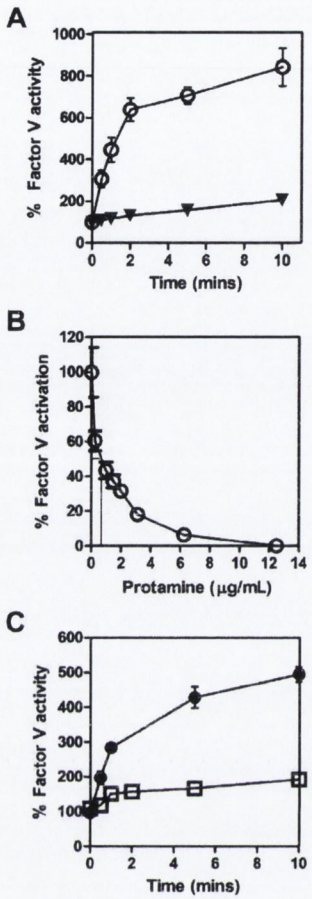


Figure 6. Protamine inhibits activation of intact FV by thrombin and by FXa. (A) The rate of activation of 100 nM purified FV by 1 nM thrombin was measured in a PT-based clotting assay using FV-deficient plasma (as described in "Methods") in the absence (○) and presence (▼) of 50 μg/mL protamine. (B) To determine the 50% inhibitory concentration for the observed effect, the activity of FV was measured after incubation with thrombin and increasing (0.25-12.5 μg/mL) concentrations of protamine for 60 seconds. Activity was expressed as a percentage of activity in the absence of protamine. (C) To assess whether FXa-mediated FV activation was affected by protamine, the rate of activation of 100 nM purified FV by 20 nM FXa in the presence of phospholipid vesicles (PC:PS:PE 60%:20%:20%, 80 μM final concentration) was assessed in the absence (●) and presence (□) of 50 μg/mL protamine in a PT-based clotting assay.

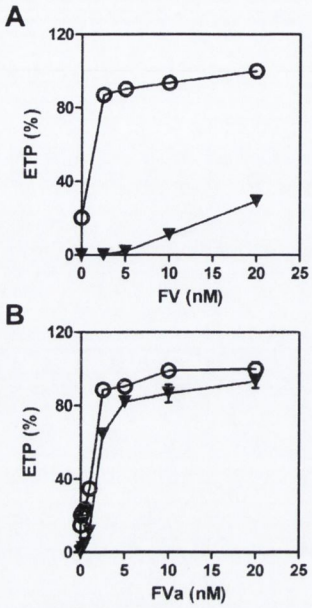


Figure 7. The anticoagulant effect of protamine is greatly reduced by preactivation of FV to FVa. (A) FV (2.5-20 nM) or (B) FVa (1-20 nM) was titrated into FV-deficient plasma in the absence (○) and presence (▼) of protamine (30 μg/mL). Thrombin generation was initiated with TF, phospholipid vesicles, and $CaCl_2$ (see "Methods"), and ETP was calculated as before.

less hemostatic support (platelets, fresh frozen plasma, and cryoprecipitate transfusions) during the perioperative period. Similarly, another prospective randomized trial of adult patients undergoing CPB also demonstrated that reduction in protamine dose was associated with significantly decreased mediastinal blood loss (~ 50%).[29]

In this study, we investigated the molecular mechanisms responsible for these clinically important protamine-mediated anticoagulant effects. We demonstrate that in vivo administration of protamine significantly reduces thrombin generation in murine plasma, and significantly prolongs tail-bleeding time. Moreover, protamine also has anticoagulant activity in normal human plasma. At pharmacologic doses (> 10 μg/mL), protamine prolonged both the PT and APTT, suggesting an effect on the common pathway. Furthermore, protamine also significantly attenuated TF-initiated thrombin generation in human plasma.

Conversion of pro-cofactor FV to active FVa occurs early in the process of TF-initiated coagulation.[31] Initial activation of FV by thrombin involves limited proteolytic cleavage of peptide bonds at Arg^{709}, Arg^{1018}, and Arg^{1545}. FVa then associates with FXa on negatively charged phospholipid membrane surfaces to form the prothrombinase complex. In this complex, FVa acts as a critical cofactor, enhancing the ability of FXa to convert prothrombin to thrombin by 300 000-fold.[32] In addition, FVa binding also makes FXa refractory to inhibition by anticoagulant tissue factor pathway inhibitor.[33] Using purified protein assays to study the anticoagulant activity of protamine, we demonstrate that FV activation by α-thrombin is reduced in a dose-dependent manner by protamine. Moreover, this novel specific inhibitory effect upon FV activation is responsible for the bulk of the anticoagulant effect of protamine on TF-initiated thrombin generation in human plasma. Indeed, protamine had only a minor inhibitory effect on thrombin generation in plasma containing preformed FVa rather than pro-cofactor FV. Further studies will be required to unravel the precise mechanism(s) through which protamine attenuates activation of FV. Nevertheless, the observation that FV activation by both thrombin and FXa is inhibited indicates protamine may form an inhibitory complex with FV.

Because arginine residues account for approximately 60% of its primary amino acid sequence, protamine is highly cationic. Interestingly, several recent studies have shown that specific anionic molecules have the opposite effect to protamine on FV activation.[34-36] In particular, polyphosphate, a linear polymer of inorganic phosphate present in the dense granules of human platelets, significantly enhanced the rate of FV activation by both thrombin and FXa.[34,37] Similarly, AV513, a sulfated proteoglycan of plant origin, has been shown to accelerate thrombin generation by significantly enhancing FV activation.[36] Finally, in antithrombin-deficient plasma, negatively charged UFH also had significant procoagulant activity due to increased FV activation.[35] The molecular interactions through which these different anionic polymers function to enhance FV activation have not been defined. Nevertheless, these reports combined with our novel findings cumulatively

support the hypothesis that charge-mediated interactions may be critical in regulating FV activation.

Previous studies have reported that protamine can also down-regulate coagulation by directly inhibiting thrombin activity.[24] However, high protamine concentrations (> 100 μg/mL) were only associated with relatively minor reductions in thrombin function.[24] Moreover, at pharmacologic concentrations (≤ 50 μg/mL), we observed no significant protamine effect on thrombin-clotting time, or thrombin amidolytic activity (data not shown). In contrast, the presence of 10 μg/mL protamine in pooled normal plasma was sufficient to prolong both the PT and APTT. In addition, the lag time and TTP of TF-initiated thrombin generation were significantly prolonged by 3 μg/mL protamine. Consequently, our findings clearly indicate that direct thrombin inhibition plays a relatively minor role in mediating the anticoagulant function of protamine. More recently, Nielsen demonstrated that clinically encountered protamine concentrations also resulted in enhanced fibrinolysis.[15] Although the mechanism(s) responsible for this effect was not defined, these data would be consistent with a down-regulation in thrombin generation, and consequent reduction in thrombin-activatable fibrinolysis inhibitor activation.

The ability of pharmacologic doses of protamine to markedly inhibit FV activation has several direct important translational implications. First, the ACT assay is routinely used to monitor UFH-induced anticoagulation during cardiac surgery, and to evaluate the efficacy of protamine reversal during the immediate postoperative period.[5,9] In other patients, including those presenting with life-threatening bleeding complications, heparin reversal after protamine administration is typically assessed using an APTT assay.[4] However, as we have shown, administration of excess protamine significantly inhibits FV activation, thereby prolonging both the ACT and APTT, respectively. Consequently, an increased ACT or APTT after protamine administration cannot be regarded as pathognomonic of inadequate heparin reversal, but rather may reflect excess free protamine. Interestingly, we observed that TF-initiated thrombin generation curves could rapidly and reliably differentiate between residual heparin and excess protamine, suggesting a potential new diagnostic application for calibrated automated thrombography in this setting.

Second, our findings have important clinical implications in relation to the use of protamine for reversing LMWH-induced anticoagulation. Although protamine reverses the antithrombin activity of LMWH, it only partially neutralizes FXa inhibition. Consequently, as we demonstrate in this study, protamine is more effective in reversing the anticoagulant activity of LMWH with lower anti-FXa:antithrombin ratios (eg, tinzaparin 2:1 compared with enoxaparin 3:1). However, we further demonstrate that rather than reversing LMWH-induced anticoagulant properties, administration of high protamine concentrations actually serves to further enhance the anticoagulant status. Furthermore, this phenomenon is more apparent in the presence of enoxaparin rather than tinzaparin, and presumably reflects residual LMWH anti-FXa activity, coupled with the inhibitory activity of excess free protamine on FV activation. Interestingly, an even more marked combined anticoagulant response was observed when protamine was titrated into plasma containing the low molecular weight heparinoid danaparoid (anti-FXa:antithrombin ratio 28:1; data not shown). Further adequately powered clinical studies will be required to define the clinical utility of protamine in reversing the anticoagulant effects of LMWH. Finally, although protamine does not directly enhance the proteolytic activity of APC, nevertheless, the combination of protamine and APC does result in a potent synergistic anticoagulant effect. Consequently, our data suggest that protamine administration should be used with caution in patients with severe sepsis receiving recombinant APC by continuous infusion.

Acknowledgments

This work was supported by Molecular Medicine Ireland Clinician Scientist Award G04005 (to F.N.A.); Health Research Board Ireland Project Grant Award RP/2006/44 (to J.S.O.); Health Research Board Ireland Postdoctoral Fellowship PD/2006/24 (to R.J.S.P.); an Irish Heart Foundation grant (to J.S.O.); and Science Foundation Ireland President of Ireland Young Researcher Award 06/Y12/0925 (to J.S.O.).

Authorship

Contribution: F.N.A. designed the research, performed experiments, analyzed results, made the figures, and wrote the paper; R.J.S.P. designed and supervised the research, analyzed results, and wrote the paper; P.V.J. and H.J.N. performed experiments and analyzed results; J.A.J. performed experiments; O.P.S. and B.W., supervised the research; P.G.F. designed and supervised the research; and J.S.O. designed and supervised the research and wrote the paper.

Conflict-of-interest disclosure: The authors declare no competing financial interests.

Correspondence: James S. O'Donnell, Hemostasis Research Group, Trinity Health Center, St James's Hospital, James's St, Trinity College, Dublin, Ireland; e-mail: jodonne@tcd.ie.

References

1. Horrow JC. Protamine: a review of its toxicity. *Anesth Analg.* 1985;64:348-361.
2. Carr JA, Silverman N. The heparin-protamine interaction: a review. *J Cardiovasc Surg.* 1999;40:659-666.
3. Baglin T, Barrowcliffe TW, Cohen A, Greaves M. Guidelines on the use and monitoring of heparin. *Br J Haematol.* 2006;133:19-34.
4. Hirsh J, Bauer KA, Donati MB, Gould M, Samama MM, Weitz JI. Parenteral anticoagulants: American College of Chest Physicians Evidence-Based Clinical Practice Guidelines (8th Edition). *Chest.* 2008;133(suppl 6):141S-159S.
5. Dunning J, Versteegh M, Fabbri A, et al. Guideline on antiplatelet and anticoagulation management in cardiac surgery. *Eur J Cardiothorac Surg.* 2008;34:73-92.
6. Brecher AS, Roland AR. Protamine inhibits formation of the covalent factor IXa-anti-thrombin complex. *Blood Coagul Fibrinolysis.* 2008;19:591-596.
7. Chu AJ, Wang ZG, Raicu M, Beydoun S, Ramos N. Protamine inhibits tissue factor-initiated extrinsic coagulation. *Br J Haematol.* 2001;115:392-399.
8. Mochizuki T, Olson PJ, Szlam F, Ramsay JG, Levy JH. Protamine reversal of heparin affects platelet aggregation and activated clotting time after cardiopulmonary bypass. *Anesth Analg.* 1998;87:781-785.
9. McLaughlin KE, Dunning J. In patients post-cardiac surgery, do high doses of protamine cause increased bleeding? *Interact Cardiovasc Thorac Surg.* 2003;2:424-426.
10. Butterworth J, Lin YA, Prielipp RC, Bennett J, Hammon JW, James RL. Rapid disappearance of protamine in adults undergoing cardiac operation with cardiopulmonary bypass. *Ann Thorac Surg.* 2002;74:1589-1595.
11. Butterworth J, Lin YA, Prielipp R, Bennett J, James R. The pharmacokinetics and cardiovascular effects of a single intravenous dose of protamine in normal volunteers. *Anesth Analg.* 2002;94:514-522.
12. Van Ryn-McKenna J, Cai L, Ofosu FA, Hirsh J, Buchanan MR. Neutralization of enoxaparine-induced bleeding by protamine sulfate. *Thromb Haemost.* 1990;63:271-274.
13. Wolzt M, Weltermann A, Nieszpaur-Los M, et al. Studies on the neutralizing effects of protamine on unfractionated and low molecular weight heparin (Fragmin) at the site of activation of the coagulation system in man. *Thromb Haemost.* 1995;73:439-443.

14. Perkash A. A comparison of the quantitative action of protamine and heparin on blood coagulation: significance in clinical and laboratory usage. *Am J Clin Pathol.* 1980;73:676-681.
15. Nielsen VG. Protamine enhances fibrinolysis by decreasing clot strength: role of tissue factor-initiated thrombin generation. *Ann Thorac Surg.* 2006;81:1720-1727.
16. Preston RJ, Tran S, Johnson JA, et al. Platelet factor 4 impairs the anticoagulant activity of activated protein C. *J Biol Chem.* 2009;284:5869-5875.
17. Harmon S, Preston RJ, Ainle FN, et al. Dissociation of activated protein C functions by elimination of protein S cofactor enhancement. *J Biol Chem.* 2008;283:30531-30539.
18. Varfaj F, Wakabayashi H, Fay PJ. Residues surrounding Arg336 and Arg562 contribute to the disparate rates of proteolysis of factor VIIIa catalyzed by activated protein C. *J Biol Chem.* 2007; 282:20264-20272.
19. Safa O, Morrissey JH, Esmon CT, Esmon NL. Factor VIIa/tissue factor generates a form of factor V with unchanged specific activity, resistance to activation by thrombin, and increased sensitivity to activated protein C. *Biochemistry.* 1999;38: 1829-1837.
20. Mittermayr M, Velik-Salchner C, Stalzer B, et al. Detection of protamine and heparin after termination of cardiopulmonary bypass by thrombelastometry (ROTEM): results of a pilot study. *Anesth Analg.* 2009;108:743-750.
21. Kresowik TF, Wakefield TW, Fessler RD, Stanley JC. Anticoagulant effects of protamine sulfate in a canine model. *J Surg Res.* 1988;45:8-14.
22. Merskey C. Defibrination syndrome or? *Blood.* 1973;41:599-603.
23. Orfeo T, Brufatto N, Nesheim ME, Xu H, Butenas S, Mann KG. The factor V activation paradox. *J Biol Chem.* 2004;279:19580-19591.
24. Cobel-Geard RJ, Hassouna HI. Interaction of protamine sulfate with thrombin. *Am J Hematol.* 1983;14;227-233.
25. Miyashita T, Nakajima T, Hayashi Y, Kuro M. Hemostatic effects of low-dose protamine following cardiopulmonary bypass. *Am J Hematol.* 2000; 64:112-115.
26. Griffin MJ, Rinder HM, Smith BR, et al. The effects of heparin, protamine, and heparin/protamine reversal on platelet function under conditions of arterial shear stress. *Anesth Analg.* 2001; 93:20-27.
27. DeLaria GA, Tyner JJ, Hayes CL, Armstrong BW. Heparin-protamine mismatch: a controllable factor in bleeding after open heart surgery. *Arch Surg.* 1994;129:944-950.
28. Despotis GJ, Joist JH, Hogue CW Jr, et al. The impact of heparin concentration and activated clotting time monitoring on blood conservation: a prospective, randomized evaluation in patients undergoing cardiac operation. *J Thorac Cardiovasc Surg.* 1995;110:46-54.
29. Jobes DR, Aitken GL, Shaffer GW. Increased accuracy and precision of heparin and protamine dosing reduces blood loss and transfusion in patients undergoing primary cardiac operations. *J Thorac Cardiovasc Surg.* 1995;110:36-45.
30. Verska JJ. Control of heparinization by activated clotting time during bypass with improved postoperative hemostasis. *Ann Thorac Surg.* 1977;24: 170-173.
31. Mann KG, Kalafatis M. Factor V: a combination of Dr. Jekyll and Mr. Hyde. *Blood.* 2003;101:20-30.
32. Nesheim ME, Taswell JB, Mann KG. The contribution of bovine factor V and factor Va to the activity of prothrombinase. *J Biol Chem.* 1979;254: 10952-10962.
33. Mast AE, Broze GJ Jr. Physiological concentrations of tissue factor pathway inhibitor do not inhibit prothrombinase. *Blood.* 1996;87:1845-1850.
34. Smith SA, Mutch NJ, Baskar D, Rohloff P, Docampo R, Morrissey JH. Polyphosphate modulates blood coagulation and fibrinolysis. *Proc Natl Acad Sci U S A.* 2006;103:903-908.
35. Smith SA, Morrissey JH. Heparin is procoagulant in the absence of antithrombin. *Thromb Haemost.* 2008;100:160-162.
36. Liu T, Scallan CD, Broze GJ Jr, Patarroyo-White S, Pierce GF, Johnson KW. Improved coagulation in bleeding disorders by non-anticoagulant sulfated polysaccharides (NASP). *Thromb Haemost.* 2006;95:68-76.
37. Smith SA, Morrissey JH. Polyphosphate enhances fibrin clot structure. *Blood.* 2008;112: 2810-2816.

THE JOURNAL OF BIOLOGICAL CHEMISTRY VOL. 284, NO. 9, pp. 5869–5875, February 27, 2009
© 2009 by The American Society for Biochemistry and Molecular Biology, Inc. Printed in the U.S.A.

Platelet Factor 4 Impairs the Anticoagulant Activity of Activated Protein C*

Received for publication, June 19, 2008, and in revised form, January 6, 2009 Published, JBC Papers in Press, January 6, 2009, DOI 10.1074/jbc.M804703200

Roger J. S. Preston[‡1], Sinh Tran[§], Jennifer A. Johnson[‡], Fionnuala Ní Áinle[‡], Shona Harmon[‡], Barry White[¶], Owen P. Smith[‖], P. Vince Jenkins[¶], Björn Dahlbäck[§], and James S. O'Donnell[‡¶]

From the [‡]Haemostasis Research Group, Institute of Molecular Medicine, Trinity College Dublin, St James' Hospital, Dublin 8, Ireland, the [§]Department of Laboratory Medicine, Clinical Chemistry, Lund University, The Wallenberg Laboratory, University Hospital, Malmö SE-20502, Sweden, the [¶]National Centre for Hereditary Coagulation Disorders, St James' Hospital, Dublin 8, Ireland, and the [‖]Department of Haematology, Our Lady's Children's Hospital Crumlin, Dublin 12, Ireland

Platelet factor 4 (PF4) is an abundant platelet α-granule chemokine released following platelet activation. PF4 interacts with thrombomodulin and the γ-carboxyglutamic acid (Gla) domain of protein C, thereby enhancing activated protein C (APC) generation by the thrombin-thrombomodulin complex. However, the protein C Gla domain not only mediates protein C activation *in vivo*, but also plays a critical role in modulating the diverse functional properties of APC once generated. In this study we demonstrate that PF4 significantly inhibits APC anticoagulant activity. PF4 inhibited both protein S-dependent APC anticoagulant function in plasma and protein S-dependent factor Va (FVa) proteolysis 3- to 5-fold, demonstrating that PF4 impairs protein S cofactor enhancement of APC anticoagulant function. Using recombinant factor Va variants FVa-R506Q/R679Q and FVa-R306Q/R679Q, PF4 was shown to impair APC proteolysis of FVa at position Arg^{306} by 3-fold both in the presence and absence of protein S. These data suggest that PF4 contributes to the poorly understood APC resistance phenotype associated with activated platelets. Finally, despite PF4 binding to the APC Gla domain, we show that APC in the presence of PF4 retains its ability to initiate PAR-1-mediated cytoprotective signaling. In summary, we propose that PF4 acts as a critical regulator of APC generation, but also differentially targets APC toward cytoprotective, rather than anticoagulant function at sites of vascular injury with concurrent platelet activation.

Protein C is a vitamin K-dependent glycoprotein zymogen, which is activated by the thrombin-thrombomodulin complex on the surface of endothelial cells (for review, see Refs. 1–3). Protein C activation is enhanced by protein C binding to its receptor, the endothelial cell protein C receptor (EPCR)[2] (4, 5). Activated protein C (APC) down-regulates the coagulation cascade by inactivation of procoagulant cofactors, factor Va (FVa) and factor VIIIa (FVIIIa) (6, 7), both of which are required for thrombin generation. The clinical importance of APC anticoagulant function is well established. Homozygous protein C deficiency causes purpura fulminans in neonates (8), whereas heterozygous deficiency is associated with significantly increased risk of venous thrombosis (9). Proteolysis of FVa and FVIIIa by APC is enhanced >20-fold in the presence of protein S, which acts as a cofactor for APC (10). Consequently, inherited or acquired protein S deficiency is also associated with significantly increased risk of thrombosis (11, 12). Recent studies have demonstrated that APC bound to EPCR via its Gla domain can also initiate protease-activated receptor 1 (PAR-1)-mediated anti-inflammatory and anti-apoptotic signaling in endothelial cells (13, 14). Furthermore, the cytoprotective properties of APC are of therapeutic benefit to patients with severe sepsis syndrome (15).

FVa inactivation by APC occurs due to limited proteolytic cleavage of FVa at positions Arg^{506} and Arg^{306} (16). Previous *in vitro* studies have demonstrated that FVa inactivation by APC occurs rapidly in the presence of negatively charged phospholipid vesicles (16, 17). In contrast, APC-mediated FVa inactivation is markedly inhibited in the presence of activated platelets (17, 18). The one or more mechanisms through which platelet-mediated APC resistance occurs are unclear. However, previous work has indicated that platelet-mediated inhibition of APC anticoagulant function is enhanced by an unidentified protein component of the platelet secretory granules released following platelet activation (19).

Accumulating evidence suggests that platelet factor 4 (PF4) may play an important role in regulating protein C activation (20). PF4 is synthesized in megakaryocytes, and subsequently stored in platelet α-granules (20). In contrast to other cationic proteins, PF4 enhances APC generation up to 25-fold on endothelial cell surfaces (21, 22). This specific enhancement has been attributed to a PF4-mediated increase in the affinity of the thrombin-thrombomodulin complex for protein C, resulting in a 30-fold decreased K_m for protein C activation (22). Moreover, subsequent studies demonstrated that enhancement is mediated through the interaction between PF4 and the protein C Gla

* This work was supported by a Health Research Board Ireland Postdoctoral Fellowship (RP/2006/44 to R. J. S. P.), a Health Research Board Ph.D. Scholarship (to J. A. J.), a Children's Medical and Research Foundation Award (RP348 to O. P. S. and F. N. A.), and a Science Foundation Ireland President of Ireland Young Researcher Award (06/Y12/0925, to J. S. O. D.). The costs of publication of this article were defrayed in part by the payment of page charges. This article must therefore be hereby marked "*advertisement*" in accordance with 18 U.S.C. Section 1734 solely to indicate this fact.

[1] To whom correspondence should be addressed. Tel.: 353-(1)896-3274; Fax: 353-(1)410-3570; E-mail address: prestonr@tcd.ie.

[2] The abbreviations used are: EPCR, endothelial cell protein C receptor; APC, activated protein C; FVa, factor Va; FVIIIa, factor VIIIa; FXa, factor Xa; PAR-1, protease-activated receptor 1; PF4, platelet factor 4; ETP, endogenous thrombin potential; PS, phosphatidylserine; PC, phosphatidylcholine; PE, phosphatidylethanolamine; BSA, bovine serum albumin; Gla, γ-carboxyglutamic acid.

Downloaded from www.jbc.org at IReL (Trinity College Dublin), on March 5, 2010

domain (23). The protein C/APC Gla domain also plays critical roles in regulating both APC anticoagulant and cytoprotective signaling properties. However, the functional consequences of the interaction between the APC Gla domain and PF4 in relation to APC anticoagulant, anti-inflammatory, and anti-apoptotic functions have not previously been defined.

In this study, we demonstrate that PF4, in contrast to its role in protein C activation, attenuates APC anticoagulant activity in plasma. Furthermore, PF4 inhibits the ability of protein S to function as a cofactor for APC. Finally, despite PF4 binding to the protein C/APC Gla domain, we also demonstrate that the APC Gla domain interaction with EPCR is preserved, such that APC in the presence of PF4 retains its ability to initiate PAR-1-mediated cytoprotective signaling. Consequently, our findings support a novel physiological role for PF4 in modulating APC function.

EXPERIMENTAL PROCEDURES

Materials—Human PF4 was purchased from both Hematologic Technologies Inc. (Essex Junction, VT) and Enzyme Research Laboratories (South Bend, IN). Human purified APC, thrombin, and protein S were purchased from Hematologic Technologies Inc. Recombinant FVa variants FVa-R506Q/R679Q and FVa-R306Q/R679Q were generated and characterized as previously described (24). Deficient plasmas and chromogenic substrates BIOPHEN CS 21(66) and BIOPHEN CS-01(38) for APC and thrombin, respectively, were purchased from Hyphen-Biomed (Neuville-Sur-Oise, France). Thrombin generation assay reagents (PPP reagent, fluorogenic substrate, and thrombin calibration standard) were all purchased from Thrombinoscope BV (Maastricht, The Netherlands). Evans Blue dye, bovine serum albumin, and staurosporine were bought from Sigma. Pre-designed primers for reverse transcription-PCR experiments were from Applied Biosystems (Foster City, CA).

Determination of APC Anticoagulant Activity in the Presence of PF4 in Plasma—The anticoagulant function of APC in the presence of PF4 in normal, platelet-poor, pooled plasma was assessed using a Fluoroskan Ascent Plate Reader (Thermo Lab System, Helsinki, Finland) in combination with Thrombinoscope software (Thrombinoscope BV), as previously described (25). 80 μl of protein C-deficient plasma was incubated with 20 μl of PPP Reagent containing 5 pM tissue factor and 4 μM phospholipids (PC/PS/PE, 60%/20%/20%) in the presence or absence of APC (1.25–10 nM, all final concentrations). Thrombin generation was initiated by automatic dispensation of 2.5 mM fluorogenic thrombin substrate (Z-Gly-Gly-Arg-amidomethyl coumarin·HCl) and 100 mM $CaCl_2$ into each well (final concentrations, Z-Gly-Gly-Arg-amidomethyl coumarin·HCl, 0.42 mM, and $CaCl_2$, 16.67 mM). Thrombin generation was determined using a thrombin calibration standard. Measurements were taken at 20-s intervals for 60 min, or until thrombin generation was complete. The endogenous thrombin potential (ETP) of each reaction was then calculated. Experiments were performed in triplicate, and data were reported as mean ETP ± S.E.

Protein S Enhancement of APC Anticoagulant Activity in Protein S-deficient Plasma—APC anticoagulant activity in protein S-deficient plasma in the presence of PF4 was determined using a similar assay to that described above. Briefly, protein S-deficient plasma was incubated with APC (10 nM) in the presence of plasma-purified protein S (6.25–100 nM). Thrombin generation was initiated and assessed using Thrombinoscope software as described previously. All experiments were performed in triplicate and data plotted as mean ETP ± S.E.

Determination of Protein S-independent and Protein S-dependent APC-mediated FVa Proteolysis—FVa degradation by APC in the absence of protein S was assessed as previously described (26). Recombinant FVa (0.8 nM, final concentration) was incubated with phospholipid vesicles (PS/PE/PC, 10%/20%/70%, 25 μM final concentration) in the presence or absence of PF4 (1 μM, final concentration) in HNBSACa buffer (25 mM Hepes, 150 mM NaCl, pH 7.7, with 5 mg/ml BSA, and 5 mM $CaCl_2$). APC (1.65 nM, final concentration) was added to initiate FVa inactivation, and aliquots were drawn at set time intervals over a 20-min time course. FVa inactivation was stopped by 1/25 dilution in ice-cold HNBSACa. The FVa activity was measured at each time point using a prothrombinase assay containing 5 nM FXa, 0.5 μM prothrombin, and phospholipid vesicles (PC/PS, 90%/10%, 50 μM final concentration) for 2 min, then stopped with 40-fold dilution in ice-cold EDTA buffer (50 mM Tris-HCl, 100 mM NaCl, 20 mM EDTA, 1% polyethylene glycol 6000, pH 7.9). The amount of thrombin formed was measured using a thrombin-specific chromogenic substrate BIOPHEN CS-01(38). The residual FVa activity was determined by comparison with the FVa activity observed prior to APC incubation. The plotted values represent the mean of at least three individual experiments ± S.E. Protein S-dependent FVa proteolysis was measured at protein S concentrations in the presence or absence of PF4. Human protein S (2.5–25 nM) was incubated with 0.8 nM APC, 8 nM FVa, and 75 μM phospholipid vesicles (PC/PS/PE, 60%/20%/20%) in 40 mM Tris-HCl, pH 7.4, 140 mM NaCl, 3 mM $CaCl_2$, 0.3% (w/v) bovine serum albumin (0.2 nM APC, 2 nM FVa, and 19 μM phospholipid vesicles, final concentrations) for 2 min at 37 °C. A 2-μl aliquot was added to 0.3 nM FXa, 1.5 μM prothrombin, and 75 μM phospholipid vesicles (0.1 nM FXa, 0.5 μM prothrombin, and 25 μM phospholipid vesicles, final concentrations) at 37 °C for 3 min. 5 μl of ice-cold 250 mM EDTA stopped the reaction. The rate of thrombin substrate cleavage was then measured as before.

Calculation of Kinetic Rate Constants for APC-mediated Cleavage at Arg^{506} and Arg^{306} of FVa—To determine the pseudo-first order rate constants for APC-mediated cleavage of FVa inactivation sites Arg^{506} and Arg^{306}, inactivation of FVa-R306Q/R679Q and FVa-R506Q/R679Q was assessed over time, and curves were fitted to the data according to a previously determined equation (27). As each variant only possesses one cleavage site, the equation was modified to reflect this, as previously described (24). FVa degradation curves for FVa-R306Q/R679Q were fitted to Equation 1,

$$Va_t = Va_0 \cdot e^{-(k_{506}) \cdot t} + B \cdot Va_0 \cdot (1 - e^{-(k_{506}) \cdot t}) \quad \text{(Eq. 1)}$$

where Va_t is the FVa cofactor activity determined at time point t, Va_0 is the FVa cofactor activity derived prior to incubation with APC, B is the remaining procoagulant activity of FVa

cleaved at amino acid position 506, and k_{506} is the rate constant for cleavage at position 506.

For determination of the rate constant for Arg^{306} cleavage, Equation 2 was used to fit the APC-mediated FVa degradation curve for FVa-R506Q/R679Q,

$$Va_t = Va_0 \cdot e^{-(k_{306}) \cdot t} + C \cdot Va_0 \cdot (1 - e^{-(k_{306}) \cdot t}) \quad \text{(Eq. 2)}$$

where C is the remaining procoagulant activity of FVa cleaved at position 306, and k_{306} is the rate constant for cleavage at position 306.

Measurement of Endothelial Cell Barrier Protection by APC—Endothelial cell barrier permeability was determined as described previously (28). Briefly, EAhy926 cells (kind gift of Dr. C. Edgell, University of North Carolina, Chapel Hill, NC) were grown to confluence on polycarbonate membrane Transwells (Costar, 3-μm pore size, 12-mm diameter) and incubated with 20 nM APC in the presence or absence of 1 μM PF4. After 3 h, the cells were treated with thrombin in serum-free media for 10 min. The cells were washed and incubated with 0.67 mg/ml Evans Blue with 4% bovine serum albumin (BSA). Changes in endothelial cell barrier permeability were determined by following the increase in absorbance at 650 nm in the outer chamber over time due to the transmigration of Evans Blue-BSA. Experiments were performed in triplicate and plotted as the mean ± S.E.

Determination of APC-mediated Protection of Apoptotic Endothelial Cells—Confluent EAhy926 cells in 6-well plates were pre-treated with APC ± PF4 for 17 h. EAhy926 cell apoptosis was induced by staurosporine (20 μM) treatment for 4 h. Cells were then trypsinized and RNA-extracted using an RNeasy Mini Kit (Qiagen). Reverse transcription was carried out (High Capacity cDNA Reverse Transcription Kit, Applied Biosystems) then Real Time PCR was performed using *Bax* (Hs00180269_m1), *Bcl-2* (Hs00153350_m1), and *β-actin* (Hs99999903_m1) TaqMan® Gene Expression Assays (Applied Biosystems) in a Applied Biosystems 7500 Real Time PCR system. Experiments were performed in triplicate and plotted as mean *Bax/Bcl-2* ratio ± S.E.

RESULTS

PF4 impairs APC Anticoagulant Function in Plasma—PF4 interacts with the protein C Gla domain, thereby significantly enhancing APC generation on endothelial cell surfaces (21, 22). However, the Gla domain also plays a critical role in regulating APC anticoagulant function. Preliminary experiments using an APC-specific chromogenic assay indicated that APC amidolytic activity was unaltered by the presence of PF4 concentrations up to 1 μM (data not shown). Consequently, calibrated automated thrombography was used to assess the impact of PF4 upon APC attenuation of tissue factor-initiated thrombin generation in protein C-deficient plasma (25). APC alone reduced thrombin generation (Fig. 1*A*). Calculation of the area under the thrombin generation curve (ETP) indicated that 10 nM APC reduced thrombin generation to 9 ± 4% of the original ETP prior to APC incubation (Fig. 1*A*). However, co-incubation of the same APC concentration with PF4 reduced the inhibition of thrombin generation conferred by APC in a dose-dependent

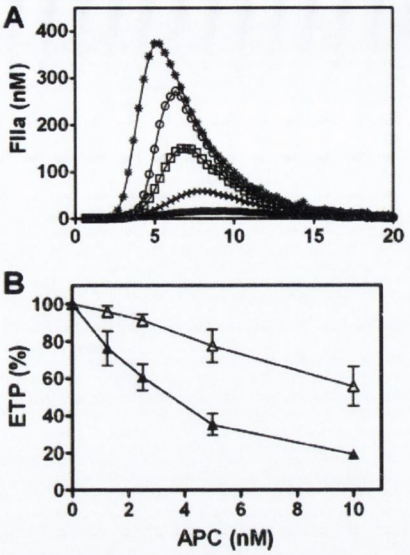


FIGURE 1. **PF4 inhibits APC anticoagulant function in platelet-poor plasma.** Coagulation was initiated in protein C-deficient plasma with 5 pM tissue factor, 4 μM phospholipid vesicles (PC/PS/PE, 60%/20%/20%), and 6.67 mM $CaCl_2$, and thrombin generation followed using a fluorogenic substrate, as described under "Experimental Procedures." *A*, thrombin generation in the absence of APC (★) was attenuated in the presence of 10 nM APC (■). Increasing PF4 concentration (0.5–2 μM) in the presence of 10 nM APC-impaired APC anticoagulant response: 0.5 μM PF4 (×), 1 μM PF4 (□), and 2 μM PF4 (○). *B*, inhibition of APC anticoagulant function in normal plasma was assessed both in the presence (△) and absence (▲) of 1 μM PF4 using respective mean ETPs ± S.E.

manner (Fig. 1*A*). In the presence of 1 μM PF4 (a concentration at which protein C activation on endothelial cells is significantly enhanced (21, 22)) the anticoagulant activity of 10 nM APC was significantly impaired, as thrombin generation was reduced to only 44 ± 4% of the original ETP, compared with 9 ± 4% in the absence of PF4 (Fig. 1*A*). To assess whether the presence of zymogen protein C altered the inhibitory activity of exogenous APC, the same experiment was performed in the presence of normal pooled plasma. Similar results were observed in APC-incubated normal pooled plasma in the presence of 1 μM PF4 (Fig. 1*B*). The same experiment was performed in the presence of a higher phospholipid concentration (25 μM), to exclude the possibility that the cationic PF4 inhibited APC anticoagulant activity by binding to and blocking access to crucial anionic phospholipid binding sites. However, PF4 was found to inhibit APC function in a similar manner (data not shown). The IC_{50} for PF4 inhibition of APC anticoagulant function was 12 μg/ml (0.4 μM), similar to PF4 serum concentration after platelet activation (22). Interestingly, PF4 in the absence of APC also mildly inhibited thrombin generation (<25% at 1 μM PF4) (data not shown). This impairment was not mediated by PF4 inhibition of contact activation, because corn trypsin inhibitor, which eliminates the contribution of contact pathway activation to thrombin generation in this system, had no effect on the observed mild reduction in thrombin generation.

Cationic Polypeptides Induce Diverse Functional Effects upon APC Anticoagulant Activity—To determine whether PF4 impairment of APC anticoagulant function represented a general functional consequence of cationic molecule association with APC, we assessed APC anticoagulant response in normal

Downloaded from www.jbc.org at IReL (Trinity College Dublin), on March 5, 2010

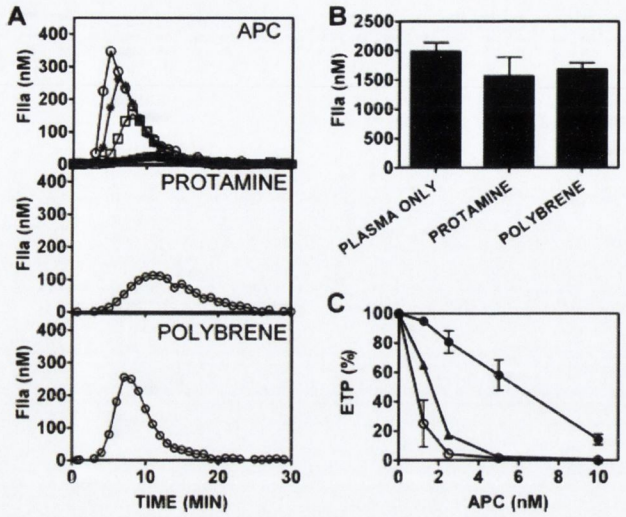


FIGURE 2. **Cationic polypeptides rapidly enhance APC anticoagulant function.** *A*, APC anticoagulant function was determined in plasma in the presence of APC (2.5–10 nM) (*top panel*: no APC (○), 2.5 nM APC (★), 5 nM APC (□), and 10 nM APC (■). 30 μg/ml protamine sulfate (*middle panel*) and Polybrene (*lower panel*), both (○) in the absence of APC was assessed. *B*, the ETP determined in normal plasma after thrombin generation in the presence of 30 μg/ml protamine sulfate and Polybrene was compared with that of normal pooled plasma alone. *C*, the susceptibility to APC anticoagulant activity with increasing APC concentration (1.5–10 nM APC) in the presence of protamine sulfate (▲) or Polybrene (○) was assessed and compared with thrombin generation in the presence of APC alone (●).

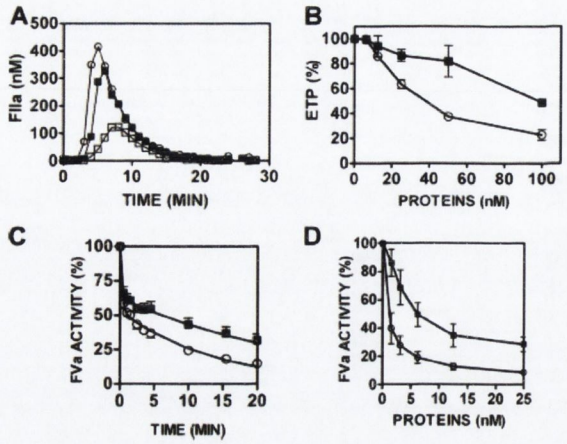


FIGURE 3. **PF4 inhibition of APC anticoagulant activity occurs via inhibition of APC-mediated FVa proteolysis.** *A*, protein S-dependent APC anticoagulant activity was measured in protein S-deficient plasma, as described under "Experimental Procedures." 5 nM APC alone (○) was compared with 5 nM APC plus 50 nM protein S in the presence (■) and absence (□) of PF4 (1 μM). *B*, protein S (6.25–100 nM)-dependent APC anticoagulant activity was assessed in the presence (■) and absence of PF4 (○) using protein S-deficient plasma. *C*, protein S-independent FVa proteolysis by APC was assessed in both the presence and absence of PF4 (1 μM). Recombinant FVa (0.8 nM final concentration) was incubated with phospholipid vesicles (PS/PE/PC, 10%/20%/70%, 25 μM final concentration) in the presence (■) or absence (○) of 1 μM PF4 in HNBSACa buffer (25 mM Hepes, 150 mM NaCl, pH 7.7, with 5 mg/ml BSA, and 5 mM $CaCl_2$. APC (1.65 nM final concentration) was added to initiate FVa inactivation, and aliquots were drawn at set time intervals over a 20-min time course. FVa inactivation was stopped by 1/25 dilution in ice-cold HNBSACa. The FVa activity was measured using a prothrombinase assay (5 nM FXa for 0.5 nM FXa, 0.5 μM prothrombin, and phospholipid vesicles (PC/PS, 10%/90%, 50 μM final concentration)). After 2 min the reaction was stopped with 40-fold dilution in ice-cold EDTA buffer (50 mM Tris-HCl, 100 mM NaCl, 20 mM EDTA, 1% polyethylene glycol 6000, pH 7.9). The thrombin formed was measured using a thrombin-specific chromogenic substrate BIOPHEN CS-01(38). The residual FVa activity was determined by comparison to the FVa activity observed prior to APC incubation. The plotted values represent the mean of at least three individual experiments ± S.E. *D*, protein S-dependent FVa proteolysis was measured in the presence (■) and absence (○) of PF4. Human protein S (1.25–25 nM) was incubated with 0.8 nM APC, 8 nM FVa, and 75 μM phospholipid vesicles (PC/PS/PE, 60%/20%/20%) in 40 mM Tris-HCl, pH 7.4, 140 mM NaCl, 3 mM $CaCl_2$, 0.3% (w/v) bovine serum albumin (0.2 nM APC, 2 nM FVa, and 19 μM phospholipid vesicles, final concentrations) for 2 min at 37 °C. A 2-μl aliquot was added to 0.3 nM FXa, 1.5 μM prothrombin, and 75 μM phospholipid vesicles (0.1 nM FXa, 0.5 μM prothrombin, and 25 μM phospholipid vesicles, final concentrations) at 37 °C for 3 min. 5 μl of ice-cold 250 mM EDTA stopped the reaction. The rate of thrombin chromogenic substrate cleavage was then measured as before.

platelet-poor plasma in the presence of two other well characterized cationic polypeptides, protamine sulfate and Polybrene. APC impaired thrombin generation in a dose-dependent fashion as previously described (25) (Fig. 2*A*, *top panel*). In the absence of APC, protamine sulfate and Polybrene both altered the dynamics of thrombin generation by reducing the peak thrombin generation and extending the time over which thrombin was generated (Fig. 2*A*, *middle* and *lower panels*). However, overall ETP was not significantly different to that determined in the absence of either cationic molecule (Fig. 2*B*).

Surprisingly, and in direct contrast to the inhibition of APC anticoagulant activity observed in the presence of PF4, both protamine sulfate and Polybrene rapidly enhanced APC anticoagulant activity. In the presence of either protamine sulfate or Polybrene (both 30 μg/ml), thrombin generation in normal plasma was entirely ablated in the presence of 5 nM APC, whereas APC alone under the same conditions only reduced thrombin generation by 41% (Fig. 2*C*). These findings demonstrate that the inhibitory effect of PF4 upon APC anticoagulant function is not solely mediated by its cationic nature.

PF4 Impairs Protein S-dependent APC Anticoagulant Activity—APC binds to anionic phospholipids, and in complex with its cofactor protein S, down-regulates thrombin generation by inactivation of procoagulant cofactors FVa and FVIIIa (6, 7). To investigate the one or more mechanisms by which PF4 inhibit APC anticoagulant activity, APC anticoagulant function was assessed in protein S-deficient plasma reconstituted with plasma-purified protein S. 10 nM APC in protein S-deficient plasma had no effect upon thrombin generation, as previously described (29) (Fig. 3*A*). However, co-incubation with protein S (6.25–100 nM) facilitated a protein S-dependent impairment of thrombin generation (IC_{50} = 36 nM, Fig. 3, *A* and *B*). Co-incubation of 1 μM PF4 with APC/protein S significantly impaired protein S-enhancement of APC anticoagulant activity in plasma ~3-fold (IC_{50} = 96 nM, Fig. 3, *A* and *B*). These data suggest that PF4 inhibition of APC anticoagulant activity in plasma is mediated in part by impairment of protein S cofactor enhancement of APC.

APC anticoagulant activity is principally determined by its ability to initiate FVa proteolysis. To gain further insight into PF4 inhibition of APC anticoagulant function, the rate of FVa proteolysis in the presence or absence of protein S and/or PF4 was determined using an APC-mediated FVa degradation reaction dependent upon the presence of anionic phospholipids for efficient APC degradation of FVa. In preliminary experiments, PF4 was shown not to influence thrombin generation by the prothrombinase reaction used in this assay (data not shown). PF4 was found to impair APC-mediated FVa proteolysis, in

particular the final stage of the characteristic biphasic FVa inactivation response (Fig. 3*C*).

A modified version of this assay was used to evaluate the ability of PF4 to inhibit FVa proteolysis by APC in the presence of protein S. PF4 inhibited APC protein S-dependent FVa proteolysis ~5-fold (Fig. 3*D*), based upon the protein S concentration required to enable half-maximal FVa inactivation in the presence and absence of PF4 (6.1 nM *versus* 1.2 nM protein S, respectively). Collectively, these results indicate that, in both plasma and purified factor assays, PF4 impairs protein S-cofactor-enhanced APC anticoagulant activity. These data are consistent with previous reports demonstrating interaction between PF4 and the Gla domain of protein C/APC and further suggest that this interaction may involve the C-terminal portion of the APC Gla domain.

PF4 Impairs Arg^{306} but Not Arg^{506} Cleavage on FVa in the Presence and Absence of Protein S—To assess the potential mechanisms by which PF4 might impair APC anticoagulant activity, the ability of APC to inactivate recombinant FVa variants in which specific APC cleavage sites (Arg^{506} and Arg^{306}) were substituted to prevent cleavage was assessed. Degradation of FVa variant FVa-R306Q/R679Q, in which only Arg^{506} cleavage by APC can occur, was unaffected by the presence of PF4, in either the presence or absence of protein S (data not shown). However, FVa degradation of FVa-R506Q/R679Q, in which only Arg^{306} cleavage takes place, was impaired by the presence of 1 μM PF4 in both the presence and absence of protein S (Fig. 4, *A* and *B*). Calculation of the rate constant for Arg^{306} cleavage by APC in FVa-R506Q/R679Q shows that the kinetic rate of Arg^{306} cleavage by APC in both the presence and absence of protein S was reduced by 3-fold (Fig. 4, *C* and *D*). PF4 therefore impairs APC anticoagulant activity in both plasma and purified protein assays via inhibition of the rate of Arg^{306} cleavage during FVa degradation by APC.

PF4 Does Not Directly Influence APC Cytoprotective Function—APC bound to EPCR via its Gla domain can activate PAR-1 on endothelial cells, triggering complex intracellular signaling that result in anti-inflammatory and anti-apoptotic cellular responses (28, 30). To ascertain whether PF4 interaction with the protein C/APC Gla domain might impair APC-EPCR-PAR-1 cytoprotective signaling, an *in vitro* assay of endothelial cell barrier permeability was used. As previously reported, thrombin markedly enhanced endothelial barrier permeability, compared with untreated cells (Fig. 5*A*). However, preincubation with APC significantly attenuated this thrombin-induced increase in permeability ($p < 0.05$, Fig. 5*A*). PF4 alone (up to 1 μM) had no independent effect upon endothelial barrier permeability, and did not protect against thrombin-mediated increased permeability. Finally, in contrast to its inhibition of APC anticoagulant activity, PF4 did not significantly inhibit the endothelial barrier protective properties of APC.

Previous studies have demonstrated that APC regulates expression of both pro- and anti-apoptotic genes to confer an anti-apoptotic phenotype in endothelial cells. Moreover, these effects are also mediated via APC-EPCR-PAR1 signaling. To determine whether PF4 might interfere with APC-mediated cytoprotection, apoptosis in EAhy926 cells was assessed by reverse transcription-PCR quantification of pro-apoptotic

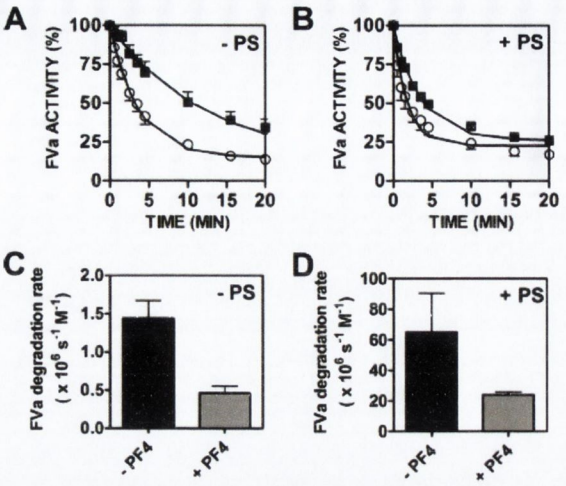


FIGURE 4. **PF4 impairs proteolysis of FVa via inhibition of APC cleavage at position Arg^{306}.** Recombinant FVa variant (506Q/679Q) (0.8 nM final concentration) was incubated with PS/PE/PC (10%/20%/70%) phospholipid vesicles (25 μM final concentration) without (*A*) or with (*B*) protein S (100 nM), in the absence (○) or presence (■) of 1 μM PF4. APC 3.3 nM (*A*) or 0.2 nM (*B*) was added to start FVa inactivation and at specified time intervals, samples were drawn, and the FVa inactivation was stopped by 1/25 dilution in ice-cold HNBSACa buffer. The FVa activity was measured with a prothrombinase assay including 5 nM FXa, 0.5 μM prothrombin, and 50 μM phospholipids (PC/PS, 90%/10%, all final concentrations) for 2 min, then stopped with EDTA buffer. The FVa activity was related to the FVa activity observed in the absence of APC. The plotted values represent the mean of at least three individual experiments ± S.E. The effect of PF4 upon rate constants for cleavage at Arg^{306} (k_{306}) using FVa degradation curves for FVa-R506Q/R679Q in the absence (*C*) or presence (*D*) of protein S was assessed. APC-mediated FVa degradation in the absence (*black bars*) or presence (*gray bars*) of PF4 (1 μM) was determined. Each *bar* represents the mean kinetic rate constant value of at least three independent experiments ± S.E.

(*Bax*) and anti-apoptotic (*Bcl-2*) gene expression following incubation with staurosporine, a well established inducer of apoptosis in endothelial cells (Fig. 5*B*). Staurosporine (20 μM) increased the *Bax/Bcl-2* ratio significantly compared with untreated cells ($p < 0.05$). Pre-treatment of EAhy926 cells with APC, however, decreased the *Bax/Bcl-2* ratio close to that determined for untreated EAhy926 cells. Furthermore, the EPCR dependence of APC-mediated cytoprotection was confirmed using an inhibitory anti-EPCR antibody (RCR-252), which entirely ablated the anti-apoptotic effect of APC. PF4 alone, or in combination with APC, had no effect upon apoptosis-related gene expression as determined by alteration of *Bax/Bcl-2* expression ratios in response to staurosporine (Fig. 5*B*). Therefore, despite PF4 enhancement of protein C activation, we demonstrate that PF4 impairs the anticoagulant response of APC by interfering with protein S cofactor enhancement. Furthermore, PF4 does not directly alter APC-mediated cytoprotection, despite its described association with the protein C/APC Gla domain.

DISCUSSION

Together with thrombospondin and β-thromboglobulin, PF4 comprises one of the major constituents of platelet α-granules (20). A number of procoagulant functions have been ascribed to PF4 that are associated with its acute release at sites of vascular injury and platelet activation. In particular, the cationic properties of PF4 facilitate high affinity heparin binding (K_D = 4 nM) and thereby attenuates the antithrombin-medi-

Downloaded from www.jbc.org at IReL (Trinity College Dublin), on March 5, 2010

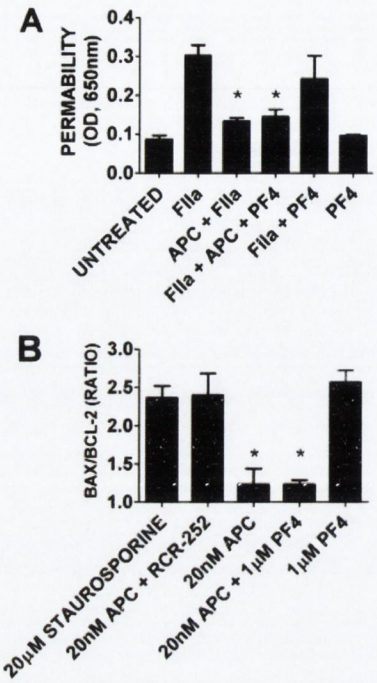


FIGURE 5. **PF4 does not alter APC-EPCR-PAR-1 cytoprotective signaling.** *A*, the effect of PF4 upon APC attenuation of thrombin-induced endothelial cell hyperpermeability was assessed as described under "Experimental Procedures." *B*, the anti-apoptotic activity of APC in the presence of PF4 was measured by determination of *Bax/Bcl-2* ratios in staurosporine-treated EAhy926 cells, as described previously (*, $p < 0.05$ when compared with staurosporine-treated EAhy926 cells).

ated anticoagulant properties of heparin and endothelial cell surface glycosaminoglycans (31, 32). Furthermore, PF4 inhibits factor XII activation by negatively charged surfaces and enhances platelet aggregation (20). In contrast, more recent studies have demonstrated that PF4 significantly enhances generation of anticoagulant APC on endothelial cell surfaces (21). Enhanced APC generation involves PF4 binding to thrombomodulin via *O*-linked chondroitin sulfate glycosaminoglycans and binding to the protein C Gla domain (23). This domain also mediates protein C binding to EPCR (33), negatively charged phospholipids, and protein S (25, 34), all of which are required for normal APC anticoagulant activity.

In vivo studies that investigated the role of PF4 upon APC generation found that low dose thrombin infusion with PF4 increased APC generation in primates 2- to 3-fold (21). However, a PF4 knockout mouse exhibited platelet aggregation defects and impaired thrombus formation, suggesting a primarily prothrombotic role for PF4 (35). Curiously, a transgenic mouse line that overexpressed PF4 exhibited similar thrombotic defects to those described for those mice lacking PF4 (35). Therefore, although PF4 appears to have a significant role in APC generation on the endothelial cell surface following platelet activation, its release from platelets is required to facilitate normal platelet aggregation and stable thrombus formation.

In this study, we demonstrate that PF4 inhibits APC anticoagulant function (Fig. 1) at PF4 concentrations described to mediate enhanced protein C activation on the surface of endothelial cells (21). Interestingly, this anticoagulant effect was specific for PF4, and was not apparent for other cationic polypeptides (*e.g.* protamine sulfate and Polybrene) (Fig. 2). Consequently, the mechanism through which PF4 impairs APC anticoagulant functions is not strictly attributable to nonspecific cationic interactions. Using purified protein assays to study APC anticoagulant activity, we observed that the inhibitory effects of PF4 were apparent when FVa inactivation by APC was assessed in the presence and absence of protein S (Fig. 3). Furthermore, despite PF4 interaction with the protein C/APC Gla domain, PF4 does not appear to interfere with the ability of the APC Gla domain to concurrently interact with negatively charged phospholipids. Instead, we demonstrate that the molecular mechanism through which PF4 inhibits APC anticoagulant function is via inhibition of the rate of Arg^{306} cleavage in FVa, which is specifically enhanced by the presence of protein S (Fig. 4).

Although protein S constitutes an essential cofactor for APC anticoagulant function in normal plasma, the protein S binding sites on APC are not well defined. However, the APC Gla domain has been shown to play a key role in mediating protein S cofactor enhancement. Recent studies have highlighted the potential importance of APC Gla residues 33–39. Although no specific PF4-Gla domain binding site has been identified, significant amino acid sequence conservation exists between the protein C/APC Gla domain and that of other vitamin K-dependent coagulation glycoproteins (36). Furthermore, previous studies demonstrated that PF4 also binds to the Gla domains of prothrombin, factor X, and protein S, although the comparative affinities of each interaction are unknown (23). It remains unclear whether the ability of PF4 to inhibit the normal protein S-APC cofactor enhancement is mediated primarily through PF4 binding to the APC Gla domain, or whether PF4 binding to the protein S Gla domain is also important.

In view of the potent anticoagulant properties of APC, the observation that PF4 increases APC generation is clearly at odds with its apparent procoagulant function. Moreover, the physiological benefit of PF4 promoting enhanced APC generation, while simultaneously inhibiting the anticoagulant function of APC, would appear somewhat counterintuitive. However, recent studies have clearly demonstrated that, in addition to its anticoagulant properties, APC bound to EPCR via its Gla domain can initiate PAR-1-mediated cytoprotective signaling on the surface of endothelial cells. *In vivo* beneficial effects of APC have been observed in a series of different animal disease models, including severe sepsis, ischemic stroke, and experimental autoimmune encephalomyelitis (13, 15, 37, 38). Also, intravenous infusion of recombinant APC significantly increased overall survival (risk reduction, 19.4%) in patients with severe sepsis in The Recombinant Human Activated Protein C Worldwide Evaluation in Severe Sepsis study (15). Accumulating evidence suggests that the efficacy of APC therapy in this setting primarily relates to its cytoprotective signaling activity, rather than its anticoagulant function (39). Nevertheless, the anticoagulant properties of APC are also of clinical importance, because APC therapy is associated with significant bleeding risk, restricting the dose and duration of recombinant APC administration (15). In an effort to reduce this risk of bleeding, recent studies have sought to develop APC variants that retain normal beneficial cytoprotective signaling but have reduced anticoagulant properties (40–42). In this study, we

demonstrate that, although PF4 specifically inhibits APC anticoagulant activity, APC generated in the presence of PF4 can still initiate PAR-1 cytoprotective signaling. Moreover, this observation is supported by recent elegant *in vivo* studies demonstrating that endogenously released PF4 from activated platelets stimulates APC generation, which reduces mortality following lipopolysaccharide challenge in mice (43).

Inherited or acquired resistance to APC anticoagulant activity in plasma constitutes the most common laboratory abnormality identified in patients with venous thromboembolism. In a majority of clinical cases, APC anticoagulant activity is caused by the FV Leiden polymorphism (R506Q). However, it is also well recognized that an acquired APC anticoagulant activity phenotype is observed in the presence of freeze-thawed platelets (44). Although a number of different potential mechanisms have been proposed (17, 19, 44, 45), the one or more molecular events underlying platelet-mediated APC resistance are not well defined. We demonstrate that PF4 inhibits APC anticoagulant function, and is therefore predicted to contribute to APC inhibition in the presence of activated platelets. Although normal plasma PF4 concentrations are low, significant amounts are secreted from activated platelets, so that concentrations in the vicinity of the platelet plug can reach ~10 μg/ml. Thus, our findings are in keeping with previous studies demonstrating that platelet activation is a requirement for the phenotype of platelet-mediated APC resistance (19, 44, 46).

In summary, we have shown that PF4 inhibits APC anticoagulant function, while retaining PAR-1-mediated cytoprotective signaling. This provides a rationale for how PF4 can exert prothrombotic effects, but also mediate enhanced APC generation on the surface of endothelial cells to induce both anti-inflammatory and anti-apoptotic events. Based on these observations, we propose that PF4 acts as a critical regulator of APC generation *in vivo* but also targets APC toward cytoprotective, rather than anticoagulant functions at sites of vascular injury.

Acknowledgments—We acknowledge Sarah Higgins and Dr. Virginie Terraube for experimental assistance.

REFERENCES

1. Dahlback, B., and Villoutreix, B. O. (2005) *FEBS Lett.* **579,** 3310–3316
2. Esmon, C. T., Gu, J. M., Xu, J., Qu, D., Stearns-Kurosawa, D. J., and Kurosawa, S. (1999) *Haematologica* **84,** 363–368
3. Griffin, J. H., Fernandez, J. A., Gale, A. J., and Mosnier, L. O. (2007) *J. Thromb. Haemost.* **5,** Suppl. 1, 73–80
4. Fukudome, K., Ye, X., Tsuneyoshi, N., Tokunaga, O., Sugawara, K., Mizokami, H., and Kimoto, M. (1998) *J. Exp. Med.* **187,** 1029–1035
5. Stearns-Kurosawa, D. J., Kurosawa, S., Mollica, J. S., Ferrell, G. L., and Esmon, C. T. (1996) *Proc. Natl. Acad. Sci. U. S. A.* **93,** 10212–10216
6. Fay, P. J., Smudzin, T. M., and Walker, F. J. (1991) *J. Biol. Chem.* **266,** 20139–20145
7. Walker, F. J., Sexton, P. W., and Esmon, C. T. (1979) *Biochim. Biophys. Acta* **571,** 333–342
8. Seligsohn, U., Berger, A., Abend, M., Rubin, L., Attias, D., Zivelin, A., and Rapaport, S. I. (1984) *N. Engl. J. Med.* **310,** 559–562
9. Reitsma, P. H., Poort, S. R., Bernardi, F., Gandrille, S., Long, G. L., Sala, N., and Cooper, D. N. (1993) *Thromb. Haemost.* **69,** 77–84
10. Walker, F. J. (1980) *J. Biol. Chem.* **255,** 5521–5524
11. Comp, P. C., Nixon, R. R., Cooper, M. R., and Esmon, C. T. (1984) *J. Clin. Invest.* **74,** 2082–2088
12. Schwarz, H. P., Fischer, M., Hopmeier, P., Batard, M. A., and Griffin, J. H. (1984) *Blood* **64,** 1297–1300
13. Cheng, T., Liu, D., Griffin, J. H., Fernandez, J. A., Castellino, F., Rosen, E. D., Fukudome, K., and Zlokovic, B. V. (2003) *Nat. Med.* **9,** 338–342
14. Riewald, M., Petrovan, R. J., Donner, A., Mueller, B. M., and Ruf, W. (2002) *Science* **296,** 1880–1882
15. Bernard, G. R., Vincent, J. L., Laterre, P. F., LaRosa, S. P., Dhainaut, J. F., Lopez-Rodriguez, A., Steingrub, J. S., Garber, G. E., Helterbrand, J. D., Ely, E. W., and Fisher, C. J., Jr. (2001) *N. Engl. J. Med.* **344,** 699–709
16. Kalafatis, M., and Mann, K. G. (1993) *J. Biol. Chem.* **268,** 27246–27257
17. Oliver, J. A., Monroe, D. M., Church, F. C., Roberts, H. R., and Hoffman, M. (2002) *Blood* **100,** 539–546
18. Stern, D. M., Nawroth, P. P., Harris, K., and Esmon, C. T. (1986) *J. Biol. Chem.* **261,** 713–718
19. Jane, S. M., Mitchell, C. A., Hau, L., and Salem, H. H. (1989) *J. Clin. Invest.* **83,** 222–226
20. Slungaard, A. (2005) *Int. J. Biochem. Cell Biol.* **37,** 1162–1167
21. Slungaard, A., Fernandez, J. A., Griffin, J. H., Key, N. S., Long, J. R., Piegors, D. J., and Lentz, S. R. (2003) *Blood* **102,** 146–151
22. Slungaard, A., and Key, N. S. (1994) *J. Biol. Chem.* **269,** 25549–25556
23. Dudek, A. Z., Pennell, C. A., Decker, T. D., Young, T. A., Key, N. S., and Slungaard, A. (1997) *J. Biol. Chem.* **272,** 31785–31792
24. Norstrom, E. A., Steen, M., Tran, S., and Dahlback, B. (2003) *J. Biol. Chem.* **278,** 24904–24911
25. Preston, R. J., Ajzner, E., Razzari, C., Karageorgi, S., Dua, S., Dahlback, B., and Lane, D. A. (2006) *J. Biol. Chem.* **281,** 28850–28857
26. Tran, S., Norstrom, E., and Dahlback, B. (2008) *J. Biol. Chem.* **283,** 6648–6655
27. Rosing, J., Hoekema, L., Nicolaes, G. A., Thomassen, M. C., Hemker, H. C., Varadi, K., Schwarz, H. P., and Tans, G. (1995) *J. Biol. Chem.* **270,** 27852–27858
28. Feistritzer, C., and Riewald, M. (2005) *Blood* **105,** 3178–3184
29. Sere, K. M., Rosing, J., and Hackeng, T. M. (2004) *Blood* **104,** 3624–3630
30. Mosnier, L. O., and Griffin, J. H. (2003) *Biochem. J.* **373,** 65–70
31. Handin, R. I., and Cohen, H. J. (1976) *J. Biol. Chem.* **251,** 4273–4282
32. Stringer, S. E., and Gallagher, J. T. (1997) *J. Biol. Chem.* **272,** 20508–20514
33. Regan, L. M., Mollica, J. S., Rezaie, A. R., and Esmon, C. T. (1997) *J. Biol. Chem.* **272,** 26279–26284
34. Smirnov, M. D., Safa, O., Regan, L., Mather, T., Stearns-Kurosawa, D. J., Kurosawa, S., Rezaie, A. R., Esmon, N. L., and Esmon, C. T. (1998) *J. Biol. Chem.* **273,** 9031–9040
35. Eslin, D. E., Zhang, C., Samuels, K. J., Rauova, L., Zhai, L., Niewiarowski, S., Cines, D. B., Poncz, M., and Kowalska, M. A. (2004) *Blood* **104,** 3173–3180
36. McDonald, J. F., Shah, A. M., Schwalbe, R. A., Kisiel, W., Dahlback, B., and Nelsestuen, G. L. (1997) *Biochemistry* **36,** 5120–5127
37. Domotor, E., Benzakour, O., Griffin, J. H., Yule, D., Fukudome, K., and Zlokovic, B. V. (2003) *Blood* **101,** 4797–4801
38. Han, M. H., Hwang, S. I., Roy, D. B., Lundgren, D. H., Price, J. V., Ousman, S. S., Fernald, G. H., Gerlitz, B., Robinson, W. H., Baranzini, S. E., Grinnell, B. W., Raine, C. S., Sobel, R. A., Han, D. K., and Steinman, L. (2008) *Nature* **451,** 1076–1081
39. Kerschen, E. J., Fernandez, J. A., Cooley, B. C., Yang, X. V., Sood, R., Mosnier, L. O., Castellino, F. J., Mackman, N., Griffin, J. H., and Weiler, H. (2007) *J. Exp. Med.* **204,** 2439–2448
40. Bae, J. S., Yang, L., Manithody, C., and Rezaie, A. R. (2007) *J. Biol. Chem.* **282,** 9251–9259
41. Mosnier, L. O., Gale, A. J., Yegneswaran, S., and Griffin, J. H. (2004) *Blood* **104,** 1740–1744
42. Mosnier, L. O., Yang, X. V., and Griffin, J. H. (2007) *J. Biol. Chem.* **282,** 33022–33033
43. Kowalska, M. A., Mahmud, S. A., Lambert, M. P., Poncz, M., and Slungaard, A. (2007) *Blood* **110,** 1903–1905
44. Taube, J., McWilliam, N., Luddington, R., Byrne, C. D., and Baglin, T. (1999) *Blood* **93,** 3792–3797
45. Camire, R. M., Kalafatis, M., Cushman, M., Tracy, R. P., Mann, K. G., and Tracy, P. B. (1995) *J. Biol. Chem.* **270,** 20794–20800
46. Camire, R. M., Kalafatis, M., Simioni, P., Girolami, A., and Tracy, P. B. (1998) *Blood* **91,** 2818–2829

Downloaded from www.jbc.org at IReL (Trinity College Dublin), on March 5, 2010

THE JOURNAL OF BIOLOGICAL CHEMISTRY VOL. 283, NO. 45, pp. 30531–30539, November 7, 2008
© 2008 by The American Society for Biochemistry and Molecular Biology, Inc. Printed in the U.S.A.

Dissociation of Activated Protein C Functions by Elimination of Protein S Cofactor Enhancement*

Received for publication, March 25, 2008, and in revised form, August 27, 2008 Published, JBC Papers in Press, September 8, 2008, DOI 10.1074/jbc.M802338200

Shona Harmon[‡1], Roger J. S. Preston[‡1,2], Fionnuala Ni Ainle[‡], Jennifer A. Johnson[‡], Moya S. Cunningham[‡], Owen P. Smith[§], Barry White[¶], and James S. O'Donnell[‡¶]

From the [‡]Haemostasis Research Group, Institute of Molecular Medicine, St James's Hospital, Trinity College Dublin, Dublin 8, the [§]Department of Haematology, Our Lady's Children's Hospital Crumlin, Dublin 12, and the [¶]National Centre for Hereditary Coagulation Disorders, St James's Hospital, James St., Dublin 8, Ireland

Activated protein C (APC) plays a critical anticoagulant role *in vivo* by inactivating procoagulant factor Va and factor VIIIa and thus down-regulating thrombin generation. In addition, APC bound to the endothelial cell protein C receptor can initiate protease-activated receptor-1 (PAR-1)-mediated cytoprotective signaling. Protein S constitutes a critical cofactor for the anticoagulant function of APC but is not known to be involved in regulating APC-mediated protective PAR-1 signaling. In this study we utilized a site-directed mutagenesis strategy to characterize a putative protein S binding region within the APC Gla domain. Three single amino acid substitutions within the APC Gla domain (D35T, D36A, and A39V) were found to mildly impair protein S-dependent anticoagulant activity (<2-fold) but retained entirely normal cytoprotective activity. However, a single amino acid substitution (L38D) ablated the ability of protein S to function as a cofactor for this APC variant. Consequently, in assays of protein S-dependent factor Va proteolysis using purified proteins or in the plasma milieu, *APC-L38D* variant exhibited minimal residual anticoagulant activity compared with wild type APC. Despite the location of Leu-38 in the Gla domain, *APC-L38D* interacted normally with endothelial cell protein C receptor and retained its ability to trigger PAR-1 mediated cytoprotective signaling in a manner indistinguishable from that of wild type APC. Consequently, elimination of protein S cofactor enhancement of APC anticoagulant function represents a novel and effective strategy by which to separate the anticoagulant and cytoprotective functions of APC for potential therapeutic gain.

Protein C is a vitamin K-dependent serine protease zymogen that circulates at a plasma concentration of ~70 nM. It has a multidomain structure comprising an N-terminal γ-carboxyglutamic acid (Gla)[3] domain (residues 1–45), two epidermal growth factor-like domains (EGF-1, residues 46–92, and EGF-2, residues 93–136) and a C-terminal serine protease domain (170–419). Protein C zymogen is activated by thrombin in complex with thrombomodulin on the surface of endothelial cells (1). Activated protein C (APC) generation is significantly enhanced by protein C binding to the endothelial cell protein C receptor (EPCR) (2). APC binds to anionic phospholipids on the endothelial cell surface and, in complex with its cofactor protein S inactivates procoagulant cofactors factor Va (FVa) (3) and factor VIIIa (4), thereby attenuating further thrombin generation and down-regulating coagulation. The physiological importance of the protein C anticoagulant pathway is well established. Individuals with homozygous protein C deficiency typically present shortly after birth with fulminant life-threatening thrombotic complications (5). Moreover, individuals heterozygous for protein C deficiency demonstrate significant lifelong increased risk of venous thromboembolism (6).

Recent studies have shown that APC bound to EPCR via its Gla domain can activate protease-activated receptor-1 (PAR-1) on endothelial cells, triggering complex intracellular signaling (7). The molecular mechanisms underlying the cytoprotective effects of APC have not been fully characterized but appear mediated independently of its anticoagulant function (8). Through mechanisms downstream of PAR-1 activation, APC has been shown to exhibit anti-inflammatory and anti-apoptotic properties via up-regulated gene expression of anti-apoptotic and anti-inflammatory mediators (9, 10), down-regulation of pro-inflammatory cytokines (10, 11), and stabilization of endothelial barrier function (12, 13).

In vivo beneficial effects of APC have been reported in a number of different animal injury models. For example, APC demonstrated significant neuroprotective effects in rat and murine stroke models (14–16) and was also recently shown to ameliorate experimental autoimmune encephalomyelitis in mice (17). Furthermore, APC was protective in a murine model of diabetic nephropathy by inhibition of endothelial and podocyte apoptosis, whereas anticoagulation with low molecular weight heparin had no such beneficial effect (18). Each of these animal studies demonstrated a consistent and critical role for the APC-EPCR-PAR-1 signaling axis.

The therapeutic potential of APC was highlighted in the activated Protein C Worldwide Evaluation in Severe Sepsis

* This work was supported by a Health Research Board Fellowship PD/2006/24 (to R. J. S. P.), an Irish Heart Foundation grant (to J. S. O. D.), a Children's Medical Research Foundation Award (to F. N. A. and O. P. S.), and Science Foundation Ireland President of Ireland Young Researcher Award 06/Y12/0925 (to J. S. O. D.). The costs of publication of this article were defrayed in part by the payment of page charges. This article must therefore be hereby marked "*advertisement*" in accordance with 18 U.S.C. Section 1734 solely to indicate this fact.

[1] These authors contributed equally to this study.

[2] To whom correspondence should be addressed. Tel.: 353-1-896-3274; Fax: 353-1-410-3570; E-mail address: prestonr@tcd.ie.

[3] The abbreviations used are: Gla, γ-carboxyglutamic acid; APC, activated protein C; EPCR, endothelial cell protein C receptor; sEPCR, soluble EPCR; Fva, factor Va; PC, phosphatidylcholine; PE, phosphatidylethanolamine; PS, phosphatidylserine; ETP, endogenous thrombin potential; PAR-1, protease-activated receptor-1; PROWESS, activated Protein C Worldwide Evaluation in Severe Sepsis.

Downloaded from www.jbc.org at IReL (Trinity College Dublin), on March 5, 2010

(PROWESS) study (19). Intravenous infusion of recombinant APC (24 μg/kg per h for 96 h) significantly reduced overall mortality (relative risk reduction, 19.4%) in adult patients with severe sepsis. In contrast, treatment with other anticoagulants (notably antithrombin (20) and tissue factor pathway inhibitor (21)) have no such effect on survival. The anticoagulant properties of APC are, however, associated with increased risk of bleeding complications and have thereby restricted its use in clinical practice. In the PROWESS study, serious bleeding complications were observed in 3.5% of the patients treated with APC compared with only 2% of the placebo group (19). Furthermore, recent post-marketing studies have reported even higher incidences of serious bleeding complications (6.5 and 6.7%, respectively) in patients treated with APC (22, 23). In this context, recent studies have sought to define the relative contributions of the cytoprotective and/or anticoagulant properties of APC toward mediating its therapeutic efficacy in different pathological settings. These studies have sought to design APC variants which retain beneficial cytoprotective actions but exhibit relative reduction in its anticoagulant properties and, thus, bleeding risk (24–26).

The anticoagulant function of APC requires the presence of its principal cofactor, protein S (27). Protein S may enhance APC anticoagulant activity by increasing its affinity for negatively charged phospholipid surfaces (27), re-positioning the APC active site for optimal substrate cleavage (28), or removing the protection of FVa in the prothrombinase complex conferred by FXa binding (29). Thus, protein S plays a critical role in mediating the anticoagulant properties of APC, but there is no evidence to date that it is important for the anti-inflammatory or anti-apoptotic effects of APC. The molecular basis through which protein S interacts with APC is not fully understood; however, a possible role for the APC Gla domain has recently been described (30). In this study, we have used a site-directed mutagenesis strategy to characterize the impact of individual amino acid residue substitutions in this putative protein S binding region upon APC anticoagulant function. We demonstrate that, surprisingly, a single amino acid substitution (L38D) is sufficient to entirely ablate the ability of protein S to function as a cofactor for this APC variant yet does not alter APC-mediated proteolysis of FVa in the absence of protein S. Consequently, in both protein S-dependent FVa proteolysis assays using purified coagulation proteins and in the plasma milieu, this APC Gla domain variant exhibited minimal residual anticoagulant activity compared with wild type APC. In addition, despite the fact that this key amino acid is located in the APC Gla domain, we also show that this APC variant interacts normally with EPCR and that it retains its ability to initiate PAR-1 protective signaling in an identical fashion to that of wild type APC.

EXPERIMENTAL PROCEDURES

Generation and Characterization of Recombinant Protein C Variants—Recombinant protein C Gla domain variants were generated by site-directed mutagenesis, expressed, and isolated from serum-free medium as previously described (30, 31). Recombinant protein C was characterized by Coomassie staining and immunodetection using a horseradish peroxidase-conjugated anti-protein C polyclonal antibody (Dako, Ely) and a mouse anti-Gla monoclonal antibody (American Diagnostica) according to standard procedures. To generate recombinant APC, wild type protein C and protein C variants were activated with Protac (Hyphen-BioMed). APC chromogenic substrate (BIOPHEN CS-21(66), Hyphen-Biomed) cleavage by each recombinant APC preparation was determined as previously described (30, 31).

Inhibition of APC in Plasma—Inhibition of APC variants in plasma was determined as previously described (32). Wild type and variant APC (20 nM) was incubated in pooled human citrated plasma at 37 °C. At designated time points, aliquots were removed, and the residual amidolytic activity was determined using a chromogenic substrate for APC (BIOPHEN CS2166). To examine the role of protein C inhibitor, the same experiments were performed in the presence of heparin (10 units/ml).

Determination of APC Anticoagulant Activity in Protein C-deficient Plasma—The anticoagulant function of wild type and variant APC upon protein C-deficient plasma was assessed using a Fluoroskan Ascent Plate Reader (Thermo Lab System, Helsinki, Finland) in combination with Thrombinoscope software (SYNAPSE BV) as previously described (30). 80 μl of protein C-deficient plasma (Hyphen-Biomed) was incubated with 20 μl of PPP reagent (Synapse) containing 5 pM tissue factor and 4 μM phospholipids (PC/PS/PE, 40%:20%:20%) in the presence or absence of wild type or variant APC (1.25–20 nM). Thrombin generation was initiated by automatic dispensation of fluorogenic thrombin substrate (Z-Gly-Gly-Arg-amidomethylcoumarin-HCl) and 100 mM $CaCl_2$ into each well. Thrombin generation was determined using thrombin calibration standard (Synapse). Measurements were taken at 20-s intervals for 60 min or until thrombin generation was complete. The endogenous thrombin potential (ETP) of each reaction were then calculated. Experiments were performed in triplicate, and data are reported as the mean ETP ± S.E.

Protein S Enhancement of APC Anticoagulant Activity in Protein S-deficient Plasma—The enhancement of APC anticoagulant activity in protein S-deficient plasma was determined using a similar assay to that described above. Briefly, protein S-deficient plasma (Hyphen-Biomed) was incubated with wild type or variant recombinant APC (10 nM) in the presence or absence of plasma-purified protein S (0.125–1.5 μM, Hematologic Technologies Inc.). Thrombin generation was initiated and assessed using Thrombinoscope software as described previously. All experiments were performed in triplicate and data plotted as mean ETP ± S.E.

Determination of Protein S-independent APC-mediated Factor Va Proteolysis—FVa degradation by APC was assessed as previously described (30, 31). 0.32 nM APC was incubated at 37 °C with phospholipids vesicles (PC/PS/PE, 60%:20%:20%; Avanti Lipids) and 4 nM FVa (Hematologic Technologies, Inc.) in 40 mM Tris-HCl, 140 mM NaCl, 3 mM $CaCl_2$, and 0.3% w/v bovine serum albumin (0.08 nM APC, 19 μM phospholipids, and 1 nM FVa, final concentration). Phospholipid vesicles were prepared as described previously (31). At the specified time points, 2-μl aliquots were removed and added to a prothrombinase mixture (25 μM phospholipids, 1 nM factor Xa, and 0.5 μM prothrombin (Hematologic Technologies Inc.) final concentra-

tions) for 3 min. Each reaction was then stopped using 5 μl of ice-cold 0.5 M EDTA. 100 μl of the reaction mixture was removed and incubated with 100 μl of 2 mM thrombin chromogenic substrate Biophen CS-01(38) (Hyphen-Biomed) to assess thrombin generation. The rate of chromogenic substrate cleavage was measured at 405 nm using a plate reader. All experiments were performed in triplicate.

Determination of Protein S-enhanced Proteolysis of FVa by APC—Protein S-enhanced proteolysis of FVa by APC was determined as previously described (30). Human protein S (2.5–25 nM) was incubated with 0.8 nM wild type or variant APC, 8 nM FVa, and 75 μM phospholipids vesicles in 40 mM Tris HCl, pH7.4, 140 mM NaCl, 3 mM $CaCl_2$, 0.3% (w/v) bovine serum albumin (0.2 nM APC, 2 nM FVa, and 19 μM phospholipids vesicles, final concentrations) for 2 min at 37 °C. After this incubation, a 2-μl aliquot was added to 0.3 nM FXa, 1.5 μM prothrombin, and 75 μM phospholipids vesicles (0.1 nM FXa, 0.5 μM prothrombin, and 25 μM phospholipids vesicles, final concentrations) at 37 °C for 3 min, then stopped with 5 μl of ice-cold 0.5 M EDTA. The rate of thrombin substrate cleavage by the consequent reaction mixture was then measured as before. Experiments were performed in triplicate, and data were plotted as the mean residual FVa cofactor activity ± S.E.

Assessment of APC Variant Binding to Soluble EPCR—APC binding to sEPCR was determined using a BIAcore X100 (GE Healthcare) as previously described (30, 31). Briefly, 10 μg/ml monoclonal anti-EPCR antibody, RCR-2 (kind gift of Dr. K. Fukudome, Saga Medical School), was immobilized on to both flow cells of a CM5 sensor chip. sEPCR (31) in HBS-P buffer (100 mM HEPES, pH7.4, 150 mM NaCl, 0.005% v/v surfactant P20) was bound to the surface of the test flow cell (400–800 response units). A reference flow cell with only RCR-2 bound was used to detect nonspecific binding. Wild type or variant APC (25–100 nM) was sequentially injected over both flow cells at a flow rate of 5 μl/min for 60 s. APC-EPCR binding was dissociated using HBS-EP buffer (HBS-P, but containing 3 mM EDTA; BIAcore) The RCR-2 surface was regenerated with 10 μl of 10 mM glycine-HCl (pH 2.5) after each experiment.

Measurement of Endothelial Cell Barrier Protection by APC—Endothelial cell barrier permeability was determined as described previously with minor modifications (13). Briefly, EAhy926 cells (kind gift of Dr. C. Edgell, University of North Carolina, Chapel Hill, NC) were grown to confluence on polycarbonate membrane transwells (Costar, 3 μM pore size, 12-mm diameter) and incubated with 20 nM wild type or variant APC. After 3 h the cells were treated with thrombin (Hematologic Technologies) in serum-free media for 10 min. The cells were washed and incubated with 0.67 mg/ml Evans Blue with 4% bovine serum albumin (Sigma). Changes in endothelial cell barrier permeability were determined by following the increase in absorbance at 650 nm in the outer chamber over time due to the transmigration of Evans Blue-bovine serum albumin. Experiments were performed in triplicate and plotted as the mean ± S.E.

Determination of APC-mediated Protection of Apoptotic Endothelial Cells—Confluent EAhy926 cells in 6-well plates were pretreated with either wild type or variant APC for 17 h. EAhy926 cell apoptosis was induced by staurosporine (20 μM, Sigma) treatment for 4 h. Cells were then trypsinized, and RNA was extracted using the RNeasy Mini kit (Qiagen). Reverse transcription was carried out (High Capacity cDNA reverse transcription kit, Applied Biosystems), then real time PCR was performed using *bax* (Hs00180269_m1), *bcl-2* (Hs00153350_m1) and β-actin (Hs99999903_m1) Taqman® gene expression assays (Applied Biosystems) in a Applied Biosystems 7500 real time PCR system. Experiments were performed in triplicate and plotted as the mean *bax/bcl-2* ratio ±S.E.

RESULTS

Characterization of Recombinant Protein C/APC Gla Domain Variants—To identify the critical amino acid residues in the APC Gla domain that mediate protein S cofactor enhancement of APC anticoagulant activity, recombinant protein C Gla domain variants were generated by site-directed mutagenesis spanning a region of the Gla domain proposed to mediate protein S cofactor function (Fig. 1*A*). Each of these variants (*APC-D35T*, *APC-D36A*, *APC-L38D*, and *APC-A39V*) contains single amino acid substitutions with the corresponding residue of the human prothrombin Gla domain. This approach enables analysis of APC-specific functions while maintaining Gla domain structural integrity (30). Each expressed recombinant protein C variant was characterized by Western blotting with an anti-protein C polyclonal antibody and an anti-Gla monoclonal antibody. Recombinant wild type and variant protein C migrated in a similar fashion to plasma-purified protein C under non-reducing conditions at the expected molecular mass of ~65 kDa. Wild type and variant recombinant protein C exhibited similar band intensity when detected with both anti-protein C and anti-Gla antibodies to that observed with plasma-purified protein C, indicative of normal expression and post-translational modification of the recombinant proteins (Fig. 1*B*). For functional studies wild type and variant recombinant protein C were activated using Protac. The amidolytic activity of each recombinant APC variant was assessed and found to be identical to that of wild type APC (Fig. 1*C*).

The rate of inhibition of each APC variant by serpins was determined in normal plasma. Inhibition of both wild type and variant APC was closely comparable (Fig. 1*D*). To examine the role of protein C inhibitor (PCI), the same experiment was performed in the presence of heparin, which accelerates PCI inhibition of APC. Accordingly, inhibition of wild type APC was enhanced 3-fold, as previously described (32). Each APC variant was inhibited in a similar manner to that of wild type APC in this system (Fig. 1*E*). Furthermore, subsequent assays indicated that APC inhibition kinetics in the presence of purified α_1-antitrypsin and protein C inhibitor were not affected by the presence of any of the APC variants tested (data not shown). Therefore, the residue substitutions present in each APC variant do not alter APC inhibition by its known plasma inhibitors.

Determination of Recombinant APC Gla Domain Variant Anticoagulant Activity—To identify the specific APC Gla domain residue(s) responsible for mediating APC anticoagulant activity in plasma, the ability of wild type and variant APC to inhibit tissue factor-induced thrombin generation was

Downloaded from www.jbc.org at IReL (Trinity College Dublin), on March 5, 2010

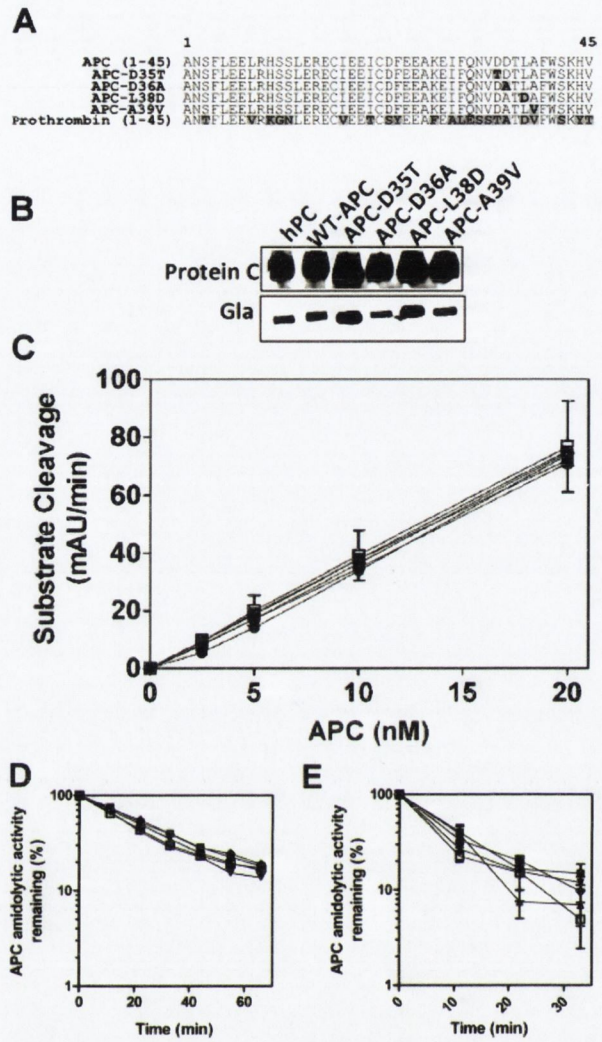


FIGURE 1. **Characterization of recombinant APC Gla domain variants.** *A*, recombinant protein C Gla domain variants were generated in which protein C residues at positions 35, 36, 38, and 39 were replaced with the corresponding residues in human prothrombin. Protein C variants were expressed in HEK 293 cells and then isolated from conditioned serum-free medium. *B*, plasma-purified, recombinant wild type (*WT*) and variant protein C preparations were assessed by Western blotting with sheep anti-protein C polyclonal and mouse anti-Gla monoclonal antibodies. *hPC*, human PC. *C*, each protein C preparation was activated using Protac, and amidolytic activity of each recombinant APC was assessed using a short APC chromogenic substrate. *mAU*, milliabsorbance units. Inhibition of wild type and variant APC in normal pooled plasma was assessed in the absence (*D*) and presence (*E*) of 10 units/ml heparin (wild type, □; *APC-D35T*, ■; *APC-D36A*, ▲; *APC-L38D*, ▼; *APC-A39V*, ◆; all 20 nM). Samples were removed at specified time points, and APC amidolytic activity was tested using a chromogenic substrate. The data shown represents the mean of three independent determinations ± S.D.

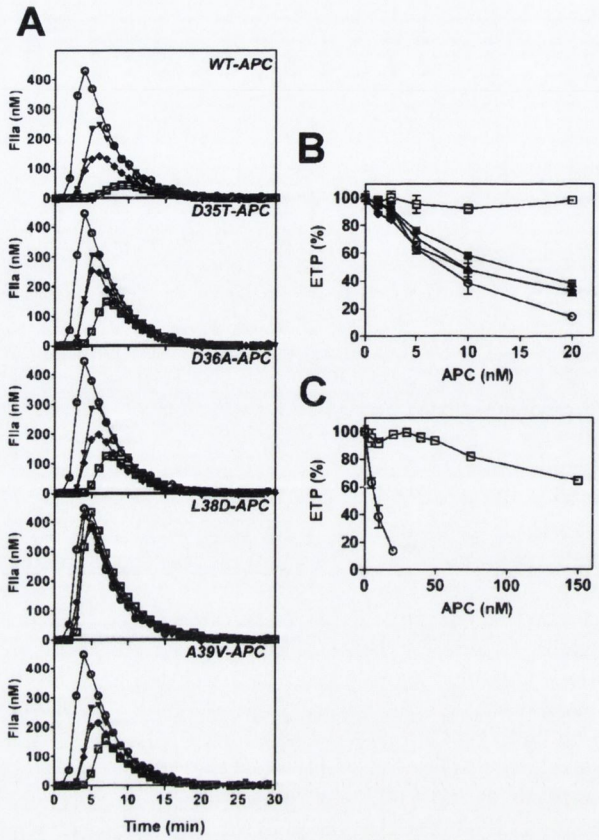


FIGURE 2. **Variant *APC-L38D* has negligible anticoagulant activity in protein C-deficient plasma.** The ability of recombinant APC variants to inhibit tissue factor-induced thrombin generation was assessed. *A*, APC (1.25–20 nM) was incubated with protein C-deficient plasma, and thrombin generation initiated with tissue factor, phospholipid vesicles, and $CaCl_2$ (see "Experimental Procedures"). Thrombin generation in protein C-deficient plasma in the absence of APC (○) was compared with 5 nM (▼), 10 nM (◆), and 20 nM (□) of each recombinant APC. *B*, the ETP for each experiment was determined and expressed as % of thrombin generated in the absence of APC (wild type APC, (○); *APC-D35T*, (■); *APC-D36A*, △; *APC-L38D*, □; *APC-A39V*, ◆. *C*, high concentrations (up to 150 nM) of *APC-L38D* (□) was compared with wild type APC (○) in the same assay.

assessed. Wild type APC diminished thrombin generation in a concentration-dependent manner, as previously described (30) (Fig. 2*A*). Variants *APC-D35T*, *APC-D36A*, and *APC-A39V* exhibited mildly impaired anticoagulant activity, with <2-fold reduced ETP compared with wild type APC (Fig. 2, *A* and *B*). Variant *APC-L38D*, however, exhibited severely impaired anticoagulant activity (Fig. 2, *A* and *B*). *APC-L38D* was unable to achieve half-maximal inhibition of thrombin generation (ETP) at concentrations as high as 150 nM APC (Fig. 2*C*), compared with half-maximal inhibition observed with wild type APC (7.2 nM; Fig. 2*B*). These data indicate that *APC-L38D* is at least 20-fold less active than wild type APC in plasma.

Leu-38 Is Required for Protein S-dependent APC Anticoagulant Function in Protein S-deficient Plasma—To clarify the role of Leu-38 in facilitating APC anticoagulant function, the ability of *APC-L38D* to be stimulated in protein S-deficient plasma reconstituted with plasma purified protein S was determined. Wild type APC had no anticoagulant function in protein S-deficient plasma, as previously observed (33). However, co-incubation of wild type APC with increasing protein S concentrations (12.5–200 nM) caused a corresponding reduction in thrombin generation (ETP) (IC_{50} = 24 nM protein S) (Fig. 3, *A* and *B*). Variant *APC-L38D*, however, was almost entirely unresponsive to protein S (Fig. 3, *A* and *B*). At the highest protein S concentration tested (1.5 μM), corresponding to 10-fold plasma free protein S concentration, thrombin generation was reduced only 22 ± 2% compared with thrombin generated in the absence of protein S. Therefore, residue Leu-38 mediates APC anticoagulant function in plasma by facilitating critical protein S cofactor function.

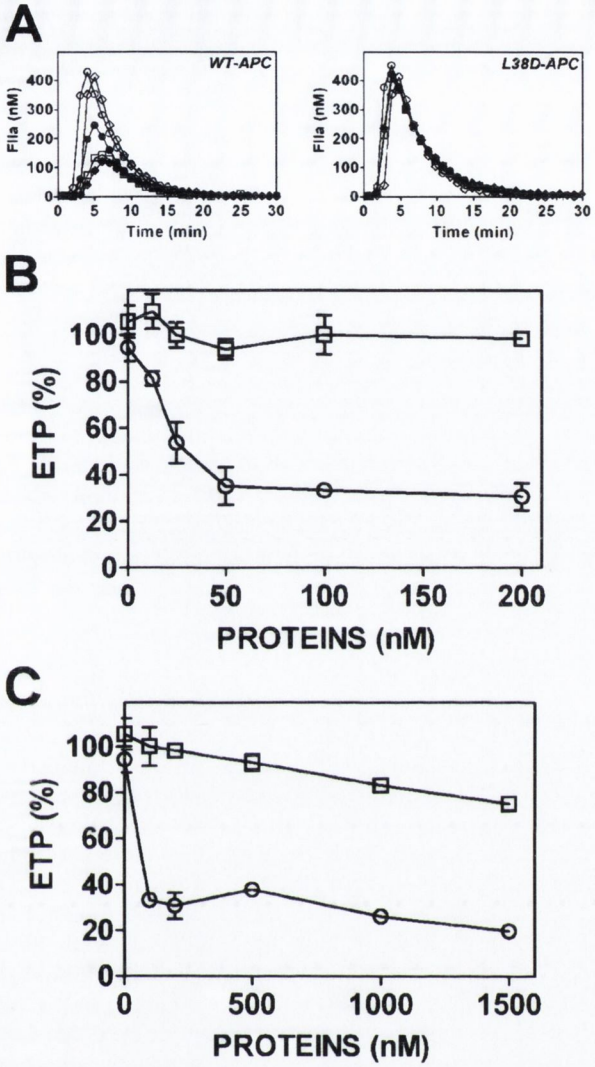


FIGURE 3. **Variant *APC-L38D* is not stimulated by protein S in protein S-deficient plasma.** *A*, the ability of recombinant wild type APC (○) and variant *APC-L38D* (□) (both 10 nM) to inhibit tissue-factor induced thrombin generation in protein S deficient plasma was assessed in the presence of increasing plasma purified protein S concentrations; no APC/protein S (◇), 10 nM APC only (○), APC + 25 nM protein S (●), APC + 50 nM protein S (□), and APC + 100 nM protein S (◆). *B*, the thrombin generation (ETP, %) in the protein S enhancement of variant *APC-L38D* (□) was compared with wild type APC (○) in the presence of protein S concentrations (*B*) (6–200 nM) and (*C*) (0.125–1.5 μM) in the same assay.

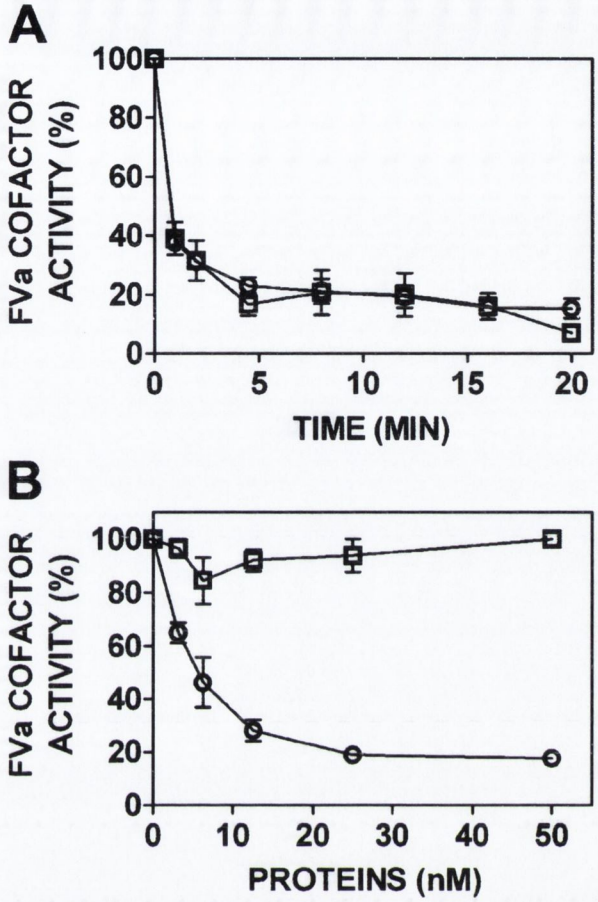


FIGURE 4. **Protein S-dependent FVa proteolysis by APC requires residue Leu-38 in the APC Gla domain.** *Upper panel*, FVa (1 nM) was incubated with wild type APC (○) or variant *APC-L38D* (□) (0.2 nM) in the presence of 25 μM phospholipid vesicles (40% PC, 20% PS, 20% PE). The FVa cofactor activity at specified time points was determined by prothrombinase assay (see "Experimental Procedures"). *B*, human plasma purified protein S (3–50 nM) was incubated with wild type APC (○) or variant *APC-L38D* (□) (0.4 nM), FVa (8 nM), and 25 μM phospholipid vesicles (40% PC, 20% PS, 20% PE). After 2 min of incubation, an aliquot was removed and added to a prothrombinase assay to assess FVa cofactor activity.

APC-L38D Exhibits Normal Protein S-Independent but Severely Impaired Protein S-dependent FVa Proteolysis—To assess the mechanism by which the impaired response to protein S by *APC-L38D* in plasma occurs, the rate of FVa proteolysis by APC in the presence and absence of protein S was determined. Using a phospholipid-dependent FVa proteolysis time course assay, the ability of *APC-L38D* to inactivate FVa in the absence of protein S was determined. Both wild type APC and *APC-L38D* rapidly reduced FVa cofactor activity (Fig. 4, *upper panel*), indicating that the observed impaired anticoagulant activity in plasma observed for *APC-L38D* is not mediated by impaired interaction with anionic phospholipids or FVa. A modified version of this assay was used to evaluate FVa proteolysis of wild type and variant APC in response to protein S. Wild type APC-mediated FVa proteolysis was rapidly enhanced by protein S (Fig. 4, *lower panel*). Half-maximal inhibition of FVa cofactor activity was observed at 5 nM protein S (Fig. 4, *lower panel*). In contrast, *APC-L38D* exhibited no protein S-enhanced FVa proteolysis at each protein S concentration tested. Therefore, *APC-L38D* loss of protein S-dependent APC anticoagulant activity observed in plasma occurs via impaired protein S-mediated FVa proteolysis.

APC-L38D Binds sEPCR with Equal Affinity to Wild Type APC—APC-mediated PAR-1 activation is dependent upon APC binding to EPCR. To ascertain whether *APC-L38D* interacts normally with sEPCR, the binding affinity of this variant compared with wild type APC was tested by surface plasmon resonance. After sEPCR immobilization, wild type APC and *APC-L38D* (12.5–100 nM) were exposed to the sEPCR surface. *APC-L38D* bound sEPCR normally (K_D = 112 ± 25 nM), similar to that previously described for wild type PC/APC (30, 31) (Fig. 5).

Downloaded from www.jbc.org at IReL (Trinity College Dublin), on March 5, 2010

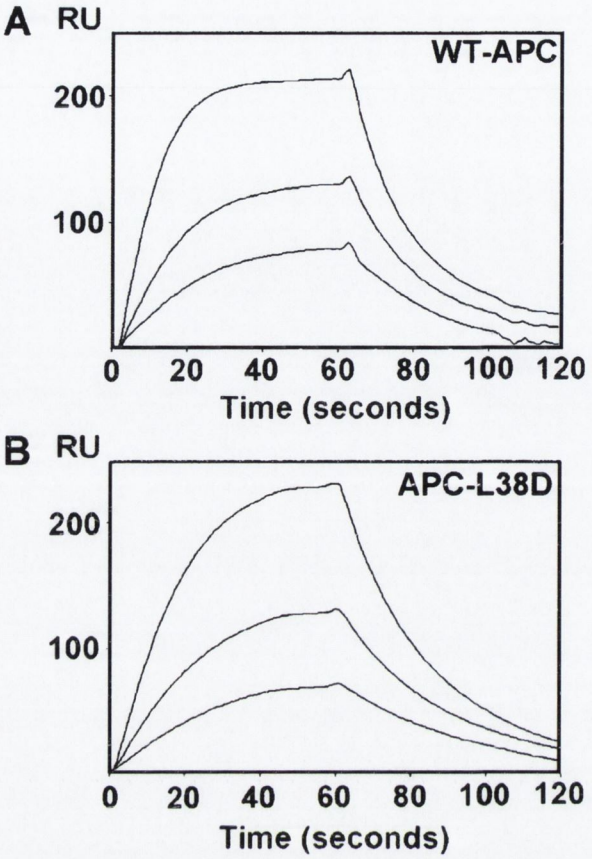


FIGURE 5. ***APC-L38D* has normal affinity for sEPCR.** Recombinant APC variant binding to sEPCR was measured by surface plasmon resonance technology. sEPCR (500–600 response units (*RU*)) was immobilized on to the surface of a CM5 sensor chip via a monoclonal anti-EPCR antibody (RCR-2) (see "Experimental Procedures"). An RCR-2 only flow cell was used to detect nonspecific binding. 25–100 nM wild type APC (*A*) and *APC-L38D* (*B*) was passed over the sEPCR surface at a flow rate of 5 μl/min. Minor differences in APC levels are due to small differences in sEPCR bound to the sensor chip surface. Binding was assessed using BIAevaluation software package.

APC-L38D Exhibits Identical Anti-inflammatory and Anti-apoptotic Activity to Wild Type APC—As *APC-L38D* bound sEPCR normally, the anti-inflammatory and anti-apoptotic properties of *APC-L38D* were evaluated. APC can regulate expression of both pro- and anti-apoptotic genes via EPCR-mediated PAR-1 signaling (10) to confer a net anti-apoptotic phenotype on endothelial cells. The ability of *APC-L38D* to protect EAhy926 cells from apoptosis was assessed by quantification of pro- (*bax*) and anti- (*bcl-2*) apoptotic gene expression after incubation with staurosporine, a well characterized inducer of apoptosis in endothelial cells. Staurosporine, as expected, significantly increased (2.3-fold) the *bax/bcl-2* ratio compared with untreated EAhy926 cells ($p < 0.005$) (Fig. 6*A*). Preincubation with either plasma-purified or wild type APC, however, significantly ameliorated the effect of the staurosporine, as indicated by the large reduction in *bax/bcl-2* ratio in APC-treated cells ($p < 0.005$) compared with those treated with staurosporine alone. The EPCR dependence of this anti-apoptotic activity was confirmed by incubation of an inhibitory anti-EPCR antibody in conjunction with wild type APC, which led to ablation of the APC-associated protective effect. Of note, *APC-L38D* significantly reduced the *bax/bcl-2* ratio compared with staurosporine only treated cells ($p < 0.005$) to the same extent as wild type APC (Fig. 6). APC activation of PAR-1 signaling has also previously been described to protect against thrombin-induced endothelial cell barrier hyperpermeability. Using an *in vitro* assay to assess endothelial cell barrier function, thrombin was found to significantly increase endothelial cell barrier permeability (Fig. 6, *B* and *C*) as previously reported (13). Prior incubation with wild type APC, however, significantly attenuated thrombin-induced endothelial barrier permeability (Fig. 6, *B* and *C*). Each of the APC variants conferred an identical and significant level of endothelial barrier protection to that of wild type APC compared with thrombin-only treated EAhy926 cells (Fig. 6, *B* and *C*). Therefore, APC variants *APC-D35T*, *APC-D36A*, *APC-L38D*, and *APC-A39V* protect endothelial barrier function to the same extent as wild type APC. These results show that the anti-inflammatory and anti-apoptotic functions of APC mediated by EPCR-PAR-1 signaling are entirely conserved in the *APC-L38D* variant despite significant loss of anticoagulant function caused by the severely impaired response to protein S.

DISCUSSION

Protein S is essential for normal anticoagulant function of APC in plasma, acting as a cofactor to enhance proteolysis of APC substrates factor Va and factor VIIIa. Although several putative APC binding sites have been described on protein S (34–40), the corresponding binding sites on APC are poorly defined. However, a previous study has demonstrated that substitution of the APC Gla domain amino acid residues 25–45 with the corresponding amino acid residues in human prothrombin prevented protein S enhancement of APC anticoagulant activity without adversely affecting anionic phospholipid or FVa interactions (41). Furthermore, a subsequent report highlighted the importance of APC Gla domain residues between 33–39, with particular significance assigned to residues Asp-35, Asp-36, Leu-38, and Ala-39 (30).

In this study we have generated and tested individual APC variants in which each of these Gla domain residues was individually substituted with the corresponding prothrombin amino acid residues. Interestingly, only the anticoagulant activity of *APC-L38D* was severely impaired, exhibiting minimal anticoagulant activity in protein C-deficient plasma compared with wild type APC, even at extremely high concentrations (only 35 ± 1% reduction in ETP observed at 150 nM *APC-L38D*; Fig. 2). Furthermore, when the protein S-dependent anticoagulant activity of this variant was assessed in protein S-deficient plasma (Fig. 3) and in FVa proteolysis assays (Fig. 4), *APC-L38D* exhibited effectively no response to protein S, even at free protein S concentrations 10-fold higher than that found in normal plasma (Fig. 3*B*). In contrast, the anticoagulant effects of *APC-D35T*, *APC-D36A*, and *APC-A39V* were only moderately impaired, exhibiting <2-fold impaired anticoagulant activity in plasma compared with wild type APC (Fig. 2). These findings suggest that APC Gla domain residues 35, 36, and 39 make a relatively minor contribution to the protein S interaction with the APC Gla domain in this region.

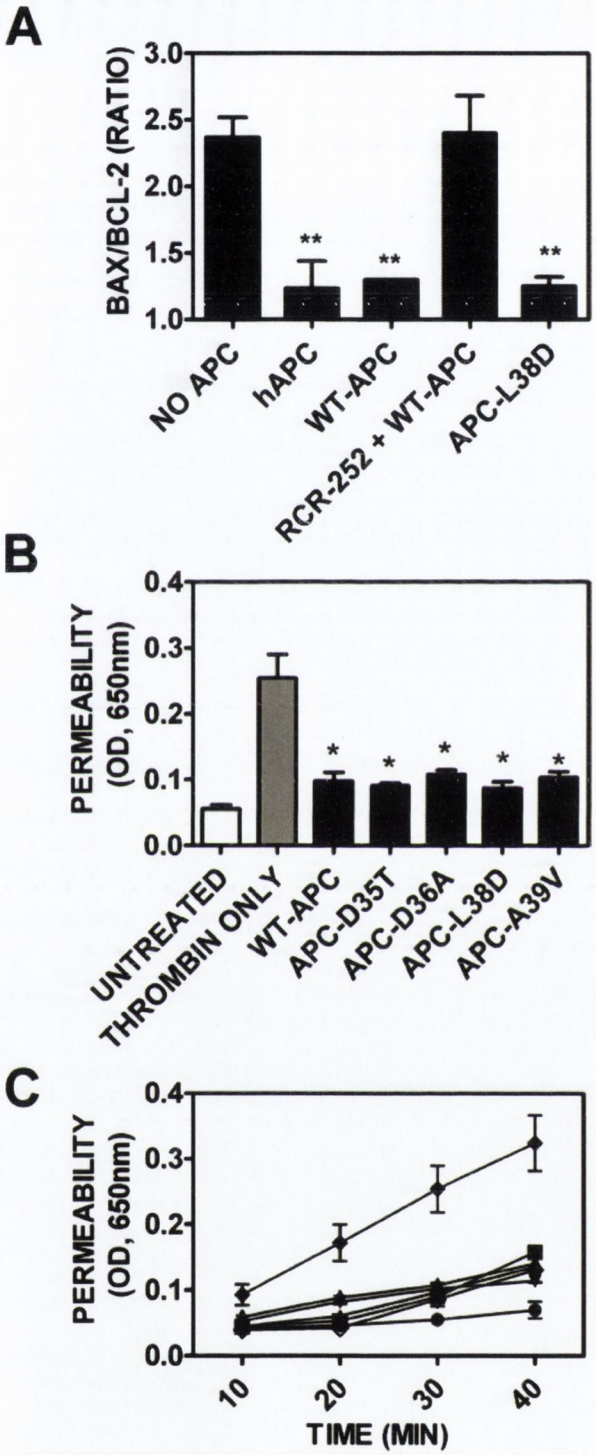


FIGURE 6. **APC variants 35–39 exhibit normal ability to inhibit apoptosis and endothelial barrier protection.** *A*, confluent EAhy926 cells were incubated with Protac-generated plasma purified APC, recombinant wild type APC, and APC Gla domain variants for 17 h. A rat monoclonal anti-EPCR antibody (RCR-252) was added (400 μM) alongside wild type APC to determine EPCR dependence. Apoptosis was induced in EAhy926 cells by incubation with 20 μM staurosporine for 4 h. RNA was extracted and reverse-transcribed as described under "Experimental Procedures." Reverse transcription-PCR was performed using specific *Bax*, *Bcl-2*, and β-actin primers. Experiments were performed in triplicate, and data are presented as the mean ± S.E. Unpaired two-tailed *t* tests were used to determine significance (**, $p < 0.005$ compared with staurosporine-only treated EAhy926 cells). *hAPC*, human APC. *B*, the protective effect of APC on the endothelial cell barrier was determined for wild type APC and each Gla domain variant. EAhy926 cells were preincubated with 20 nM wild type or variant APC (*black bars*) for 3 h. Untreated cells (*white bar*) were used as a negative control. EAhy926 cells were then treated with 5 nM thrombin in serum-free media for 10 min (cells treated with thrombin only, *gray bar*), and endothelial barrier permeability was assessed after 30 min using Evans Blue-bovine serum albumin (see "Experimental Procedures"). Unpaired two-tailed *t* tests were used to determine significance (*, $p < 0.05$ compared with thrombin-only treated EAhy926 cells). *C*, endothelial barrier protection was assessed over time as described above: untreated EAhy926 cells, ●; 5 nM thrombin, ◆; WT-APC, ▲; *APC-D35T*, ■; *APC-D36A*, △; *APC-L38D*, ◇; *APC-A39V*, ▼.

Protein S binding to APC has historically proved refractory to meaningful assessment in the absence of phospholipid vesicles, making it difficult at this stage to ascertain whether Leu-38 constitutes a key residue as part of a protein S binding site on APC or is critical for a protein S-mediated conformational change that facilitates enhanced APC substrate proteolysis. Further studies will be required to unravel the precise role of Leu-38 in regulating protein S cofactor enhancement.

Accumulating evidence from different animal disease models suggests that the cytoprotective signaling activity of APC may be of greater significance than its anticoagulant function in protection against various disease states, including severe sepsis, inflammatory bowel disease, and ischemic stroke (16, 19, 42). Nevertheless, the anticoagulant properties of APC are important in that APC administration is associated with a significant increased bleeding risk (19). Although protein S constitutes a critical cofactor for the anticoagulant function of APC, there is no suggestion that it plays any role in regulating PAR-1-mediated anti-inflammatory or anti-apoptotic effects. Thus, disrupting the interplay between APC and protein S constitutes an attractive and novel strategy that may be exploited to generate APC variants with discrepant anticoagulant to cytoprotective properties. However, previous studies have demonstrated that mutations in other regions of APC may influence the ability of the APC Gla domain to effectively bind EPCR, which is a prerequisite for PAR-1 signaling (24). As we have demonstrated, despite having almost entirely lost the ability to interact with protein S, the *APC-L38D* variant bound sEPCR with the same affinity as wild type APC (Fig. 5). Furthermore, *APC-L38D* exhibited PAR-1-mediated cytoprotective properties that were indistinguishable from those of wild type APC (Fig. 6).

Recombinant APC variants possessing APC modifications that have significantly reduced anticoagulant activity but retained significant PAR-1 signaling function have previously been generated using alternative strategies. Mosnier *et al.* (25) demonstrated that clustered alanine mutations (R229A/R230A) and (K191A/K192A/K193A) in two surface loops of the APC serine protease domain disrupted the anion binding site on APC for FVa exosite binding. Consequently, when these five alanine substitutions were combined (5A-APC), APC anticoagulant activity was markedly reduced (<3% residual APTT clotting assay) (26). Because the APC serine protease exosite for PAR-1 is distinct from that of FVa, this combination of mutations did not influence the cytoprotective properties of 5A-APC, which were identical to those of wild type APC. Thus the anticoagulant and anti-inflammatory profiles of this 5A-APC variant are comparable with that exhibited by the

Downloaded from www.jbc.org at IReL (Trinity College Dublin), on March 5, 2010

APC-L38D variant described herein despite the fact that the respective mutations occur at opposite ends of the APC molecule, are located in distinct structural domains, and target two different specific APC functional interactions.

Using an alternative approach, Bae *et al.* (24) engineered a disulfide bond (Cys^{67}–Cys^{82}; chymotrypsin numbering) within the APC serine protease domain, which prevented Ca^{2+} binding to the functionally critical Ca^{2+} binding 70–80 loop. As a result, the anticoagulant activity of the variant Cys^{67}–Cys^{82}APC was again dramatically impaired, but it was shown to retain PAR-1 activation mediated anti-apoptotic, anti-inflammatory, and endothelial barrier protective functions. However, in contrast to 5A-APC and the *APC-L38D* variant, the cytoprotective effects of Cys^{67}–Cys^{82}-APC required a 2-fold higher concentration of mutant APC to produce equivalent effects to wild type APC. Interestingly this reduction in the cytoprotective properties of Cys^{67}–Cys^{82}APC was subsequently shown to result from a reduced affinity of the variant APC for EPCR.

On the basis of their specifically reduced anticoagulant activity, one would anticipate that these two previously described recombinant APC variants together with the novel *APC-L38D* variant should all be associated with significantly reduced bleeding risk *in vivo*. Because of their reduced bleeding risk, these variants may permit the use of significantly higher APC doses and also longer duration APC administration. Such altered APC therapeutic regimens may be particularly relevant in severe sepsis where overall mortality in the group of patients treated with wild type APC in the PROWESS trial still exceeded 24% (19). A recent *in vivo* study has confirmed for the first time that APC variants with reduced or minimal anticoagulant activity may confer important therapeutic benefit. In a murine model, Kerschen *et al.* (8) demonstrate that 5A-APC was as effective as wild type APC in reducing overall mortality after LPS challenge.

In addition to the complete ablation of anticoagulant activity for *APC-L38D*, we observed a 2-fold reduced anticoagulant activity for each of the variants *APC-D35T*, *APC-D36A*, and *APC-A39V* respectively. Each of these variants also retained entirely normal PAR-1-mediated cytoprotective properties. Thus, these three variants demonstrate anticoagulant/cytoprotective phenotypes that are intermediate between wild type APC and the *APC-L38D* variant. Consequently, these variants may prove useful adjuncts for defining the relative importance of the anticoagulant and cytoprotective effects of APC in different disease states. Moreover, such APC variants with reduced but residual anticoagulant activity may also offer novel therapeutic opportunities. For example, a beneficial effect of APC has recently been described in a murine model of experimental autoimmune encephalomyelitis (17). In this animal model of multiple sclerosis, it was clearly demonstrated that both the cytoprotective and the anticoagulant properties of APC were required for maximal therapeutic efficacy. These findings suggest that second generation therapeutic recombinant APC variants that retain some residual anticoagulant activity may constitute the treatment of choice in specific disease settings. Further *in vivo* studies will be necessary to fully dissect the relative contributions of APC anticoagulant *versus* cytoprotective properties across such a wide variety of pathophysiological processes.

In conclusion, we have demonstrated that a single amino acid substitution (*L38D*) in the Gla domain of APC is sufficient to almost entirely ablate APC anticoagulant activity due to severely impaired protein S cofactor response. This variant, however, retains normal EPCR binding and PAR-1 signaling properties, suggesting a novel mechanism by which the anticoagulant and cytoprotective properties of APC can be separated for potential therapeutic gain.

REFERENCES

1. Esmon, C. T. (1989) *J. Biol. Chem.* **264,** 4743–4746
2. Stearns-Kurosawa, D. J., Kurosawa, S., Mollica, J. S., Ferrell, G. L., and Esmon, C. T. (1996) *Proc. Natl. Acad. Sci. U. S. A.* **93,** 10212–10216
3. Walker, F. J., Sexton, P. W., and Esmon, C. T. (1979) *Biochim. Biophys. Acta* **571,** 333–342
4. Fay, P. J., Smudzin, T. M., and Walker, F. J. (1991) *J. Biol. Chem.* **266,** 20139–20145
5. Seligsohn, U., Berger, A., Abend, M., Rubin, L., Attias, D., Zivelin, A., and Rapaport, S. I. (1984) *N. Engl. J. Med.* **310,** 559–562
6. Reitsma, P. H., Poort, S. R., Bernardi, F., Gandrille, S., Long, G. L., Sala, N., and Cooper, D. N. (1993) *Thromb. Haemostasis* **69,** 77–84
7. Riewald, M., Petrovan, R. J., Donner, A., Mueller, B. M., and Ruf, W. (2002) *Science* **296,** 1880–1882
8. Kerschen, E. J., Fernandez, J. A., Cooley, B. C., Yang, X. V., Sood, R., Mosnier, L. O., Castellino, F. J., Mackman, N., Griffin, J. H., and Weiler, H. (2007) *J. Exp. Med.* **204,** 2439–2448
9. Joyce, D. E., Gelbert, L., Ciaccia, A., DeHoff, B., and Grinnell, B. W. (2001) *J. Biol. Chem.* **276,** 11199–11203
10. Riewald, M., and Ruf, W. (2005) *J. Biol. Chem.* **280,** 19808–19814
11. White, B., Schmidt, M., Murphy, C., Livingstone, W., O'Toole, D., Lawler, M., O'Neill, L., Kelleher, D., Schwarz, H. P., and Smith, O. P. (2000) *Br. J. Haematol.* **110,** 130–134
12. Feistritzer, C., Lenta, R., and Riewald, M. (2005) *J. Thromb. Haemost.* **3,** 2798–2805
13. Feistritzer, C., and Riewald, M. (2005) *Blood* **105,** 3178–3184
14. Domotor, E., Benzakour, O., Griffin, J. H., Yule, D., Fukudome, K., and Zlokovic, B. V. (2003) *Blood* **101,** 4797–4801
15. Cheng, T., Liu, D., Griffin, J. H., Fernandez, J. A., Castellino, F., Rosen, E. D., Fukudome, K., and Zlokovic, B. V. (2003) *Nat. Med.* **9,** 338–342
16. Griffin, J. H., Zlokovic, B., and Fernandez, J. A. (2002) *Semin. Hematol.* **39,** 197–205
17. Han, M. H., Hwang, S. I., Roy, D. B., Lundgren, D. H., Price, J. V., Ousman, S. S., Fernald, G. H., Gerlitz, B., Robinson, W. H., Baranzini, S. E., Grinnell, B. W., Raine, C. S., Sobel, R. A., Han, D. K., and Steinman, L. (2008) *Nature* **451,** 1076–1081
18. Isermann, B., Vinnikov, I. A., Madhusudhan, T., Herzog, S., Kashif, M., Blautzik, J., Corat, M. A., Zeier, M., Blessing, E., Oh, J., Gerlitz, B., Berg, D. T., Grinnell, B. W., Chavakis, T., Esmon, C. T., Weiler, H., Bierhaus, A., and Nawroth, P. P. (2007) *Nat. Med.* **13,** 1349–1358
19. Bernard, G. R., Vincent, J. L., Laterre, P. F., LaRosa, S. P., Dhainaut, J. F., Lopez-Rodriguez, A., Steingrub, J. S., Garber, G. E., Helterbrand, J. D., Ely, E. W., and Fisher, C. J., Jr. (2001) *N. Engl. J. Med.* **344,** 699–709
20. Warren, B. L., Eid, A., Singer, P., Pillay, S. S., Carl, P., Novak, I., Chalupa, P., Atherstone, A., Penzes, I., Kubler, A., Knaub, S., Keinecke, H. O., Heinrichs, H., Schindel, F., Juers, M., Bone, R. C., and Opal, S. M. (2001) *J. Am. Med. Assoc.* **286,** 1869–1878
21. Abraham, E., Reinhart, K., Opal, S., Demeyer, I., Doig, C., Rodriguez, A. L., Beale, R., Svoboda, P., Laterre, P. F., Simon, S., Light, B., Spapen, H., Stone, J., Seibert, A., Peckelsen, C., De Deyne, C., Postier, R., Pettila, V., Artigas, A., Percell, S. R., Shu, V., Zwingelstein, C., Tobias, J., Poole, L., Stolzenbach, J. C., and Creasey, A. A. (2003) *J. Am. Med. Assoc.* **290,** 238–247
22. Bertolini, G., Rossi, C., Anghileri, A., Livigni, S., Addis, A., and Poole, D. (2007) *Intensive Care Med.* **33,** 426–434

23. Kanji, S., Perreault, M. M., Chant, C., Williamson, D., and Burry, L. (2007) *Intensive Care Med.* **33,** 517–523
24. Bae, J. S., Yang, L., Manithody, C., and Rezaie, A. R. (2007) *J. Biol. Chem.* **282,** 9251–9259
25. Mosnier, L. O., Gale, A. J., Yegneswaran, S., and Griffin, J. H. (2004) *Blood* **104,** 1740–1744
26. Mosnier, L. O., Yang, X. V., and Griffin, J. H. (2007) *J. Biol. Chem.* **282,** 33022–33033
27. Walker, F. J. (1984) *Semin. Thromb. Hemostasis* **10,** 131–138
28. Yegneswaran, S., Smirnov, M. D., Safa, O., Esmon, N. L., Esmon, C. T., and Johnson, A. E. (1999) *J. Biol. Chem.* **274,** 5462–5468
29. Nicolaes, G. A., Tans, G., Thomassen, M. C., Hemker, H. C., Pabinger, I., Varadi, K., Schwarz, H. P., and Rosing, J. (1995) *J. Biol. Chem.* **270,** 21158–21166
30. Preston, R. J., Ajzner, E., Razzari, C., Karageorgi, S., Dua, S., Dahlback, B., and Lane, D. A. (2006) *J. Biol. Chem.* **281,** 28850–28857
31. Preston, R. J., Villegas-Mendez, A., Sun, Y. H., Hermida, J., Simioni, P., Philippou, H., Dahlback, B., and Lane, D. A. (2005) *FEBS J.* **272,** 97–108
32. Berg, D. T., Gerlitz, B., Shang, J., Smith, T., Santa, P., Richardson, M. A., Kurz, K. D., Grinnell, B. W., Mace, K., and Jones, B. E. (2003) *Proc. Natl. Acad. Sci. U. S. A.* **100,** 4423–4428
33. Hackeng, T. M., Sere, K. M., Tans, G., and Rosing, J. (2006) *Proc. Natl. Acad. Sci. U. S. A.* **103,** 3106–3111
34. Dahlback, B., Hildebrand, B., and Malm, J. (1990) *J. Biol. Chem.* **265,** 8127–8135
35. Giri, T. K., de Frutos, P. G., Yamazaki, T., Villoutreix, B. O., and Dahlback, B. (1999) *Thromb. Haemostasis* **82,** 1627–1633
36. He, X., Shen, L., and Dahlback, B. (1995) *Eur. J. Biochem.* **227,** 433–440
37. He, X., Shen, L., Villoutreix, B. O., and Dahlback, B. (1998) *J. Biol. Chem.* **273,** 27449–27458
38. Mille-Baker, B., Rezende, S. M., Simmonds, R. E., Mason, P. J., Lane, D. A., and Laffan, M. A. (2003) *Blood* **101,** 1416–1418
39. Saller, F., Kaabache, T., Aiach, M., Gandrille, S., and Borgel, D. (2006) *J. Thromb. Haemost.* **4,** 704–706
40. Saller, F., Villoutreix, B. O., Amelot, A., Kaabache, T., Le Bonniec, B. F., Aiach, M., Gandrille, S., and Borgel, D. (2005) *Blood* **105,** 122–130
41. Smirnov, M. D., Safa, O., Regan, L., Mather, T., Stearns-Kurosawa, D. J., Kurosawa, S., Rezaie, A. R., Esmon, N. L., and Esmon, C. T. (1998) *J. Biol. Chem.* **273,** 9031–9040
42. Scaldaferri, F., Sans, M., Vetrano, S., Graziani, C., De Cristofaro, R., Gerlitz, B., Repici, A., Arena, V., Malesci, A., Panes, J., Grinnell, B. W., and Danese, S. (2007) *J. Clin. Investig.* **117,** 1951–1960

Downloaded from www.jbc.org at IReL (Trinity College Dublin), on March 5, 2010